Integration and Optimisation of Bio-fuel Micro-Tri-Generation with Energy Storage

By Xiangping Chen

Thesis Submitted for the Degree of

Doctor of Philosophy

Newcastle Institute for Research on Sustainability

Newcastle University

Newcastle upon Tyne

United Kingdom

June 2013

List of Publications

1) **X. P. Chen**, Y. D. Wang, H. D. Yu, D. W. Wu, Y. P. Li, A. P. Roskilly, "A domestic CHP system with hybrid electrical energy storage", *Energy and Buildings*, Vol. 55, Dec 2012: 361-368.
2) **X. P. Chen**, Y. D. Wang, J. T. Li, A. P. Roskilly, "Hybrid electrical storage and power system for household tri-generation application", *Advanced Materials Research*, Vol. 614-615, 2012: 829-836.
3) Y. Wang, Y. Huang, E. Chiremba, A. P. Roskilly, N. Hewitt, Y. Ding, D. Wu, H. Yu, **X. Chen**, Y. LI, J. Huang, R. Wang, J. Wu, C. Tan, "An investigation of a household size trigeneration running with hydrogen", *Applied Energy*, Vol. 88:6, 2011: 2176-2182.
4) **X. P. Chen**, M. Zhang, F. Wen, "Min-shaft safety monitoring system based on zigbee technology", *Journal of Sichuan University (Natural Science Edition)* Vol. 45, Issue 2, 2008: 129-131.
5) **X. P. Chen**, Y. D. Wang, D. W. Wu, H. D. Yu, Y. P. Li, A. P. Roskilly, "Investigation of a combined CHP with energy storage system", *ICAE'12*, 5th -8th July, 2012.
6) F. Ronilaya, Y. D. Wang, **X. P. Chen**, A. P. Roskilly, "Modeling and assessment of electrical energy storage system and the integration with fuel cell system", *The 2nd PRO-TEM Network Conference*, 25th-26th Oct. 2011.
7) **X. P. Chen**, K. L. Teng, C. He, Y. D. Wang, A. P. Roskilly, "A study of innovative electrical energy storage and power supply system in a household tri-generation", *International Conference on Sustainable Energy Technologies*, Shanghai, China, 24th-27th Aug. 2010.
8) Y. Wang, Y. Huang, A. P. Roskilly, N. Hewitt, Y. Ding, C. Charalambous, D. Wu, H. Yu, **X. P. Chen**, F. Y. Zhao, J. Huang, R. Wang, J. Wu, Z. Xia, C. Tan, "A study of a diesel genset based trigeneration running with raw jatropha oil", *The 2009 Heat Powered Cycles Conference*, TU Berlin, Germany, 7th-9th Sept. 2009.

Abstract

This study addresses the global technical challenges of resource depletion and climate change by developing the first demonstration of incorporating smart energy storage (super-capacitors and batteries) with bio-fuel micro-tri-generation (BMT-HEES) for domestic applications. The developed system is capable of producing required heat, electricity and refrigeration from renewable bio-fuels for an average British household usage, and dynamically regulating the energy distribution within the system by using a novel energy storage system and a following electric load (FEL) energy management method.

In this study, an extensive literature review has been carried out to investigate previous tri-generation and hybrid energy storage systems with a particular focus on their features, advantages and challenges which provide a basis for further improvements. The research work started with a preliminary investigation to fully understand the dynamic characteristics of lead acid batteries and super-capacitors used in combination to provide the desirable electrical output. The test results suggested that the super capacitors performed better than batteries in meeting transient electrical demands.

In order to develop a complete BMT-HEES system, computational modeling and simulation was then conducted in the *Dymola* simulation environment, where the complete BMT-HEES system with advanced operational strategies has been implemented followed by case studies. System performance was assessed by evaluating key performance indicators including fuel consumption, dynamic response of each power sources, operational durations and energy efficiencies.

A full experimental setup of the proposed system was also developed. Experimental tests on individual components and the BMT-HEES system as a whole have validated the effectiveness of the developed methodologies and techniques. Specific case studies have proved that the system can improve over the existing ones in terms of energy efficiency (with 47.86% improvement compared to one tri-generation system without HEES) and dynamic response for selected days as reported in the case studies. Test results from both simulation and physical experiments show that BMT-HEES can satisfy the fluctuating energy demands faithfully and instantly with high system efficiency for domestic applications.

In addition, the predicted performance based on the developed methodologies has a good agreement with actual measurements. The low error of each assessment indicator provides

the confidence that the system models can predict the system performance with good accuracy (all of the errors were within 3%).

The developed technologies in this study can help cut down the carbon footprint in domestic environments, facilitate a shift towards an environment-friendly lifestyle, and in the long run, improve the quality of human life. Moreover, the established system is flexible, scalable and inter-connectable. That is, the system can incorporate other types of bio-fuels or other sources of new and renewable energy (wind, solar, geothermal, biomass etc.), depending on the availability of the energy and location of the system used. In addition to the small-scale domestic environment, the physical system can be scaled up to be used in larger commercial and industrial environments. It may be used as a stand-alone energy system or it can be inter-connected with neighboring energy systems or connected with the power grid as a distributed generation set if there is a need (or a surplus) of generated electricity. Without doubt, this will require further work on this inter-disciplinary topic as well as new innovations in the fields of energy networks and smart grids.

Acknowledgements

I would like to take this opportunity to gratefully appreciate the great support from my supervisors, Professor Tony Roskilly and Dr. Yaodong Wang throughout my entire PhD study. I also thank Stephen Crosby and Ian Milne for their industrious work by building up the experimental bench and Dr. Rosemary Norman for guidance and proofreading.

Thanks also need to be given to the colleagues and friends including Chris Mullen, Petros Missailidis, Jonathan Heslop, Guohong Tian, Yiji Lu, Huashan Bao, Leigh Ingle, Jan Fairless, Paul Watson, and Michelle Wagner, for the assistance and laughter.

Last I shall express my deepest appreciation to my family. Without their consistent support and encouragement, I would never be nearing the completion of my PhD work.

Contents

List of Figures

List of Tables

Nomenclature

AGM	absorbent glass mat
BMT-HEES	bio-fuel micro-tri-generation with hybrid electrical energy storage
CAES	compressed air energy storage technology
CCHP	combined cooling, heating and power
CDE	carbon dioxide emissions
CEF	charge efficiency factor
CES	cryogenic energy storage
CHP	combined heat and power
COP	coefficient of performance
DG	distributed generation
DOC	discharge of capacity
ECDL	electrochemical double layer super-capacitors
ESR	equivalent series resistance
EPR	equivalent parallel resistance
FEL	following electrical loads
FTL	following the thermal load
GA	genetic algorithm
HEES	hybrid electrical energy storage
LP	linear programming
MCFC	molten carbonate fuel cells
OC	operational cost
PV	photovoltaic
PEC	primary energy consumption
PEMFC	proton exchange membrane fuel cell
PER	primary energy ratio
PLC	programmable logic controller
PMSM	permanent magnet synchronous motor
PSB	polysulphide bromide battery
PWM	pulse width module
SMES	superconducting magnetic energy storage
VC	vapour combustion
VRB	vanadium redox battery
ZBB	zinc bromine battery

Symbols

E_{ave}	overall electrical efficiency
E_{Bat}	average operational efficiency of batteries
E_{Gen}	engine electric efficiency
$f_{eng}(t, p_e)$	electric efficiency of the engine at time t(s) with electric output p_e
$f_{ch}(t, p_e)$	storage system charging efficiency at time t with electric power output p_e
$f_{ch_{disc}}(t, p_e)$	electric transmission efficiency of the storage system over charge/discharge at time point of t with electric power output p_e
$f_{Gen}(p)$	generator efficiency at power output p
$p_{co}(t, p_e)$	heat power recovered from coolant system at time t with electric output power p_e
p_{eng}	nominal electric power of the engine
$p_{exh}(t, p_e)$	heat power recovered from exhaust gas at time t with electric output power p_e
P_{max}	maximum power
$p_{rec}(t, p_e)$	total heat power recovered at time t with electric output power p_e
$p_{storage}$	electric output power of the energy storage system
P_η	discharge power at discharge efficiency η
Q	total heat energy recovered
Q_{co}	total heat energy recovered from coolant system
Q_{exh}	total heat energy recovered from exhaust gas
R_b	resistance
T_{eng}	engine operational duration
T_{ees}	storage system discharging duration
T_i	engine operation time during the duration i
$T_{together}$	peak hour
V_{oc}	open-circuit voltage
η	efficiency
$\eta_{ch}(i)$	average charge efficiency of the storage system over t_i duration
η_{eng}	average electric efficiency of the engine operation
$\eta_{storage}$	electric efficiency of the storage system
η_{sys}	overall efficiency of the system

Chapter 1 Introduction

1.1 Global energy challenges

Over the last 50 years, the global economy has been developing rapidly with the aid of "cheap" fossil fuels. Currently, the majority of energy is still being derived from primary sources of energy (coal, gas, oil, etc.). On one hand, fossil fuel reserves are finite and it is only a matter of time before they run out. On the other hand, burning them in large quantities generates excessive greenhouse gases (mainly CO_2) and collectively causes the so-called "global warming" phenomenon. As a result, it is now universally accepted that this way of development is not sustainable.

In 1992, the United Nations Framework Convention on Climate Change (UNFCCC) proposed a voluntary target for greenhouse gas emissions in 2000 to be lower than 1990 levels. But the result showed that only the UK, Germany and Luxembourg achieved this aim. In 1997, "The 3rd Conference of the Parties to the United Nations Framework Convention on Climate Change" was held in Kyoto (Japan). The world leaders agreed that a drastic target of a 5% reduction in greenhouse gas emissions below 1990 levels by 2010 was to be set for developed countries. However, this Kyoto Protocol was weakened by several countries especially by the United States who later withdrew its signature on the treaty. At the 2012 UN Climate Change Conference in Doha (Qatar), the international community agreed to launch a new commitment period under the Kyoto Protocol in order to achieve its goals, and to set a timetable to adopt a universal climate agreement by 2015, which will come into effect in 2020. Overall, international effort to limit greenhouse gas emissions has been taken forwards in two directions: (i) utilising new and renewable energy in place of fossil fuels; (ii) Improving the energy efficiency of major components in the power chain (generation, transmission, distribution, and consumption).

The work in this thesis addresses the global energy challenges in both directions by developing novel technologies to utilise new and renewable energy, and by improving the efficiency of small-scale tri-generation systems for domestic applications. It is thus hoped that this work will play a small part in worldwide energy demand reduction moving towards tackling global warming issues. Progress is indeed made in small steps.

1.2 **Energy policy in the UK**

The UK government has always been proactive at facing global energy challenges. In 2008, the Climate Change Act 2008 [1] was launched with an important objective of reducing 80% of greenhouse gas emissions by 2050 compared to the 1990 levels. In order to achieve this long-term objective, an intermediate goal was set to reduce emissions by at least 34% by the year 2020 with respect to the 1990 baseline levels. Later in 2011, the first Renewable Energy Roadmap was published and the Department of Energy and Climate Change (DECC) which proposed a target of 15% renewable energy generation by 2020 [2]. This will require approximately 239 TWh of renewable energy to be delivered in the UK, including onshore and offshore wind power, large and small-scale hydropower, biomass and bio-wastes (including co-firing), solar photovoltaic (PV) and active solar heating, wave and tidal power, and geothermal aquifers. In 2012, the UK government further proposed to increase the proportion of renewable energy to 30% by 2020 with an emphasis on electricity consumption, as compared to around 11% in 2012 [3].

Among all the end-users, domestic energy consumption accounts for approximately half of the UK greenhouse gas emissions according to an energy analysis report [4] from the Department for Environment, Food and Rural Affairs (DEFRA). Domestic electricity consumption is regarded as a major contributing factor (31%) of total demand for electricity in the UK according to official statistics in 2011 [5].

Without doubt, electricity generation derived from renewable sources is one of the most important objectives and a crucial development in the UK government energy strategy. An incentive was the introduction of the Feed in Tariff (FiT) scheme in April 2010 which attempted to expand renewable electricity generation. As a consequence, wind turbine installations have increased and now play a dominant role in UK renewable electricity generation [6], especially for large-scale renewable power generation. Solar PV installations expanded rapidly with 94% growth across the spectrum of renewable electricity generation [7], especially for small-scale domestic applications. Similarly, micro combined heat and power (CHP) schemes demonstrate substantial growth with 241 installations from a total of 354 cases according to an investigation performed by DECC [7].

These government initiatives demonstrate the inclination of the UK authorities towards building a low-carbon economy with reduced dependency on conventional fuel resources for

energy generation. In the UK, bio-fuels as alternative fuels are playing an increasingly significant role in meeting the target of cutting down greenhouse gas emissions because they are non-toxic, sulphur-free, oxygenated and bio-degradable [8]. Traditionally, some of these bio-fuels have been burnt as wastes releasing a large quantity of CO_2 and other gases. As a result, there is a doubly added value to the utilisation of bio-fuels which may be used directly in diesel engines without substantial modification. Furthermore, distributed CHP (or tri-generation) fed by bio-fuels is one of the key technologies suited for domestic applications which are the main focus of this work.

1.3 **Domestic energy demands and supplies**

A comprehensive review of domestic energy consumption across England and Wales was provided by DECC in [9]. In the year 2009, the energy consumption was 294 million MWh (for gas) and 69 million MWh (for electricity) in England while the corresponding figures for Wales during the same period were 16.2 million MWh (for gas) and 44.6 million MWh (for electricity). The annual energy consumption of the average household was approximately at comparable levels in both regions ranging from 13,709 kWh (South west) and 15,777 kWh (Yorkshire and Humber) in gas and 3,407 (North east) to 4,115 kWh (South east) in electricity. The average gas and electricity consumption was 15,342 kWh and 3,784 kWh, respectively, across England and Wales. Furthermore, statistical data from the Office of the Gas and Electricity Markets (OfGEM) indicated that the average heat demand in a typical property in the UK ranged from 16,500 kWh to 20,500 kWh and the average electricity consumption was 3,300 kWh over the year 2011 [10] which are adopted in this study.

1.3.1 **Household electricity demands**

The day-time variation of household electricity utilisation over a two-year period is depicted in Fig. 1.1 [11]. The average demand of electricity is generally below 2 kW. In rare situations, electricity consumption exceeding 6 kW can also be observed. In practice, there is a need to consider a power system to accommodate the demands of 2-6 kW.

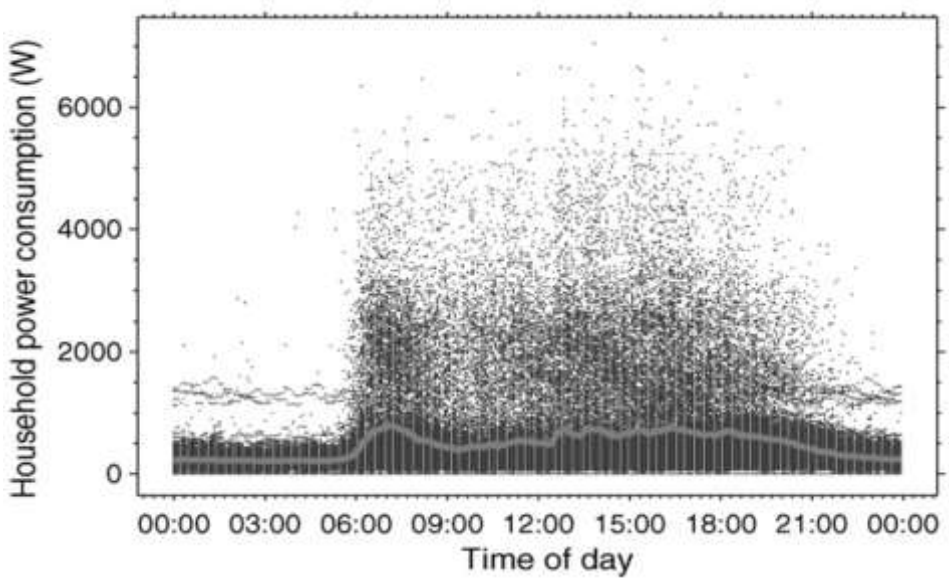

Fig. 1.1 Household electric consumption over 2 years [11]

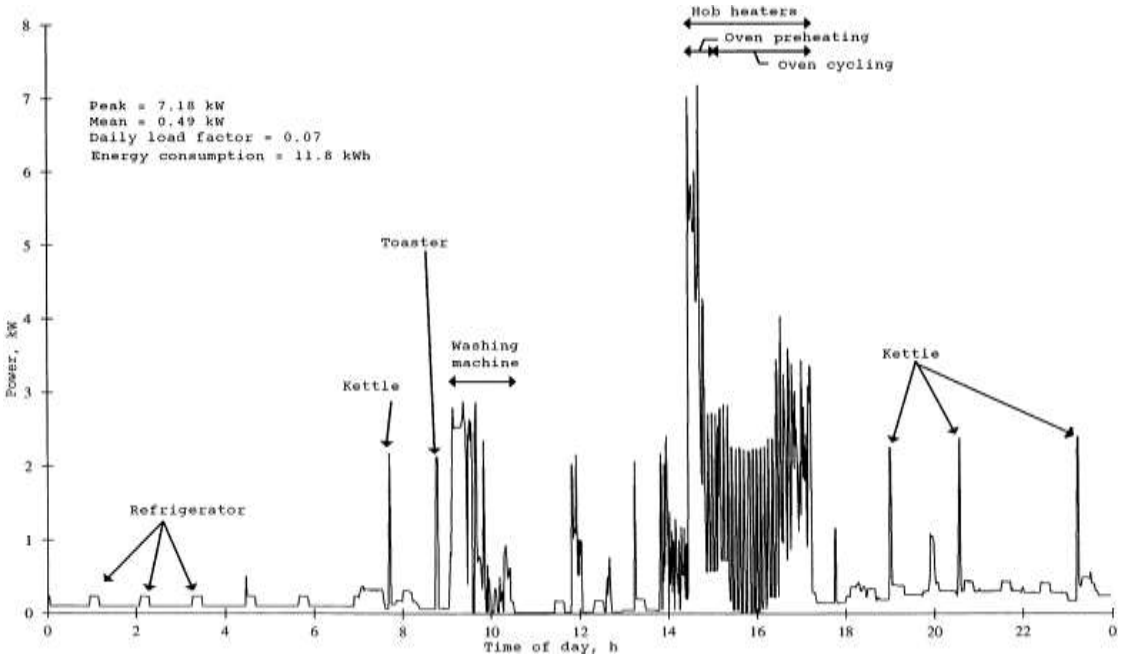

Fig. 1.2 Electricity demand profile from an individual household [12]

Fig. 1.2 shows daily electricity consumption in the premises of a household [12]. The household consumption varied dramatically within a day depending on the use of different electrical appliances. Although one appliance may use less than 1 kWh per day and some appliances (e.g. kettles, ovens and tumble dryers) may create an individual peak demand of 2–2.5 kW, the cumulative appliance usage could result in high demands for electricity at peak times. For instance, during dinner times, a peak demand of 10 kW can be produced. In the

UK as a whole, the difference between peak demand (45.0 GW at 18:00) and the lowest demand (29.6 GW at 04:30) [13] can be as much as 50% over the course of a day.

Fig. 1.3 shows the electricity consumption/demand profile over 24 hours for a selected house from Lawson's research [14]. From the figure, it can be seen that the minimum demand of electrical power was around 100 W and the maximum demand reached 6.544 kW. It can also be found that the electricity consumption was lower than 1 kW for most of the time during

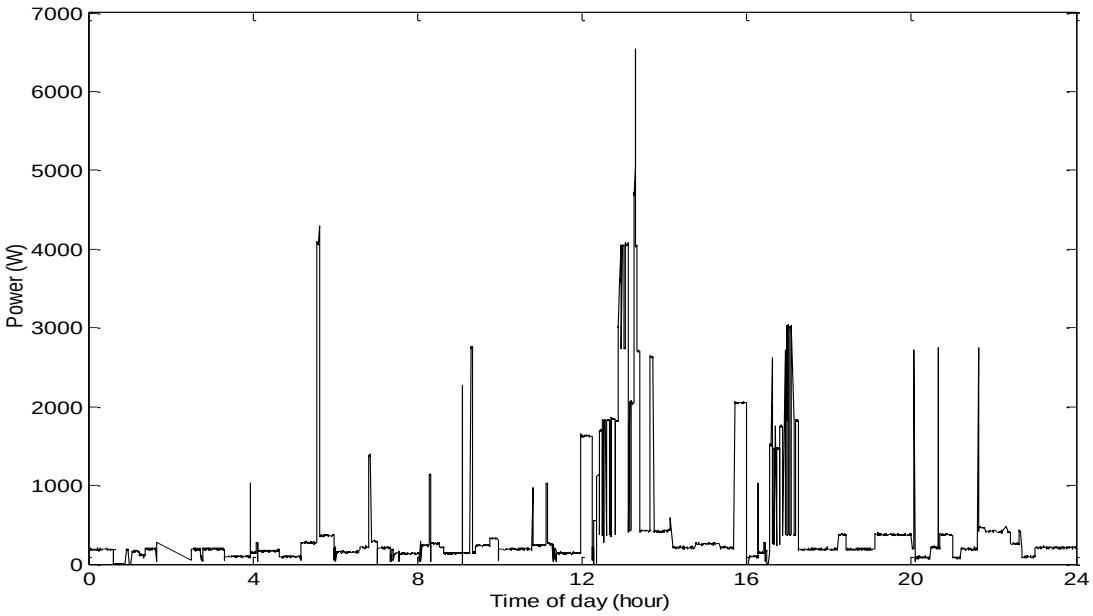

Fig. 1.3 Household electricity consumption profile over a single day [14]

the 24-hour period while the duration of peak demands was relatively short. For example, the demand was as high as 6.544 kW at 13:11 and soon plunged to 400 W just 5 minutes later. The peak demands over 2.5 kW occurred 3 times: at 05:22, 13:11, and 21:22. In total, the electricity consumption for this household over the chosen day was 9.85 kWh.

Based on the fluctuating nature of electricity demands depicted in Fig. 1.1-1.3, the major characteristics of a household electricity supply system for design consideration hereafter can be developed, which are:

- Electricity consumption fluctuates considerably over a wide range, from 0 to 9 kW.
- Off-peak household electricity fluctuates around the 6 kW range.
- Transient peak demands are of short duration.

1.3.2 **Household heating demands**

According to a report published in 2011 by OfGEM, the average heating demand in a typical

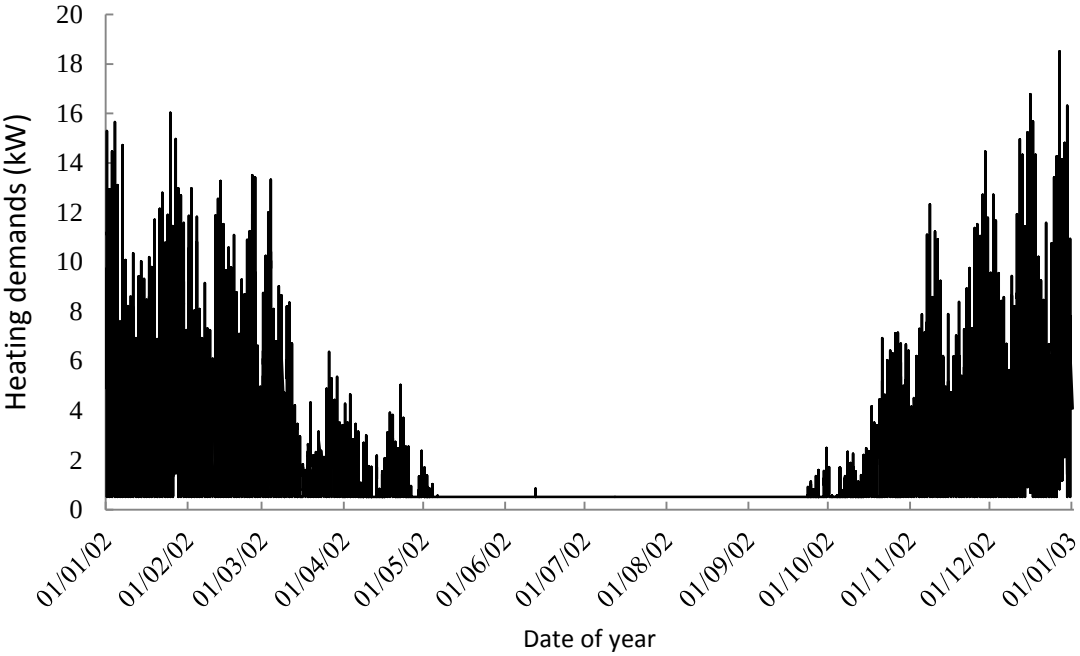

Fig. 1.4 Yearly heat consumption profile in a UK household [10]

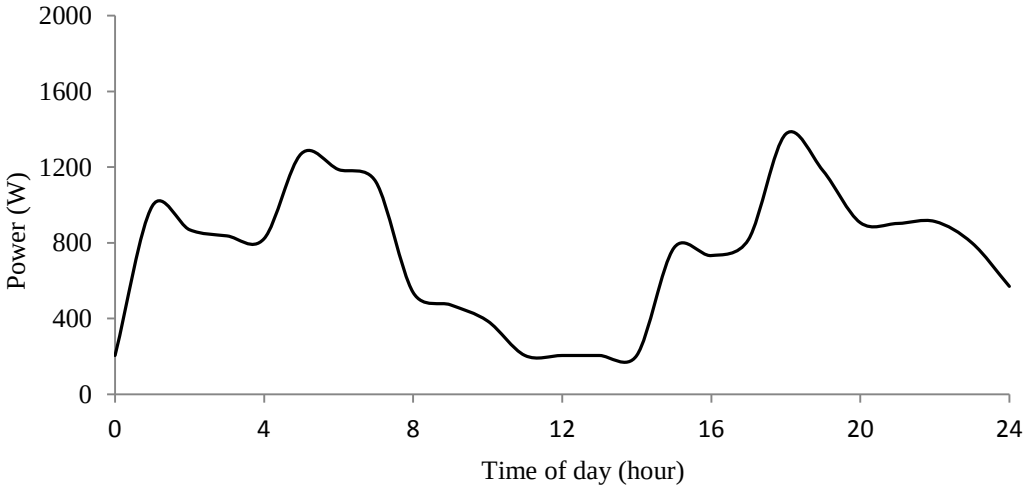

Fig. 1.5 Daily heat consumption profile in a UK household [10]

property in the UK ranged from 16,500 kWh to 20,500 kWh [10]. This data provide the basic knowledge required for the design of a domestic CHP system shown in Fig. 1.4 and 1.5 are the annual and daily heat consumption for an average UK household, respectively. It can be seen that the heat demands exhibit seasonal characteristics. That is, the demand for heating is significantly higher during the winter than in the summer. This is remarkably different to the demand for electricity.

1.4 Design challenge of the domestic energy system

CHP can satisfy both the electricity and heat demands and thus is particularly applicable to domestic environments. However, the heat demands present a distinct seasonal difference with little daily variation as the electricity demands fluctuate dramatically within a day but change little over the seasons. Moreover, the demand for electricity can fluctuate rapidly within minutes whilst the rate of change in heat demands was relatively small. Therefore, a following electrical loads (FEL) strategy should be adopted for designing a domestic CHP energy system. In this regard, the versatile generating capability and fast response of the CHP system are key issues to meet electric load profiles in household dwellings.

1.5 Research contribution

This PhD work was fully supported by the British Engineering and Physical Sciences Research Council (EPSRC) under the grant EP/F061978/1.

The aim of this work was to develop a micro-tri-generation system fed by bio-fuels and incorporating advanced energy storage. The principle objectives were:

- To develop an innovative energy storage prototype and investigate its dynamic characteristics.
- To investigate advanced energy management and operational strategy to optimise the energy generation process
- To set up complete system models to predict system performance in a simulation environment.
- To implement a complete BMT-HEES system and evaluate the whole system performance.

The main contributions of this research are outlined as follows:

- This research has developed an innovative hybrid electrical energy storage system (HEES) consisting of lead-acid batteries and a super-capacitor module. The HEES had both power and energy benefits to meet the fluctuation of the energy demands. The super-capacitors can provide a quick dynamic response to the electrical power demand whilst batteries are capable of generating electrical outputs to meet the base electrical demand. When used in combination, the capacitors operate firstly to meet the peak demands followed

by the batteries supplying electricity to the load with increasing current when the super-capacitor current decays gradually.

- An advanced energy management and operational strategy has been developed under the principle of FEL in the *Dymola* simulation environment. The engine in this system can be switched on over a shorter duty time with higher energy efficiency compared to traditional engine-based tri-generation. The proposed BMT-HEES can deliver a required amount of energy to meet electricity and heating demands for domestic applications in the case studies. By doing so, the need for excessive heat energy in conventional engine-based tri-generation is avoided meanwhile the system efficiency is improved.

- This research has developed an experimental demonstrator for bio-fuel micro-tri-generation with hybrid electrical energy storage (BMT-HEES). The system employs a small-scale diesel engine to provide the main energy required in household usage and the system dynamic response is managed by the coordination of super-capacitors and batteries. The test results from both simulation and experimental case studies have validated the effectiveness of the proposed technologies.

- The developed technologies can be extended to include other types of new and renewable sources of energy such as solar, wind and geothermal energy. The developed physical setup can also be scaled up or interconnected to share generating capabilities with neighbouring systems. In the long term, these systems can also be employed as grid-connected distributed generation (DG) with the help of "smart grid" technologies.

1.6 **Organisation of the thesis**

This thesis is arranged in the following manner. Chapter 2 introduces the relevant technologies of existing tri-generation and electrical energy storage through an extensive literature review. Chapter 3 presents the outcomes of the preliminary design and tests which were aimed to investigate the dynamic performance of the HEES prior to establishing a complete BMT-HEES. Based on the in-depth knowledge of bio-fuels, tri-generation and electrical energy storage from the preliminary study, Chapter 4 presents the design of the whole system. The system models of both small-scale HEES and the complete BMT-HEES were developed in the Dymola environment, and are presented in Chapter 5. Experimental work using the physical system for household applications is described in detail in Chapter 6.

Test results from both simulation and experiments on the performance of the developed system are presented and compared in Chapter 7, followed by Chapter 8 to conclude major research findings of this PhD and further work in this field.

Chapter 2 Literature Review

2.1 Introduction

This chapter provides an overview of the topics covered in the study. Section 2.2 reviews the general characteristics of renewable bio-fuels which are suited for combustion engines for domestic applications. The basic features of tri-generation are presented in Section 2.3 followed by the introduction of HEES technologies covering common categories and diverse combination applications in Section 2.4. A review of energy management strategies and operational algorithms is presented in Section 2.5. Section 2.6 introduces computational simulation software package "Dymola". Section 2.7 provides a brief summary of this chapter.

2.2 Bio-fuels

The term bio-fuel refers to a type of fuel whose energy comes from biological carbon fixation. Biofuels generally include fuels derived from biomass conversion, solid biomass, liquid fuels and biogases and can be classified as bio-diesel, bio-ethanol, bio-methanol, pyrolysis oil, biogas, synthetic gas (dimethyl ether) and hydrogen from renewables. Typical bio-fuels include straight (unprocessed) plant oils (sunflower, rapeseed, jatropha and croton) and are considered to be alternative fuels to fossil fuels. Biofuels are gaining in popularity with the ever-increasing oil prices and increased concern of energy security. Within this group, bio-ethanol and bio-methanol are petrol additives or substitutes whilst bio-diesel attracts much attention because it can be used in standard (unconverted) diesel engines. Moreover, biodiesel can be used alone or mixed with petro-diesel. Overall, bio-diesel is an environmentally-friendly alternative liquid fuel to diesel fuel [15] that can be produced economically from a variety of vegetable oils [8, 16].

Advantages of bio-diesel are:

- They are oxygenated, non-toxic, sulphur-free, bio-degradable, and thus environmentally-friendly and sustainable.
- Use of bio-diesel in a conventional diesel engine results in substantial reduction in unburned hydrocarbon (UBHC), carbon monoxide (CO) and particulate matters (PM) emissions [17].

- The emissions of polycyclic aromatic hydrocarbons (PAH) and nitro PAH compounds when burning bio-diesel are substantially lower than conventional diesel fuel [18].

- The engine performance with bio-diesel and vegetable oil blends of various origins is similar to that of a typical diesel fuel with nearly the same thermal efficiency [19].

However, the major disadvantage of bio-diesels and vegetable oils is their inherent high viscosity [20] that may cause fuel flow and ignition problems [21]. Compared to standard diesel fuel, a higher mass fuel flow is required to maintain constant energy input to the engine in order to produce the same output power [18].

2.3 Tri-generation technologies

2.3.1 CCHP and micro-tri-generation

Tri-generation is widely considered as a key method to enhance energy efficiency and reduce carbon dioxide emissions for small-scale energy users. In most cases, it can also be termed a combined cooling, heating and power (CCHP) system. As its name suggests, the tri-generation system can supply three types of energy: electrical, heating and refrigeration. In theory, tri-generation systems can meet the energy demands at high operational efficiency and therefore reduce overall energy consumption and environmental impacts compared with conventional generation.

Despite research and development efforts in traditional tri-generation, there are limited studies on bio-fuel-based micro-tri-generation (combined power, heating and cooling) systems for small- and medium-scale domestic, industrial and commercial applications. There are several technical and economic obstacles limiting the widespread use of micro tri-generation systems. The technologies are still evolving in matching bio-fuels with diesel engines, managing the energy distribution and improving the system efficiency. Furthermore, they generally require relatively high initial cost and complex optimisation of different parts of the system. Relevant research issues were discussed by Huangfu [22] who asserted that electricity efficiency should be prioritised in micro-tri-generation systems. Miguez [23, 24] pointed out that the introduction of a tri-generation system in the domestic sector requires it to be compact, cost efficient and easily installed. Gigliucci [25] identified key issues for this technology, including the ability to deliver waste heat to a useful thermal sink, variable heat to power ratio and the potential for rapid change of electrical load during operation.

A Conventional tri-generation construction and categories

Generally, a tri-generation system consists of five basic units: the prime mover, electrical generator, heat recovery system, thermally activated equipment, the management and control system, as show in Fig. 2.1.

The prime mover consists of five types: steam turbines and combustion turbines, reciprocating internal combustion engines, micro-turbines, Sterling engines and fuel cells. Major thermally activated technologies include absorption chillers, adsorption chillers, and desiccant dehumidifiers. These cooling and dehumidification systems can be driven by steam, hot water or hot exhaust gas derived from prime movers. Existing tri-generation systems including laboratory-sized units and models vary from site to site, with diversity in prime movers, cooling options, connecting forms, rated size ranges, heat-to-power rates, and demand limitations.

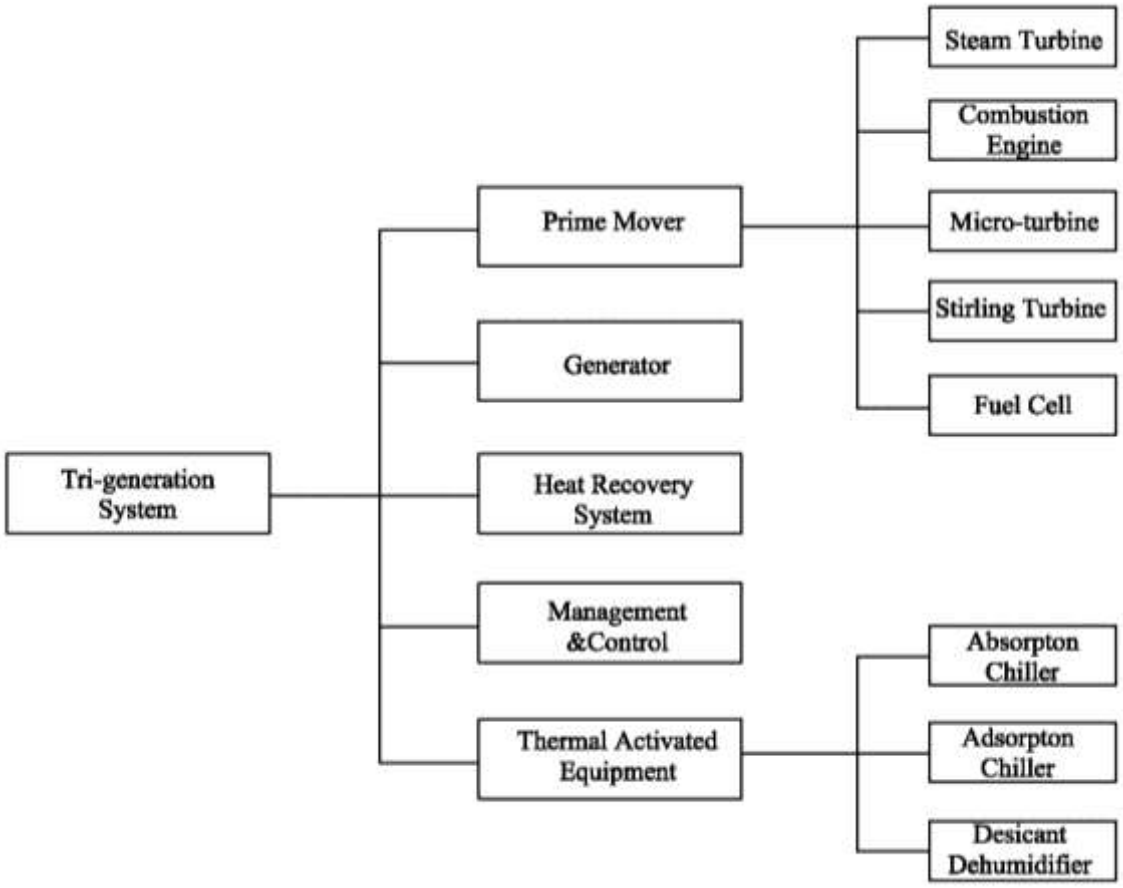

Fig. 2.1 Construction units of tri-generation system

In terms of system rating, tri-generation systems are categorized into large-scale, medium-scale, small-scale and micro-tri-generation systems, ranging from 10MW and above, 1-10MW, 20kW-1MW and under 20kW [26]. Some examples of these tri-generation systems are summarized in Table 2.1 for detailed information.

Fig. 2.2 shows the schematic diagram of a typical micro tri-generation system [27] which is comprised of an internal combustion gas engine coupled with an adsorption chiller.

According to the functions performed, the whole system is divided into the following units: heat and power generation unit (gas engine/generator set), cooling unit (adsorption chiller), domestic hot water supply unit (water tank), and floor heating unit (plate HE). The engine is powered by fuels and mechanically connected to the electrical generator through a shaft, which transfers mechanical energy into electricity which can then be supplied to the end users or feed back to the power grid. At the same time, jacket water exchanges heat from the exhaust gas via a heat recovery unit before it is fed into an adsorption chiller for cooling applications. Some hot water coming from the heat recovery unit is delivered into the plate heat exchanger for space heating or is stored into the insulated water tank for storing domestic hot water.

Under its rated power operation, the system electrical efficiency is 21.4%, heat recovered from the exhaust gases and from the cylinder jacket cooling are 13.6 kW (24.3%) and 14.4 kW (25.7%), respectively. It can be seen this system functions to produce the energy required but suffers from low system efficiency, without an electrical energy storage unit.

B Improved tri-generation system

Tri-generation or CCHP [26, 28] technology, as a popular research topic, ranges from large-scale tri-generation in power plants to small-scale generation in stand-alone domestic applications [29, 30]. Recently, new technologies have been developed with the main objectives of improving their system performance and energy efficiency. Other research employed highly efficient components, for instance, micro gas turbines [31], fuel cells [30], or PV cells as the prime mover. Additionally, a variety of developments have been attempted to integrate biomass [32, 33], solar sources [34-40] or hydrogen [41] into tri-generation.

Table 2.1 Technical specification in four specific tri-generation systems

Size	Example	Specification
Large-scale systems (above 10MW)	Tri-generation plant at the University of Illinois at Chicago [26]	Two units of 6.3MW Cooper-Bessemer dual-fuel reciprocating engine generators; Two units of 3.8MW Wart-sila 18V-28SG gas reciprocating engine generators; A 3.5MW Trane two-stage absorption chiller; Two units of 7MW York International electrical centrifugal chillers; Several remote building absorption chillers activated by the hot water loop (4.7MW maximum cooling capacity).
Medium-scale systems (1– 10MW)	The system in the Domain Plant of Austin [42-44]	A gas-based combustion turbine and generator for electricity demands (4.6MW 28.6% electricity efficiency); A two-stage indirect-fired absorption chiller for cooling and heating (8918 kW of cooling power).
Small-scale systems (20 kW– 1MW)	Tri-generation at the University of Maryland [45]	A micro-turbine/generator (60 kW electricity at 90 k rpm and exhausts flue gas at 310 1C after recuperation, 26.9% electricity efficiency); A single absorption chiller (65 kW of cooling power at the COP of 0.65); RTU (316 kW direct expansion electric rooftop cooling units); Solid desiccant dehumidifier system.
Micro systems (under 20 kW)	Tri-generation system at Shanghai Jiao tong University [26, 46]	A 12 kW gas-fired reciprocating engine (21.4% electricity efficiency); A 10 kW adsorption chiller (0.3-0.4 COP at 65-95ºC) & a cooling water tower; A floor radiate heating system & a hot water tank; A waste heat recovery.

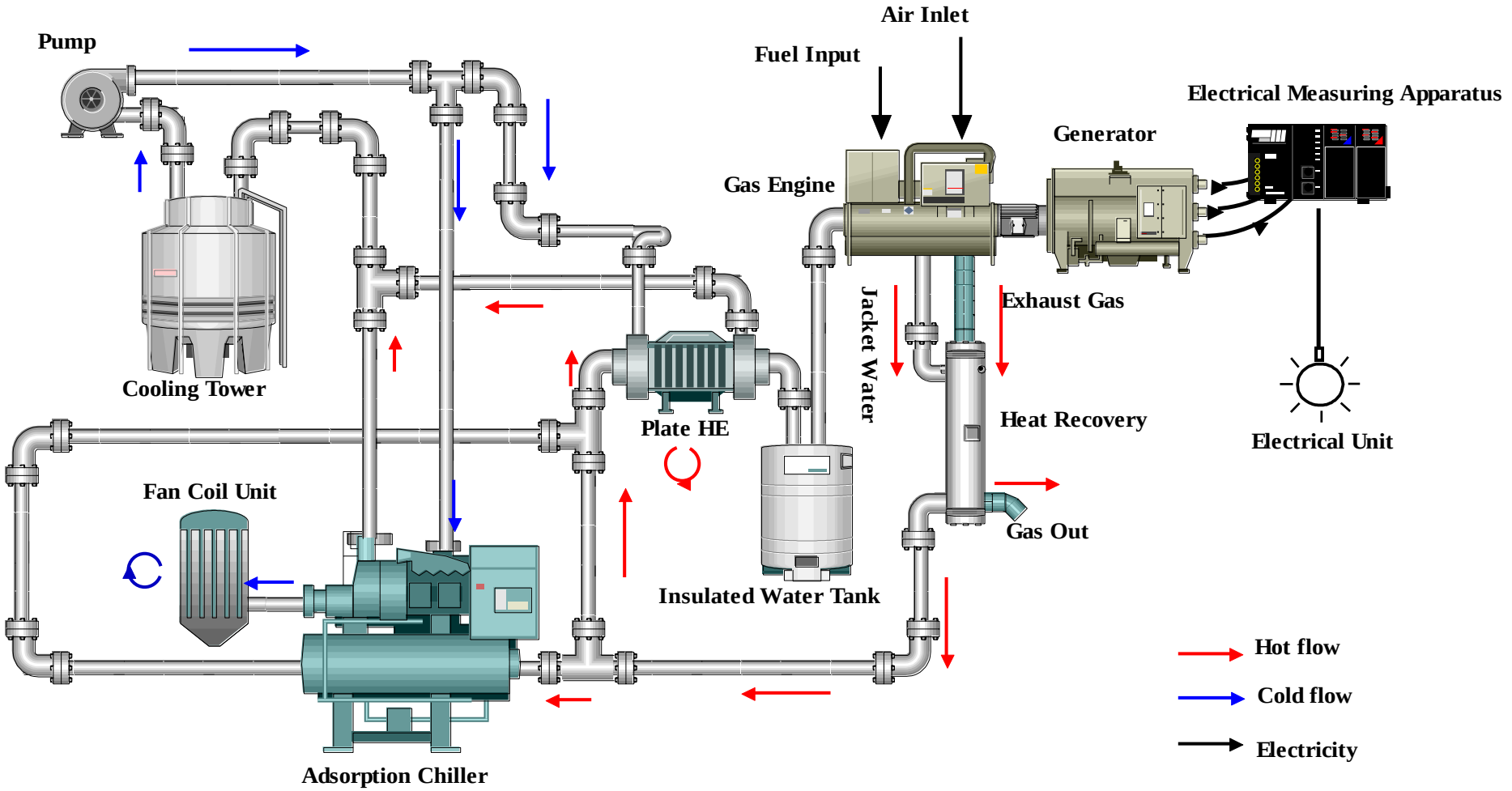

Fig. 2.2 Facility layout of a micro tri-generation system[27]

C Bio-tri-generation

Bio-fuels are a renewable and sustainable type of fuel which can be utilised to power engines and in turn to generate power to the supply. In the literature, there are a limited number of publications available to cover this topic.

Parise et al. [47] and Galvao et al. [33] have developed a bio-tri-generation model for simulation purposes. They considered and discussed several important aspects of using a tri-generation system, including energy consumption, CO_2 emission and system efficiency.

Parise et al. [47] studied a tri-generation system fired by bio-fuel, which employed a heat engine and a vapour compression chiller, along with a boiler as an auxiliary thermal device. This system could produce 1.5 kW of electrical power, 19.6 kW heating, and 9.1 kW cooling power at maximum capacity. Clearly, this system has a large heating power output and was preferred in applications with relatively large heating demands. The outcomes from the calculations illustrated that total energy consumption was considerably reduced (by as much as 50%) and CO_2 emission decreased 95%, as compared with a conventionally fuelled tri-generation system of the same size.

Galvao et al. [33] carried out a study on bio-tri-generation and compared two kinds of biomass (wood chips and pellets) in a practical tri-generation system used in a hotel. In this case, a general heat engine, thermal processor and an alternator equipped with PV panels as supplement were developed and validated. The electrical requirements for the tri-generation energy system were a maximum power of 26.3 kW per day and a maximum energy of 318 kWh per month. This investigation verified that this tri-generation system has an overall efficiency of 75% and consumed approximately 720 kg wood chips per day or 529.3 kg wood pellets per day to provide electrical power of 20 kW and thermal power of 87.8 kW.

D Hybrid tri-generation

In household environments, it would be ideal to utilise other new or renewable sources [35, 36, 38-40] available to the end users along with the tri-generation systems. Various hybrid types of tri-generation systems have been proposed to include renewable energies (solar, wind, geothermal energy etc). Immovilli et al. [35] compared solar based tri-generation systems in terms of electrical efficiency, coefficient of performance (COP) and cooling power density. In this paper, solar as a primary energy source was utilised both for thermal and electrical purposes. Six categories of cooling technologies for tri-generation were

discussed in this paper, followed by a comparison of three types of thermal solar panels, including flat plate solar collectors, evacuated collectors and concentrators. Solar based tri-generations with different combinations were studied in detail. Simultaneously generated cooling energy was taken into account. Among these different combinations, solar tri-generation consisting of photovoltaic (PV) panels and vapour combustion (VC) cooling was determined to be a superior option due to its compactness, simplicity and reliability.

Furthermore, Carmeli et al [36] proposed a hybrid distributed system, in which a PV source with a conventional CHP were employed to improve the system's thermal and electricity efficiency. In this study, PV arrays were used as electricity supplement and were integrated into an internal combustion engine equipped CHP with two operation options. This system can provide a nominal 15.2 kW of electrical power and 30 kW of thermal power.

With the development of solar collection technologies [37] and cost reduction due to mass production, PV technologies have been commercially successful.

Overall, hybrid tri-generation may provide much promise to cut down the carbon emissions as well as to make tri-generation commercially viable. However, drawbacks are generally associated with high capital costs and some similar technical challenges to optimise the system configuration and performance.

2.3.2 **Micro-tri-generation systems**

Micro-scale tri-generation systems refer to those tri-generation systems with a capacity of less than 20kW and are typically used for domestic applications.

A Energy cascading utilization and energy saving

Fig. 2.3 shows a simple calculation of prime energy utilisation based on traditional energy supply mode and a typical tri-generation mode. Some assumptions are made based on empirical data including 33% for electrical efficiency, 85% for heating efficiency of a boiler, and electrical air-conditioner with COP 4 in a traditional mode. It is obvious that energy cascading utilization facilitates the energy savings in a micro tri-generation system. For example, a tri-generation system requires 100 units of prime energy to provide energy needs, including 33 units of electric power, 40 units of cooling power and 15 units of heating power for a typical summer day [22, 26]. In contrast, the consumption is 148 units in a traditional energy supply model with 33 units of electricity, followed by 34 units of cogenerated waste

heat utilised to obtain 40 units of cooling power with COP of 1.2. Another 18 units of waste heat can be recovered to provide 15 units of heating to domestic water at efficiency of 85%.

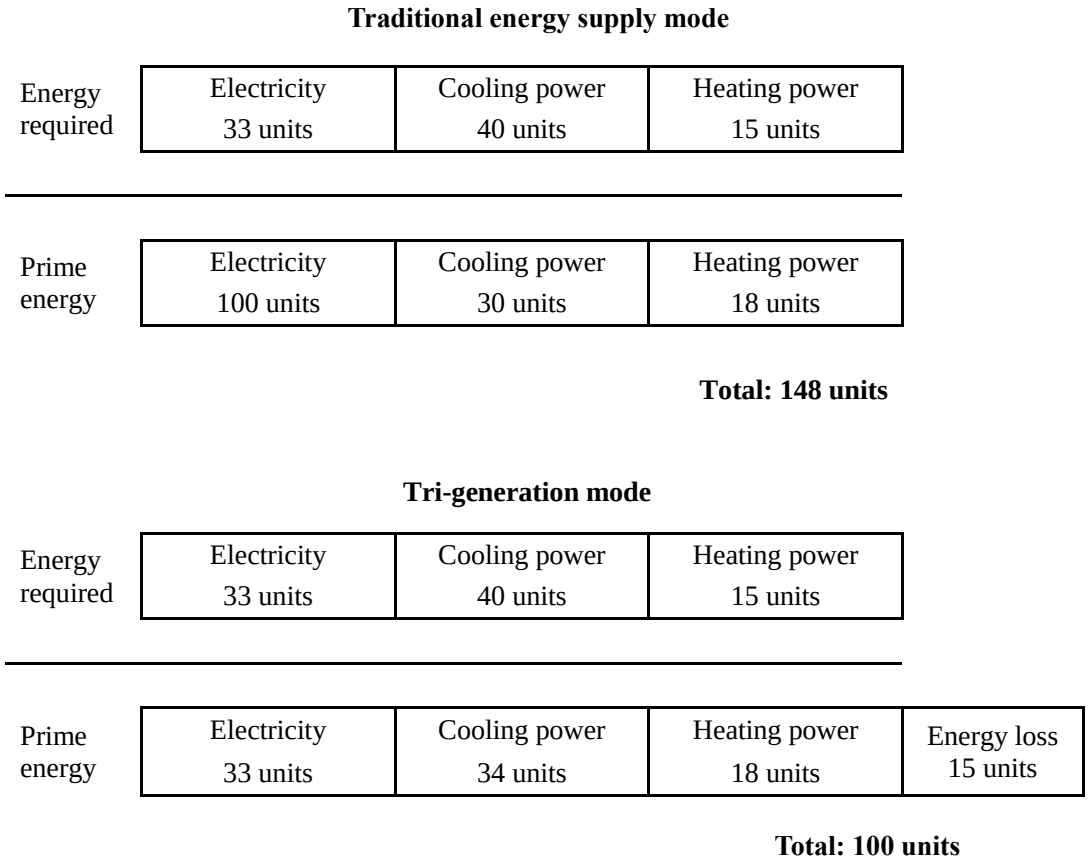

Fig. 2.3 Prime energy consumption comparison between traditional energy supply mode and tri-generation system [26]

B Cost-effectiveness and economic efficiency

A key issue for developing any commercial product is the capital and operational cost. The micro tri-generation systems are no exception. Huangfu, et al. [22] analysed a typical micro-tri-generation system in detail with an economic evaluation for a traditional electricity power mode and a tri-generation mode. This micro-tri-generation system can supply 12 kW electricity and 28 kW heating load and 9 kW cooling power to the load. The economic evaluation shows that this micro-tri-generation system has a good economic efficiency with a payback period of approximately 3 years based on the then energy price. This should be commercially appealing to potential customers. Similar conclusions had also been drawn by other researchers in this field [22, 48, 49].

C Environmental impacts and greenhouse gas emission reduction

A primary aim of developing tri-generation technologies is to reduce greenhouse gas emissions by using different prime movers such as fuel cells and micro-turbines. Although the fossil fuel-based centralised power plants release a large quantity of CO_2 and NOx, some smaller tri-generation systems connected with certain prime movers may emit more greenhouse gases per kW electricity generated. Therefore, it would be advantageous in the meantime to promote energy efficiency of tri-generation systems while still meeting the same energy demand requirements with reduced emissions.

2.4 Energy management strategies and operational algorithms for tri-generation

2.4.1 Energy management strategies and performance indicators

The operational strategy of a tri-generation system is key to the efficient operation, depending largely on the specific goals the designers and users want to achieve. Furthermore, optimisation techniques are the route to meet these goals. Commonly, the optimisation criteria are: (1) reduction of operational cost (OC), (2) primary energy consumption (PEC), (3) carbon dioxide emissions (CDE) and (4) a combination of the above listed criteria [24, 49-61].

However, the optimal energy management strategy of tri-generation systems calls for complex mathematic algorithms and experimental justification. In the literature, the majority of these strategies are operated in two basic ways: following the electric load (FEL) and following the thermal load (FTL) [48, 50, 53, 60, 61]. In the case of the FEL operation strategy, the prime mover is primarily operated to satisfy the electric demand in the application. For the FTL strategy, the prime mover is controlled to ensure the recovered waste heat will be adequate to meet heating and cooling requirements.

2.4.2 The application of optimisation algorithms

As a promising technology for efficient and clean provision of energy, tri-generation systems demonstrate vast potential for energy savings and emission reduction. Therefore, significant research attention and investment are directed towards developing efficiency improvement

technologies for tri-generation systems. In order to meet the optimisation criteria, various optimisation algorithms associated with different tri-generation models have been proposed, as tabulated in Table 2.2 and explained as follows.

Table 2.2 Optimisation algorithms for tri-generation systems

Algorithm	Optimisation objective
Genetic algorithm	Minimising operational costs or emission
Multi-objective evolutionary algorithm	Exergetic efficiency, total levelised cost rate of the system product, the cost rate of environmental impact
Decomposition technology	Cost-efficient operation
Lagrangian relaxation	Minimising annual costs
Optimal energy dispatch algorithm	Minimising operational costs, PEC, or CDE
The particle swarm optimization algorithm	Minimizing costs
Fuzzy multi-criteria decision-making	Energy saving potential, carbon dioxide emission reduction and annual total cost savings

A Genetic algorithm

The genetic algorithm (GA) is an optimisation technique based on natural genetics. Researchers including Sakawa and Ahmadi [62, 63] applied it to search operational variables in the tri-generation operation aiming to achieve an optimum overall design and to minimise the operating costs and emissions simultaneously.

B Multiple-objective evolutionary algorithm

The evolutionary algorithm was employed by Burer et al [64-66] to solve the thermoenvironomic or exergoeconomic optimisation in the tri-generation systems. Thermoenvironomic or exergoeconomic criteria are used to evaluate the thermal efficiency for the purpose of improving the design of energy systems and reducing the impact on the environment.

C Decomposition technology

Successful application of decomposition technology requires the modelling of the tri-generation system and then operational tri-generation algorithms are developed. Lahdelma, Rong and Makkonen [67-69] adopted decomposition technology to deal with tri-generation problems in which they built up the system models as linear programming (LP) models and

decomposed the tri-generation system into a large number of hourly models. LP models can be solved independently without influence of dynamic dependence between different hourly models.

D Lagrangian relaxation

Rong et al [70] proposed a Lagrangian relaxation based algorithm to analyse a tri-generation system where a storage system was integrated into the tri-generation system and, therefore, some dynamic factors relating to energy storage system performance were taken into account as the system model was constructed.

E Optimal energy dispatch algorithm

Cho et al employed an optimal energy dispatch algorithm to identify an optimal operating mode for the specific CCHP system in the most economical manner. They built up a linear programming model after outlining an energy flow chart with various efficiency limitations with an aim to minimise an objective function based on the operational cost, primary energy consumption (PEC), and carbon dioxide emission (CDE) [71].

F Particle swarm and fuzzy logic algorithms

Other optimization algorithms, such as the particle swarm optimisation algorithm [72] and fuzzy multi-criteria algorithm [73] were also proposed for the analysis and optimisation of tri-generation economic solutions.

Overall, all the algorithms have their own merits and shortcomings. There does not exist a best algorithm for all optimisation situations. It is always a matter of balance to strike between convergence, efficiency and computational time.

2.5 Electric energy storage system

2.5.1 Relationship between electric energy storage system and tri-generation optimisation

From previous discussions, an energy storage system is of critical importance to be added in tri-generation systems in order to improve energy efficiency and to meet the complexity of load requirements. The energy storage can serve the four following functions:

- An electrical energy storage system in the tri-generation system would help to achieve energy efficient operation of the prime mover so that wasted generation is minimised.

- Under the operation of the FTL energy management strategy, an electrical energy storage system could meet the transient changes in demand to best match the load.

- Auxiliary electrical energy storage devices could facilitate supplying complicated fluctuations of electric load domestically.

- An energy storage system makes it possible for optimisation strategies to be exerted to manage the power distribution within the tri-generation system.

First of all, implementation of an electric energy storage subsystem is the prerequisite of efficient operation of prime movers. Huangfu et al [22] pointed out that the electricity efficiency is the most influential factor in improving the primary energy ratio (PER) for high efficiency and regulation performance where the PER is a common evaluation indicator of micro-tri-generation efficiency. They further suggested that the efficiency reaches a high level and varies slightly when the electricity output is greater than half load. Therefore, for better energy utilisation, the prime mover should be operated with an electrical output of greater than half load. When generated electricity is not used, it should be stored in an auxiliary electric energy storage system or fed back to the power grid.

Secondly, the preferable energy management strategy (e.g. FTL), requires specific equipment for storage of electricity. Mago et al [53] studied the performance of Tri-generation and CHP systems operating under both FEL and FTL, based on primary energy consumption, operational costs, and CO_2 emissions for different climate conditions. Their results show that FTL is the preferred energy management strategy over FEL.

However, with the following thermal load method, the prime mover is controlled to generate heating or cooling power to meet the thermal demands from the load. As a result, generation of electrical power cannot perfectly match electrical loads. Thus, extra electricity should be stored into the electric energy storage devices or supplied from them, depending on the mismatch of the supply and the load.

Clearly, the electric energy storage system can accommodate the complicated demand changes in a tri-generation application. Compared to the thermal load in tri-generation, the

FEL requirement is comparatively complicated, which can be observed from fluctuating daily household electricity demands. In this case, there are obvious differences between peak and off-peak power demands. Additionally, the fluctuation of electrical demands varies instantly, making the stand-alone generator difficult to adapt to these changes. Auxiliary electric power sources in the loop can shave the peak and fill the trough of electric demands.

Moreover, the electricity profile is changeable under different optimisation strategies from FEL to FTL. Thus, the electric energy storage system can be regarded as a favourable solution to adapt to different electricity requirements. Miguez [23] integrated an electric energy storage system into a tri-generation system to improve its performance. In that case, batteries were employed as an electricity energy storage device to assist the tri-generation operation.

Obviously, an electric energy storage system is indispensable for the tri-generation system if its performance and efficiency are to be improved. But how to select appropriate electric storage devices and to coordinate the energy distribution within the tri-generation system will be the next question to ask. Accordingly, relevant investigations will be presented in the following section.

2.5.2 **Electric energy storage technologies**

The basic function of an energy system is to generate sufficient electricity to meet demands at acceptable prices and to do so with a clean, safe and reliable source of energy [73]. Electric energy storage is regarded as a crucial factor associated with reliable and reasonable use of primary electric sources. It can be described as a process that can store electricity by diverse means and convert it back to electricity when needed. In general, energy storage can be employed in various applications [74, 75], such as generation-based applications, transmission and distribution, energy services, and renewable energy applications. Electric energy storage systems can be categorised in terms of their forms and functions. Firstly, there are four different forms of energy which can be stored, namely, electrical, mechanical, chemical energy, and thermal energy storage, as illustrated in Fig. 2.4. Each form of storage has different features. For instance, the technology of super capacitors is largely dependent on the development of optimised electrode materials and electrolytes whilst the lithium-ion batteries depends on materials science to deliver new electrodes and electrolytes [76].

Secondly, they can function primarily for improving power quality/reliability, and energy management. Taking super-capacitors for example, they are activated in a fraction of a second to ensure a reliable response to the demand change in the system. On the other hand, energy storage devices such as fuel cells or sodium-sulphur (Nas) batteries are better suited to energy management [73, 77, 78].

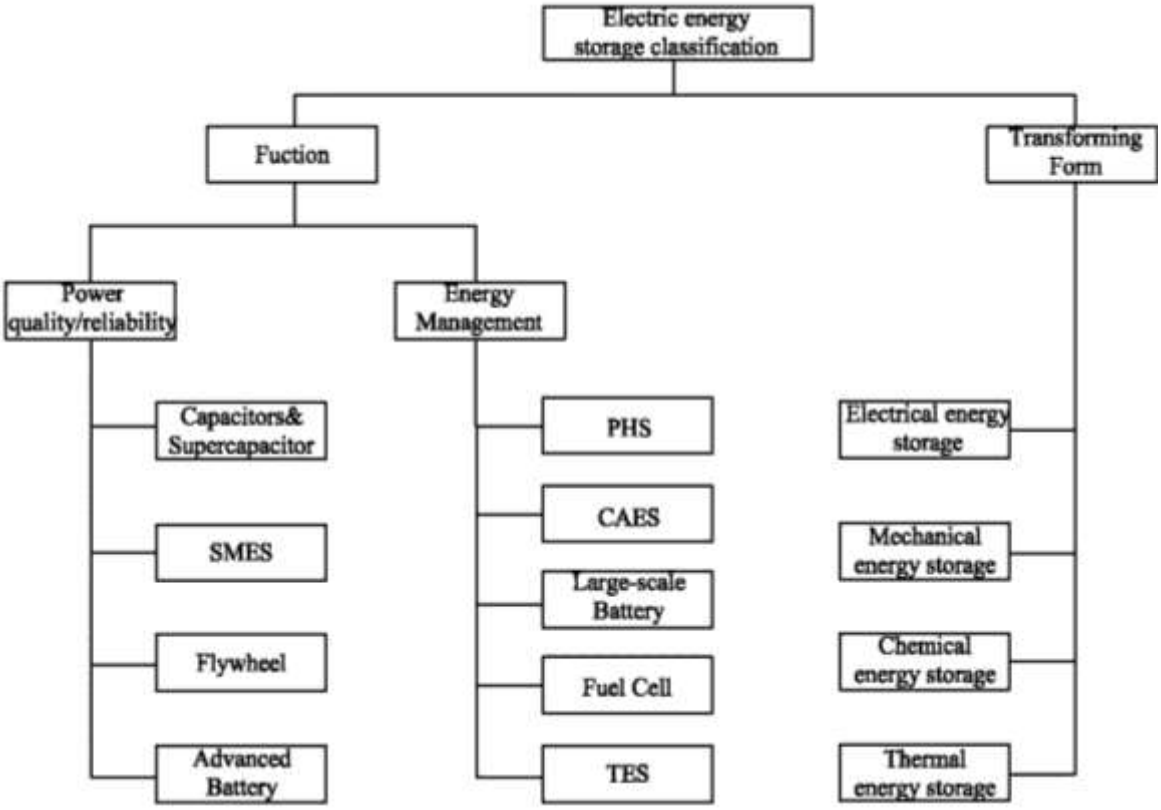

Fig.2.4 Classification of electric energy storage system [73-81]

Recently, the use of hydrogen storage has received much attention but the novel hydrogen storage systems require extremely demanding properties and low heat loss during normal operations [79]. As the only commercially-proven large-scale electric energy storage technology, pumped hydraulic energy storage systems have gained in popularity especially as they can be incorporated with variable renewable generation such as wind energy technology [80].

In the literature, a wide range of investigations has been carried out by researchers to understand the technological characteristics, application environments and energy storage capacity of different systems [73-81]. In order to achieve optimal system operation in this

study, specifications of the storage devices needed to be studied thoroughly, prior to a decision being made on device selection.

A Batteries storage technology

Rechargeable batteries are a traditional energy storage device associated with electrochemical reactions to store electricity. These types of reaction are reversible, allowing the batteries to be recharged through current generated by electrochemical reaction between two electrodes. Generally, the most popular devices in this category include lead acid batteries, nickel cadmium batteries, sodium sulphur (NaS), sodium nickel chloride, and lithium ion batteries. Some of them can be employed in energy management and usual candidates are lead-acid and nickel cadmium batteries. Other have superior power capability and are more suitable for applications where power quality and peak shavings are of importance. For example, the sodium sulphur battery has a power density of 150-230w/kg with the capability of pulse power of 6 times over their rating [73]. The sodium nickel chloride battery is a new type of battery. The power version has been applied to hybrid electric vehicles while the high energy version is used for storing renewable energy and levelling loads in industry. Very high efficiency (almost 100%) and relatively high cycle life (10,000 cycles) makes the lithium ion battery the promising branch in the battery family [73, 75, 82]. Despite high costs, it is widely employed in portable electrical and electronic devices. Table 2.3 shows the pros and cons of typical batteries for comparison.

Clearly, batteries have widely proliferated into various electricity storage systems. Meanwhile, technology improvement in terms of cost reduction, lifetime increase as well as reduction of flammability will contribute to the promotion of batteries in a plethora of applications.

Table 2.3 Various types of batteries comparison [73,75,82]

Types	Advantages	Drawbacks
Lead-acid batteries	Mature technology; High energy efficiency; (85%-90%) Low level of maintenance and investment cost; Very low self-discharge rates(2% per month)	Low cycle life and operational lifetime Be affected by depth of discharge and temperature
Nickel-based batteries:	Superior operational life and cycle life(1500-3000) Higher energy densities than lead-acid one(50Wh/kg – 80Wh/kg)	10 times than lead-acid Lower energy efficiency Inferior self-discharge rate(10% per month)
Lithium-based batteries (lithium-ion &lithium-polymer)	Higher energy density(100Wh/kg – 150 Wh/kg) Energy efficiency (90%-100%) Lower self-discharge rate(maximum 5% per month) Extremely low maintenance High power density(500W/kg-2000W/kg)	High cost
Sodium sulphur (NaS) battery	High power density High energy efficiency (89-92%)	Highly operating temperature/ highly corrosive nature of sodium

B Flow battery

Flow battery is an emerging technology based on reversible electrochemical reactions. Unlike conventional batteries, flow batteries have the capability of fully discharging without any damage, and they exhibit very low self-discharge. The electrolytes are stored in separate sealed tanks. Flow batteries therefore are a long life and low maintenance system that allows energy storage over a long period of time.

There are three commercially available flow batteries: vanadium redox battery (VRB), zinc bromine battery (ZBB) and polysulphide bromide battery (PSB). Since their operation is based on reduction and oxidation reactions of the electrolyte solutions, they are also called redox flow batteries [83].

C Fuel cells

Fuel cells are regarded as a promising renewable energy device with immense popularity due to their clean, easily scalable and zero self-discharge characteristics [84]. Similar to batteries, fuel cells are also commonly used as electric energy facilities associated with electrochemical conversion approaches. However, unlike batteries, fuel cells exhibit both high energy and high peak power capabilities. There are five main types of fuel cells available: hydrogen fuel cell, proton exchange membrane fuel cell (PEMFC), solid oxide fuel cells, metal-air battery and molten carbonate fuel cells (MCFC). Among them, the PEMFC is a commonly used device in practice and its development is closely associated with hydrogen storage and electrolyser progress.

D Flywheel storage technology

The flywheel storage system stores kinetic energy by means of electromechanical conversion [74, 75]. Energy is delivered by the rotational part of the system. During the charging period, the flywheel is spun up by a motor; during the discharging period, the same device acts as a generator producing electricity from the rotational energy of the flywheel. The flywheel storage system has some prominent advantages such as high efficiency and long cycling life. However, the drawbacks of this technology include relatively short storage duration, high standing loss, as well as high self-discharge (at least loss of 20% per hour). The applications of flywheels are principally on high power/short duration applications [75]. The most common application is to be utilised as a power quality device that is incorporated with stand-by generators. The flywheels can also be integrated with renewable energy source

power plants (e.g. photovoltaic cells or wind turbines), used for power-quality-sensitive customers such as communication facilities and computer serve centres.

E Super capacitor storage technology

Super capacitors (or ultra-capacitors) are technologically promising devices for electricalenergy storage. They generally have high surface areas along with a molecule-thin layer of electrolyte as the dielectric to separate charges. The super-capacitor resembles a regular capacitor except that it offers very high capacitance in a small package.

Super-capacitors can be categorised into electrochemical double layer super-capacitors (ECDL), pseudo-capacitors, and hybrid capacitors according to their electrodes used. The ECDL super-capacitors are currently the least costly to manufacture and are the widespread type of super-capacitors.

Super capacitors can have extremely high power density (up to 10kW/kg) but low energy density (2-5Wh/kg). Therefore, they are mainly adopted in power quality applications such as ride-through, bridging, and energy recovery in mass transit systems [73, 85, 86]. Other features, such as long life (50,000-100,000 cycles), high efficiency (90% and above) make this technology a promising storage candidate [85, 86].

F Superconducting magnetic energy storage (SMES)

The SMES stores energy in a magnetic field supplied by DC current through a large superconducting coil at cryogenic temperature [87-89]. Higher energy density is available with superconducting technology (40 MJ/m) than that of flywheels and conventional batteries. Besides, SMES systems have very high energy efficiency of over 90%. SMES can reach its rated power within a very short period (200kW within 20ms). In addition, SMES systems have a very long cycle life of tens of thousands of cycles. Despite the advantages of this technology, SMES has limited applications due to its high costs. The capital cost may vary between 1000 and 10,000$/kW. Besides, cooling is a very strict requirement in applications in order to keep superconductor coils in a cryogenic state rendering its applicability questionable.

G Cryogenic energy storage (CES)

CES is a relatively new electricity energy storage system. The CES stores energy by gas liquefaction as a cryogen (e.g. liquid nitrogen -196°) using electricity and then releases energy through a boiling liquid by cryogenic heat engine. The operational principle of such a technology is shown in Fig. 2.5. CES has a relatively high energy density (100-200 Wh/ kg), and a relatively long storage period. One additional benefit is that it produces less greenhouse gas in solid form (dry ice) which is easy to capture and process. However, CES has a relatively low efficiency (40-50%) and the technology is still under developed [74].

H Pumped hydroelectric storage technology (PHS)

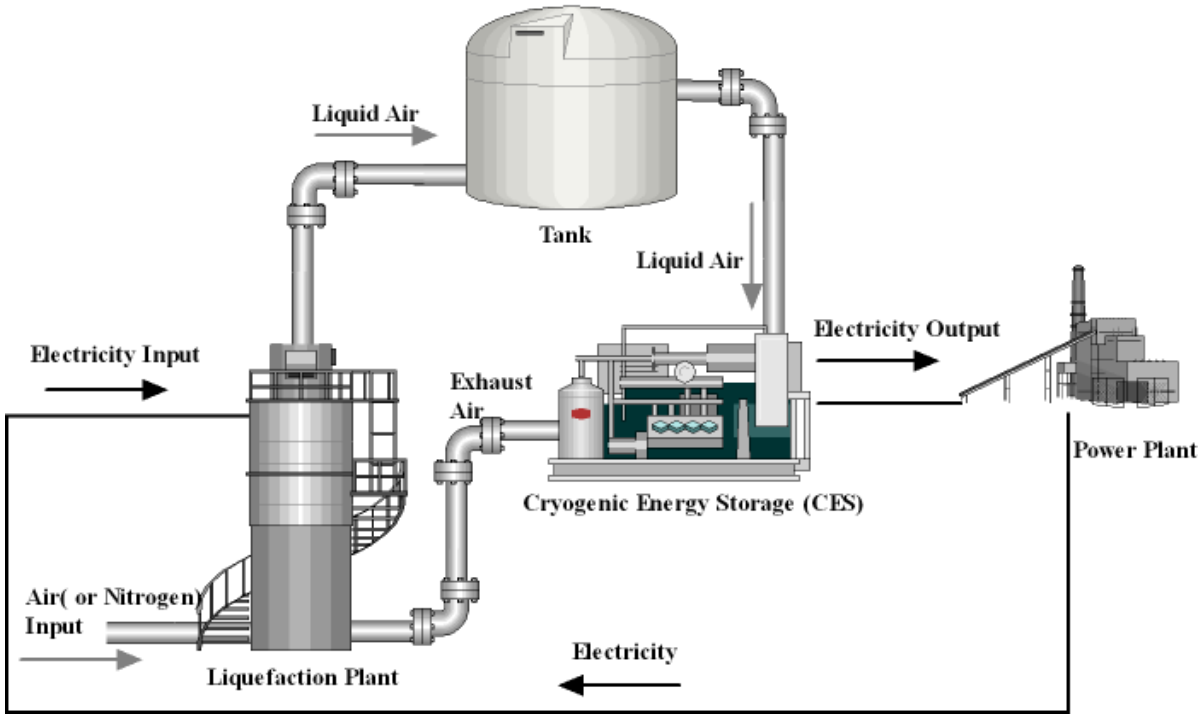

Fig.2.5 Schematic diagram of cryogenic electricity storage system [74]

PHS is a mature storage technology and the only commercially proven large-scale (>100MW) energy storage technology with over 300 plants installed worldwide and a total installed capacity of over 95GW [80]. The PHS is applied in energy management due to its mass capacity of energy storage in mechanical energy form. This technology exploits the hydraulic potential energy of two reservoirs at different elevations to store and produce electricity by reversible turbine/pump. In the case of low electricity demands, excessive

electricity is stored in the form of potential energy. Turbine pumps propel the water into the high reservoir. On the other hand, water is released back into the low reservoir through a turbine which generates electricity to satisfy the peak electricity demands. Overall, PHS plays the dominant role in energy management applications due to the technological maturity, long-term storage and long cycling life.

However, the high initial capital cost, relatively low energy density as well as its geographic dependence are obstacles limiting the wide adoption of PHS technology.

I Compressed air energy storage technology (CAES)

Similar to the PHS technology, CAES is large-scale electrical storage technology in energy management applications. It stores the electricity in the form of elastic potential energy of compressed air [74]. Typically the output power of CAES systems is in the range of 50-300MW. Preferable merits include long life time (40 years) and long storage duration, low self-discharge and high efficiency (71%) [83]. The major barrier for CAES implementation is its geographic reliance.

The analysis has given a brief introduction to the diverse electrical energy storage technologies. Their main characteristics have been summarised in Table 2.4.

2.5.3 Hybrid electric energy storage

As mentioned before, different electric storage devices have different applications. Super capacitors, SMES, flywheels and batteries can be used as the power quality and reliability in electric systems thanks to their superior kinetic properties. Meanwhile, in energy management applications, energy devices with favourable energy capacities, such as PHS, CAES, large-scale batteries, Fuel cell and CES, can function properly. Meanwhile, the basis of an energy system is the capacity of this system to generate sufficient energy to meet demand. Therefore, electric energy storage has always been a challenge since these applications require energy storage devices to supply ranging from fractions of a second in high power applications to hours in high energy applications [73, 77, 78]. However, some specific situations require electricity energy storage systems that can accommodate bothhigh-level power and energy demands. A combination of devices with high-level power properties

Table 2.4 Electric energy storage technologies

Name	Classification	Characteristic
Capacitor/super capacitor [73, 85, 86]	Power quality/ electric energy storage	Low energy density & high power density Short duty duration & high self-charge ratio Transient charge/discharge period High efficiency & long life Developed technology
Flywheel [74, 75]	Power quality/ mechanical energy storage	Long cycling life & high efficiency High power & short duration Developed technology
Battery	Power quality/reliability & energy management/ chemical energy storage	Multi-types Low standby losses & high energy efficiency Short cycle life/ limited discharge capability Mature technology
Superconducting magnetic [87-89]	Power quality/reliability	High energy density Prompt response Long cycle life & high energy efficiencies High cost
Pumped hydroelectric storage (PHS)	Energy management/ Mechanical energy storage	Mature technology, large-scale Long-term discharge time & long-term storage duration & long cycle life Low-range capital cost per KWh High efficiency & relatively low energy density Dominant EES system
Compressed air energy storage (CAES)	Energy management/ Mechanical energy storage	Developed technology Long-term discharge time & long storage period Low-range capital cost per KWh High efficiency & medium energy density Rapid commercial development
Fuel cell [50, 82, 85]	Energy management/ chemical energy storage	Clean technology & long storage period Fast response/non self-discharge High energy density (0.6- 1.2kWh/kg) Low efficiency (20-50%) & high cost ($6-20/kWh)

		Developing technology
Cryogenic energy storage	Energy management/ Thermal energy storage	Developing technologies Medium-storage period Low-range capital cost per KWh Low efficiency & medium energy density Long cycle life

and devices with superior energy capacities can be incorporated to satisfy the complex load scenario. Hybrid electric energy systems are seen increasingly such as combined flywheels and wind turbines, integration of fuel cells and batteries, amalgamation of super-capacitors, fuel cells and batteries. How to validate a hybrid electric energy storage system relies on a systematic consideration to include power density, energy capacity, cost, cycle lifetime and energy efficiency as well as technology maturity.

Among all these electric energy storage technologies, super-capacitors provide much promise in high power density applications, which is a few orders of magnitude higher than the power density achieved with batteries. Besides, they have preferable features including several million full charge-discharge cycles and deep discharge capacity [85] and thus were selected in this study as an energy storage device.

However, due to their low energy density, this high amount of power will only be available for a very short duration. Furthermore, cost is a main barrier constraining super capacitors from commercial applications. Fortunately, these drawbacks can be compensated by the use of batteries. Especially lead-acid batteries, as a mature electric energy storage technology, possess very high energy density and can be used in combination with super-capacitors. Other energy storage methods such as micro pumped hydro, compressed air, or flywheel are not economical at the small scales this research is concerned with.

In the literature, research on dynamic response has been reported on different experimental benches [85, 86, 90-92]. From the current perspective, the application of hybrid energy systems can be found in use in hybrid electric vehicles, power quality regulation, and regenerative braking for energy recovery. However, research on the integration of hybrid energy storage system into tri-generation is hardly reported.

In this research, because domestic electricity demands have a complicated profile, the energy system should feature fast response in a short period and long-term energy supplying capability. As a result, a combination of batteries and super-capacitors is an appropriate option because of their output characteristics, size, capital and operational costs, for the targeted domestic applications.

2.6 **Dymola simulation environment**

Before a physical system is set up, computational simulations for predicting system performance and validating the feasibility of the system should be employed. This involves developing analytical models for simulation. In this study, the software "Dymola" was selected. Dymola refers to "dynamic modelling laboratory" which employs hierarchical model composition. Components and connectors are reusable. Model libraries include diverse physical systems such as mechanical, electrical, thermodynamic, hydraulic, pneumatic, thermal and control system. Based on the Modelica language, Dymola features an object-oriented approach and performs multi-domain modelling simultaneously, and is regarded as a powerful tool appropriate for multidisciplinary applications [93, 94].

Its features include:

• Handling of large, complex multi-engineering models.

• Faster modelling by graphical model composition.

• Open for user defined model components.

• Open interface to other programs, such as Matlab.

• Plotting and 3D Animation.

• Real-time simulation.

Dymola can also import data in other forms including graphics files. Furthermore, Dymola contains a symbolic translator generating *C* code for simulation making Dymola compatible with Matlab/Simulink. Scripts can be used to manage experiments and to perform calculations.

2.7 **Summary**

This chapter reviewed tri-generation technologies in terms of their type, configuration, advantages and drawbacks. The analysis of different technologies demonstrated that integrating auxiliary storage units into the tri-generation system was necessary and can improve system performance and energy efficiency. Therefore, electrical energy storage

technologies have been investigated following the discussion of general energy management strategies and control algorithms in the applications.

Hybrid electrical energy storage technologies can employ various components for specific applications. A combination of super-capacitors with batteries was chosen in this study which provides both power and energy benefits due to high power capability of super-capacitors. This study uses these technologies in the bio- tri-generation systems. The integration of a hybrid electrical energy storage system into tri-generation system provides much promise in reducing the CO_2 emissions and increasing the system efficiency. In the last section, the computational simulation tool Dymola was introduced and used to develop computational models for testing the proposed system in simulation before the physical system was built up.

Chapter 3 Preliminary hybrid electrical energy storage (HEES) system

3.1 Introduction

This chapter presents the investigations of the initial experimentation of the HEES. The key aim was to develop a power system to charge/discharge automatically. In order to build up this system, a couple of relevant preliminary experiments had been executed to test the performance of the devices used. The objectives included testing Hall-effect sensors, inverter/charger and super-capacitors. These tests ranged from simple to sophisticated, along with the experimental bench being improved gradually to build up a small-scale, controlled hybrid electric storage and power system, in which electricity can be either stored or be released by hybrid power sources. The control strategy was implemented in a programmable logic controller (PLC) to allow hybrid DC storage sources to be discharged automatically after being fully charged.

In the system, the hybrid power sources consisted of super capacitors and batteries. The load was represented by an AC resistive load (bulb board). A super capacitor module with high power density was connected in parallel to the lead acid battery group as energy devices. Therefore, the small-scale HEES system had both the desired power and energy advantages as proposed. The purpose of this test was to obtain the characteristics of the HEES system.

The test bench of the HEES included: (1) a HCC super capacitor module with 40F/60V; (2) 3 units of lead acid batteries (12V/12Ah for each); (3) inverter/ charger (HBC-3000PVA) ; (4) load bank (up to 600W) ; (5) data detection devices; (6) Controller (Simens S7-200 PLC) and monitoring software *Kingview*.

3.2 HEES system components

3.2.1 Super capacitors

In the preliminary test, a super capacitor module was selected to be one of main components in the energy storage system. This module was constructed with 27 super-capacitors units (2.7 V/1200 F for each) connected in series.

Fig.3.1 (a) Super capacitor module

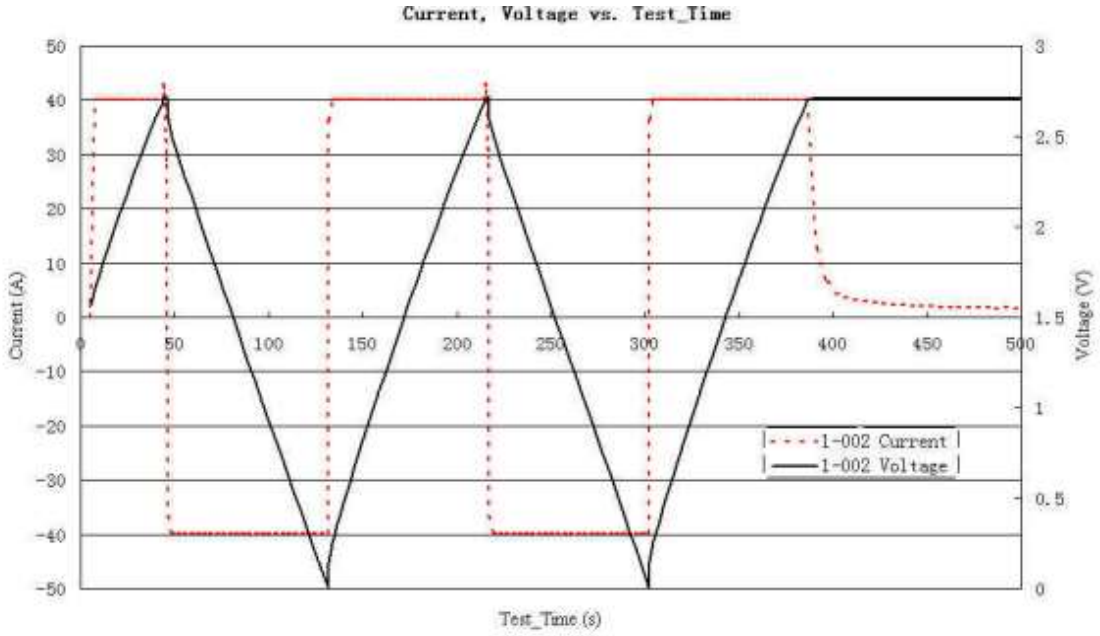

Fig.3.1 (b) Charge/discharge performance

Fig. 3.1 (a) illustrates the layout of this module and Fig. 3.1 (b) demonstrates charge/discharge performance of single super capacitor unit. This test used 40 A DC current to charge/discharge the super capacitor constantly. The voltage increased or decreased in a linear manner. Table 3.1 shows the specifications of the super capacitor unit. From the table, it can be seen that the HCC super capacitor has small internal resistance which results in

current leakage during operation. Meanwhile, the high power density of the super capacitor allows high-level current release transiently and the maximum transient current reached as high as 550 A within 1s for a single unit. Long cycle life is another good characteristic of a super capacitor where it is 500,000 cycles in this case.

Table 3.1 Specification of super capacitor (single unit)

Item	Value	Note
Rated voltage	2.7V	
Surge voltage	2.85V	
Internal Resistance	0.0016 Ω	
Capacitance	1200F	
Energy stored (at V_R) E	4.4kJ (1.2Wh)	$E=1/2CV_R^2$
Nominal current (25ºC)	235A	Discharge to 1/2 V_R within 5S
Maximum current (25ºC)	>550A	Discharge to 1/2 V_R within 1S
Power density	5.1Wh/kg	
Maximum leakage current	8mA	
Operational temperature	-40 ～60 ºC	
Life	90000h(at V_R, 25ºC)	
	1000h (at V_R, 70ºC)	
Cycle life	500,000	
Size	Ø50×110	
Volume	216ml	
Mass	240g	

3.2.2 Batteries

Three units of batteries were selected as the main DC source and were linked together in series, and then coupled with super capacitor module in parallel later in the test as the

Fig. 3.2 Batteries

electrical hybrid sources. Each battery was a 12 V/12 Ah lead-acid used as a common electrical energy storage device by storing/releasing DC power for a backup power supply. The layout of the batteries in series is illustrated in Fig. 3.2.

3.2.3 Load bank

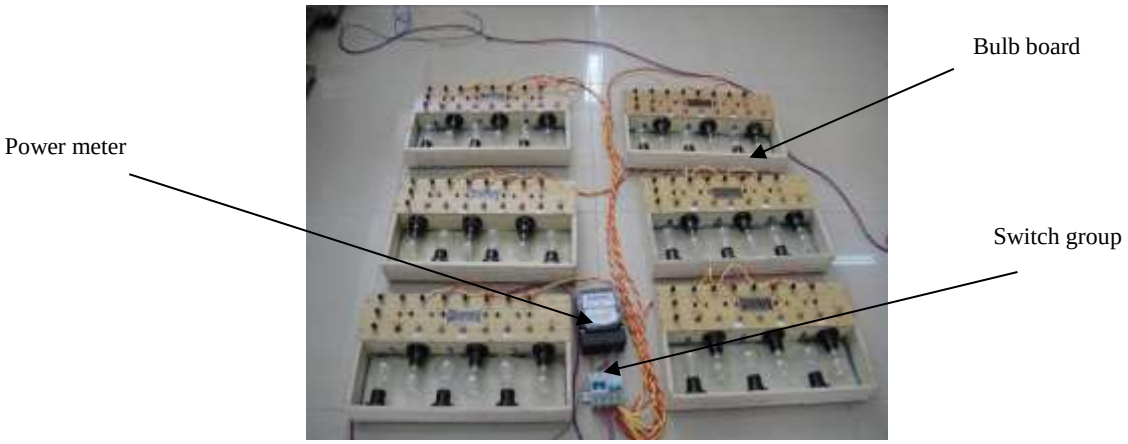

Fig. 3.3 Load bank

The load bank in Fig. 3.3 consisted of 6 groups of bulb boards with 100 W for each. Therefore, the load power could change between 0-600 W according to the demands. The change of power demand was accomplished by switching on and off. The power meter connected with the load bank recorded the real-time power signal for further analysis.

3.2.4 Inverter/charger

Fig. 3.4 (a) Inverter/Charger

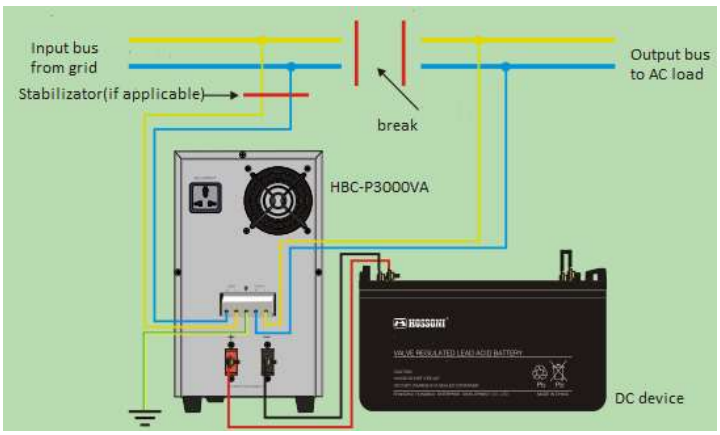

Fig.3.4 (b) Common connection with HBC-P3000VA

As a central control device, HBC-P3000VA shown in Fig 3.4 played a crucial role to charge/discharge the hybrid DC power sources (super capacitors and batteries). It was fed with AC current from the grid and transformed it into DC to charge DC devices and in turn to convert DC current into AC current back to the grid for regeneration. Therefore, the inverter acted as an inverter or charger with the capacity of bi-directional power delivery.

3.2.5 Signal detection devices

The test with the DC hybrid sources aimed to detect the current and voltage changes along with the charge/discharge operation. Therefore, current and voltage sensors were employed in the signal measuring circuits. Fig. 3.5 illustrates these connections.

3.2.6 Signal conversion, control and display

The signals detected by the sensors were analogue and needed to be transformed into digital signals before being analysed for further processing. In this test, a Siemens S7-200 PLC (Programmable Logic Controller) extension module EM231 was selected for accepting analogue signals and transferring them for further calculation by the CPU unit in the PLC. Meanwhile, these digital signals were displayed on a desktop by software *Kingview* which communicated with the PLC. Fig. 3.6 illustrates the PLC and monitoring software *Kingview* in the test.

The experiments employed a Siemens S7-200 PLC as the controller to perform the charge/discharge tasks for HEES automatically. It accepted the signals from the data detection devices via an I/O module and calculated the control output to the execution devices relay 1 and relay 2. Table 3.2 lists all of the constituents of the PLC employed.

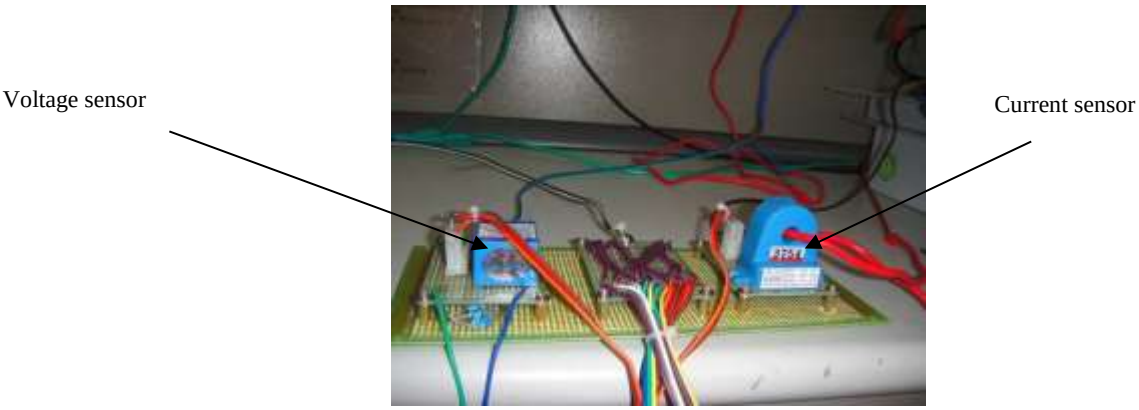

Fig. 3.5 (a) Measuring board

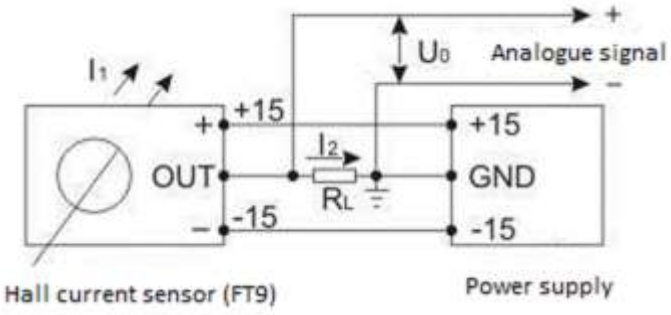

Fig. 3.5 (b) Current measuring circuit

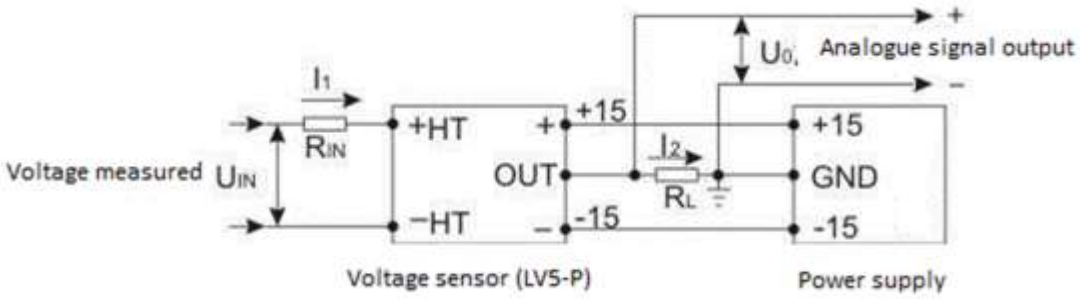

Fig. 3.5 (c) DC voltage measuring circuit

3.3 Experimental circuit design

The experimental bench is illustrated in Fig. 3.7. A super capacitor module was connected to 3 units of lead acid batteries as energy devices and fed to the inverter/charger via the DC input port. The bulb boards, as load bank, were linked with the inverter/charger via the AC output port while the AC power from the grid took the role of the main electrical source to

supply the HBC-P3000. HEES parameters were detected by the sensors placed in the DC circuits and sent to the PLC for calculation. A PC interacted with the hardware circuit via serial communication RS485 and interfaced with the software *WINCC* and the utility *Kingview* for monitoring and control purposes.

The programme implemented in the PLC was used to assess the data collected by the input

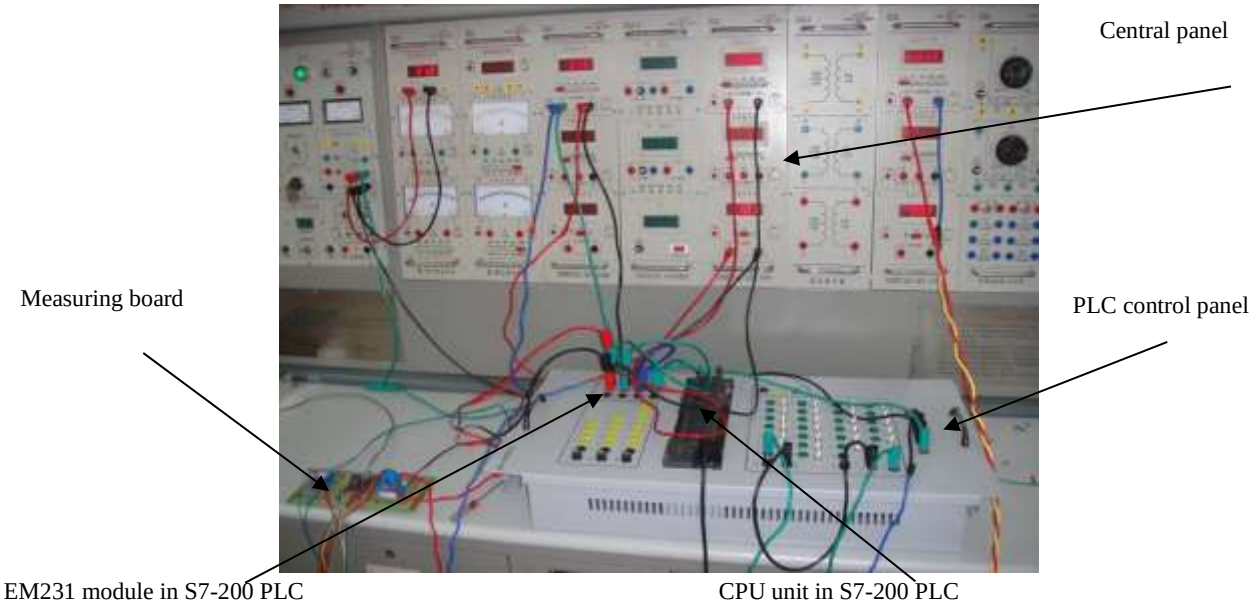

Fig. 3.6 (a) Signal conversion and processing bench

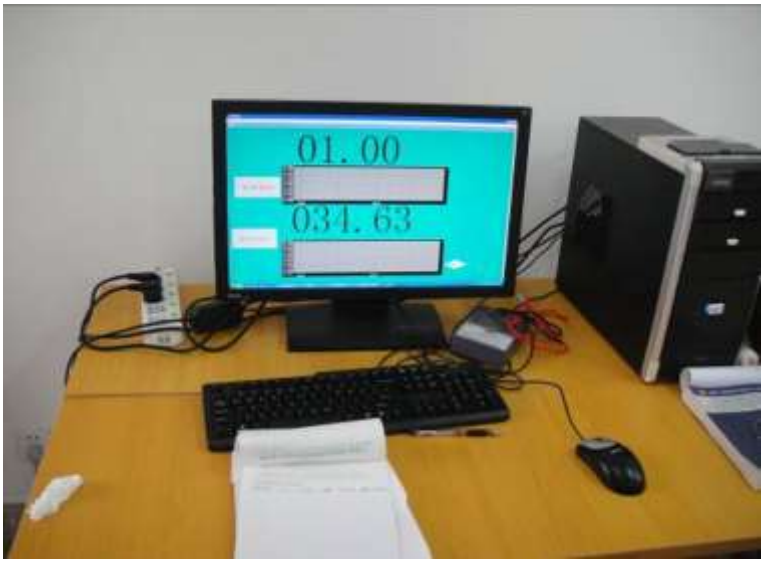

Fig. 3.6 (b) Kingview interface on a desktop

ports which linked with the sensors and DC meters and then to drive the actuator elements (relay 1 and relay 2) via output ports for charging and discharging the hybrid power system. Simultaneously, the data that the PLC received was sent to the supervisory software *Kingview*

on a desktop for display. The allocation of input/output (I/O) ports and the registers of the PLC are summarised in Table 3.3.

The complete PLC programme is shown in Appendix 1.

Table 3.2 S7-200 PLC

Item	**Specification**
CPU module	CUP-224
I/O module	EM231/EM232 (8 analogue in/4 analogue out)
Communication	RS485 (built-in)
Power module	220V In / 24V Out
Software	HMI-Software WinCC

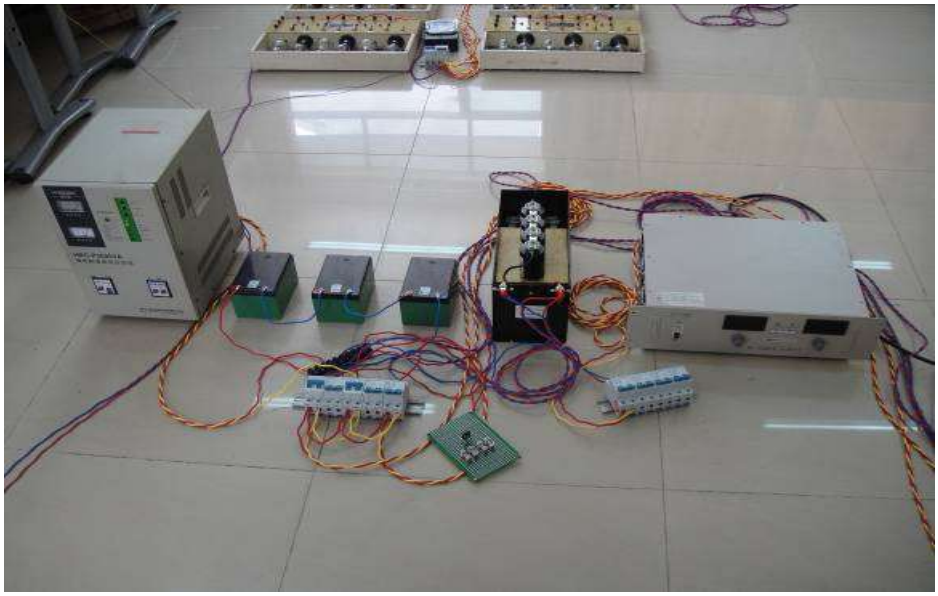

Fig. 3.7 (a) Layout of the primary test bench

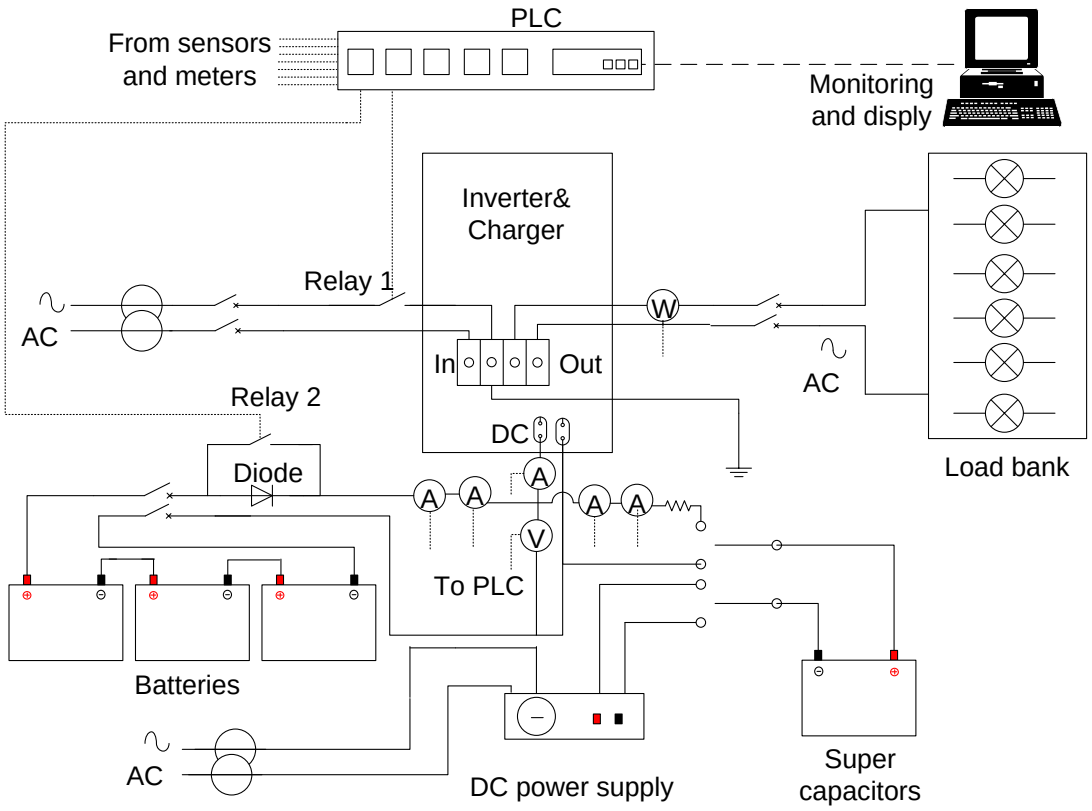

Fig. 3.7 (b) Circuit of the preliminary test

Table 3.3 Variables allocation

Item	PLC I/O Port	PLC Register	*Kingview* Variable
Battery charge current	AIW0	VD100	AI0
Battery discharge current	AIW2	VD104	AI1
Super capacitor charge current	AIW4	VD108	AI2
Super capacitor discharge current	AIW6	VD112	AI3
DC voltage value	AIW8	VD200	AI4
Total discharge current	AIW10	VD204	AU0
Transient load power	AIW12	VD208	AW0
Output 1 to relay 1	AOW0	Q0.0	-
Output 1 to relay 2	AOW4	Q0.4	-

3.4 Test plan and procedures

The experimental bench was developed to charge and discharge hybrid power sources automatically.

Tests were carried out in two steps:

Charge batteries and super capacitors : relay1 on and relay 2 on

Discharge batteries and super capacitors: relay 1 off and relay 2 off

The inverter charged the DC sources (batteries and super capacitors) along with electricity supplies to the load bank. After the batteries and super capacitors were fully charged, the inverter started to convert DC power originating from batteries and super capacitors into AC power to supply the load bank. During the operation, the load demand was 100 watts.

3.5 Test results

Three diagrams in Fig. 3.8 show voltage and current waveforms as a result of charging and discharging the DC sources.

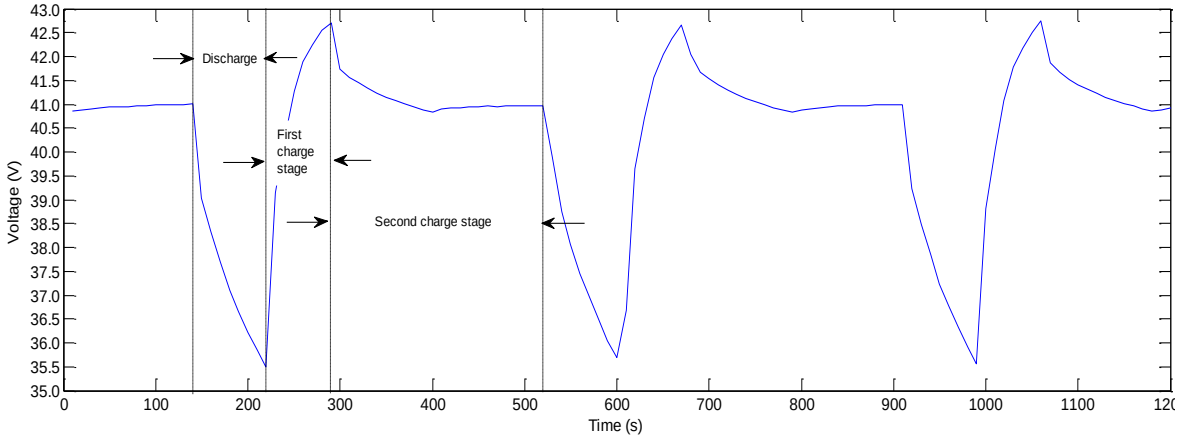

Fig. 3.8 (a) Voltage waveforms of the DC sources

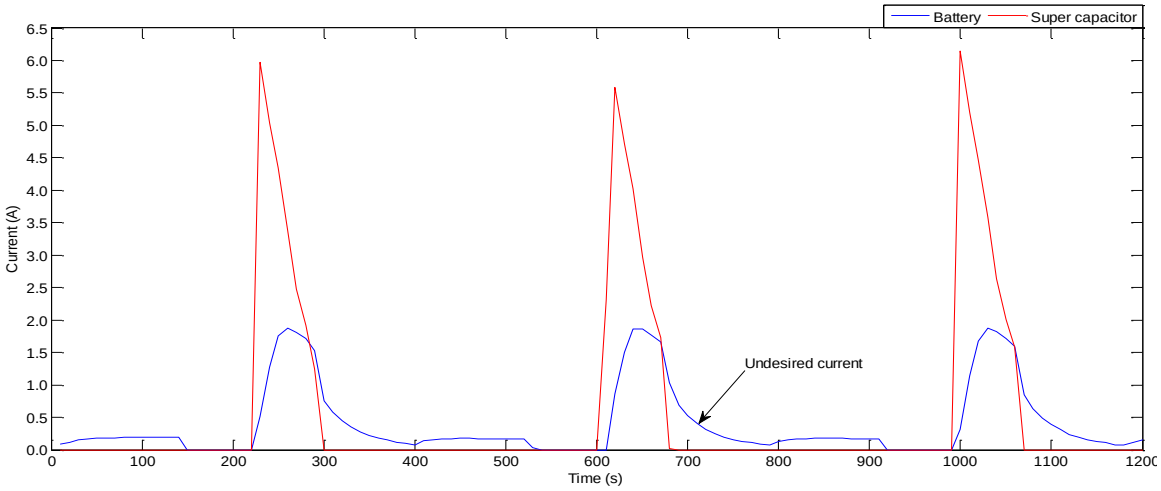

Fig. 3.8 (b) Current waveforms of charging the DC sources

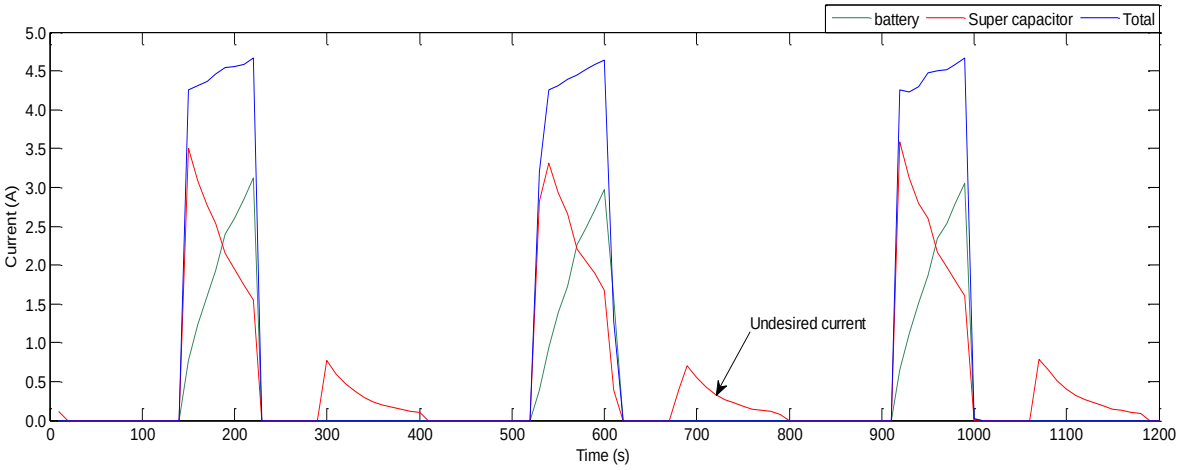

Fig. 3.8 (c) Current waveforms of discharging DC sources

Fig. 3.8 (a) presents the experimental result of the voltage curve of the hybrid power sources during both the charging and discharging processes. From the figure, the charge process can be divided into two stages.

Three-stage charging is a widely used method for lead-acid batteries. It is the combination of constant-current and constant-voltage and float stages. The batteries were charged with constant current in the first stage and with constant voltage in the second stage. Float charge provided a small current to charge the batteries. When the charging started, an immediate high current was supplied to the batteries and their voltage increased gradually. This is the first stage, constant-current charging. Afterwards, the batteries were charged with constant voltage for a period of time. In this stage, the current decayed to a preset value, the charging process transferred from the second stage to the third stage the purpose of float charging is to charge the batteries with a low rate that is approximately equivalent to the internal losses of the battery over long-period operation.

In the tests, the batteries were charged by the first two stages of the three-stage charging method. Therefore, the voltage variation over the charging process can be divided into two parts.

The voltage dropped swiftly in the discharge phase of the test because the hybrid DC sources offered the maximum power to the load. However, the total energy supplied by the hybrid power sources was relatively limited. As a result, the voltage plunged when hybrid power sources discharged with relatively high power.

Fig.3.8 (b) presents the current curves of the hybrid power sources being charged. From Fig.3.8 (b), it can be seen that the super capacitors responded more rapidly compared to the batteries'. The charging current for the super capacitor increased from 0 to 6A within 5s. In contrast, the charging current for the batteries only increased to 1.8A.

On the other hand, there was an undesired current rushing to the batteries at the last stage of the charge process. It was mainly due to the higher voltage of the super-capacitor compared to the batteries' at the transient time. This undesired current can be seen in Fig. 3.8 (b).

Fig. 3.8 (c) shows the current curves of the hybrid power sources being discharged. From the figure, it can be seen that during the period of discharge, the super capacitor module showed active characteristics and fast response capability. Super capacitors provide a higher current

to the load instantly than batteries at the start of the discharging period. However, the current plunged along with the voltage while the batteries' current increased dramatically.

3.6 Summary

The preliminary tests were conducted to gain in an understanding of the small-scale HEES system and were used later as a basis for developing the complete BMT-HEES system. Some points could be summarised as follows,

- Super capacitors exhibit excellent dynamic characteristics and they responded promptly both in charging and discharging, which will benefit the complete system in terms of satisfying the dynamic electrical loads.

- Hybrid DC sources operated with their maximum capability to supply power to the load demand.

- Due to the parallel connection between the batteries and the super capacitors, there was a voltage difference between them at the start of second charging stage (constant-voltage stage). As a result, DC current released from super capacitors flowed into batteries even though it was in the charge phase, which was undesired in this system. This issue could be sort out by adding a diode in the circuit in the complete system.

- In-depth investigation was followed in developing a complete bio-fuel tri-generation with hybrid energy storages system.

Chapter 4 The design of the BMT-HEES

4.1 Introduction

In this section, a full-sized HEES system based on that presented in Chapter 3 was used for the BMT-HEES and configured in the laboratory. The system was composed of the following parts: (1) Diesel engine & generator; (2) Waste heat recovery system; (3) Absorption refrigerator and exhaust heat recovery system; (4) HEES; (5) Energy management and control unit.

The design of the complete BMT-HEES system proposed is presented in the schematic

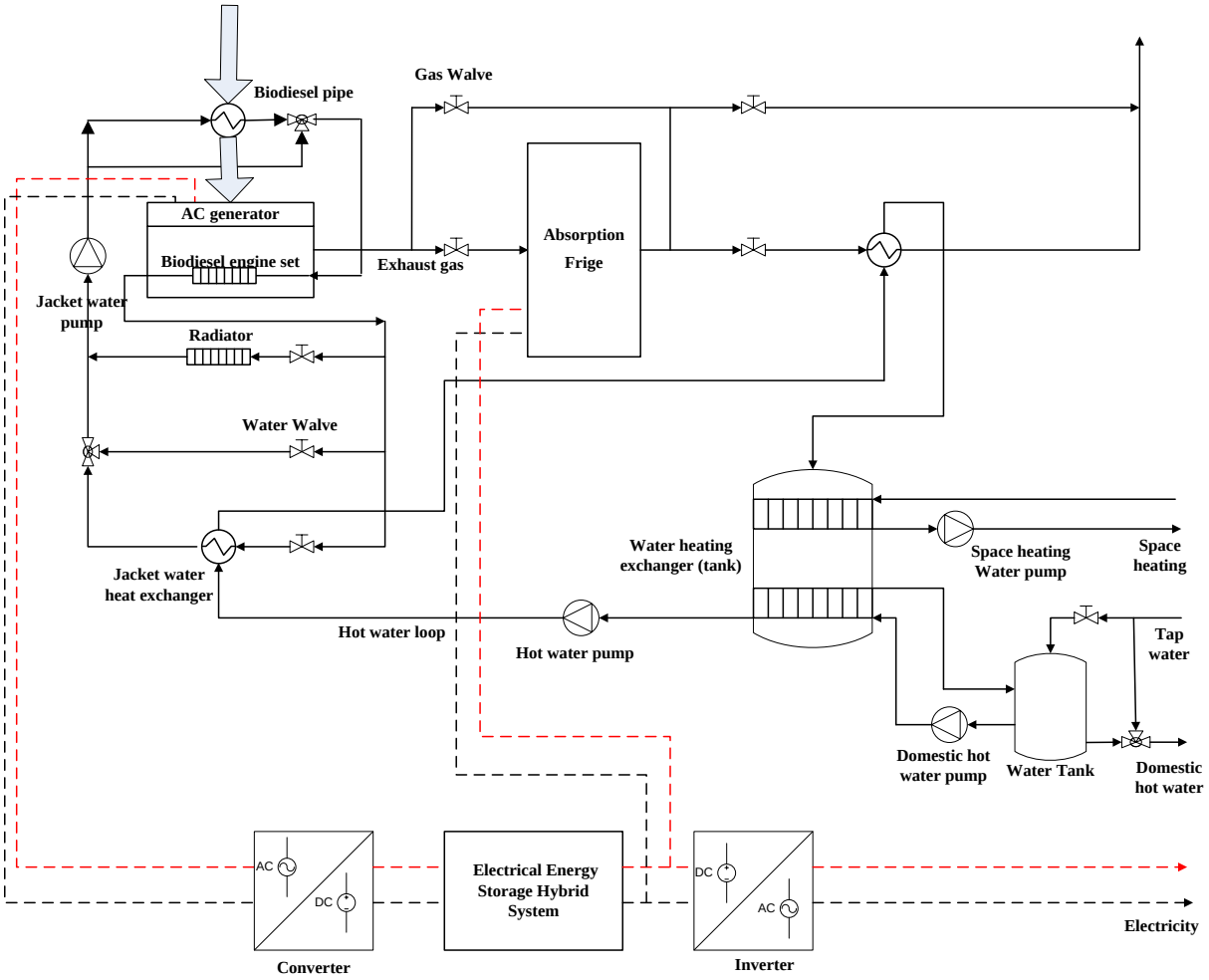

Fig. 4.1 Schematic diagram of the BMT-HEES system

diagram shown in Fig. 4.1. The system includes an engine-based bio-fuel micro- tri-generation and a hybrid energy storage system. The system was stand-alone and allowed three different types of energy (electricity, heat and cooling energy) to be generated locally. The engine was fuelled with bio-diesel and was used to satisfy basic electricity demand; the waste heat from the engine cooling system and the exhaust gas was recovered and stored in a tank; and the hot water was utilised to supply heating and hot water for the house. Heat was exchanged between jacket water and hot water in the heat exchanger in the engine cooling system. Hot water then continued to be heated up by waste heat from exhaust gas before it flowed into the water heat exchanger for third heat exchange. Therefore, waste heat was recovered from both coolant source and exhaust gas. The water heat exchanger supplied hot water for both space heating and domestic hot water consumption.

The HEES consisted of battery banks and a super capacitor module. It was connected to the diesel generator. The electric energy produced from the generator but not used at off-peak hours was stored in the HEES system and then released along with electricity directly produced from the generator to satisfy the electricity demands at peak time. Since both branches of electricity generated by the engine were AC while electricity for charging/discharging the HEES was DC, the system included a rectifier and an inverter for power conversion purposes.

Experimental equipment were selected based on computational simulation and preliminary study. Component performance tests had been carried out, especially for batteries which are a key component in HEES system. After that, the HEES system performance was investigated followed by testing the complete system of BMT-HEES based on daily electricity consumption in the selected examples in the UK.

4.2 System components

4.2.1 Diesel engine & generator

The developed BMT-HEES system employed a Yanmar diesel engine (series YTG6.5S) as the prime mover. It provided a nominal power output of 6.5 kW electrically and both engine coolant as well as exhaust heat recovery systems were adopted for heat recovery/delivery purposes.

The fuel supply system is a key part in an engine system. Fuel from a fuel tank was preheated

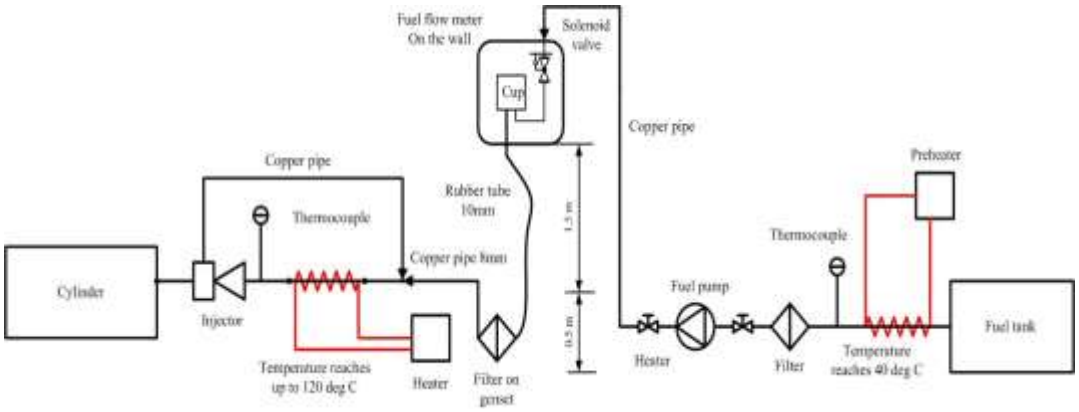

Fig.4.2 Diagram of the fuel supply system

at two levels before it went through the injector and was then burnt in the cylinder. The pre-heater, controlled by a set of temperature/process controllers, could facilitate reduction of viscosities of the oils to a diesel oil level as fuel temperature could go up to 120°C. Fig.4.2 below illustrates the construction of the fuel supply system. Table 4.1 lists the main devices in this subsystem.

Table 4.1 Device list in the diesel engine & generator subsystem

Device name	Unit
Engine/generator	1
Fuel tank	1
Valve	2
Pre-heater	2
Thermal couple	2
Fuel flower meter	1
Pump	1
filter	1

The curves in Fig. 4.3 and Fig. 4.4 represent the trial test outcomes of the engine/generator associated with energy indicators, including efficiency, consumed energy and acquired energy respectively. Fig. 4.3 illustrates both electric and heat efficiency on the basis of the diesel engine fuelled by bio-diesel. Table 4.2 summarises the testing values in detail. Electric efficiency ranged from 7.8% to 28.1% when electric power output varied from 0.64 kW to 6.35 kW and heat efficiency changes from 38.45% to 41.03% under the same circumstances. Fig. 4.4 demonstrates energy consumed and heat recovered over the electric power output from 10% to full load. The fuel consumption ranged from 8.19 to 22.62 kWh while heat recovered from 3.15 to 9.28 kWh and electric power outputs altered from 0.64 kW to 6.35 kW.

Table 4.2 Engine performance

Load (%)	Engine power (kW)	Fuel energy(kWh)	Total heat recovered (kWh)	Heat Efficiency (%)	Electricity efficiency (%)
10	0.64	8.19	3.15	38.45	7.81
25	1.61	9.86	3.4	34.49	16.30
50	3.28	13.53	4.93	36.44	24.23
75	4.81	17.66	7.25	41.05	27.25
100	6.35	22.62	9.28	41.03	28.09

4.2.2 **Waste heat recovery system**

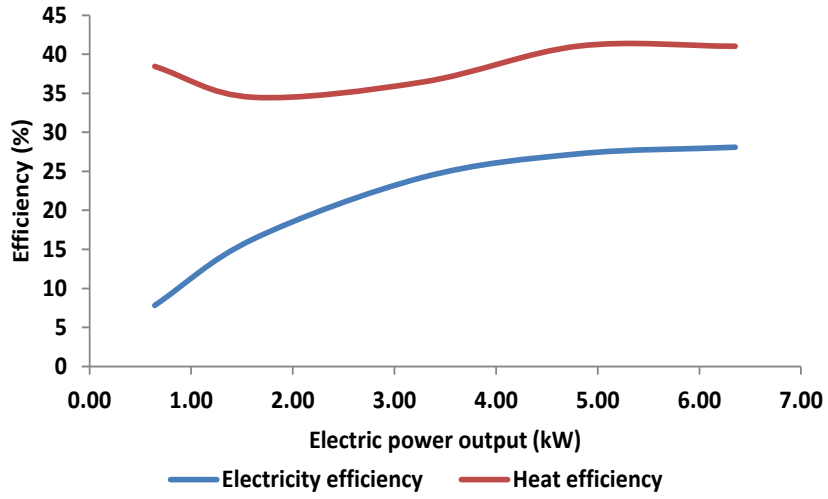

Fig. 4.3 Electric and heat efficiency of the engine

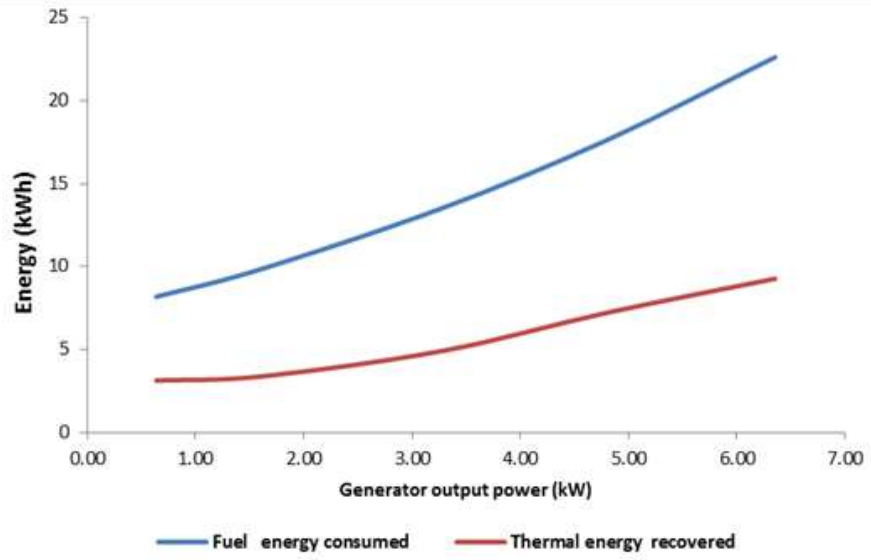

Fig. 4.4 Energy versus electric power

Two kinds of waste heat source could be utilised for heating and cooling purposes after waste heat was recovered. One main heat source was the engine cooling system by means of coolant heat recovery. The other was derived from the exhaust heat recovery system. Fig. 4.5 and Fig. 4.6 demonstrate their layout.

Heat from the engine cooling system was dispatched into two branches. One branch went through the radiator along with the other branch flowing through the coolant heat exchanger. Within the loop, they were later pumped back into the coolant jacket. At the same time, heated fluid coming from the coolant heat exchanger flowed into the exhaust heat exchanger and absorbed heat from the exhaust gas and went through the heat dumper before flowing back to the coolant heat exchanger. Three flow meters were utilised to measure heat fluid

Table 4.3 Main devices in the subystem

Device name	unit
Engine cooling system	1
Radiator	1
Coolant heat exchanger	1
Exhaust heat exchanger	1
Heat dumper	1
Pump	2
valve	9
Flow meter	3
Thermal couple	12

cycling within these three heat circuits. The main components in this subsystem can be summarised as shown in Table 4.3.

4.2.3 **Absorption refrigerator and exhaust heat recovery system**

Table 4.4 Main devices in heat recovery system

Device list	Unit
Engine exhaust gas channel	1
Absorption refrigerator	1
Exhaust pipe	1
valve	5
Exhaust flow meter	1
Air flow meter	1
Thermal couple	5

High-temperature exhaust gas was divided into three branches. In one branch, waste gas exchanged heat with water in exhaust heat exchanger before it was disposed of through the

exhaust pipe. The second one was used for preheating bio-fuel. The absorption refrigerator generated cooling by means of waste heat where the third branch of the engine exhaust heat was consumed. After that, these three branches of exhaust gas converged together and were disposed of through the exhaust pipe. Table 4.4 shows main components in this section.

4.2.4 **HEES**

A Introduction of HEES

The HEES system consisted of batteries and super-capacitors. Batteries are commonly regarded as an energy storage device which can store and supply large amounts of energy in a relatively small volume. Super-capacitors are used as an auxiliary power device to store electricity. Compared to batteries, they have much lower energy density but higher power density, long cycle life and fast charge/discharge capability. Super capacitors have become essential components to shave peaks and responded to the fluctuating load in storage applications.

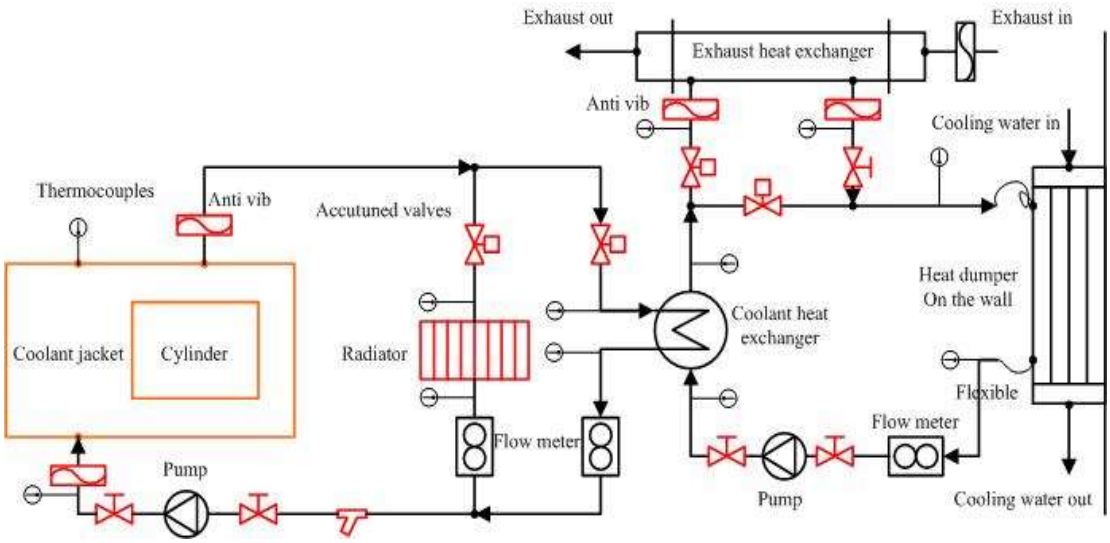

Fig. 4.5 Diagram of coolant heat recovery system

Andrew [108] explained the reason why super-capacitors are better than batteries in high

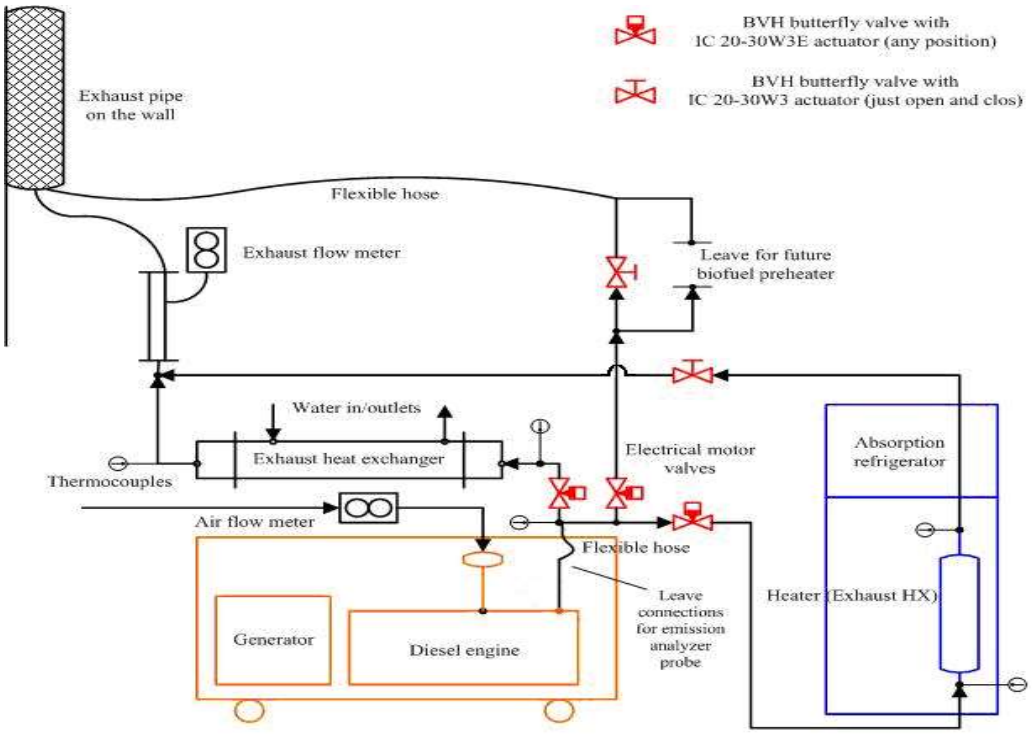

Fig. 4.6 Diagram of exhaust heat recovery system

power applications. For instance, the super capacitor module Superfarad 50V/250F has an energy density of 5.4 Wh/kg but a power density of 219 W/Kg where as the Varta NiHD battery has 70 Wh/kg energy densities and 46 W/kg power densities.

B Batteries

As one of main components in the BMT-HEES system, batteries stored and released most of energy in the HEES. Valve Regulated Lead Acid (VRLA) batteries manufactured by Victron were selected as the energy device. Because the batteries were required to couple with the engine/generator to supply electricity over the 24-hour test, the energy capacity of the battery

Fig. 4.7 (a) Valve Regulated Lead Acid battery

Fig. 4.7 (b) Battery set

set could be calculated based on the energy consumption of 1 kW power for 12 hours. Therefore, the total energy required was equal to 12 kWh (1 Kw × 12 hours). Therefore 6 units of Victron VRLA batteries (12 V/220 Ah) were selected in this study. Fig. 4.7 illustrates the exterior image of the battery and the battery set on the bench.

C Super capacitor module

The super-capacitor module employed in the complete BMT-HEES system was the same one as in preliminary test. It was a 30 V/160 F HCC module.

D Centre unit

A key unit of the electrical system was the *Multiplus 24V/5000VA* manufactured by Victron which has a nominal output 5000VA power capacitity when coupled with 24V DC power devices. It performed the monitoring and governing function by analysing the signals and deciding which operation should be implemented. It accepted the signal for the power output and set out the commands of power demand to the AC input device and HEES system as well to the logic controlling regulation which had been programmed in the control unit in the Multiplus. Fig. 4.8 shows this unit on the bench.

E DC link box

The DC link box provided the connections for all DC power sources and it had functions of primary DC protection, DC monitoring and sensors in one enclosure. The key components were (1) 4 Mega fuses (2x 300A, 1x 200A, 1x 100A) and 1 Midi fuse (60A) as default for DC source connections under protection (2) connection points for the sensors, which were used to link with MultiPlus voltage sensor and BMV-600 (battery monitor) (3) DC output connection points joined with the Multiplus DC points. Fig. 4.9 illustrates its exterior layout.

F Protection circuit and DC actuators

In addition to the main functional circuit in the system, an emergency circuit and a protection device were designed and configured. These included: (1) the air-break switches (2) the DC circuit protection devices (2 emergency buttons and 4 safety relays) for stopping current from the batteries and the super capacitors flowing into the main circuit when the fault condition happened. (3) diodes, which allowed the current to flow from the batteries, the super capacitors and the DC power supply unit (4) voltage contactors, which provided the function

Fig .4.8 Multiplus 24V/5000VA

Fig. 4.9 DC link box

of voltage monitoring and prevent under-voltage and over-voltage of the super capacitors. (5) two relays as acuators in the DC circuits, which accepted the commands from the control unit in the *Multiplus* and switched on/off DC current from the batteries and super capacitors. The exteriors are illustrated as in Fig. 4.10.

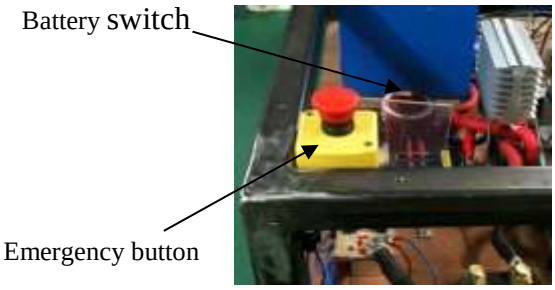

Fig. 4.10 (a) Part 1

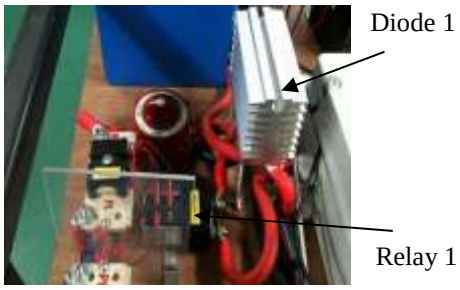

Fig. 4.10 (b) Part 2

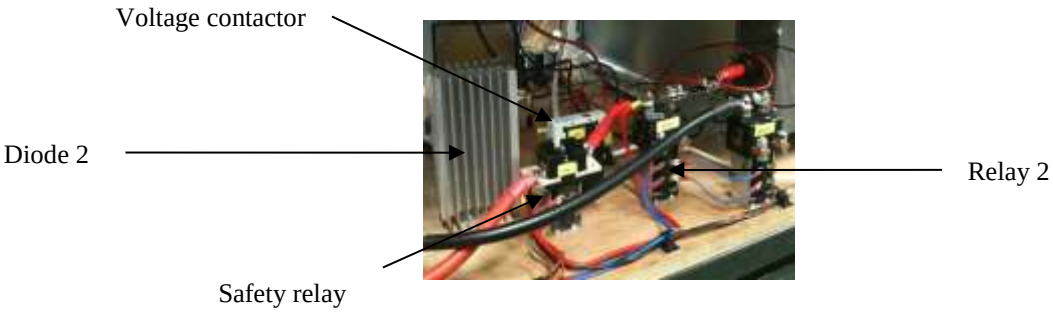

Fig. 4.10 (c) Part 3

Fig. 4.10 Protection circuit and DC actuators

G Input/ output circuit

The input/output circuit accepted the AC electricity from the grid or other AC power sources,

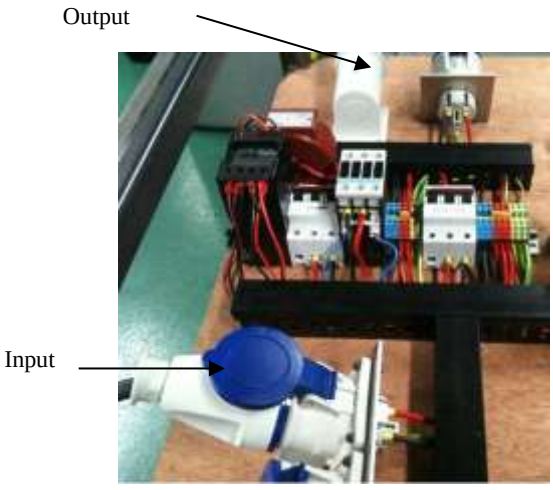

Fig. 4.11 Input / Output

Fig. 4.12 Load bank

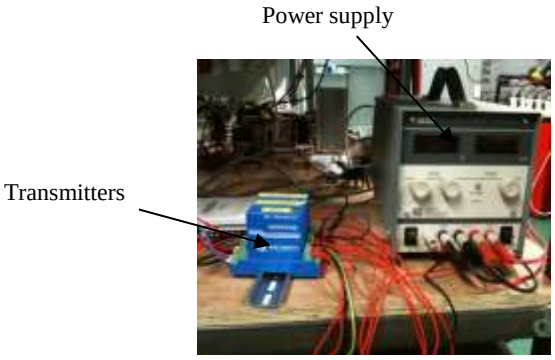

Fig. 4.13 (a) Transmitters and power supply

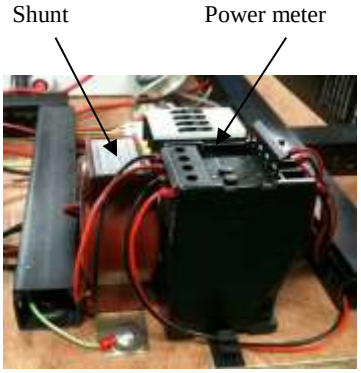

Fig. 4.13 (b) Shunt and power meter

such as a generator or other renewable resources in AC form. After combining DC power sources in the *Multiplus* system the electrical energy was sent out via the output port shown in Fig. 4.11.

H Load bank

Load bank provided electrical demands of up to 16,570W power by employing 2 units of adjustable load box and 1 bulb board, shown in Fig. 4.12.

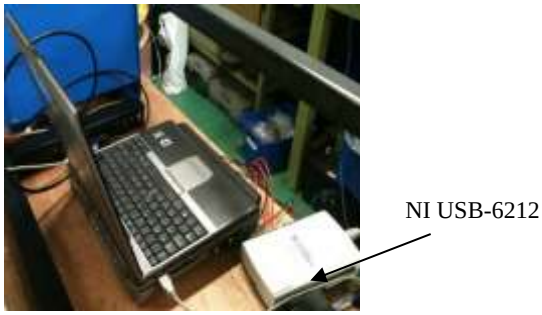

Fig. 4.14 (a) Data conversion and laptop

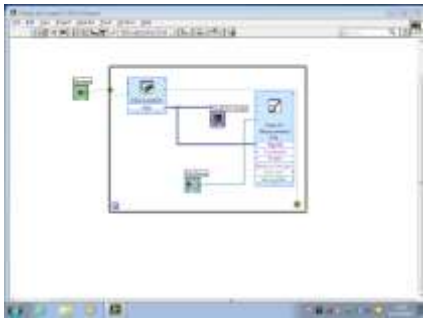

Fig. 4.14 (b) Labview interface

Fig. 4.14 (c) Battery monitor

Fig. 4.14 (d) Real-time data

I Analogue signal detection

There were 5 necessary signals to be monitored by the system, including 2 DC currents, 1 DC voltage and 2 power signals (system input/output). They were analysed and served as the basis of the controller output. These 5 signals were detected by the transmitters or the power meters as analogue signals within 4-20 mA output. Fig. 4.13 (a) and (b) show the exteriors of them on the bench.

J Signal conditioning devices and monitoring interface

The signals from the transmitters and power meters were unable to be directly read by the controller or displayed with monitoring software. Therefore, these analogue signals were firstly transformed into digital form by the NI USB-6212 data log (Fig. 4.14 (a)). The monitoring software accepted these digital signals and then they were recorded by *Labview* (Fig. 4.14 (b)) via the interface or the data files. Real-time data related to batteries were shown via battery monitor (Fig. 4.14 (c)) and recorded by the interface (Fig. 4.14 (d)) via serial communication.

4.2.5 Control circuit design

In the main unit, *Multiplus* was used to execute the embedded control command in relevant codes input to the control unit according to the user applications. A programmable relay controlled relay 1 and relay 2 in the external circuit.

4.3 BMT-HEES circuit design

Fig. 4.15 provides the details of the whole BMT-HEES electrical design. The system consisted of three main power sources, including engine/generator, AGM batteries and the super capacitor module. The batteries and super capacitor were connected in parallel. Multiplus is a bi-directional converter device, and it transferred AC current to DC to charge the DC power sources (batteries and super capacitors) or converted DC power source outputs to AC electricity to supply the load or for grid connection. The signals during the tests were acquired by the current/voltage sensors then transformed into digital signals by the NI data logger. Meanwhile, the data was sent to the control unit in the Multiplus for analysis and control purpose and also sent to real-time monitoring and recorded in data files on the laptop.

Fig.4.15 (a) Photograph of the BMT-EES system

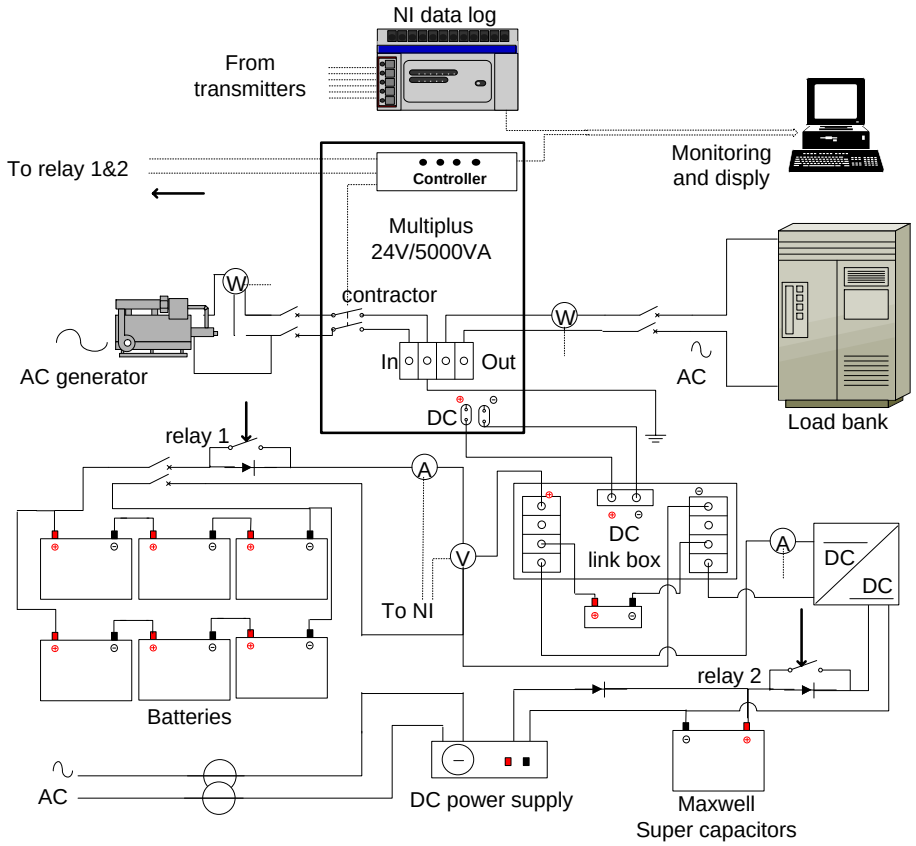

Fig.4.15 (b) Schematic test rig of the BMT-HEES

4.4 **Summary**

The designed system reported in this chapter was developed in the laboratory and in the Dymola modelling and simulation environment. In order to evaluate system performance, case studies were carried out and will be reported in the following chapters.

Chapter 5 Bio-fuel tri-generation and HEES system modelling and simulation

5.1 Introduction

A system performance assessment was necessary before the experimental tests were carried out. Computational modelling and simulation was used to determine control strategies and predict system performance.

5.2 System configuration

On the basis of tri-generation technologies and the preliminary design, a complete BMT-

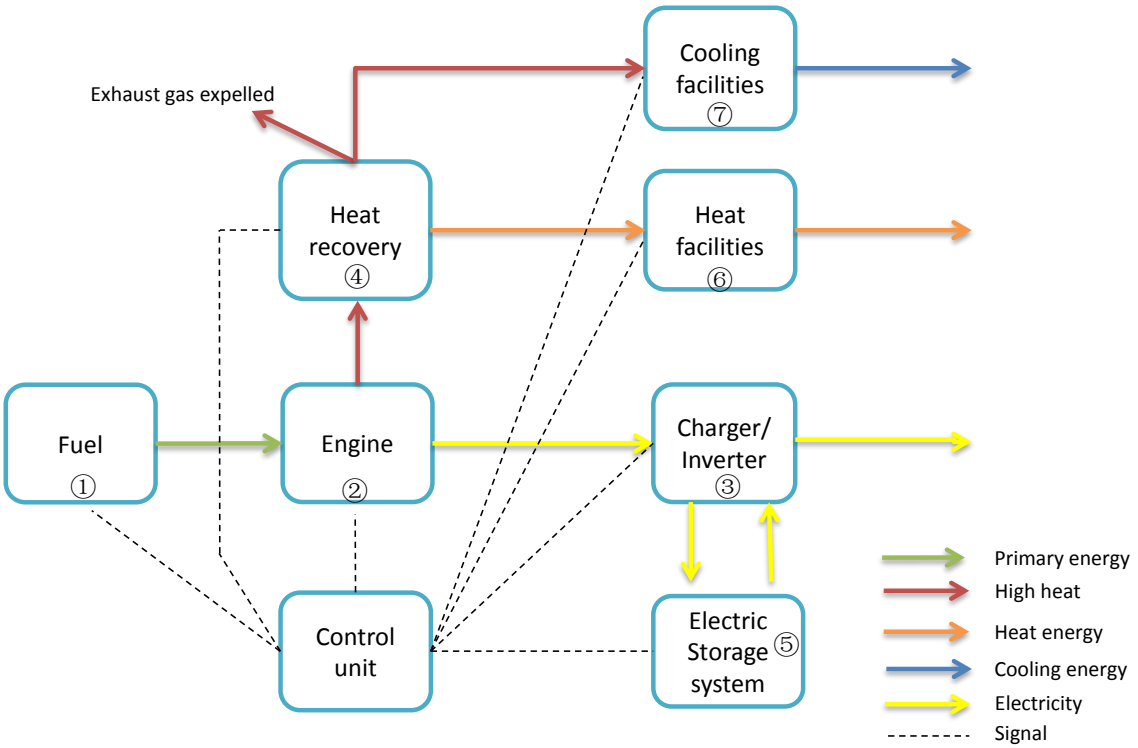

Fig. 5.1 Energy flow chart in a tri-generation

HEES system is developed in this chapter in the computational environment. The system consisted of the following components: a diesel engine generator set, a waste heat recovery unit, a hybrid electric energy storage system, and a control unit. The tri-generation system can provide three different forms of energy (electricity, heating and cooling) simultaneously for one application. Traditionally, such systems do not include an energy storage system.

This study integrated a novel electric energy storage system to improve the energy efficiency and dynamic performance in this tri-generation arrangement.

The generator set includes an engine and a generator. The generator set produces electricity and meanwhile the heat energy coming from the jacket water and the exhaust gas is collected. Part of the heat produced is then transferred into cooling energy through absorption or adsorption refrigeration unit. The rest of the heat that is collected is used for space heating or domestic hot water if the system is adopted in the domestic sector. In this research, FEL energy management strategy was adopted. Therefore, the system primarily satisfied the electric demands along with producing the required amount of heat and cooling energy for domestic usage.

5.2.1 **Generator set**

The generator set is the heart of the whole system since all energy is generated from this unit.

A **Mathematic analysis of a diesel-engine based generator set**

In terms of energy conversion, the generator set can be considered as a bilateral energy converter so that the developed mechanical power is just equal to the generated electrical power. Equations (5-1) to (5-3) describe the relationship between mechanical and electrical power based on the equivalent circuit [95] shown in Fig. 5.2.

$$T_d\Omega = EI_A \quad (5\text{-}1)$$

$$E = K\Phi\Omega \quad (5\text{-}2)$$

$$T_d = K\Phi I_A \quad (5\text{-}3)$$

Where,

E	generated Electromotive Force (EMF) in volts
Φ	air gap flux per pole in webers
Ω	angular velocity in radians per second
T_d	developed torque in newton-meters
I_A	armature current in amperes
K	constant for the given machine

However, this model presents the static state of a generator set with respect to the relationship between the mechanical and electrical sections. Dynamic characteristics of the generator set should also be considered. Normally, a diesel engine is mechnically linked to a synchronous permanent magnet generator for the purpose of electricity generation. The mathematic model of a generator set based on the dynamic characteristics of a diesel engine with a generator (electrical part) can be described as Fig. 5.3 [96, 97]. The two parts are analysed as follows,

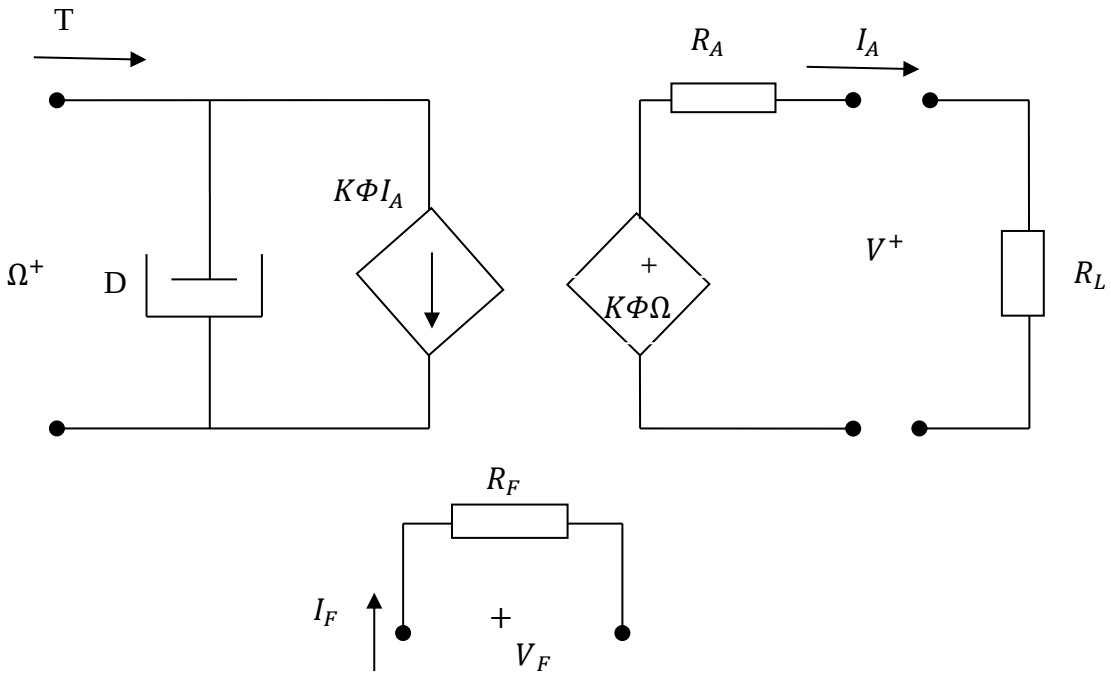

Fig. 5.2 Equivalent circuit for an engine/generator

- Mechanical part of a generator set

$$\frac{d\omega_m}{dt} = \frac{1}{J}(T_e - F\omega_m - T_m) \tag{5-4}$$

$$\frac{d\theta}{dt} = \omega_m \tag{5-5}$$

Where,

ω_m	Mechanical rotational speed
J	Combined inertia of rotor and load
F	Combined viscous friction of rotor and load

θ	Rotor angular position
T_m	Shaft mechanical torque

Equations (5-4) and (5-5) give the relationship between rotor angular position, rotor rotation, and the torque values.

- Electrical part of a generator set

Mechanical energy is transformed into electricity by a generator. This investigation adopted a mathematical model of a PMSM (permanent magnet synchronous motor) to describe a generator that is derived in the two-axis d-q synchronous rotating reference frame. Equations (5-6) to (5-9) give the relationship between the variables.

The d-q component of the current vector are calculated through a state transformation of the stator currents phases i_a , i_b , i_c and the rotor angular position θ

$$\begin{pmatrix} i_d \\ i_q \end{pmatrix} = \sqrt{\frac{2}{3}} \begin{pmatrix} \cos(p\theta) & \sin(p\theta) \\ -\sin(p\theta) & \cos(p\theta) \end{pmatrix} \cdot \begin{pmatrix} 1 & -\frac{1}{2} & -\frac{1}{2} \\ 0 & \frac{\sqrt{3}}{2} & -\frac{\sqrt{3}}{2} \end{pmatrix} \cdot \begin{pmatrix} i_a \\ i_b \\ i_c \end{pmatrix} \tag{5-6}$$

The machine equations associated with the rotor frame are as follows,

$$v_d = R \cdot i_d + L_d \cdot \frac{d}{dt} i_d - L_q \omega_r i_q \tag{5-7}$$

$$v_q = R \cdot i_q + L_q \cdot \frac{d}{dt} i_q + L_d \omega_r i_d + \omega_r \Phi \tag{5-8}$$

$$T_e = 1.5p\left[\lambda i_q + (L_d - L_q) i_d i_q\right] \tag{5-9}$$

Where,

L_q, L_d	q and d axis inductances
R	Resistance of the stator windings
v_q, v_d	q and d axis voltages
ω_r	Angular velocity of the rotor
Φ	Permanent magnet flux coupled with the stator windings
p	Number of pole pairs

B **Generator set model in Dymola**

Fig. 5.3 illustrates an improved model for an engine/generator set which consists of the models including *Accessories*, *Engine* (mechanical part), *Generator* (electrical part) and

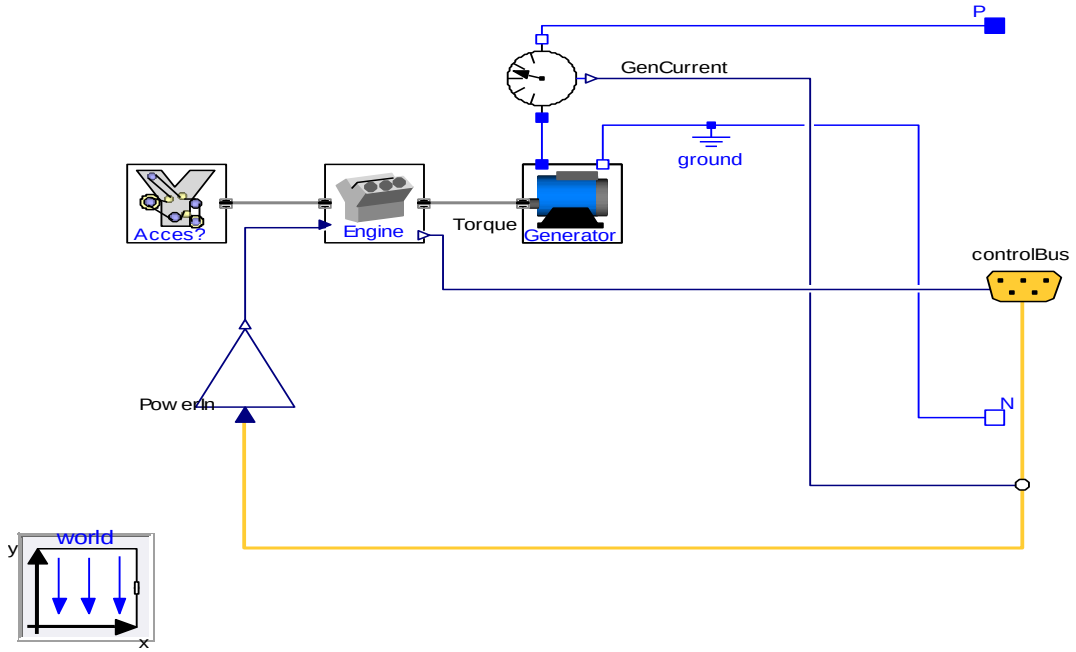

Fig. 5.3 Dynamic model for engine/generator

Control_Bus. The model *world* is used to set up the environmental variables such as gravity, temperature. *Current sensor* is used to acquire circuit current associated with the generator for analysis and control. The details of three main components *Accessories*, *Engine*,

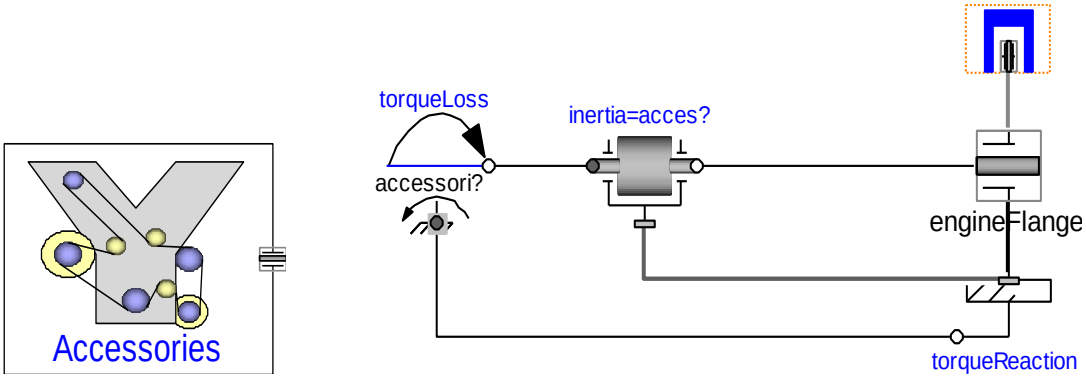

(a) Exterior (b) Interior

Fig. 5.4 Model Accessories

Generator are discussed thereafter.

- *Accessories*

In addition to the consideration of the essential sections in the engine system, in most cases, the mechanical or other power losses should be taken into account for more accurate simulation. Therefore, a model to describe the mechanical losses within the component *Accessories* is illustrated in Fig. 5.4.

This model represents mechanical loss during operation. Referring to Fig. 5.5 (b), friction loss is represented by the variable *torqueLoss*, which is sent out via the component *engineFlange* associated with the mechanical calculation.

- *Engine*

The engine model includes mechanical inertia, engine torque and speed. This model includes two inputs and two outputs, as shown in Fig. 5.5 (a). This model accepts the signal coming from model 'Accessories' via input1 and the value of the load via input (the small tri-angle at the left corner). On the other hand, there are two outputs from this model, namely mechanical power and mechanical torque. Mechanical power is delivered to the model *Generator* via *transmission flange* on the right hand side (the middle one). The real-time value of the mechanical torque is sent out by output2 (the small triangle at the right corner).

Fig. 5.5 (b) provides the model details. This module links with module *Accessories* via accessory flange at the left hand side where mechanical loss delivered into engine model is involved in the calculation. The load demands are sent into this model by input signal *PowerIn* via the unit *engine_tau* which then links to the flywheel before the energy is output via the 'transmission flange' on right hand side.

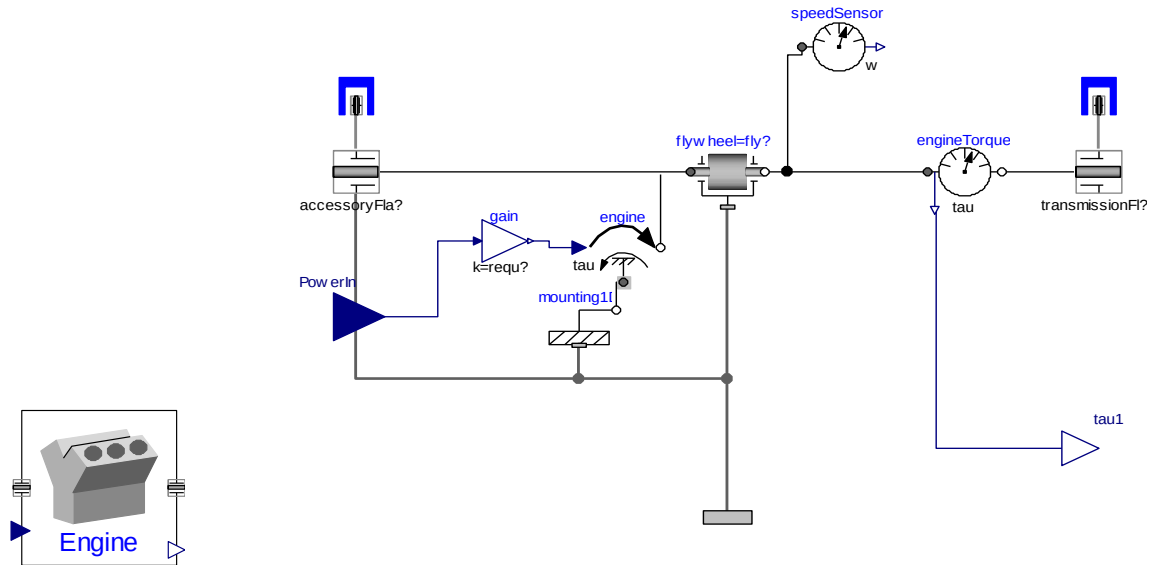

(a) Exterior (b) Interior

Fig. 5.5 Model Engine

- Generator

The generator model is shown in Fig. 5.6. It is another key component of an engine/generator, which accepts mechanical energy derived from an engine and then transfers it electrically. Terminals *pin_p* and *pin_n* in Fig. 5.6 stand for positive and negative connections of the electrical part, respectively. The item *shaft_b* is used to link to the model *Engine* to accept mechanical variables. variables *L* and *R* are the equivalent inductor and resistor in the circuit, respectively.

The model *controlBus* is for communication where three signals are transmitted including generator current, mechanical torque and power in operation. These signals are used for overall control by exchanging information with other models.

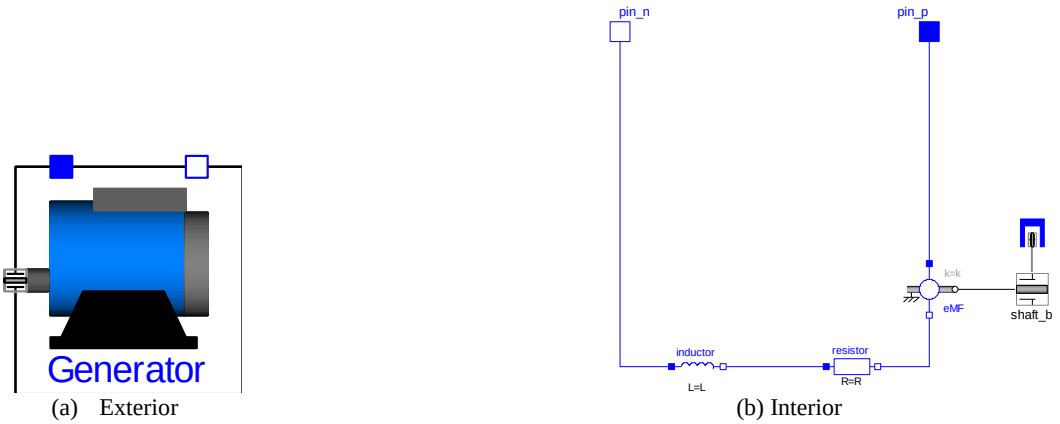

(a) Exterior (b) Interior

Fig. 5.6 Model Generator

C Simulation on engine starting

Generally, an engine has to undergo a transient process before it approaches a steady state. In this section, simulation with respect to engine response during the starting process is presented. In the simulation, model 'Engine' is based on the specifications of the Yammar engine discussedin Chapter 4, at nominal rotation speed and power.

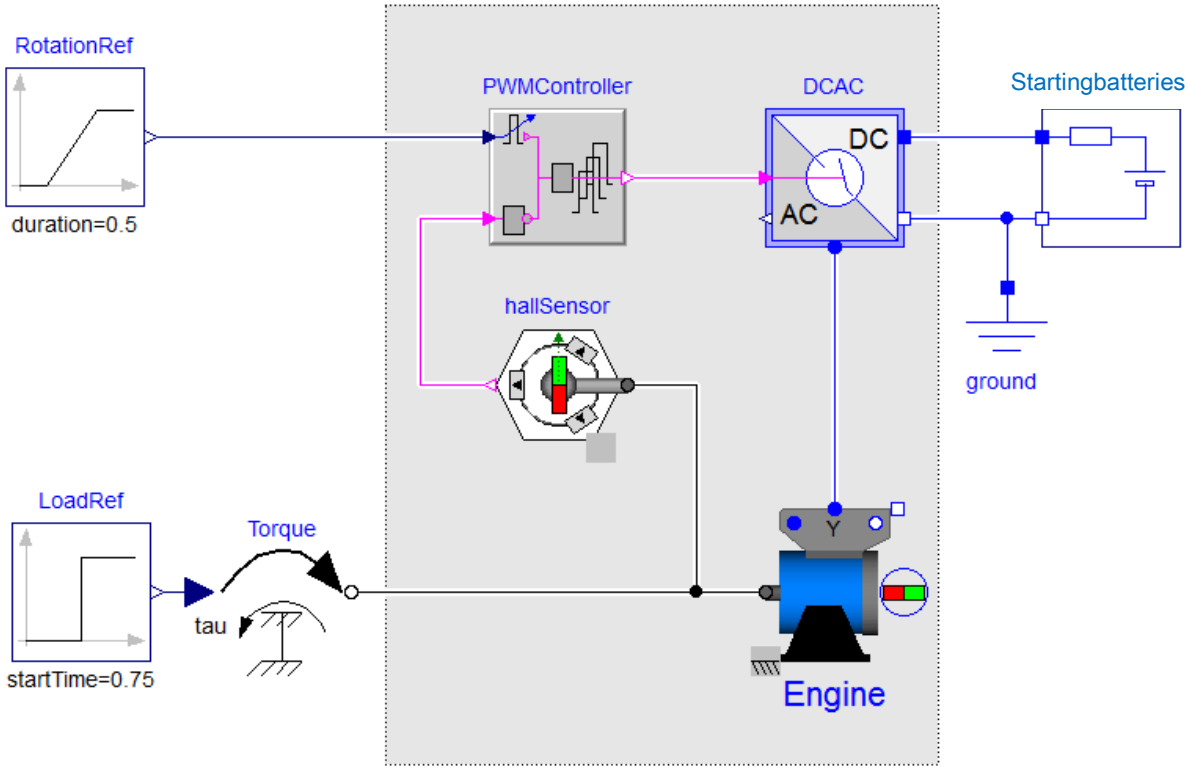

Fig. 5.7 (a) Dynamic simulation of the starting process of an engine

The model in Fig. 5.7 was used to simulate the starting of a diesel engine. The components in this model include (1) *RotationRef*, it is used to provide rotation reference of the engine over the starting process; (2) *PWMController*, it is a PWM (Pulse width module) signal generator. It accepts the rotation reference and compares it with the feedback of the engine rotational speed to generate the signal to control the device *DC/AC*; (3) *DC/AC*, which is a converter. It transforms DC power from 'StartingBatteries' to AC power to crank the engine; (4) *StartingBatteries* is a small-scale set of batteries providing initial power over the starting process; (5) *Engine* represents the Yanmar engine; (6) *LoadRef* provides the load demand over the simulation without dimension. (7) *Torque* is a conversion component that accepts a non-dimensional variable and transforms it to mechanical torque with the same value to link with the engine as a torque demand.

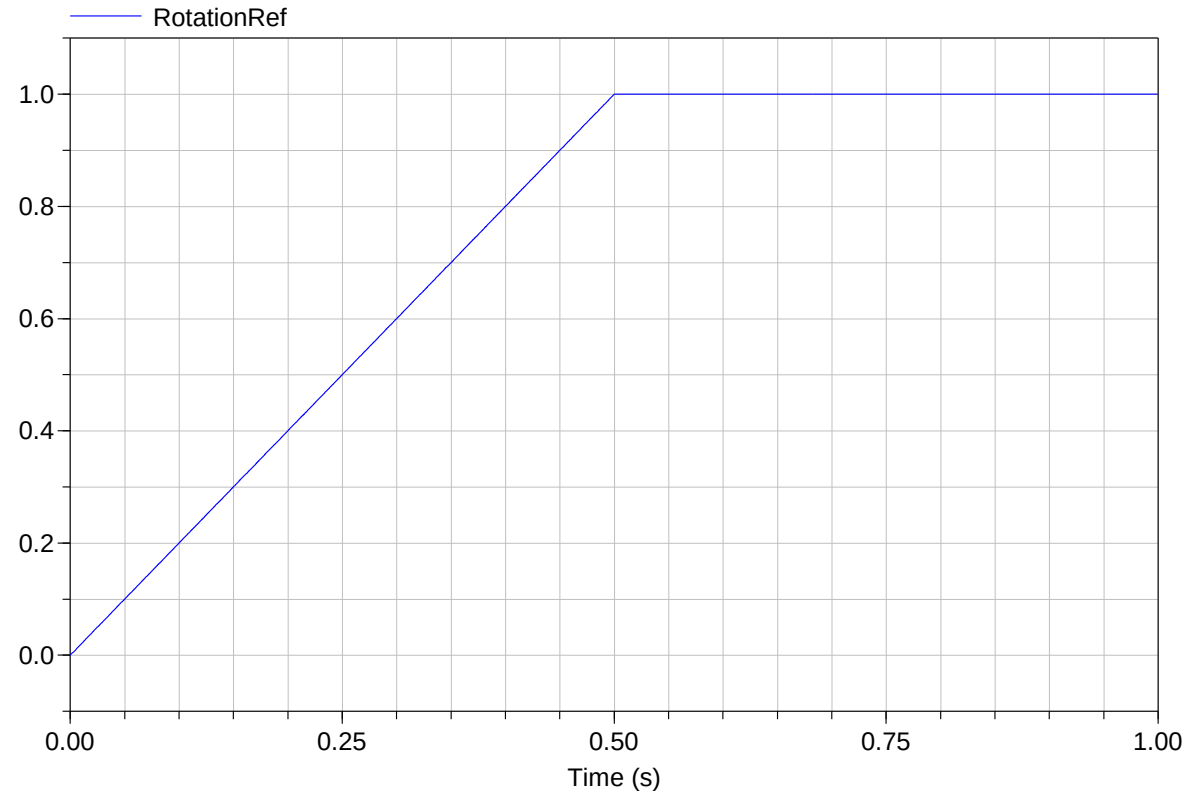

Fig. 5.7 (b) Rotation reference (unified)

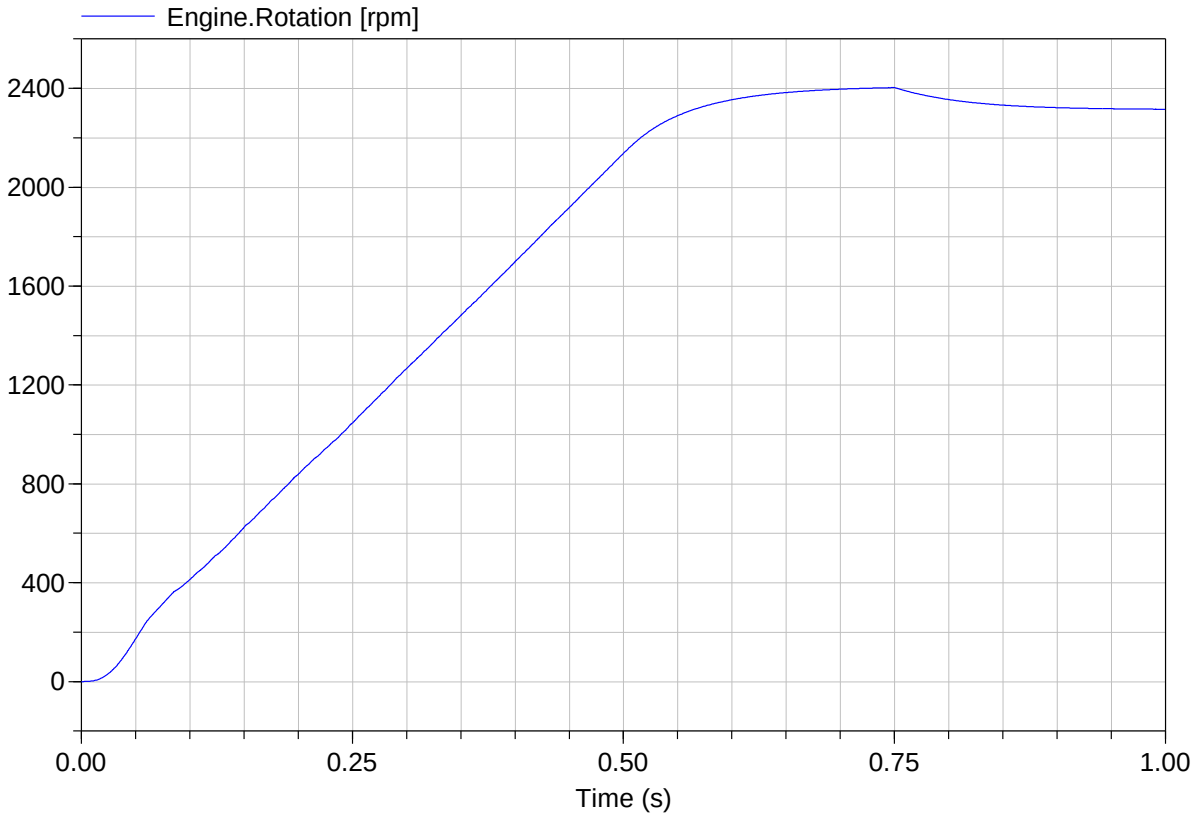

Fig. 5.7 (c) Enigne rotation

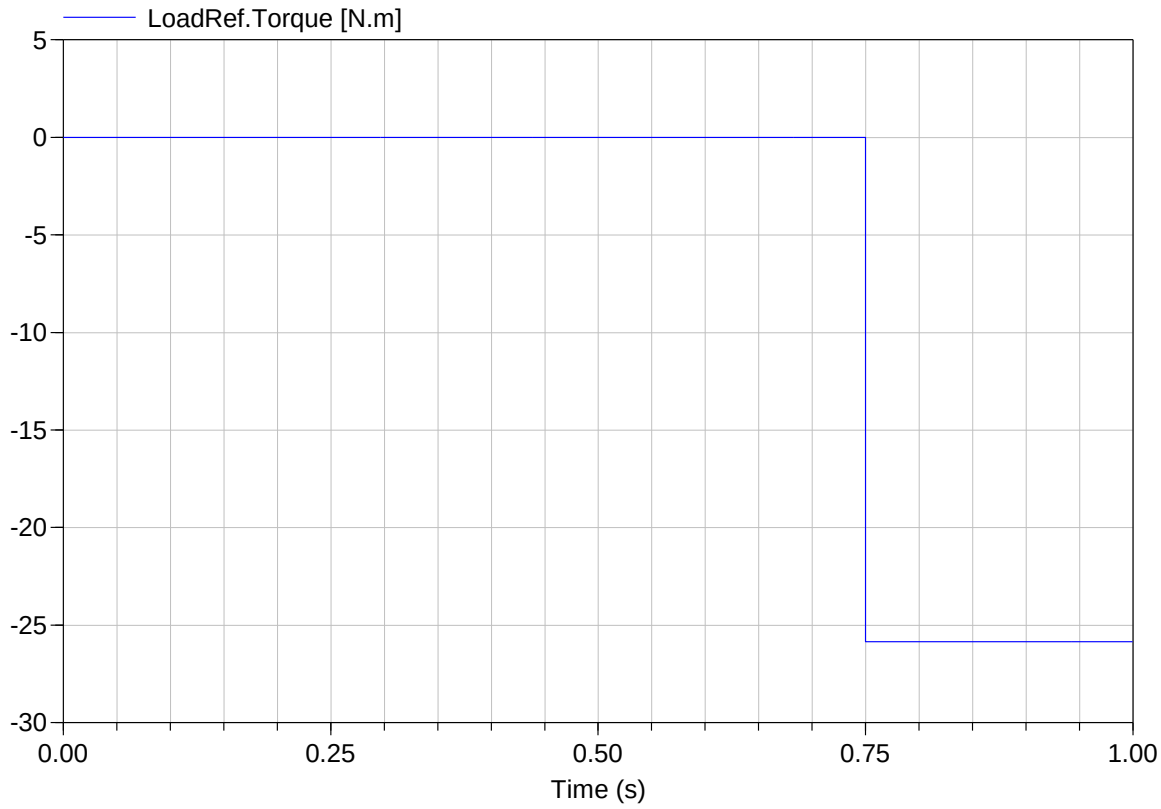

Fig. 5.7 (d) Load torque

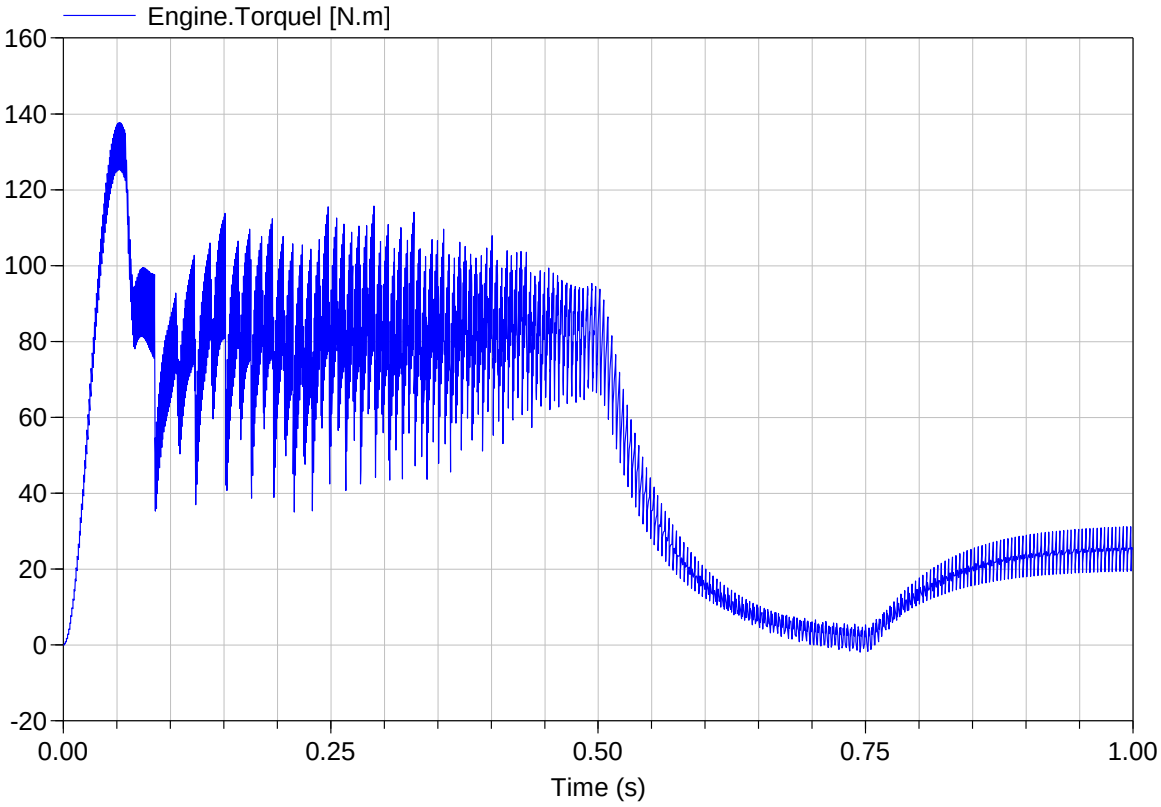

Fig. 5.7 (e) Enigne torque

The engine was started by the power from the *starting batteries* after the DC current had been transferred to AC current by the DC-AC inverter. A speed reference lasted 0.5 seconds to reach the nominal value of 2400rpm. Load demand was applied to the engine 0.75 seconds later. The outcomes derived from the starting process can be seen as Fig. 5.7. The curves in Fig. 5.7 (b)-(e) represent a series of dynamic indicators during the process, including rotation reference, rotation response of the engine, load torque and response torque of the engine, respectively. The engine rotational speed increased gradually to the nominal value of 2400rpm, as shown in Fig. 5.7 (c), under the demand from the module 'RotationRef'. After the engine reached a stable point, a 6500W load requiring a torque of 25.86 N.m. and was connected at 0.75s (seen as in Fig. 5.7 (d)). The engine rotational speed dropped slightly when the load was applied suddenly as seen in Fig. 5.7 (c). High level torque was required as shown in Fig. 5.7 (e) at the begining of the engine starting process, which was followed by some fluctuations until 0.5 seconds and it then dropped to nearly zero. From 0.75 seconds onward, the torque increased again to reach the demand of 25.86 N.m. as requested by the load.

The simulation output illustrates that the engine has unstable torque for the first 0.6 seconds and it took 0.1 seconds to reach the torque required of the engine when the load changed at 0.75 seconds. In practice, the engine may take longer to reach the stable level. During the transient process, the generator set cannot provide the expected output. Therefore, an auxiliary power source, such as energy storage and a power system would be preferable options to satisfy the transient load demands and improve the system dynamic performance electrically.

5.2.2 **Batteries**

In the literature, there are three types of battery model commonly employed: (1) simple model consisting of constant voltage source and constant resistance; (2) Ceraolo model including variable voltage source, constant capacitor and three resistors with variable values; (3) defined model consisting of a constant capacitor, a variable resistor and variable current source.

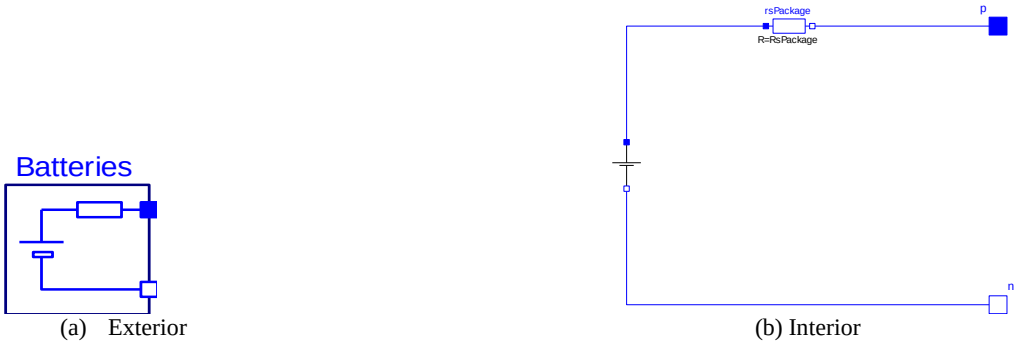

(a) Exterior (b) Interior

Fig. 5.8 Simple battery model

A **Simple battery model**

A simple model for batteries consists of a constant voltage and resistance as shown in Fig. 5.8. However, this model is over simplified and cannot take into account the different characteristics of battery charging/discharging operations.

B **Ceraolo battery model**

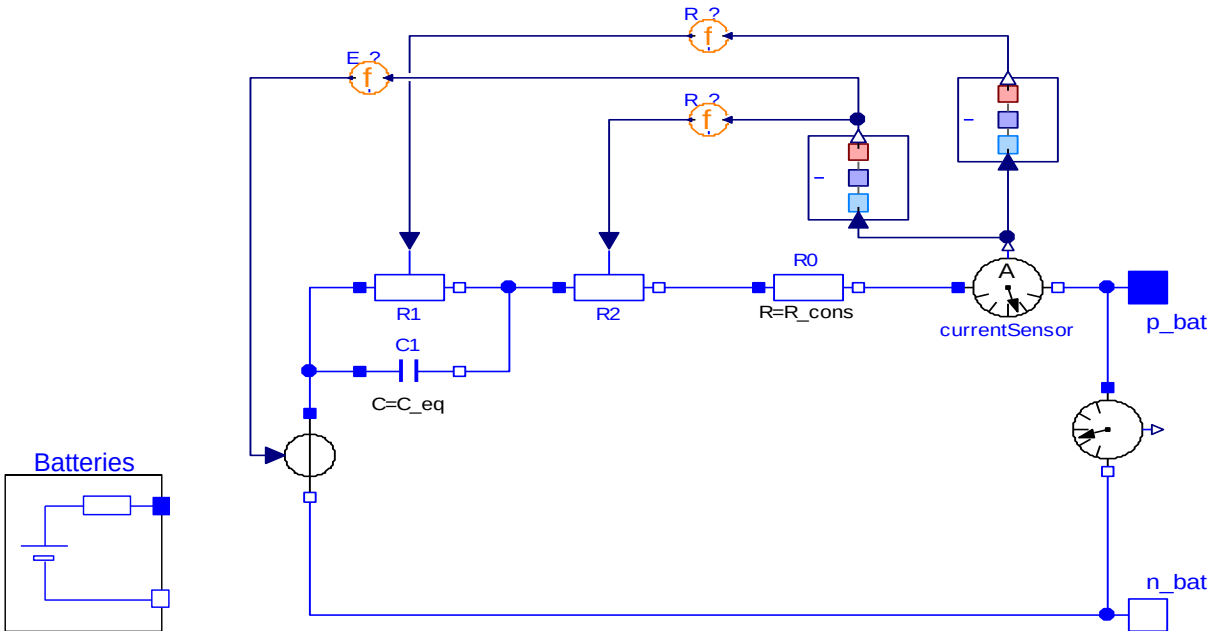

(a) Exterior (b) Interior

Fig. 5.9 Ceraolo battery model

As shown in Fig. 5.9, the dynamic model used for this battery bank employs the lead-acid battery prototype proposed by Massimo Ceraolo with an electrochemical battery model for electrical systems [98]. This model takes into account of the heating influence, non-linear

characteristics during battery operation and parasitic reaction at the end of charging. This prototype was further improved by Barsali [99], Jackey [100] and Glavin[101]. In this model, the parameter R0 is set with the value of 0.12Ω. Meanwhile, the variable resistances R1 and R2 are calculated by module SOC (state of charge)/DOC (discharge of capacity) and the initial values are 0.02 Ω and 0.006 Ω respectively.

Ceraolo developed the lead-acid model where equivalent resistance in the circuit changes dependent on charging and discharging processes. The calculation of the coefficients in the equation was determined experimentally.

C **Defined model**

This model was set up on the basis of the experimental outcomes of the batteries being charged or (and) discharged where battery current and voltage were detected. The equivalent resistance was equal to the voltage v_r against current i_r. Meanwhile, the state of charge (SOC) was calculated by equation (5-10). The experimental circuit is illustrated in Fig. 5.10 (a).

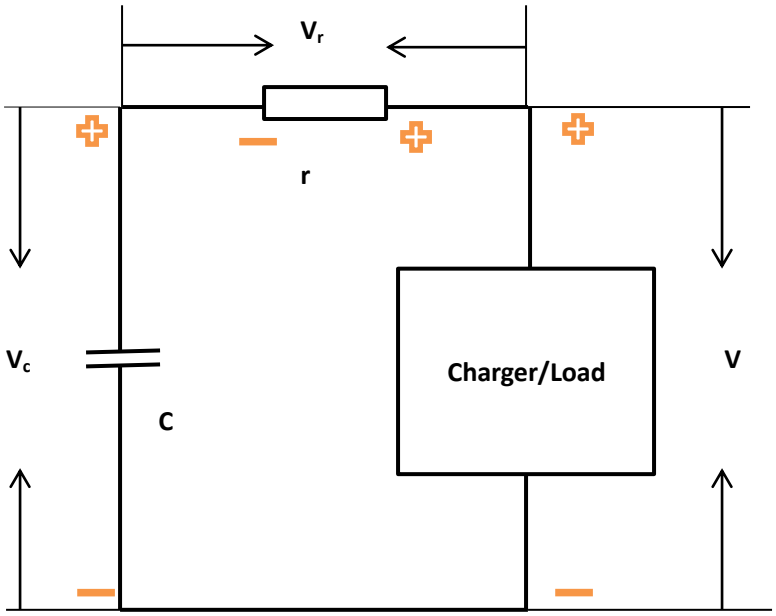

(a) Equivalent circuit for battery charging/discharging tests

(b) Exterior

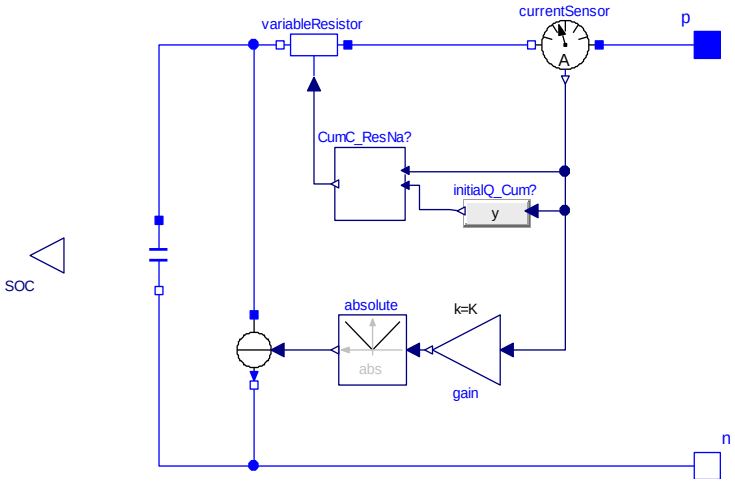

(c) Interior

Fig. 5.10 Defined model

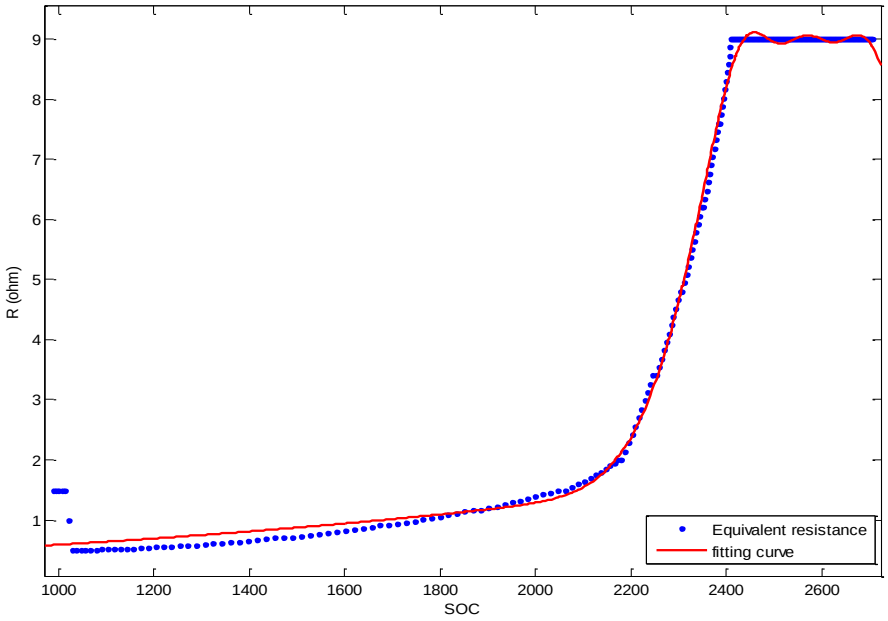

(a) Charging duration (i<0)

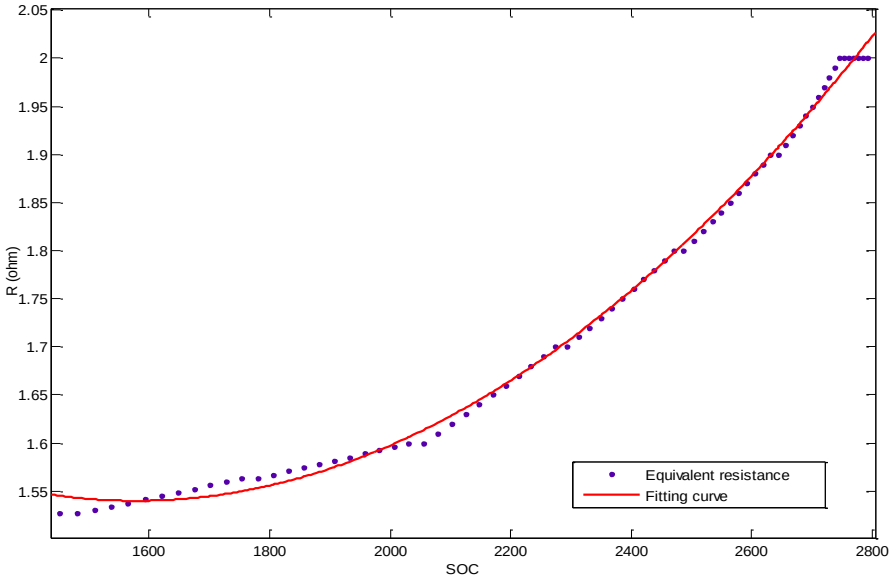

(b) Discharge duration (i≥0)

Fig. 5.11 Battery equivalent resistance

The model in Fig. 5.10 (c) considers the influence caused by stray current and consists of a variable resistor and a constant capacitor. The resistance is calculated from experimental results as follows,

$$SOC = Q_{initial} + k\int i\,dt \tag{5-10}$$

$$r = \begin{cases} a1 * e^{(-(soc-b1)/c1)^2)} + a2 * e^{(-(soc-b2)/c2)^2)} \\ +a3 * e^{(-(soc-b3)/c3)^2)} + a4 * e^{(-(soc-b4)/c4)^2)} & i < 0 \\ \\ p1 * soc^2 + p2 * soc + p3 & i \geq 0 \end{cases} \tag{5-11}$$

(5-12)

Fig. 5.11 illustrates curves used for the equivalent resistance calculation. The dotted lines represent the equivalent resistance curve from experimental tests while the solid lines represent the computed resistance found by curve fitting.

When the batteries are charged, the relationship between the equivalent resistor and the indicator SOC can be expressed with a quartic Gaussian equation given in equation (5-11) along the curves demonstrated in Fig. 5.11 (a). When they are discharging, this relationship can be described with a cubic polynomial as in equation (5-12) and the curves in Fig. 5.11 (b). The values of these coefficients in the equations are listed in Table 5.1 and Table 5.2.

Table 5.1 Coefficients in fitting curve for charging (i<0)

Coefficient	a1	a2	a3	a4	b1	b2	b3	b4	c1	c2	c3	c4
Value	6.14	11.69	14.82	-10.62	2569	2563	8939	2568	76.94	228.3	4421	95.67

Table 5.2 Coefficients in fitting curve for discharging (i>0)

Coefficient	p1	p2	p3
Value	3.232 e-007	-0.00102	2.345

5.2.3 **Super capacitors**

The super capacitor model is illustrated in Fig. 5.12 as a classical RC equivalent circuit,

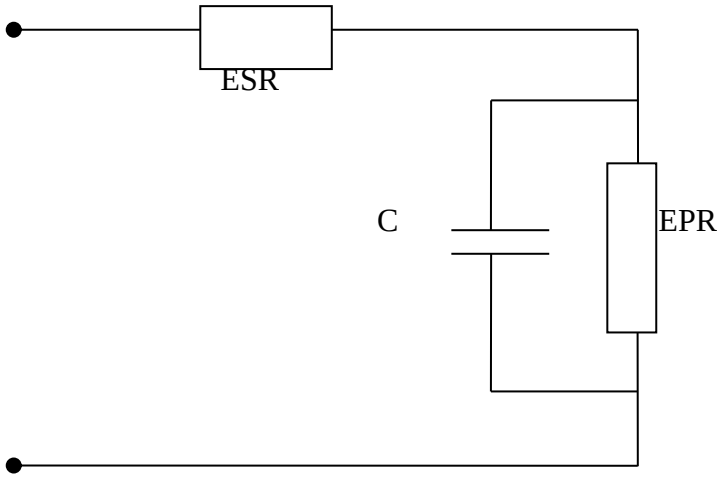

Fig. 5.12 Classic equivalent circuit for single unit of super capacitor

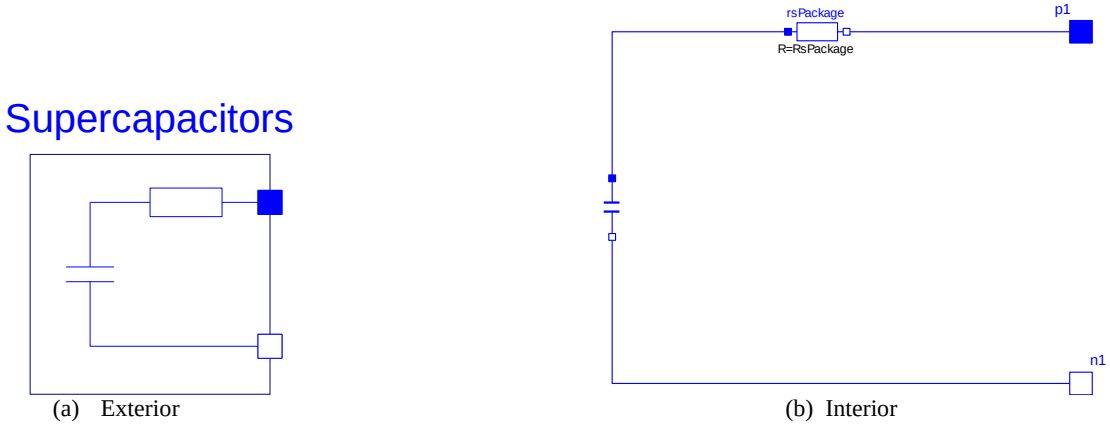

Fig. 5.13 Super capacitors model in DYMOLA

which is commonly used in super capacitor modelling due to its simplicity. Uzunoglu [102, 103] and Spyker [104, 105], carried out investigations by using this model. This model contains three main elements, an equivalent circuit capacitance (C), an equivalent series resistance (ESR) and an equivalent parallel resistance (EPR). ESR represents the charging and discharging resistance and EPR accounts for current losses or leakage which affects the long term energy storage performance of super capacitors. In most applications for super capacitors, EPR is ignored for simplicity.

Normally, a super capacitor bank includes a number of single units connected to build up to a whole bank. In these cases, relevant parameters can be describe as follows,

$$R_{total} = n_s \frac{ESR}{n_p} \tag{5-13}$$

$$C_{total} = n_p \frac{C}{n_s} \tag{5-14}$$

$$E = \frac{1}{2} * C_{total} * (v_i^2 - v_f^2) \tag{5-15}$$

R_{total} The total resistance of super capacitor bank (Ω)

C_{total} *The total capacitance of super capacitor bank (F)*

n_s *The number of super capacitors connected in series*

n_p *The number of super capacitors connected in parallel*

E *The amount of energy released or stored in super capacitor bank (Ws)*

v_i *The initial voltage of super capacitors before discharging starts (V)*

v_f *The end voltage of super capacitors after discharging ends (V)*

The *Dymola* model of the super capacitors is shown in Fig. 5.13, which includes one capacitor and one resistance, the values of R and C are dependent on the total number of super capacitors which are connected in parallel or series.

5.2.4 **Charger/Inverter**

The conversion device is necessary because that the DC devices (batteries and super capacitors) are charged by an AC device (generator). Also, DC electricity from the batteries and super capacitors has to be converted to AC current before it is provided to the AC load. Therefore, this conversion device can accept a DC power input and transmit it as AC power

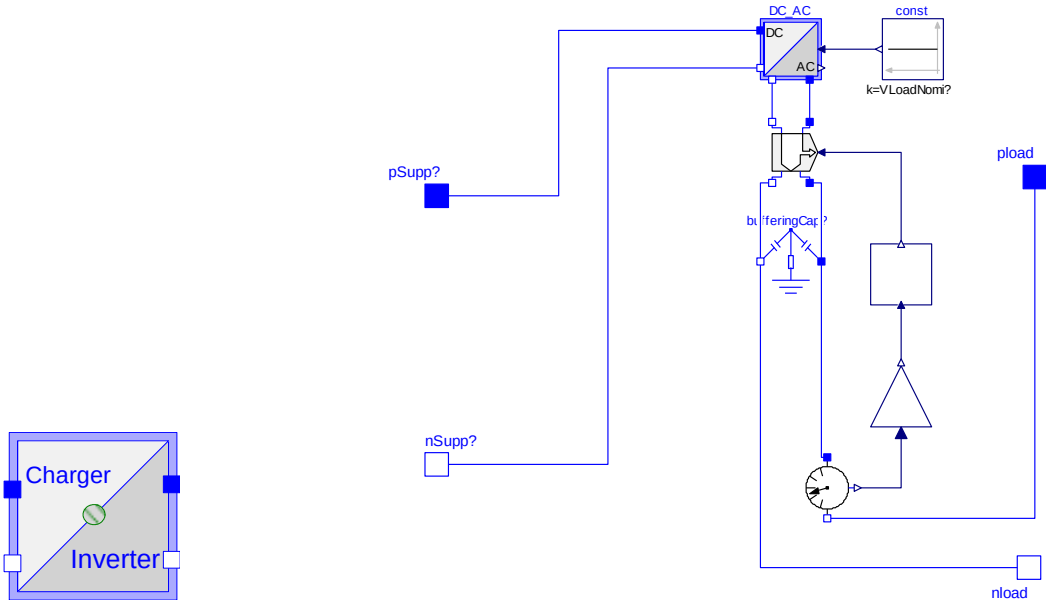

(a)Exterior (b) Interior

Fig. 5.14 *Charger/Inverter*

to connect with other AC loads. The conversion device in Fig. 5.14 converts DC to AC or AC to DC electricity. The Charger/Inverter model is a bidirectional device which can transfer DC power to AC power and vice versa. Three main modules have been included, *DC_AC*, *efficiency* and *f* function. Energy loss over delivery has been taken into account by using the function module *f*.

5.2.5 **Grid/Load**

The *Grid/Load* model in Fig. 5.15 is a simple model consisting of a *powerLoad* component and a *PowerData* model. The *PowerLoads* component has electrical property and decides how much load power should be applied. The element PowerData provides the power value of the load/charger in the simulation. For the purpose of simplicity, the data representing the power from the grid and from the load demand were included into one table (*PowerData*) where negative values represent grid power for charging purposes and positive ones stand for discharging power to supply the load.

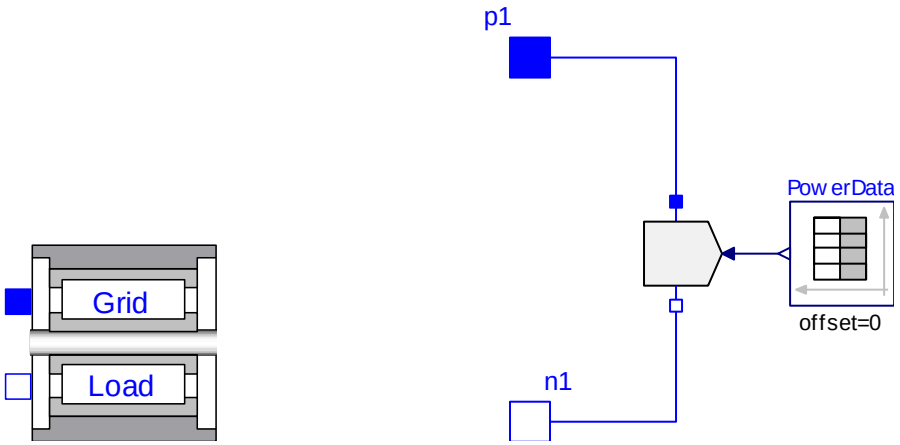

(a) Exterior (b)Interior

Fig. 5.15 Grid/Load model

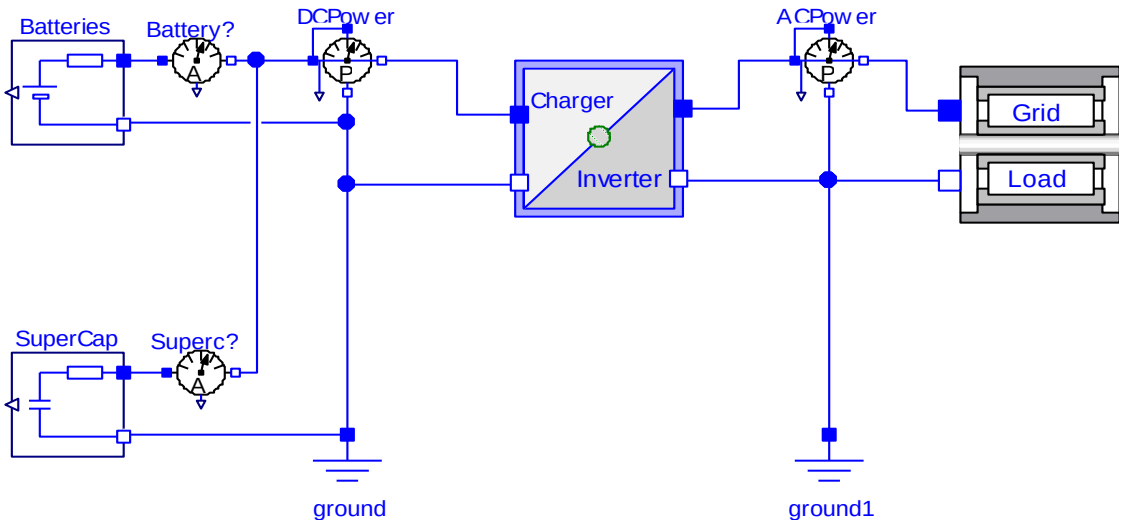

Fig. 5.16 Simulation for HEES performance test

5.3 **Modelling and simulation for the preliminary tests**

5.3.1 **Methodology**

The HEES system is shown in Fig. 5.16 where the batteries and super capacitors were connected in parallel and then linked with the Charger/Inverter. The DC sources (batteries and super capacitors) deliver the power to the load via the inverter which converts the DC current into AC current. Similarly, AC power from the grid was converted by the charger when it is used to charge DC sources. Power loss during the process is accounted for in the component 'charger/inverter'.

The curve in Fig. 5.17 shows the power demand profile which was applied by the 'Grid/Load' model where both positive and negtive values were included. The positive power shows periods when the power was supplied from the DC sources (batteries and super capacitors) whilst negtive values represented the power from the grid used to charge the DC sources (batteries and super capacitors).

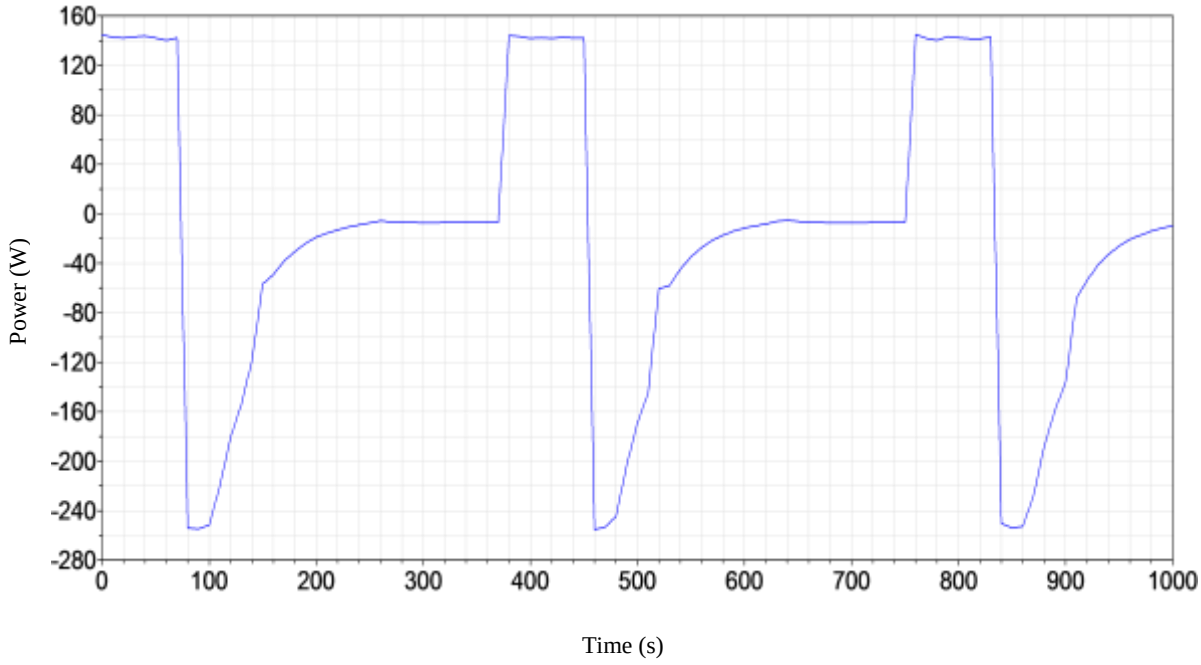

Fig. 5.17 Power from Grid/Load

5.3.2 **Outcomes and analysis**

A **Power delivery**

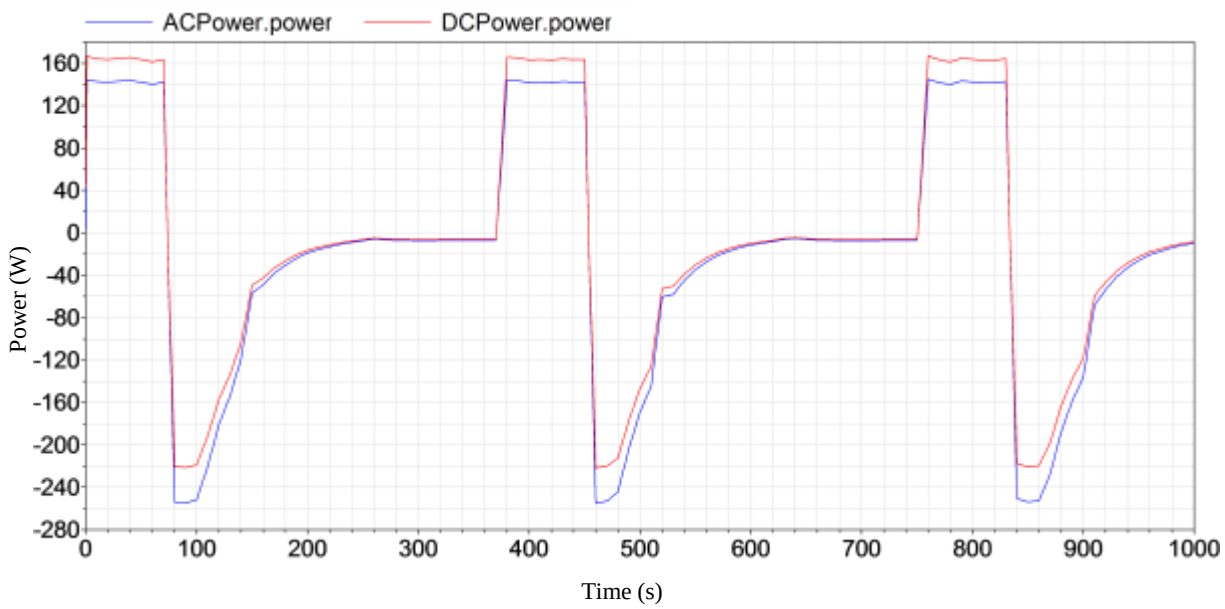

Fig. 5.18 Power scenario

The charging and discharging of the DC sources can be seen in Fig. 5.18. The blue curve in Fig. 5.18 represents the power required by the electrical load or coming from the grid while the red one shows the DC power to/from the DC sources. The difference between these two curves is due to the power loss within the inverter/charger as mentioned earlier. For instance, 251.7 W of AC power is provided by the grid while 218.8 W of DC power is delivered to the DC sources (batteries and super capacitors) at 100 s. The efficiency of the inverter/charger is 86.95%. In another case, there was 163.7 W of DC power provided by the batteries and super capacitors while 142.2 W of power was transmitted to the AC load at the time of 450 s. The efficiency was 86.92% this time. Energy efficiency had a 0.03% difference between these two cases with the efficiency at 100s being slightly higher than that at 450 s due to the different amount of power delivered at each point in time. The higher the power that was delivered, the higher the efficiency in these tests.

B **Current flows**

Fig. 5.19 shows the current scenarios of the batteries and super capacitors during charge/discharge operations. The blue line, red line and green line in the figure represent the super capacitor current, battery current and the total current respectively.

Initially, both the super capacitors and batteries were discharged. The current from the super capacitor to the load increased more rapidly than did that from the batteries. The super capacitor initially supplied 3.35 A while the batteries provided 0.94 A. However, the current from the super capacitors reduced quickly as its voltage decreased. At the same time, the batteries increased their output current. Therefore, the total power output from the DC sources was able to keep the same level as expected even though the total current (green line) from both the super capacitors and batteries increased slightly due to the DC voltage dropping.

The performance of these two sources during charging has a similar trend to their discharge. The super capacitors absorbed much more current than the batteries did initially. As seen at the time point 80 s, the super capacitors absorbed 5.23 A current where only 0.34 A current was achieved by the batteries. The super capacitor current decreased rapidly as the voltage increased quickly. By contrast, the batteries absorbed current increasingly with a small amount initially.

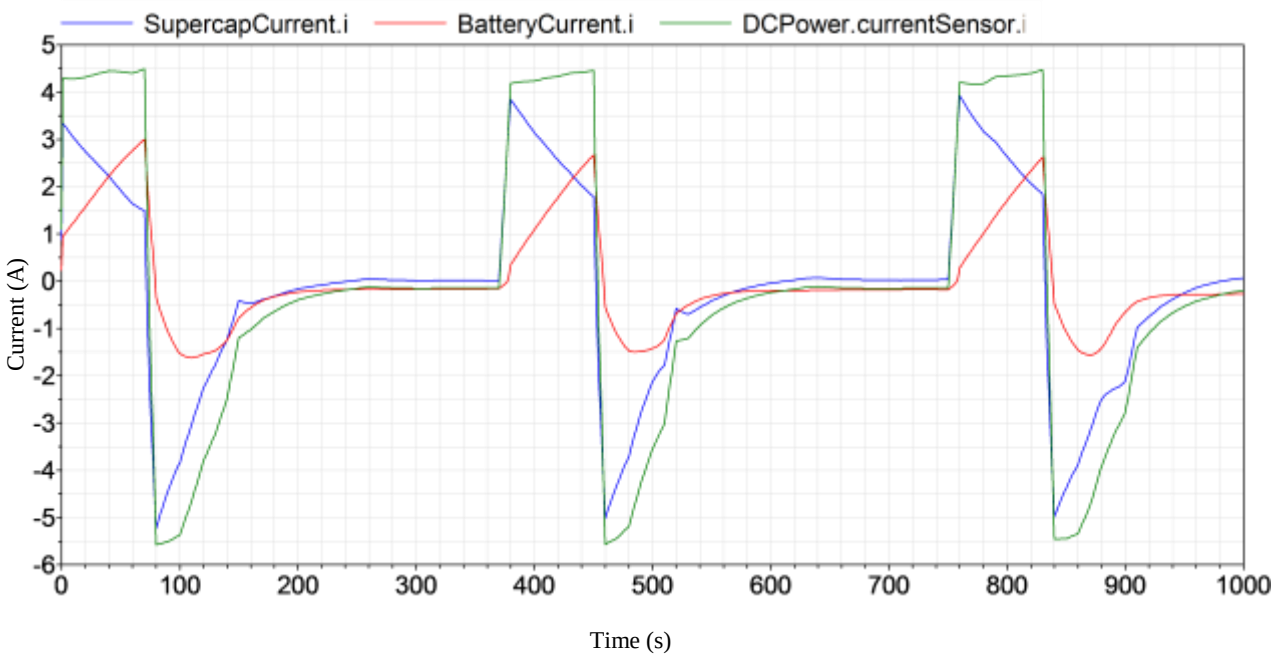

Fig. 5.19 Current scenario of the DC sources

In both charging and discharging, the super capacitor showed fast response while the batteries had a relatively slow response.

C **DC voltage scenario**

Fig. 5.20 shows the voltage curve during the charge/discharge operation. Over the period between 0 s to 80 s, the DC sources were discharged and the voltage decreased from 39.5 V to 36.4 V. During charging, the voltage increased gradually with the three stage charging procedure. Again, the discharging/charging cycle repeated after 370s. At this time, the voltage maintained the same level for some time and this indicated that the sources were fully charged.

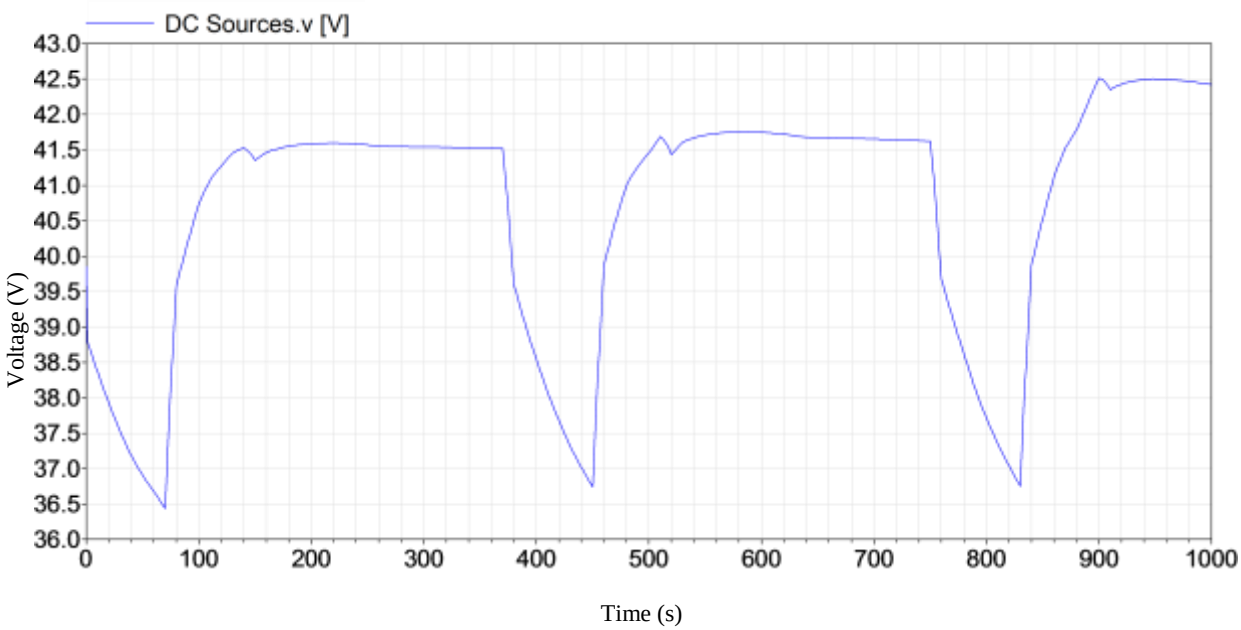

Fig. 5.20 The voltage curve of the DC sources

Overall, the purpose of the preliminary simulation was to assess the performance of the hybrid DC sources before the physical system was set up. In the simulation, the super capacitors exhibited good dynamic characteristics over short time scales, more suitable for household applications. The DC voltage reflected both the voltages of the batteries and super capacitors due to the parallel connection between them. The conversion model of the *Charger/Inverter* was built up on the basis of the principle of energy balance and energy efficiency along with power variation, which made the model close to the practical case.

The preliminary simulation employed a simple power demand profile to assess the hybrid electric energy storage system (HEES) without consideration of integration with the main power source, e.g. engine system. Therefore, the following section carries out further investigation improving the system step by step.

5.4 System improvement and performance evaluation

The aim of this research was to develop a complete BMT-HEES system which could accommodate complex domestic energy demands. In order to build up the whole system, the performance in large scale applications needed to be estimated along with an initial system

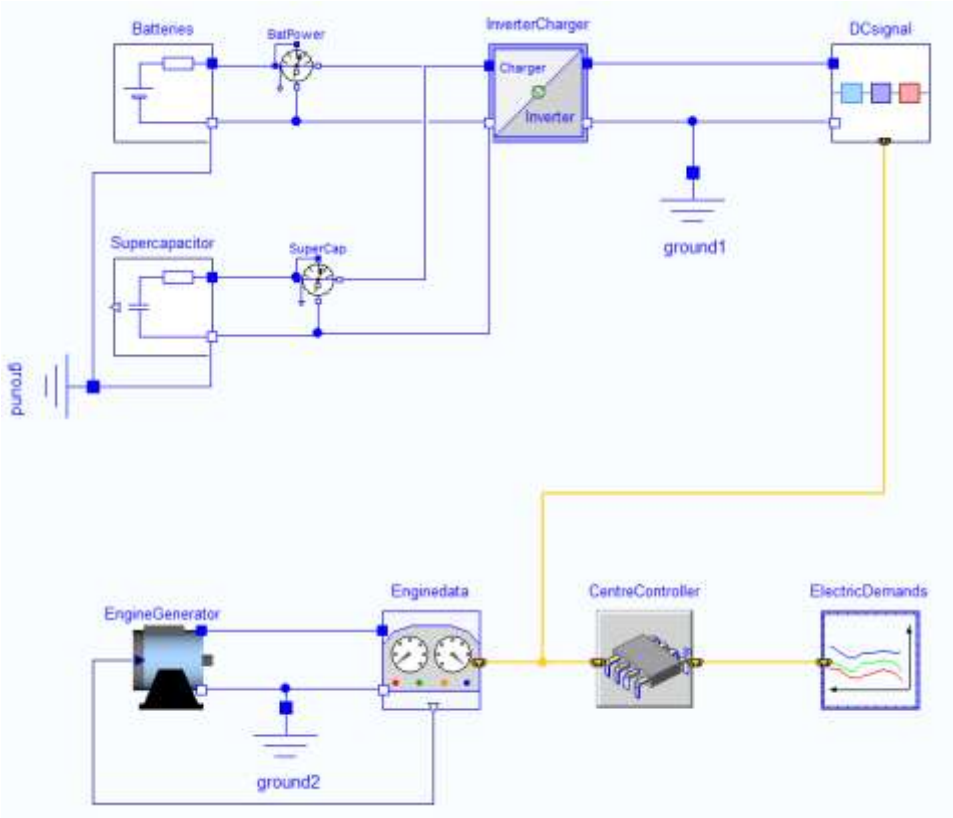

Fig. 5.21 Initial BMT-HEES system model on the top level

model, as shown in Fig. 5.21. The system model included the key control unit *CentreController* as seen in Fig. 5.21 which realised the operational method under the energy management strategy. System performance was estimated and compared with the common tri-generation system without HEES. Compared indicators included energies (electricity and heat), duration (e.g. engine operational duration,etc), efficiencies (e.g. electrical or heat efficiency, etc.), and power range (e.g. engine power output range for two different systems,etc.).

5.4.1 Energy management

A normal domestic electricity profile over 24 hours varies over a wide range and an engine-based tri-generation was hardly able to meet this demand for the reasons below,

- First of all, domestic electrical power demands typically consist of a couple of hundreds watts over most time of a day but with several thousand watts within short period (1-2 minutes). To meet peak demands, the nominal power of the engine has to match the power demands of a household. But an engine might have low electrical efficiency due to running at low power output over most of the time.
- Electricity demands fluctuate over a day and the change in demands occurs quickly and by a large amount. However, an engine has to undergo a transient process to reach the stable output.

Table 5.3 Description of the operational state

State	State description	Power source(s) in operation
1	In peak-demand : electricity demands greater than output of the generator set	Engine/generator with DC sources
2	Non-peak demand Generator supplies electricity to the load and meanwhile charges DC devices	Engine/generator with DC sources
3	Low demand DC devices supply electricity to the load without generator	DC sources

Table 5.4 Variables summary

Variable name	Explanation	Note
Flags	Engine operational state	=True Engine on =False Engine off
flagEnd	State variable (true or false) represents charge state	=True Charge end =False Charging
p_{charge}	Default charge power for storage system	Default setting charge curve $f(t, SOC)$
p_{gen}	The maximum value of output power from generator	Constant
p_{load}	Load power demands	--
$P_{Storage}$	Maximum discharge power from storage system	Constant

Therefore, an electric storage system was required to be integrated into the system to improve the performance of the system. The key issue arises in terms of coordinating the engine and the electric energy storage system. The system operates in different modes

depending on the SOC of the DC sources and the demand. The engine provides electricity to satisfy household demands while also charging the hybrid DC devices (batteries and super capacitors). The DC sources supplied electricity as a supplement to assist the engine over the peak period and then were charged by the engine/generator within a certain duration when the demands were relatively low. Table 5.3 describes the system operation, in relation to an initial plan for energy supply management as shown in Fig. 5.22. Table 5.4 summarizes the variables applied to the control process. There were three main states and two sub states applied to the system operational procedures. State 1 is for the condition that both the generator set and DC sources are supplying electricity. In operating state 2, the generator set supplies both the electric load and the DC source charging. In operating state 3, the electric storage system (DC sources) provided electricity to the domestic appliances alone and the generator set is switched off in the period of low electricity requirement. Sub-state 2-1 and 2-2 stood for two different charging approaches. In sub-state 2-2, the HEES was charged by default charging curves. Otherwise, the demand must be met first and the charge power is equal to the generator power minus the demand load. The optimisation energy management strategies were programmed in the control system for energy demands analysis as well as decision-making for energy allocation.

5.4.2 **Operational methods**

According to the principle of operation stated above, relevant models were built up. In simulation, the models on the top level represented the whole structure of the electricity supplying system. Batteries and super-capacitors were linked together in parallel. On the other hand, the generator set was an AC power source connected with the unit of *Enginedata*, in which power for the generator set was decided by the component of *CentreController*. The role of the *CentreController* model was to decide the operational state based on the electricity demand data before calculating the energy amount to both AC sources and DC sources.

A **Model *CentreController***

The state diagram shown in Fig. 5.22 was implemented by the *CentreController*. During the period of low power requirement (state 3), power was supplied from the storage system with a power demand less than 4000W. In this case, the power storage system would not be able

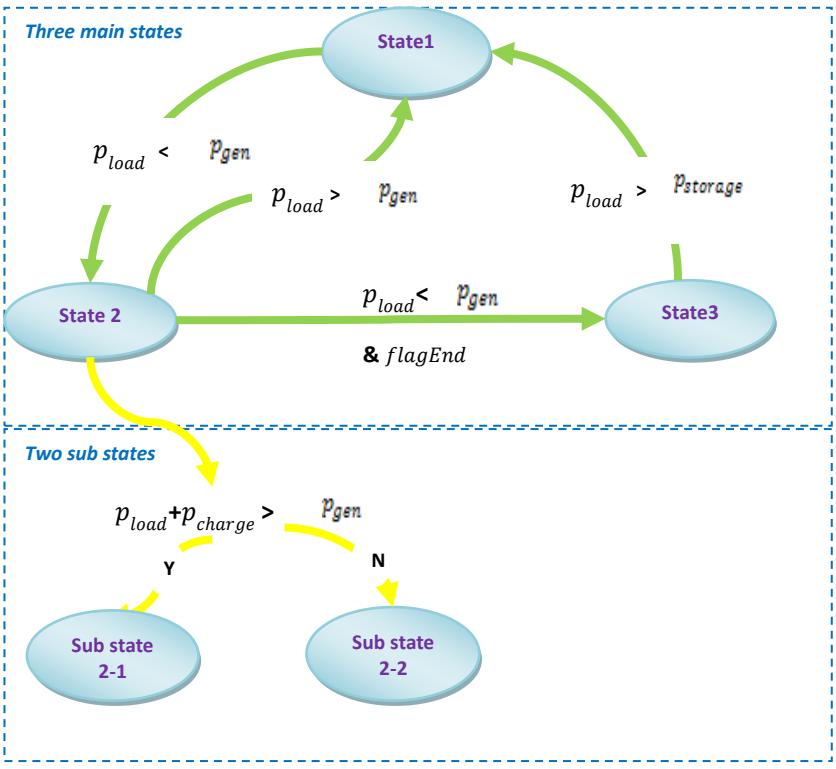

Fig. 5.22 State flow chart for the operation of the system

to provide enough power for the household load and the system would go back to state 1 where the generator set worked together with the HEES to satisfy the load requirements over

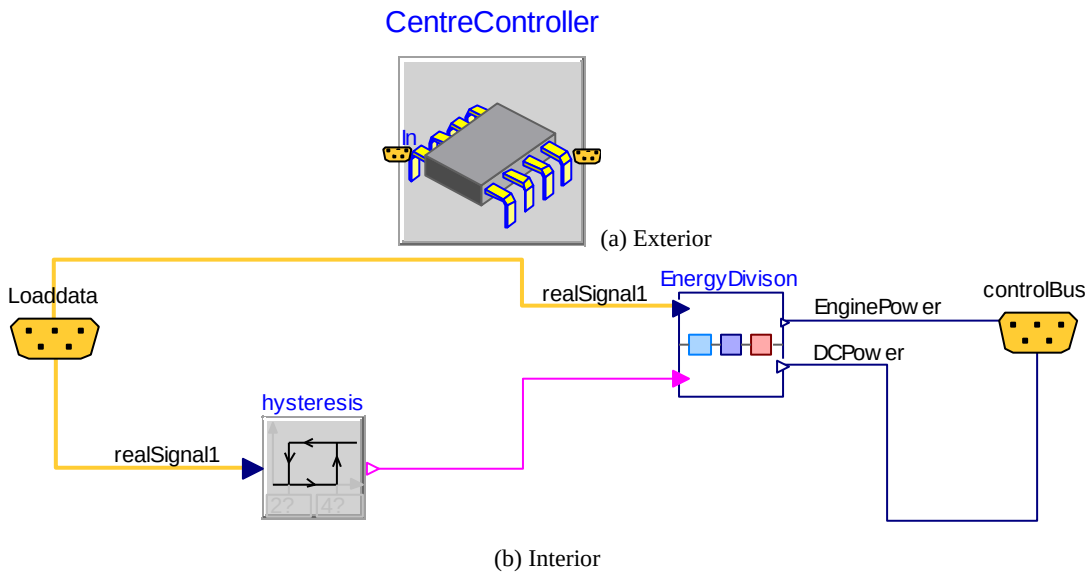

Fig. 5.23 Model CentreController

peak time. If the load power demand reduced to below 2500W, the available power drawn from the generator was greater than the household demand. Therefore, extra current could be provided to charge the storage system and the system entered state 2. The system entered state 3 when HEES was fully charged and household electricity demands were within 2500 W. Otherwise, the system transferred from state 2 to state 1 when the electricity demand was more than 2500 W. In fact, state 2 included two different operational sub-states. In one case, HEES was charged by the engine with pre-setting charge equation *f(t)* if the engine was able to supply enough electricity for both the load and charging requirements. Otherwise, the majority of electricity generated by the engine/generator was used to supply to the load and the remaining electricity was used to charge the HEES. The model *CentreController* fulfilled the function stated above. Fig. 5.23 (a) shows the exterior when it was employed by the higher level model (in the system in Fig. 5.21 or Fig. 5.26, for instance) and Fig. 5.23 (b) shows detailed model with its construction. The model *CentreController* accepted external data via data bus *Loaddata* and then sent it to the model *EnergyDivision* and meanwhile fed into the model *hysteresis*.

In the model *CentreController* in Fig. 5.23, *hysteresis* had two threshold values, the upper

one of 4000 and the low one of 2500. The component *hysteresis* accepted the signal *realSignal1* representing load data and compared with these two thresholds. If *realSignal1* increased above the upper limit (4000), the binary output signal of the *hysteresis* model would be set to *1* (true). By contrast, if the input decreased below the lower limit (2500), the output would be set to *0* (false). This binary signal was sent to the component *EnergyDivison* along with the load data (*realSignal1*) as two inputs to calculate the output data for the amount of power the engine (*EnginePower*) and DC sources (*DCPower*) should provide. Signals *EnginePower* and *DCPower* were sent out via the component *controlBus* linked with the other models outside *CentreController*.

B ***Model EnergyDivision***

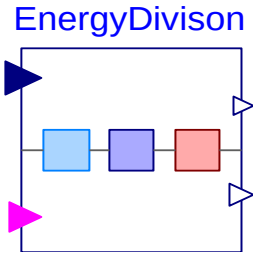

Fig. 5.24 (a) Model EnergyDivision

Fig. 5.24 (a) illustrates the top level of the model *EnergyDivision*, in which the system operation state and energy amount for each power sources (generator, DC devices) were decided. After that, the value of the transient power amount needed was sent out via *controlBus*. The *EnergyDivsion* component was programmed by using the language *Modelica*. The programme flow chart is presented as Fig. 5.24 (b).

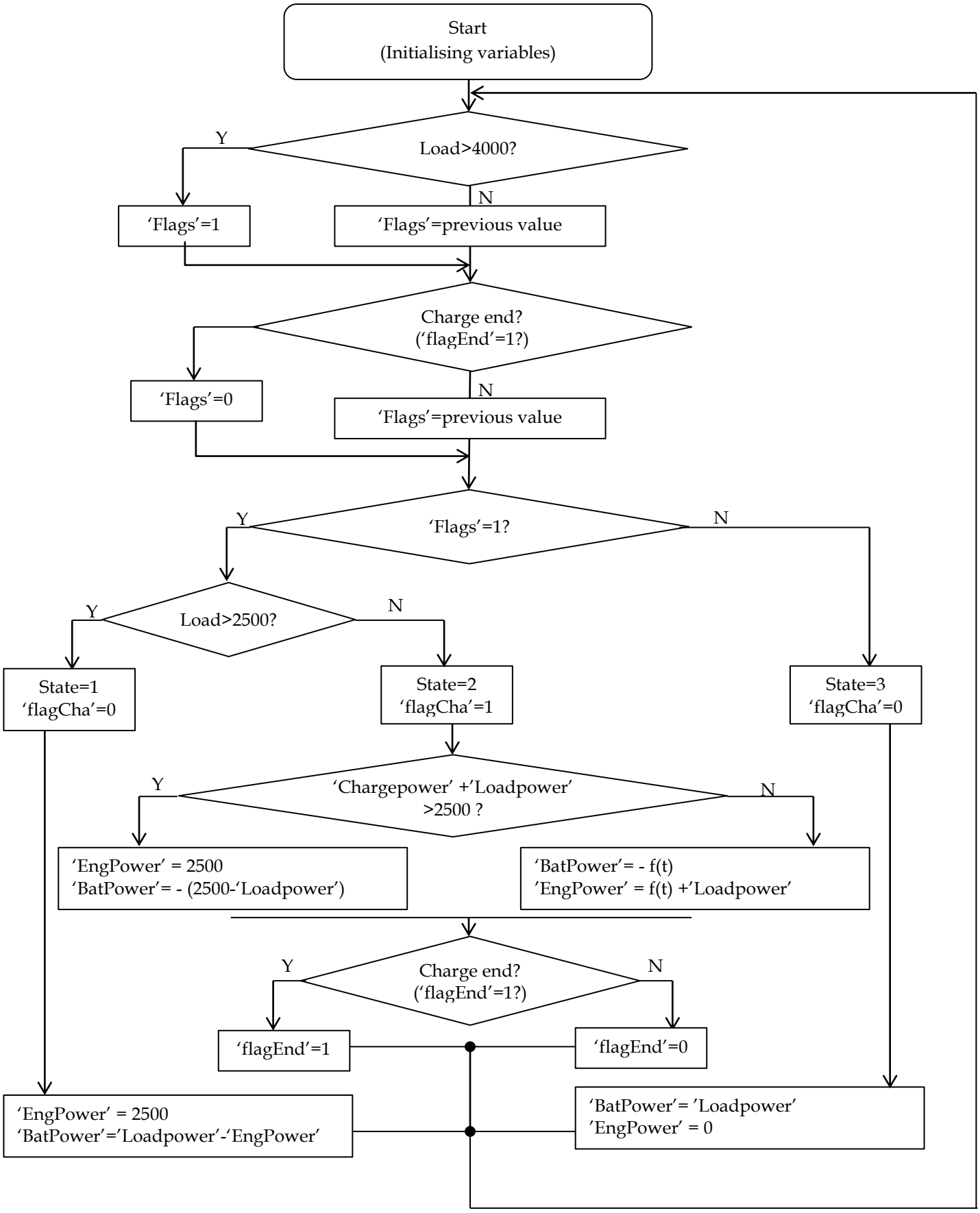

Fig. 5.24 (b) Main program flow chart for the model EnegyDivision

The flow chart in Fig. 5.24 (b) presents the whole process of energy distribution. Here, the variable *flags* represents the engine operation state. *Flags=true* means running the generator set and vice versa. The variables *flagEnd* stands for the charging state for the batteries and super-capacitors. *flagEnd=true* represents end of charge and vice versa.

5.5 Case studies

5.5.1 Case 1-domestic investigation with 2500W generator set

A Load power profiles

Fig. 5.25 (a) shows the electricity demand profile over 24 hours for a selected house in the UK [14]. From the figure, it can be seen that the minimum demand of electrical power was around 100W and the maximum demand reached 6544 W. The electricity consumption was lower than 1 kW during the majority of the 24-hour time while the peak demand occurred over relatively short periods. For instance, at 13:11 (47448s), the demand was as high as 6544 W before it plunged to 400 W 5 minutes later. The peak demands over 4000W took place twice, at 05:22 (19296s) and 13:11 (47448s). Electricity consumption for this household over 24 hours is 9.85 kWh in total.

In this case study, the following assumptions were made based on its electrical demand profile,

① The maximum power demand was set to 6544.85 W

② An engine was selected with 2500 W power output.

③ The HEES supplied the load with a maximum of 4 kW

④ This system was also compared with an engine-only system of 6500 W to check its effectiveness.

B Outcomes

Fig. 5.25 (b) to (d) illustrates various power profiles of the outputs.

- Engine/generator power profile

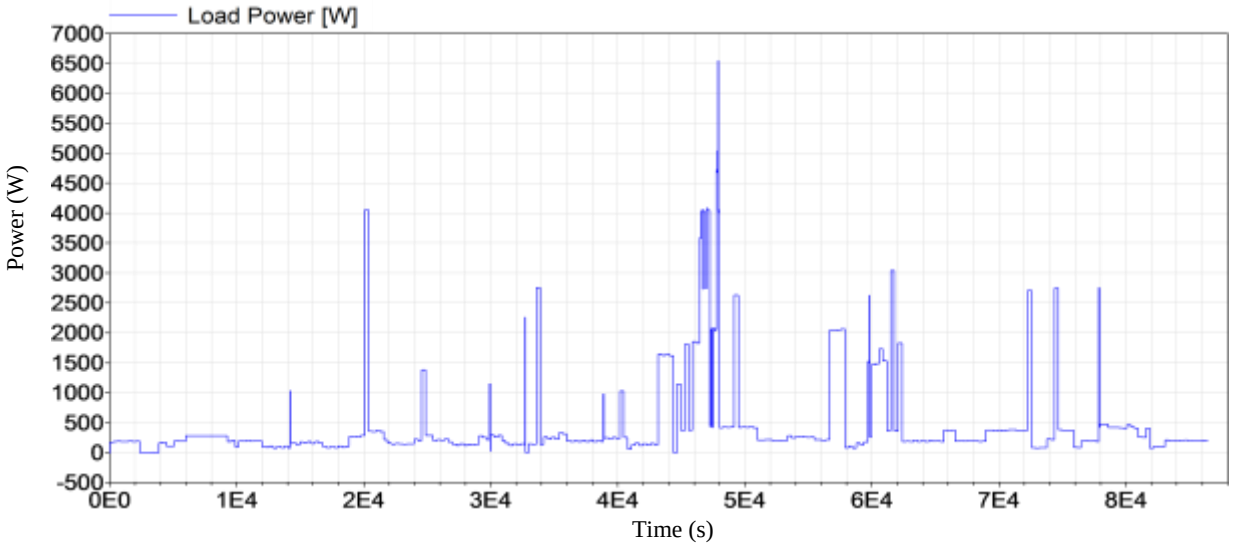

(a) Load power profile over 24 hours (86400 s)

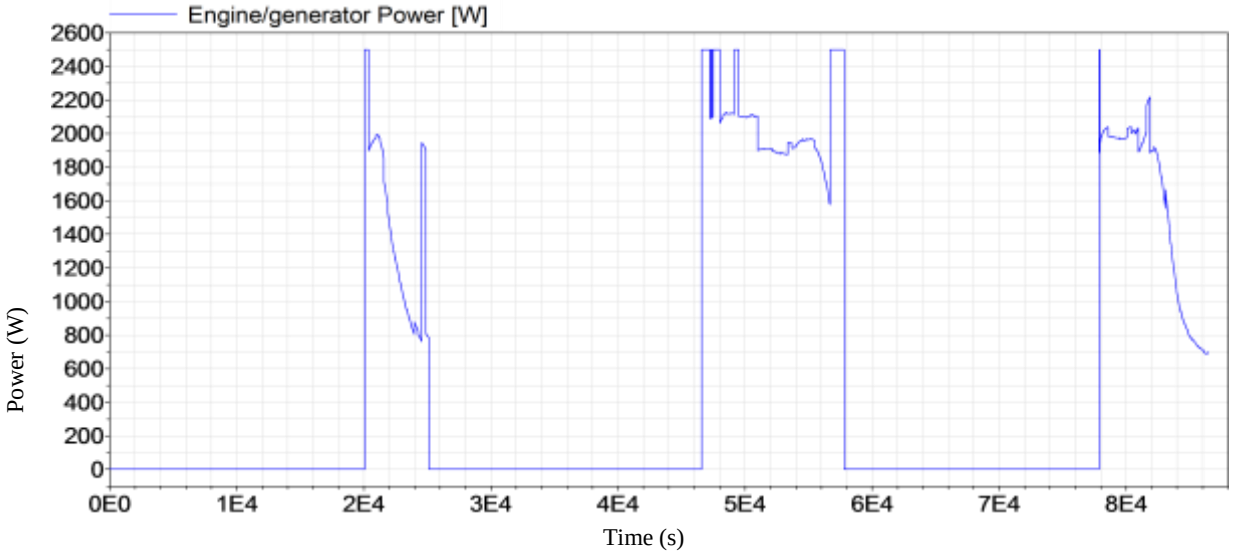

(b) Power profiles of the Energy/generator

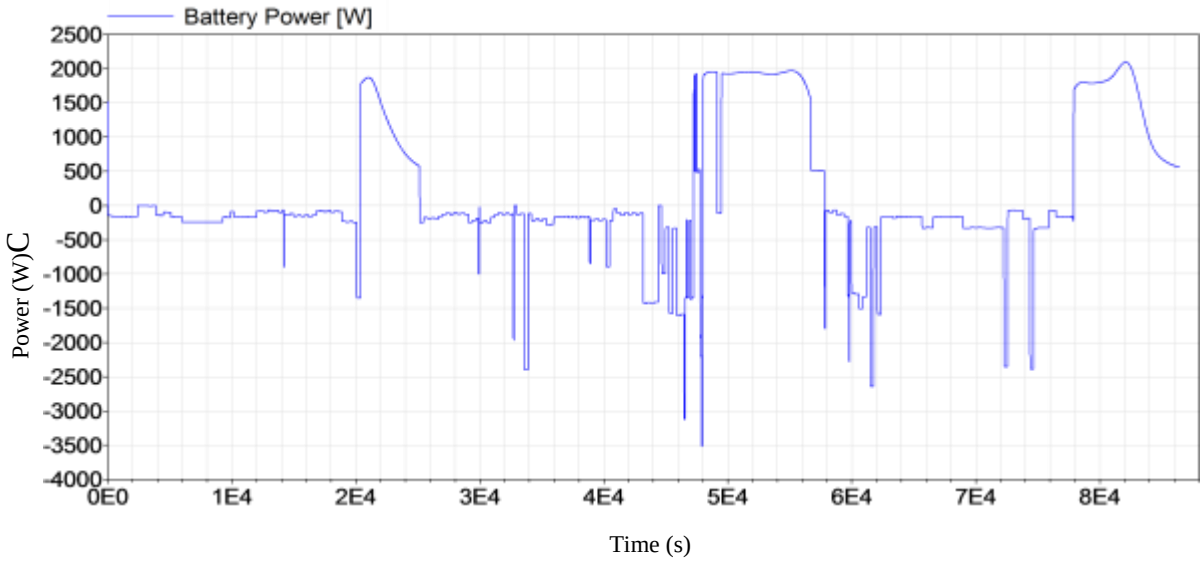

(c) Power profiles for the batteries

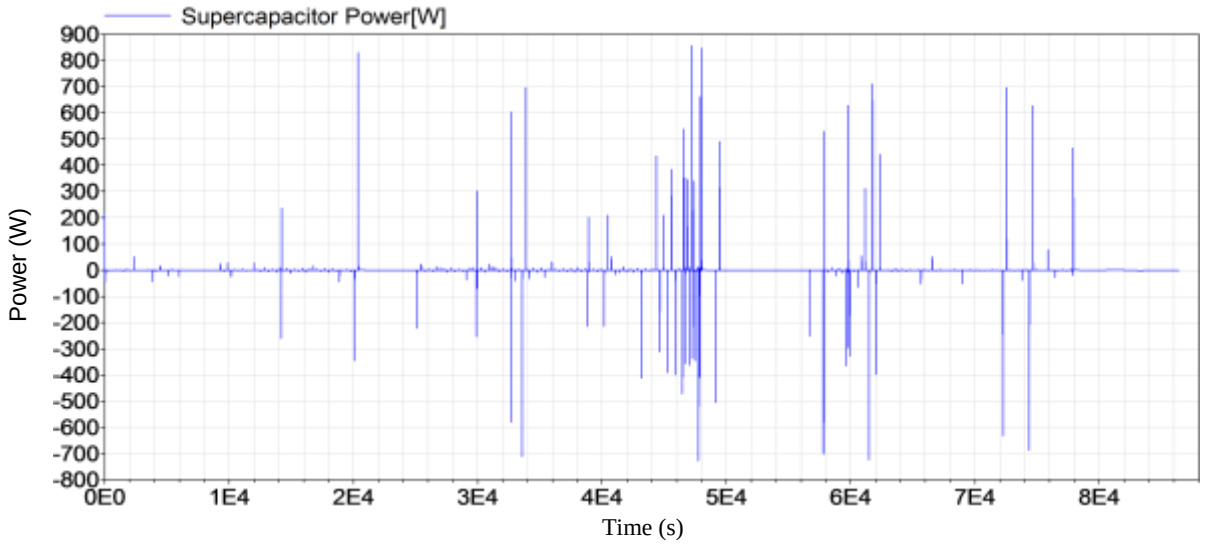

(d) Power profiles for the Super capacitors

Fig. 5.25 Power demands and supplies

The engine was switched on three times over the 24-hour investigation according to Fig. 5.25 (b). The decision on operating the engine mainly depended on the level of load power. If load power went beyond 4000W, the energy storage system was unable to supply enough power to the electrical loads and the engine needed to be started as the main power source to feed the load. Before midnight in this case, the engine needed to be switched on to charge the energy storage system to make sure there would be enough energy available over night. On

the basis of these operational arrangements, the engine started three times and its overall operation duration was 6.87 hours calculated from the simulation outputs.

- Battery profiles

Similarly, there were three times of the battery charging as presented in Fig. 5.25(c). The first two started after the end of the peak hours as the engine was still running. The last charging took place at 21:22 (76932 s) to make sure the storage devices had enough energy to cover the consumption over night. The batteries were able to operate within the power range from -3514.23 W to 2097.64 W in the simulation.

- Super-capacitor power profile

In Fig. 5.25 (d), the super-capacitors exhibited prompt response capability in the simulation. However, they could contribute limited energy to the system over an extended period. In other words, the amount of the energy supplied by the super capacitors was significantly less than the batteries. Meanwhile, the power of the super capacitors was quite limited, ranging from -663.7 (discharging) to 866.6 W (charging).

C **System efficiency analysis**

In order to identify the benefits of integrating the HEES, a comparison between the conventional engine-based system without HEES and the system with HEES was conducted. All the criteria associated with the efficiencies refer to arithmetic average value over the duty duration.

- Engine electric efficiency

According to the actual engine operation, the engine/generator started three times. Therefore, average efficiency over the operational duration of engine is calculated as,

$$E_{Gen} = \frac{\sum_0^K f_{Gen}(p)}{K} \qquad (5-16)$$

$f_{Gen}(p)$	Generator efficiency at power output p
K	Generator operational duration

- Battery operational efficiency

The battery operational efficiency is equal to its charge efficiency multiplied by its discharge efficiency.

$$E_{Bat} = \frac{\sum_0^M f_{Gen}(p)}{M} * \frac{\sum_0^N * f_{Bat}(p)}{N} \quad (5-17)$$

Where,

E_{Bat}	Average operational efficiency of batteries
$\frac{\sum_0^M f_{Gen}(p)}{M}$	Average charge efficiency of batteries operated over duration of M
$\frac{\sum_0^N * f_{Bat}(p)}{N}$	Average discharge efficiency of batteries operated over duration of N

- Overall electrical efficiency

The system operational efficiency including the HEES and supplying system is equal to the average efficiency of the power sources over the supply duration. Therefore, it can be expressed as follow,

$$E_{ave} = \frac{E_{Gen} + E_{Bat}}{2} \quad (5\text{-}18)$$

D **Comparison of the system with and without HEES**

Two types of electrical supply systems were compared as given in Table 5.5. The traditional energy system employed an engine only and the proposed system included an engine with an electrical energy storage system. From Table 5.5, it can be observed that the operational duration of the engine/generator decreased from 24 hours to 6.87 hours for the whole day while the engine efficiency increased dramatically from 5.0% to 25.9 %. On the other hand, the overall efficiency for the electrical supply system increased from 5.00% to 23.57% using the HEES.

Table 5.5 Comparison table of performance indicator in two electrical systems

System type / Item	Engine only	Engine with energy storage system
Engine nominal Power (kW)	6.5	2.5
Operational range (kW)	0 – 6.54	0 – 2.51
Engine operation duration (hours)	24	6.87
Storage system charge duration(hours)	N/P	6.46
Storage system charge range (W)	N/P	567.3 – 2097.6
Storage system discharge duration	N/P	17.05
Storage system discharge range (W)	N/P	0-4044.9
Storage system charge efficiency (%)	N/P	23.1
Storage system discharge efficiency (%)	N/P	21.2
Engine efficiency (%)	5.0	25.9
Overall electrical system efficiency (%)	5.0	23.6

Therefore, the engine/generator worked at a relatively high operational power level.

The above illustrated the operational efficiencies of the engine and the storage system over 24 hours. In the case of the engine without HEES, it provided all electricity required during the 24 hours and the instantaneous efficiency depends on the electricity requirement. The average electrical efficiency in the system with the engine only was low due to the fact that the engine operated with both low and high electrical load for the whole day. In the case of the engine with HEES, it was able to work with high efficiency continuously according to the optimal strategy. The engine was switched on three times with limited duration and the total duty period was 6.87 hours under the same load demand scenario. Accordingly, the engine efficiency increased dramatically and operational time was reduced.

5.5.2 **Case 2- domestic application with 6500 W generator set**

For case 2 study, the following assumptions were made,

① The maximum power demand was 10,290 W

② An engine was selected with 6.5 kW power output.

③ The HEES supplied a maximum power output of 4 kW

④ This system was also compared with an engine-only system of 10 kW.

In case study 2, the model of the system was further improved. A complete system model of the BMT-HEES was set up, as shown in Fig. 5.26. This system consisted of a diesel engine-based tri-generation and HEES units where fuel consumption, electricity generated, heat recovered and refrigeration temperature in real time were monitored. Meanwhile, dynamic response of the relevant units, including engine/generator, batteries and super capacitors were recorded.

In the system shown in Fig. 5.26, the HEES consisting of batteries and super capacitors was coupled with the 6.5 kW engine/ generator (main power source). All control signals governing the whole system were provided by the unit *centrecontroller* which collected the data of electrical demands before control signals were generated under the control strategy. Component *Fuel* calculated the instantaneous fuel consumption and meanwhile gave the total amount accumulated based on fuel types, in which the fuel characteristics were loaded before the calculation was carried out. The components *cooling* and *Heat* used the equations representing the heat and cooling characteristics of the systems. Therefore, simulation data was obtained from these calculations and shown via display units, such as *FuelConsumption*, *Totalfuel* and *Temperature* etc.

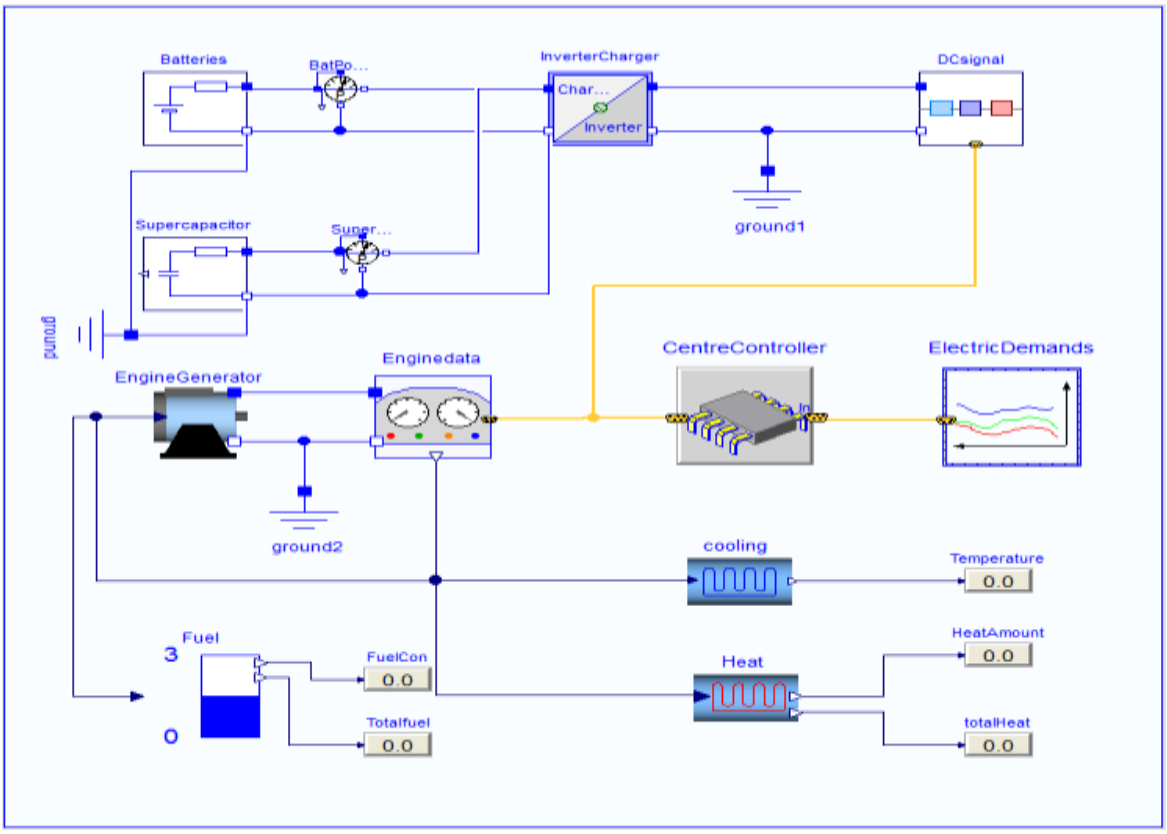

Fig. 5.26 Schematic layout of BMT-HEES system in Dymola

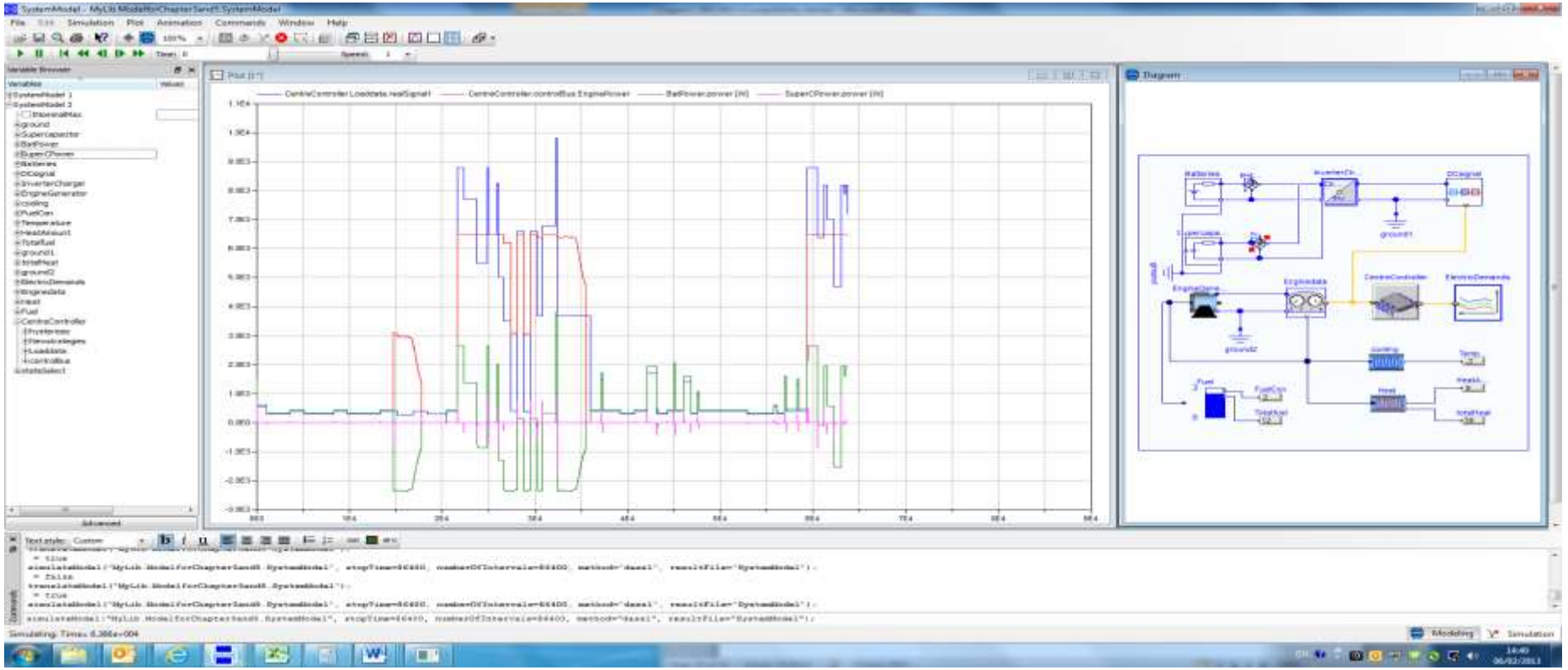

Fig. 5.27 Real-time simulation

Fig. 5.27 illustrates a dynamic picture corresponding to real-time simulation of the BMT-HEES under the control of the optimal energy management strategy. At the time 19:13 (69750s), the engine fuelled by rapeseed oil was running to generate a 6500 W power output to satisfy 3600 W of domestic electricity demand and charging the HEES with 2900 W. Heat recovered simultaneously was 9280 W and part of which was used in the absorption refrigerator at a temperature of -25.45°C. The real-time fuel consumption was 2.33 kg/h and the amount of fuel consumed by that time was 15.47 kg in total.

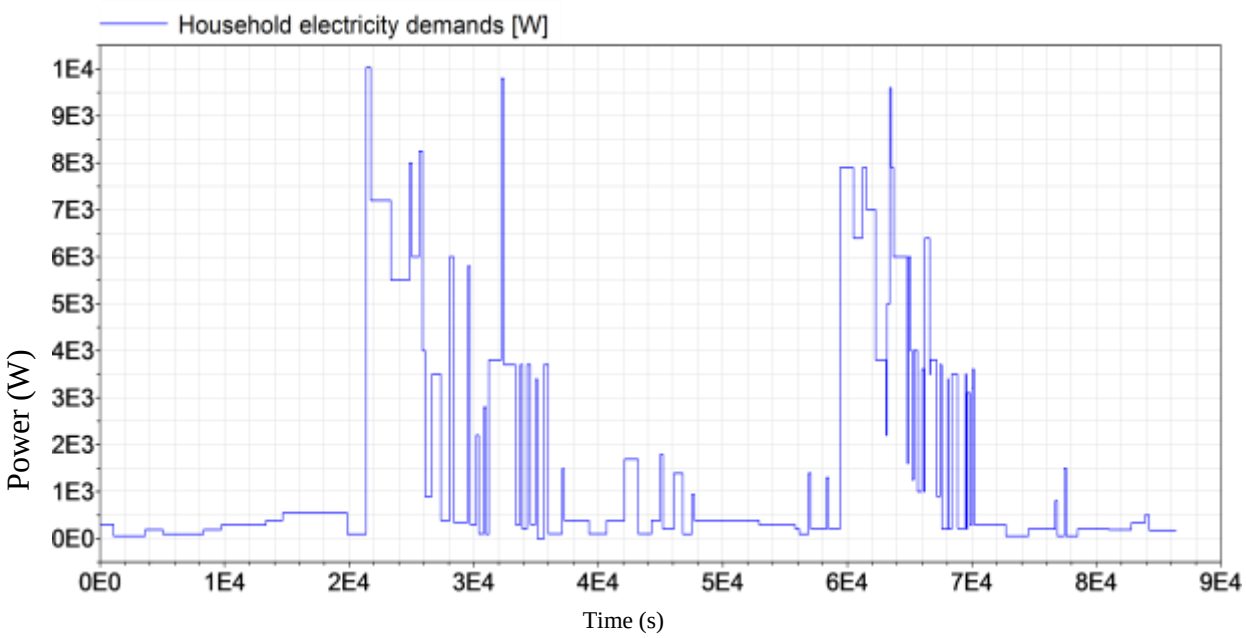

Fig. 5.28 Household electricity demands profile over 24 hours in case 2

A **Electricity demands scenario**

Case study 2 adopted a typical electricity demand scenario for a household as depicted in Fig. 5.28 [14]. There were two peak durations which took place at around 6am and 5pm. The maximum power reached approximately 10 kW while the minimum power was only 250W on this day. Basically, there was constant fluctuation from 0am to 6am, 12 o'clock to 4 pm 18 minutes where the load power varied from 290W to 540W, 250W to 1390W respectively.

B **Outcomes**

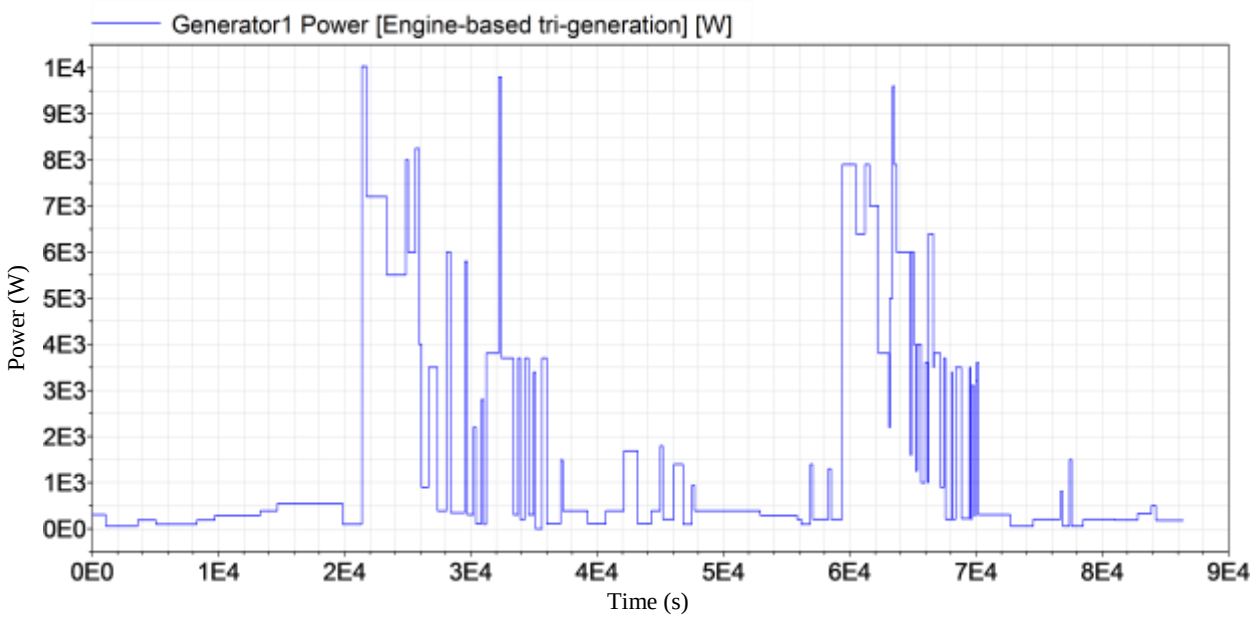

Fig. 5.29 Electric power output in system 1

Fig. 5.29 and Fig. 5.30 depict electric power output from system 1 and system 2. System 1 represented the engine-based tri-generation system without HEES. The output power from the generator set followed the household electric profile ranging from 250 W to 10 kW. Therefore, an engine/generator set with nominal electrical output of at least 10 kW was used. The electric efficiency of this system fluctuated from 7.8% to 28.1% over the whole 24 hours of operation. Meanwhile, the generator had average electric efficiency of 9.3% due to being operated with low efficiency for the majority of the time in one day. The system was able to recover 146.7 kWh thermal energy in total for household heating and hot water purposes.

By comparison, system 2 in Fig. 5.30 was the BMT-HEES system proposed which employed electric energy storage system and a set of energy management and control systems were included as well. From Fig. 5.30, it can be seen that the generator in this case was operated with relatively high electric output over limited duration. Therefore, relatively high electric efficiency was achieved under this operation. Meanwhile, the HEES as the main supplying source was operated over low electricity demands, for instance, from 0 am to 6 am. While it also assisted the engine as an auxiliary power source during peak demands from 6 am to 12 o'clock or from 16:18 to 18:18. The engine with nominal 6.5 kW electrical output in system 2 achieved 25.94% electrical efficiency on average over 24 hours of operation where 51.03

kWh of thermal energy was recovered. Relevant performance parameters in the simulation are summarised in Table 5.6.

Fig. 5.31 illustrates the response curves of the system in case study 2 with key variables of fuel consumption, heat and cooling characteristics shown. Fuel consumption, instantaneous heat power, accumulated amount of heat energy and cooling temperature are shown in Fig. 5.31 (a) to (d) respectively. With these diagrams, dynamic characteristics of the system could be learned, analysed and assessed.

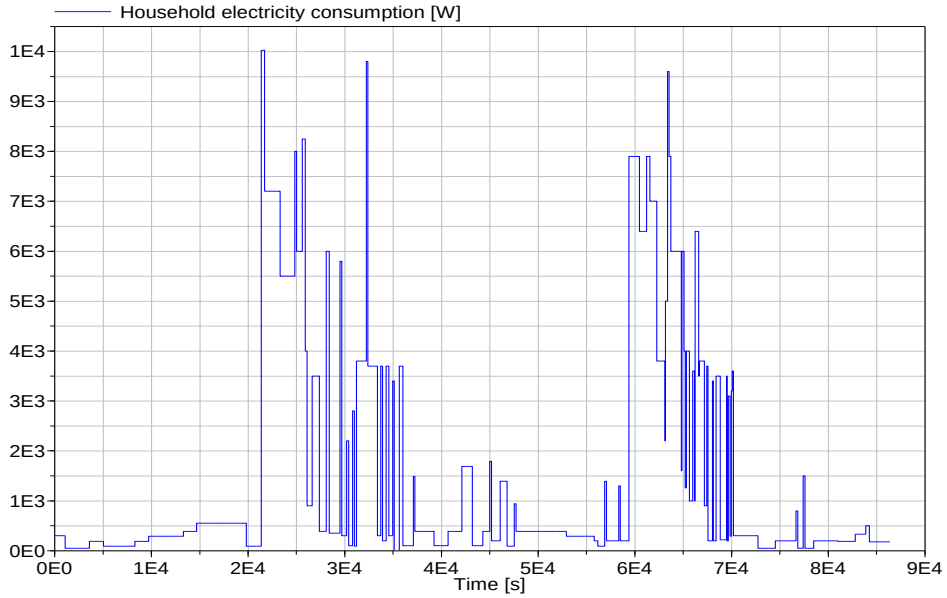

(a)

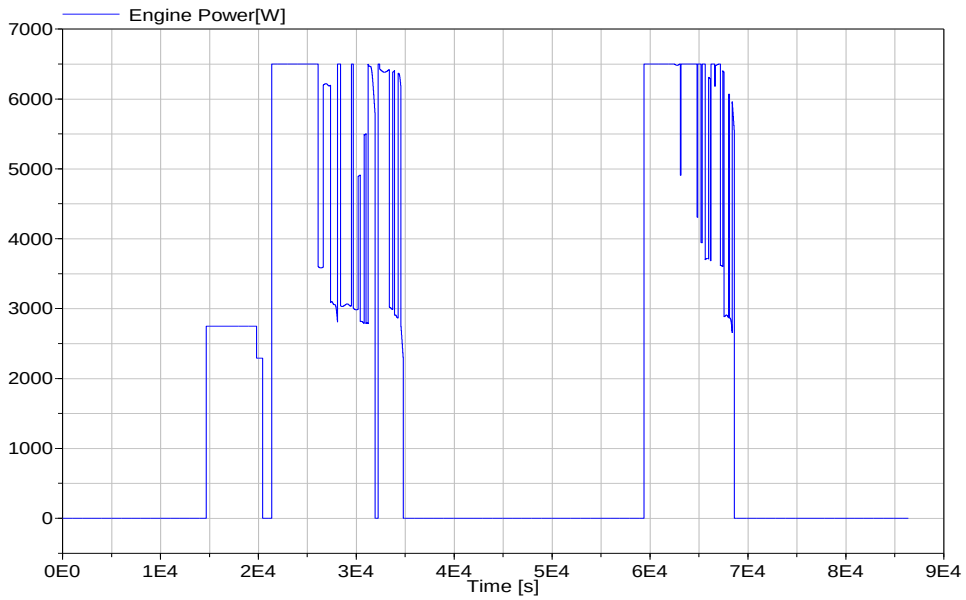

(b)

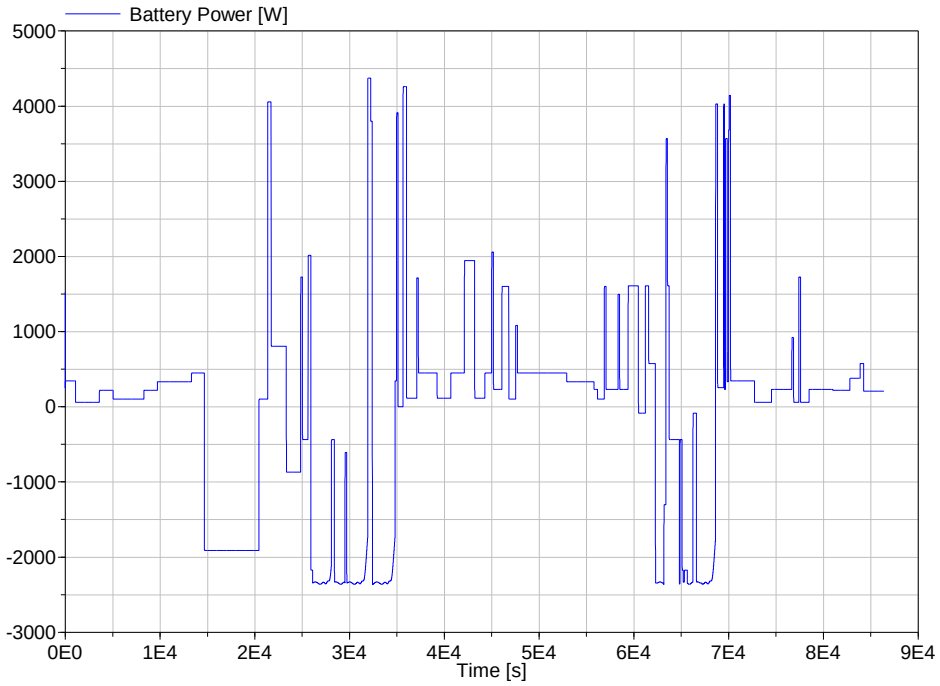

(c)

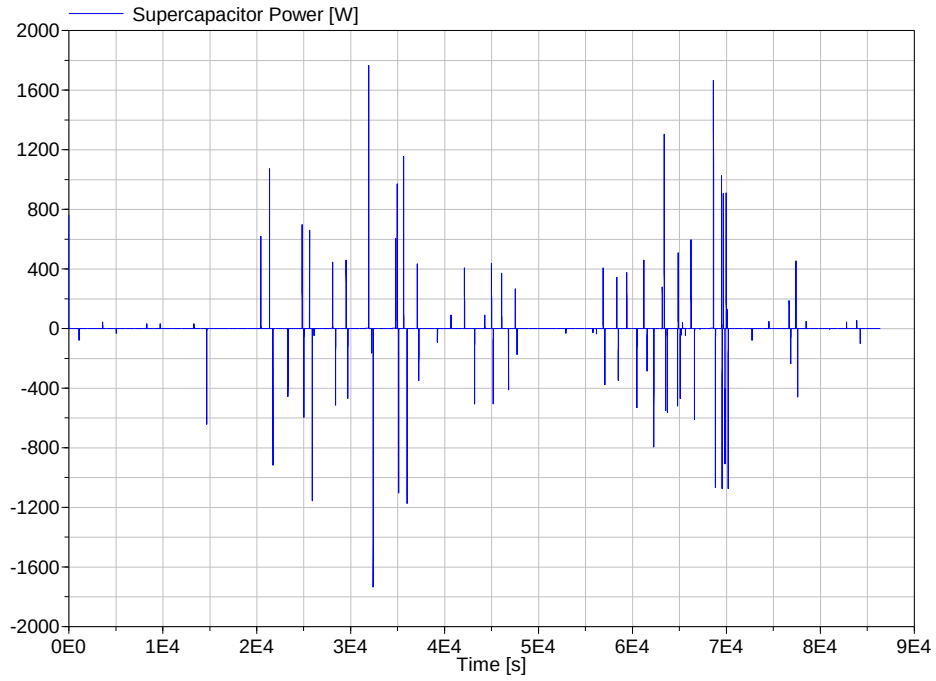

(d)

Fig.5.30 Electric power output in system 2

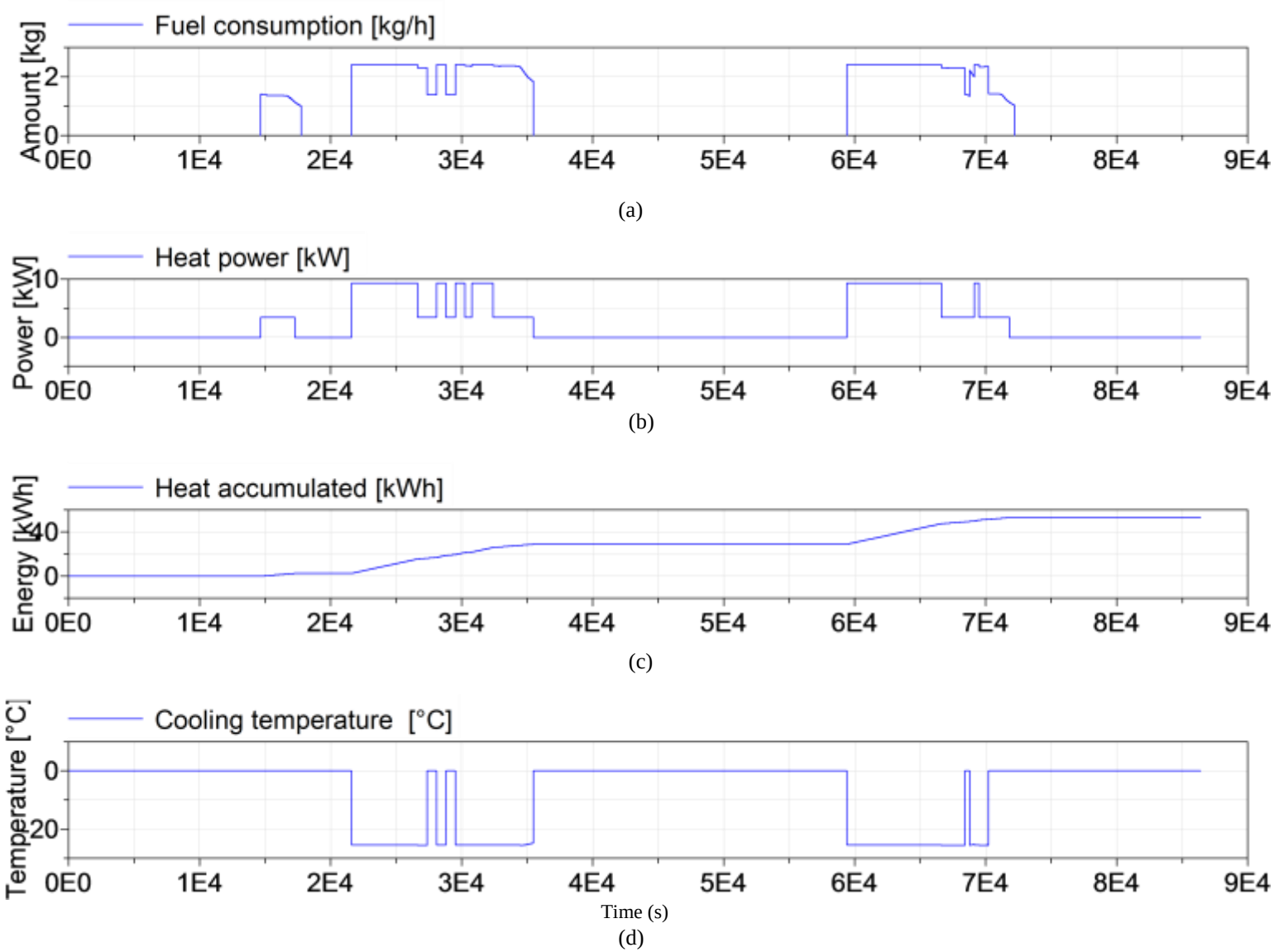

Fig. 5.31 Fuel consumption, heat and cooling curves over 24 hours

Table 5.6 Performance parameters summary in case 2 study

		System 1 Tri-generation (without HEES)	System 2 Tri-generation (with HEES)
Energy(kWh)	Discharge energy from HEES	-	9.12
	Electric energy from engine	32.96	34.41
	Energy supplying to load directly from engine	32.96	24.97
	Energy for charging energy storage system	-	15.05
	Electricity consumed by load	32.96	32.96
	Thermal energy recovered	140.40	51.03
Time (hrs)	HEES discharge duration	-	18.24
	Engine running	24.00	7.22
	Charge period for HEES	-	5.8
Efficiencies (%)	HEES electric efficiency	-	24.45
	Engine electric efficiency	7.20	25.94
	Heat efficiency	40.40	38.72
	System electric efficiency	7.20	25.20
	System overall efficiency	47.60	63.92
Power (W)	Variation of power, HEES	-	-2364/4373
	Variation of power, engine	0/10,290	0/6500
	Load power	0/10,290	0/10,290

C **Analysis**

Table 5.6 provides simulation results from case 2. The performance indicators include energy, operational duration, efficiencies, and power indicators. Compared to system 1, system 2 (Tri-generation with HEES) had apparently higher operational efficiency due to the assistance of electric energy storage that took on the majority of operation over the duration of low electricity demands. Meanwhile, even though electrical power as high as 10 kW was

requested over the 24 hours of operation, a smaller engine with nominal electric output of 6.5 kW was selected as the prime mover in the tri-generation-HEES while system 1 had to adopt a 10 kW engine to satisfy the same needs. Meanwhile, the operational duration of the engine

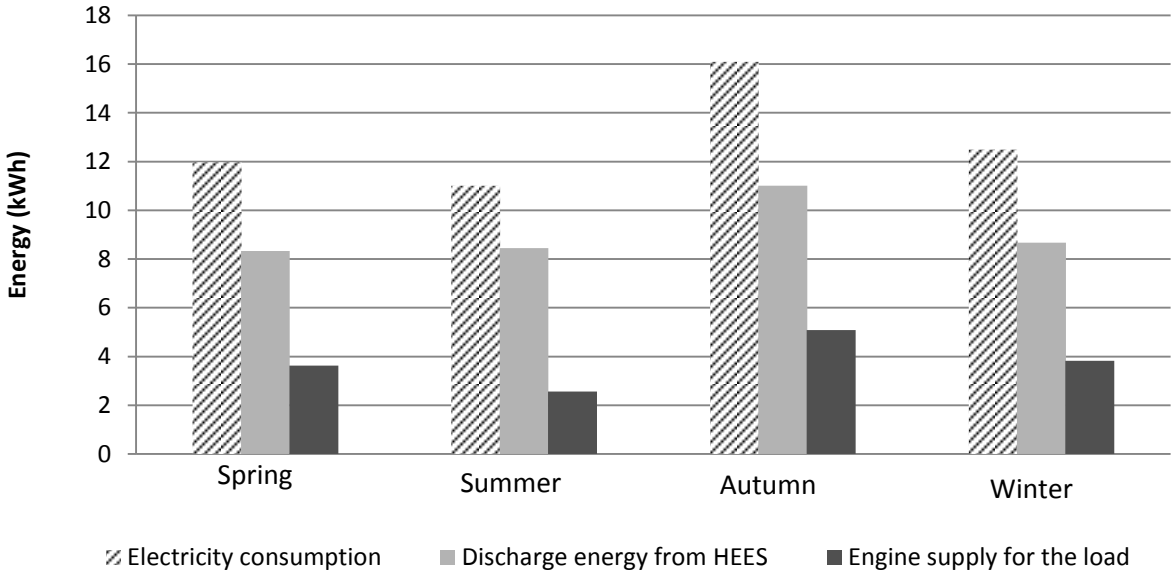

(a) Energy consumption and contribution

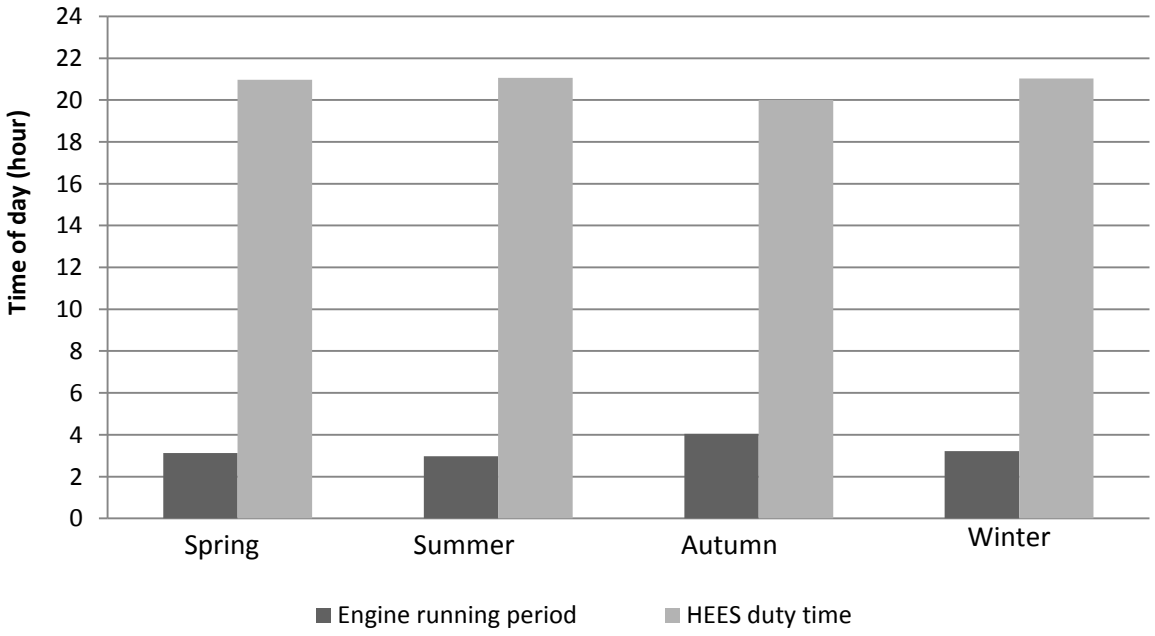

(b) Duty duration of the supplying sources

Fig. 5.32 Daily electricity consumption and supplies

declined from 24 hours (for 10 kW engine) to 7.22 hours (for 6.5 kW engine).

Under the same electrical demands with 32.96 kWh over 24 hours, the engine in system 2 supplied 34.41 kWh of electrical power with higher electrical efficiency (25.94%) while the tri-generation without HEES had only 7.2% electrical efficiency to contribute 32.96 kWh of electricity output. In other words, the amount from system 2 was almost the same as that from system 1 but the electrical efficiency improved dramatically. Meanwhile, the overall system efficiency increased as well, from 47.60% to 63.92% with a 16.32% improvement.

Clearly, the combination of batteries and super capacitors boost the dynamic performance of the energy storage system. There were two obvious advantages. On one hand, the batteries were not over-discharged even when the power demand increased suddenly because the super capacitors provided part of the electricity required. On the other hand, frequent fluctuation of power demands from the load within a short period of time was satisfied by super capacitors due to their speedy response capability. Therefore, over and frequent discharge of the batteries was avoided. In this application, a 30 V/160 F super capacitor module was linked with the batteries in parallel to assist their operation. In fact, alternate topologies of the HEES could benefit the system by decreasing the size of the super capacitor further and therefore reducing the system cost. This could be one option for system optimisation for future research. Naylor et al. [106] give a detailed discussion on the topic of hybrid energy system topologies.

The engine operation in system 2 was in good agreement with the findings explored by Huangfu, et al [22] who regarded the electricity efficiency as the highest influence factor concerning improving PER in CHP systems. He further advised that the prime mover should be operated with the electricity output greater than half load. This was proved by the results from system 2.

According to the statistics from the Office of Gas and Electricity Markets (OfGEM), end-user energy demand for average household is 21,000 kWh/year, 61% space heating and 23% hot water. So, the average thermal demand over one year was 48.3 kWh/day [10]. However, thermal energy recovered by off-grid CHP was apparently far more than this amount with 140.4 kWh recovered per day and much more energy was wasted. By contrast, 51.3 kWh of thermal energy was available in the tri-generation system with HEES. This was therefore the reason that the tri-generation with HEES system performed better than tri-generation without

HEES for common domestic applications where both electricity and heating energy produced by the tri-generation-HEES system can supply all the household demands properly.

5.5.3 Case 3 -BMT-HEES performance investigation based on domestic electricity consumption in four seasons

Case study 3 was carried out to consider four different daily electricity consumption profiles with respect to four seasons in one house where different bio-fuels or bio-oils were compared. Results of the BMT-HEES are shown in Appendix (A2).

Fig. 5.32 (a) illustrates daily electricity consumption and the contributions from each energy source. Taking the case of Spring for example, the total electricity demand in that day was 11.97 kWh and 8.33 kWh of electricity came from discharging the HEES and the rest 3.36 kWh, was provided directly by the engine running at the peak demand time. Actually, the total electricity generated by the engine was 9.59 kWh of which 5.96 kWh of electricity was used to charge the HEES and the rest 3.63 kWh was for supplying electric loads. In accordance with the supply contribution in Fig. 5.32 (b), the duty duration of the engine and the HEES were 3.12 hours and 20.97 hours respectively in this case. Table 5.7 summarizes performance indicators of the BMT-HEES over the four-season case study. Compared to the engine-based tri-generation, electric efficiency of the BMT-HEES increased dramatically by 441.4% and overall efficiency (electric and heat) was 58.08%, increasing by 29%. Obviously, system performance was promoted by integrating HEES into the engine-based supply system. The main reason for that was due to performance improvement of the engine that ran in limited periods with relatively high efficiency. For most of time, energy was derived from the HEES unit which was charged by the engine over a period of time.

Table 5.8 summarises various the fuel consumptions on a daily basis for the engine to satisfy domestic electricity demands in the simulation. From the table, it can be seen that consumption amounts for different fuels in the same case were slightly different. Take ‘Spring’ for example, fuel consumption for diesel, Rapeseed oil, Sunflower and Croton were 2.54 kg, 3.12 kg, 3.10 kg and 3.16 kg respectively for the single day demands. Autumn had a significant increase in terms of fuel consumption for various fuels. Croton consumed most in all these case studies while diesel was the least used.

The aim of the computational simulation based study was to assess the performance of the BMT-HEES system proposed before building up a full prototype. The following conclusions can be drawn:

First of all, the BMT-HEES system has superior energy efficiency which profited from the integration of HEES. Secondly, the implementation of super capacitors assisted the dynamic performance of the HEES system and prevented from over and frequent discharge of the batteries. Furthermore, the design of the BMT-HEES satisfied the criteria of system optimisation. Last but not least, both electricity and thermal energy generated by the BMT-HEES system met with the common domestic energy requirements, which was much better than the system without HEES.

Furthermore, in order to improve system dynamic response, the super capacitor module was integrated into system, which apparently increased system cost. However, the price of super capacitors has dramatically decreased along with the technology development. The cost of a 3 kF capacitor dropped from $5,000 in 2000 to $50 now[107]. The implementation of the BMT-HEES proposed is one of the competitive options for domestic energy supply system in the future.

Table 5.7 Performance summary in the case studies in four seasons

	Electricity consumption(kWh)	Engine supplying for the load(kWh)	engine supply in total(kWh)	discharge energy(kWh)	charge energy(kWh)	heat recovered(kWh)	Electric efficiency (%)	Increase of the electric efficiency (%)	Overall efficiency (%)	Increase of the overall efficiency (%)	Engine start time	Engine running period(Hours)	charge duration(Hours)	HEES duty time(Hours)
Spring day	11.97	3.63	9.59	8.33	5.96	15.98	20.79	441.4	58.08	29	30000/66840	3.12	3.03	20.97
Summer day	11.01	2.56	9.04	8.45	6.47	14.91	21.21	477.93	58.17	27.5	29050/63000	2.97	2.94	21.06
Autumn day	16.1	5.09	14.01	11.01	9.01	22.2	22.7	340.78	60.15	30.73	26350/62850	4.04	3.99	20.01
Winter day	12.5	3.83	9.57	8.67	5.72	15.53	21.72	424.64	58.67	28.35	31750/59950	3.22	2.97	21.03

Table 5.8 Daily fuel consumption in four seasons

Fuel consumption (kg) / Season	Diesel	Rapeseed oil	Sunflower	Croton
Spring	2.54	3.12	3.10	3.16
Summer	3.06	3.75	3.74	3.85
Autumn	5.42	6.64	6.61	6.75
Winter	2.43	2.97	2.96	3.02

5.6 **Summary**

This section presented the simulation outcomes before the practical investigation was carried out. Outcomes validated that the system with an optimal energy management strategy had relatively high efficiency where the engine was operated for limited duration with high electric efficiency. In this section, work has been done as follows,

The engine/generator mathematical model was discussed both in the process of starting and continuous operation before the computer model was built up in Dymola. Preliminary performance test of the engine system was carried out after that.

Key component models were introduced, including batteries, super capacitors, conversion device (Inverter/Charger), communication devices, energy management strategy and centre controller. Preliminary performance simulation for the HEES was carried out for estimation purpose before the prospective system was set up physically.

The BMT-HEES system was improved step by step along with the investigation of the case studies where diverse daily electricity consumptions were applied. Comparison between the BMT-HEES and a conventional CHP system with engine only were presented.

Furthermore, instantaneous fuel consumption and refrigeration temperature were displayed over the simulation and performance criteria were summarised, which provide detailed information for physical system estimation.

Chapter 6 Physical experiments of BMT- HEES

6.1 Introduction

In this chapter, experimental tests of the BMT-HEES system are introduced followed by the presentation of the preliminary test results from the HEES system.

6.2 Test plan

The performance tests of the system were divided into two parts. Firstly, the performance of the energy storage devices was evaluated. The purpose of this section was to investigate the performance of deep discharge or power/energy capacities with various discharge powers. Thus, how to operate the engine/generator to accommodate the fluctuations of the load demand with an appropriate operational strategy could be estimated. For this purpose, 4 groups of tests were carried out in which the batteries were operated with different discharge powers after the same charge process.

The second part of the tests aimed to evaluate the performance of the integrated BMT-HEES system. First of all, a Yanmar engine/generator was coupled with the HEES to supply the electrical loads under different power levels. For this purpose, different levels of electrical load were applied into the BMT-HEES system and continuous tests under these loads were carried out. Based on the outcomes of this test, a grid power of 2.5 kW was used to replace the engine/generator to match the HEES system and to carry on the experiments relating to the entire system performance with a specific household electrical profile over 24 hours. Finally, the HEES system was supplied with AC power to carry on the second study. From this experiment, the whole system performance indicators could be evaluated through the outcomes and the complete system could be built up as a result.

6.3 Test procedure

6.3.1 Battery performance tests

These tests aimed to evaluate the perfomance of the batteries as they were discharged with different power levels ranging from 1kW to 4kW. The circuit used for the test is illustrated in Fig. 6.1. The batteriess were linked with the 'Multiplus' via the DC port where the batteries received or released the power as commanded by the control unit in the 'Multiplus'. Data relating to the battereies was detected by the battery monitor and recorded in the files simultaneously.

Table 6.1 Parameters setting

Parameters	value
Current value (maximum AC input current)	16A
Maximum charge current	120A
Bulk Charge voltage	(Up to) 28.8V
Absorption Charge voltage	28.8V
Float Charge voltage	27.6V

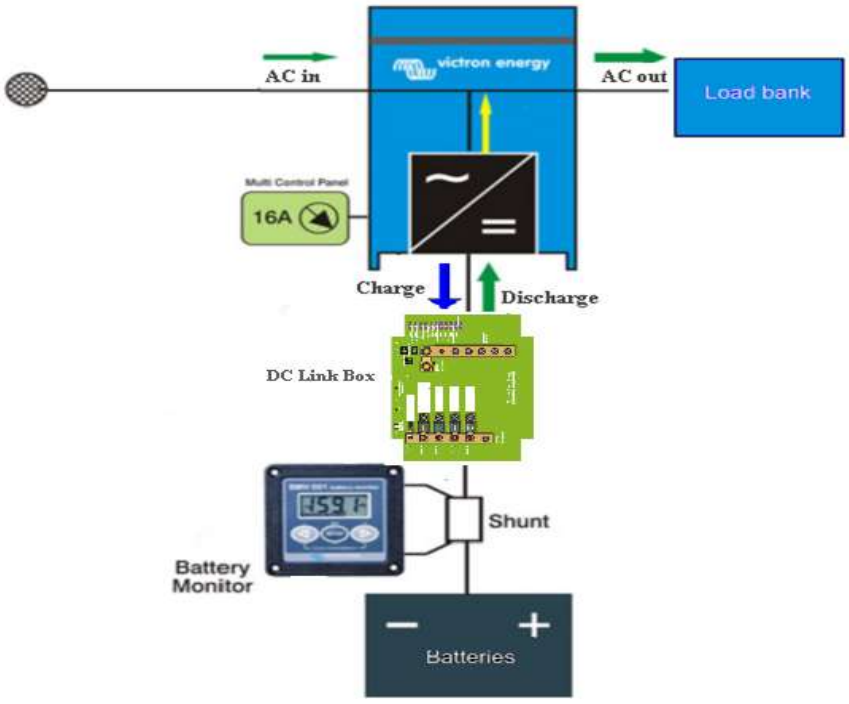

Fig. 6.1 Schematic diagram of the battery tests

Step 1

To set the key operational parameters shown in Table 6.1 before the test, other parameters related to the battery operation were maintained at their default values before the batteries were charged.

Step 2 Launch charging and then record the relevant parameters

Step 2 was to charge the batteries with the three-stage method, including bulk, absorption and float charging periods. The batteries were charged with a maximum current of 120A unitl the voltage reached 28.8V. In the third stage, float charge, the batteries were charged with a small current to compensate the losses during the battery operation.

Step 3 Display and save real data

After starting the charge cycle, real-time parameters were shown on the visual monitor panel. Meanwhile relevant data was saved to a file in CSV format which could be imported into other applications, such as Microsoft Excel, for further processing.

These relevant procedures on how to save real-time data to CSV files are referenced from the document 'BMV-602 Data Link Manual'.

Step 4 Set power level of load bank, launch discharge, record parameters

Four tests with different discharging power were carried out, which was to identify the discharge capacity of the batteries under different rates. These consumed power levels ranged from 1 kW to 4 kW.

6.3.2 **Electrical performance tests for the engine/generator with the HEES**

Five different electrical conditions were tested, including

(1) Base demands: 1000W

(2) Peak demands: increasing loads from 6500W to 10,000W

(3) Medium-level demands: 5000W

(4) Increasing demands followed by maintaining the value.

(5) Extremely high and fluctuating power demands

6.3.3 **Case studies**

The two cases followed the same testing procedure.

Case study 1: AC grid power of 2.5 kW with HEES supplying a household electrical demand over 24 hours.

(1) Operational strategy plan and control code programming

(2) Detection device check and preparation

(3) Applied household profile to the whole system by adjusting the load bank output

(4) Data collection and analysis

Case study 2 AC grid power up to a maximum of 6.5kW with HEES supplying a household electrical demand over 24 hours.

The test steps (1) - (4) were the same as above.

6.4 **Test results**

6.4.1 **Battery performance results**

The data collected was divided into 4 files which included the parameters mainly concerned in each charge and discharge cycle. Since each charge cycle started from the end of a discharge cycle, the complete charge/discharge data could be saved into a single file to represent the complete process for charge and discharge.

A Discharge with 1 kW power:

In this cycle, the batteries were discharged with an energy released of 8000.3Wh in total. SOC decreased from 100% to 41.1% with a duration of 7 hours 50 minutes. The alarm relay switched on at an SOC equal to 49.9% when the energy consumed was 6846.71 Wh and this took 6 hours 42 minutes.

After discharge to an SOC of 41.1%, the batteries began to be charged with a maximum current setting of 120 A. After 3 hours 53 minutes, the SOC increased to 100% that meant the batteries were fully charged. The total energy supplied for charging the batteries was 8694.1 Wh. After that, the charge voltage decreased slowly as the current was released until the float charge stage was reached. It is noteworthy that the current at the beginning of the charge cycle was 108.996 A even though the default setting value was 120 A. Energy efficiency in this test was 92.02% ; that was calculated from the ratio between energy supplied by the batteries to energy consumed for charging the batteries.

B Discharge with 2 kW power:

In this cycle, the batteries were discharged with an energy release of 7296.26 Wh along with 298.614 Ah in total. The discharge duration was 3 hours 33 minutes. Here, the battery voltage decreased to 23.503 V and after that, the batteries began to be charged. After 3 hours 29 minutes, the SOC had increased to100% that meant that the batteries were fully charged. The total energy supplied for charging the batteries was 8257.03 Wh. After that, the charge voltage decreased slowly with the current until the float charge stage was reached. It is noticeable that the current at the beginning of charge cycle was 109.588 A even though the default setting value was 120 A. Energy efficiency in this test was 88.36%, again calculated as the ratio between energy supplied by the batteries to energy consumed for charging the batteries.

C Discharge with 3 kW power:

In this cycle, the batteries were discharged with an energy release of 6887.23 Wh in total. The SOC decreased from 100% to 30.8% within 2 hours 25 minutes. The alarm switched on at a SOC equal to 49.3% when the energy consumed was 5138.6 Wh and took 1 hours 39 minutes.

After discharge to a SOC of 30.8%, the batteries began to be charged with the maximum current setting of 120 A. After 3 hours 19 minutes, the SOC increased to100%. The total energy supplied for charging the batteries was 7849.1 Wh. After that, charge voltage decreased slowly with current decreasing evenly until the float charge stage. It is noticeable that the current at the beginning of the charge, cycle was 108.142 A even though the default setting value was 120 A. Energy efficiency in this test was 87.75 % which was calculated

from the ratio between energy supplied by the batteries to energy consumed for charging the batteries.

D Discharge with 4 kW power:

In this cycle, the batteries were discharged with an energy released of 6588.06 Wh in total. SOC decreased from 100 % to 25.5 % with duration of 1 hours 38 minutes. Alarm relay switch on at SOC equal to 49.8% when the energy consumed was 4536.565 Wh and this took 1 hours 5 mins.

After discharge to an SOC of 25.5%, the batteries began to be charged with a maximum current setting of 120 A. After 3 hours 11 minutes, the SOC increased to 100%. The total energy supplied for charging the batteries was 7516.11 Wh. After that, the charge voltage decreased slowly with the current descending evenly until the float charge stage. It is noticeable that the current at the beginning of the charge cycle was 108.829 A even though the default setting value was 120 A. Energy efficiency in this test was 87.65%, which was calculated from the rratio between energy supplied by the batteries to energy consumed for charging the batteries.

E Analysis and discussion

- Initial charge current and energy efficiency

If the initial charge current and energy efficiency are taken into account, it is easy to understand why the charge current wwas 108 A at the start of the charge cycle even though the value was set to 120 A as the maximum charge current. Due to the charge efficiency factor (CEF), 90% current can be absorbed by the batteries when they are in a good condition or new. Meanwhile, the CEF will be affected by other factor such as temperature change. The higher the operational temperature of the batteries, the longer it takes to fully charge them.. In this series of tests, energy efficiency was used instead of the CEF factor. Accordingly, the overall energy efficiency ranges from 87.7% to 92%, which shows us the batteries performing well in the tests.

- Ah capacity of the batteries

According to the theory of the Peukert exponent, it is easy to understand the change of the Ah capacity of a battery under different discharge currents. It is noticeable that the higher the discharge current, the lower the discharge Ah capacity will be. The discharge begins from 100% SOC but will not reach zero percent due to the safety and protection concerns for the batteries concerns. However, from Fig. 6.2 (c), it can be seen that discharge capacity is significantly decreased along with the increase of discharge current. Meanwhile, energy efficiency tends to reduce gradually, which can be seen in Fig. 6.2 (d).

Table 6.2 shows a summary of the important performance parameters. Fig.6.2 shows three graphis of the charging/discharging performance. Four levels of discharge duration have been

Table 6.2Performance indicators summary

Performance indicators \ Discharge power level	1kW	2kW	3kW	4kW
Energy released (Wh)	8000.3	7296.26	6887.23	6588.06
Energy consumed (Wh)	6846.71	8257.03	7849.10	7516.11
Discharge duration (hours)	7.83	3.50	2.42	1.63
Charge duration (hours)	3.88	3.48	3.32	3.18
Energy efficiency (%)	92.02	88.36	87.75	87.65
SOC at discharge end (%)	41.1	35.5	30.8	25.5
Discharge Capacity (Ah)	325	299	287	284

compared on the basis of different discharge power rating alongside different charge duration. Furthermore, total energy released and consumed has been compared as below. Energy efficiency, deepest discharge capacity and cumulative discharge capacity have been presented in Fig. 6.2

According to the results of the battery tests and their subsequent analysis, it is reasonable to draw the following conclusions,

- Moderate discharge with appropriate current levels is beneficial to extend the battery life and to increase their discharge capacity.

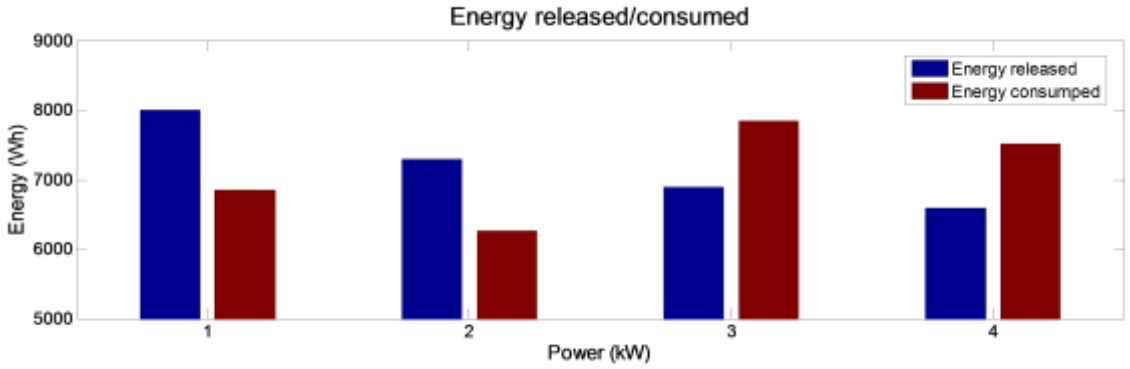

(a)

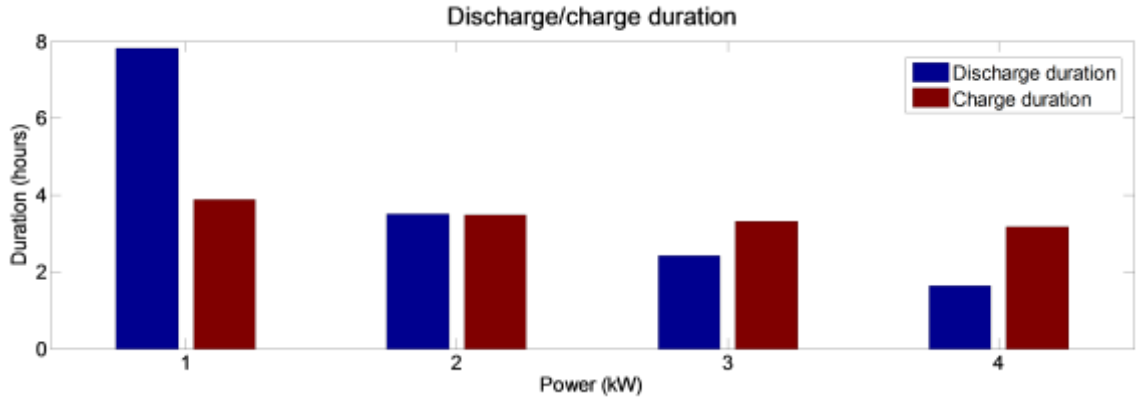

(b)

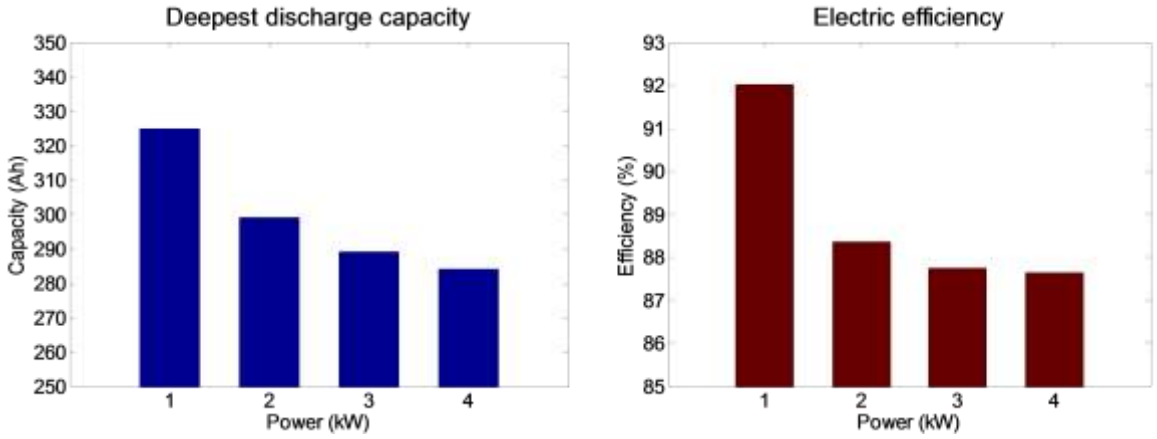

(c) (d)

Fig.6.2 Performance diagrams

- Due to the CEF factor, only part of charge current can be absorbed by the batteries in practice. CEF will affect the energy efficiency of battery systems due to power loss, in the form of waste heat and temperature rise.
- Under different discharge schemes, it has taken a similar time to charge the battery to 100% SOC, about 3 to 4 hours. However, it should take a longer time for float charge to reach the fully charged state.

- Energy efficiency ranged from 87.65 % to 92.02 %, which showed that the batteries performed well in tests. However, both energy efficiency and discharge capacity tend to decrease with large discharge currents. These findings provide guidelines to improve the performance of the batteries.

6.4.2 **BMT-HEES system results**

The components in the BMT-HEES system may perform differently with changing loads. Fig. 6.3 provides the overall profile of the test conducted over 11 minutes on the generator set, batteries, super capacitors subject to different processes. Sometimes, electricity from the generator set was used to meet load demands assisted by the charging hybrid sources. Otherwise, both engine/generator and hybrid sources collaborated to satisfy the demands as the power requirements increased. The overall test can be generally divided into three

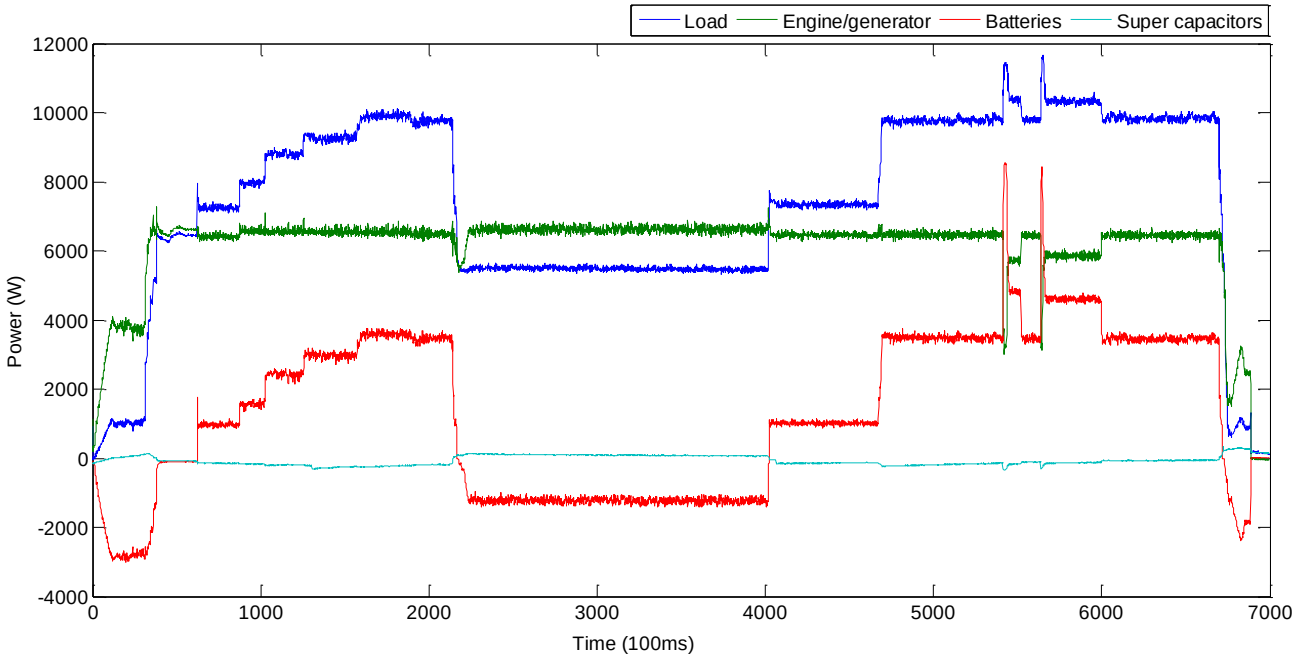

Fig .6.3 Performance test for the BMT-HEES

sections. Each section reflected a different power demand scenario as well as power source responses over the period.

Phase 1 Load power increase from low to high

At this stage, the generator set supplied electricity to the load along with charging the energy storage system. Fig. 6.4 (a) demonstrates the load profile over this stage. In these diagrams, the positive values represent the electricity derived from power sources and negative values are power absorbed. It can be seen that load demands increased gradually from 0 up to 10 kW. Correspondingly, power generated from the engine increased as shown in Fig. 6.4 (b). At the time of 38.2 s, the engine power increased to the nominal value of 6.5 kW and remained at this output level even though the load requirements increased continuously. The hybrid power sources, namely batteries and super capacitors provided the shortfall between the load demand and the engine power output. Note that, the batteries were charging with relatively high charge power under the situation of demands lower than 6.5 kW. This scenario appeared from the beginning to the time of 38.2 s. After that, the batteries changed from the charge to discharge state, providing the gap between load demand and the engine output. The Super capacitors absorbed or released power as supplement over a very short period when the demand altered. Compared to engine or battery, the power level of the super capacitors was relatively low due to their small size.

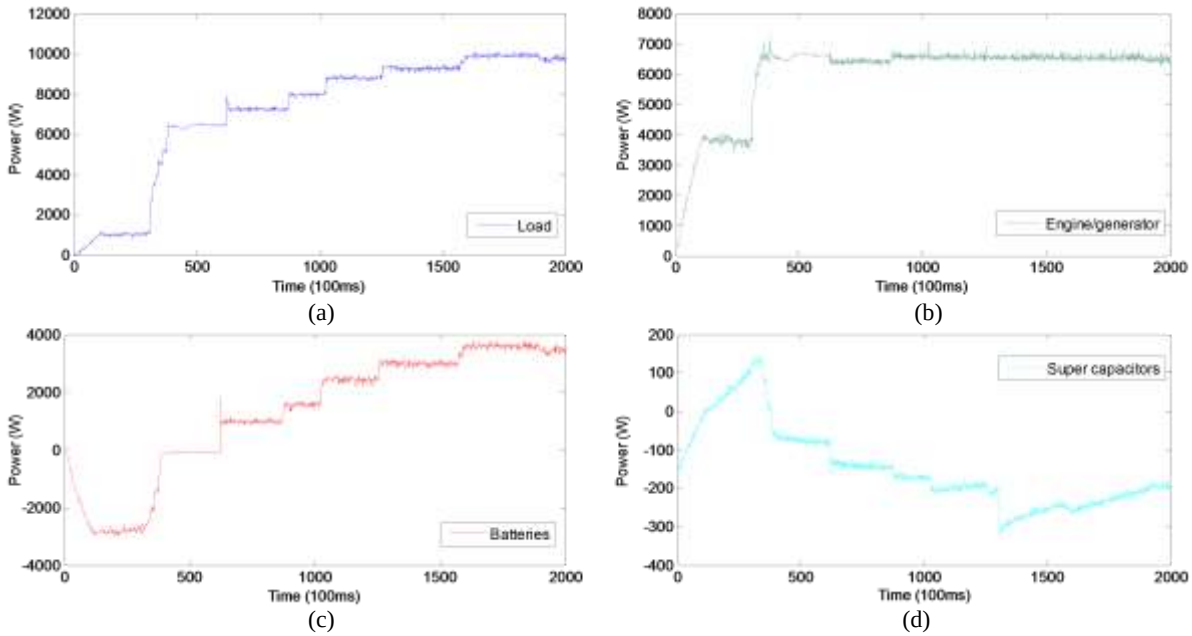

Fig. 6.4 Performance in the phase 1 of the test

With the integration of the energy storage devices, the batteries and super capacitors, the hybrid power system can satisfy the load increase up to 10 kW. Meanwhile, the engine can work stably at nominal output despite demand variations.

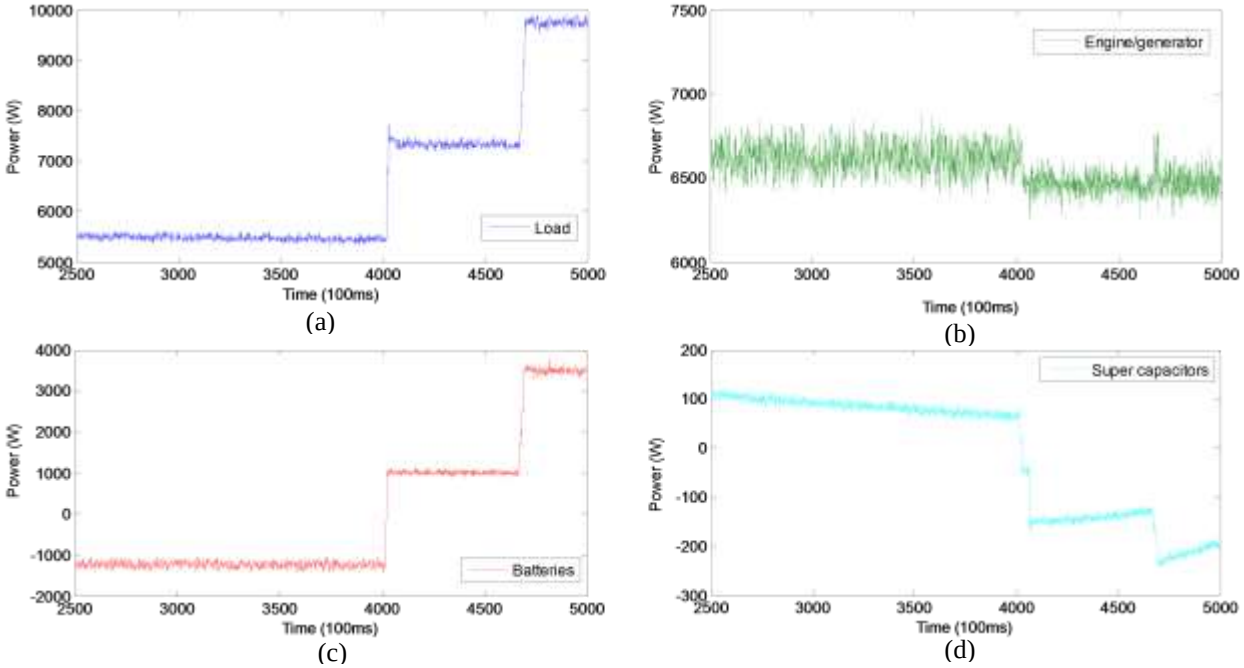

Fig. 6.5 Performance in the phase 2 of the test

Phase 2 load demands consistent increase

Due to the small difference between the engine supply and load demand, there was an amount of electricity available to charge the batteries. After time 400s in Fig. 6.5, the batteries started to discharge along with the electricity from the engine to satisfy the load requirement of over 6.5 kW. The variation of the battery output was quite similar to the load demand. Therefore, the batteries responded to the load variation much more than the engine did. It can be observed from Fig. 6.5 (d) that the super capacitor responded to the sudden variation of the load demand rapidly even though the power level was relatively low.

Phase 3 high and sudden changes of the electric load

Over this stage, the energy storage system discharged along with the engine working at its nominal output. When the electric demand fluctuated, the energy storage system responded to the change before the engine. Therefore, it enabled the engine output to alter smoothly. From the time 533.5 s to 571.6 s, there were two sudden changes of the load demand. All of the power sources, engine, batteries as well as super capacitors followed these changes.

However, the batteries responded to this sudden change by increasing their power output by 142.8% while the engine decreased by 50.8%. Fig. 6.6 shows the details of these results.

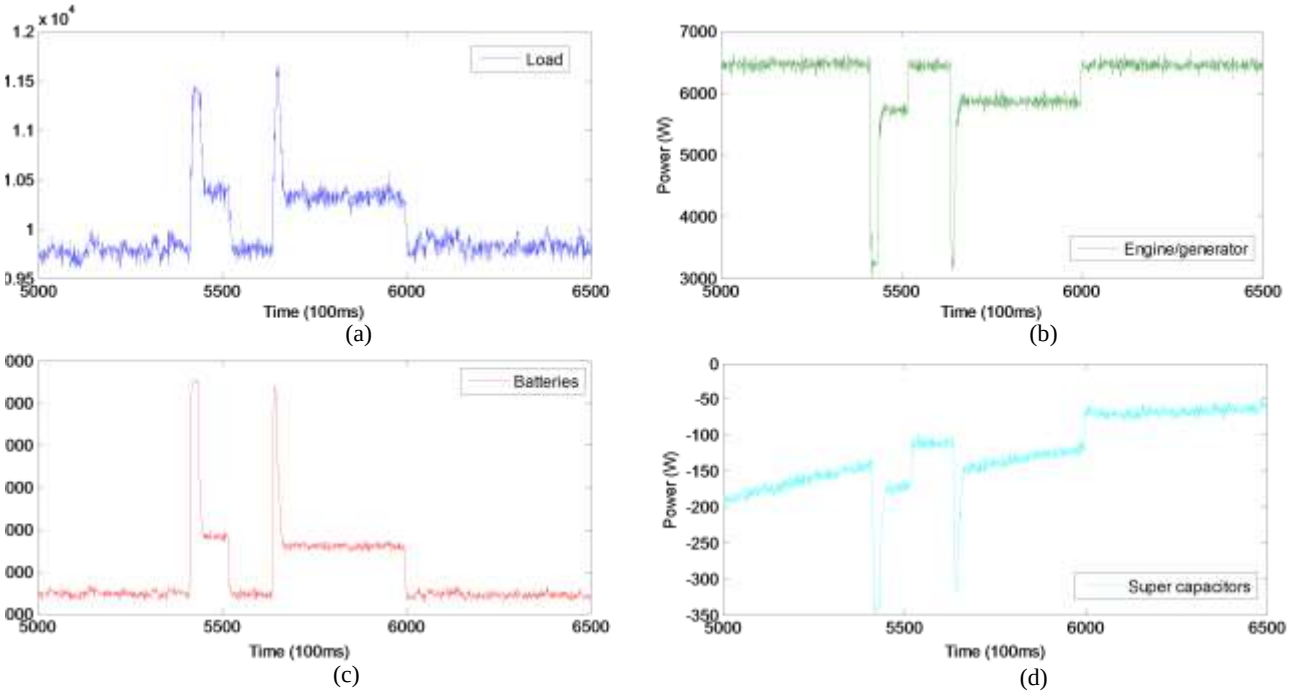

Fig. 6.6 Performance in the phase 3 of the test

This test confirms the feasibility of the integration of the Yanmar engine with the energy storage system. The engine-based HEES was able to match the load fluctuation over a wide range which provided significant benefit for the domestic case studies.

6.4.3 **Case studies**

There were two cases employed to study the effectiveness of the proposed system.

A Case 1

The first case study was set up based on an electricity profile over one working day in a UK house where hybrid power system employed a generator, AGM (Absorbent Glass Mat) batteries and supercapacitor module as electricity supply sources.

Fig. 6.7 (a) illustrates the electricity demand scenario adopted by the case 1 study. The electricity demand fluctuated over 24 hours with a large power difference between the minimum of 120 W and the maximum of 10.02 kW respectively. Furthermore, the overall amount of electricity over the 24 hours was 33.63 kWh. Actually, the peak hour (electricity

demands over 6.5 kW) lasted 1.48 hours in this case but it is impossible for a stand-alone 6.5 kW engine to satisfy this without assistance from other power sources. Therefore, the engine/generator being assisted by auxiliary power sources and operating with an optimal operational strategy was a superior solution in this case study. Otherwise, a bigger engine/generator would have to be chosen to satisfy higher power demands but it would exhibit inferior option due to its low energy efficiency.

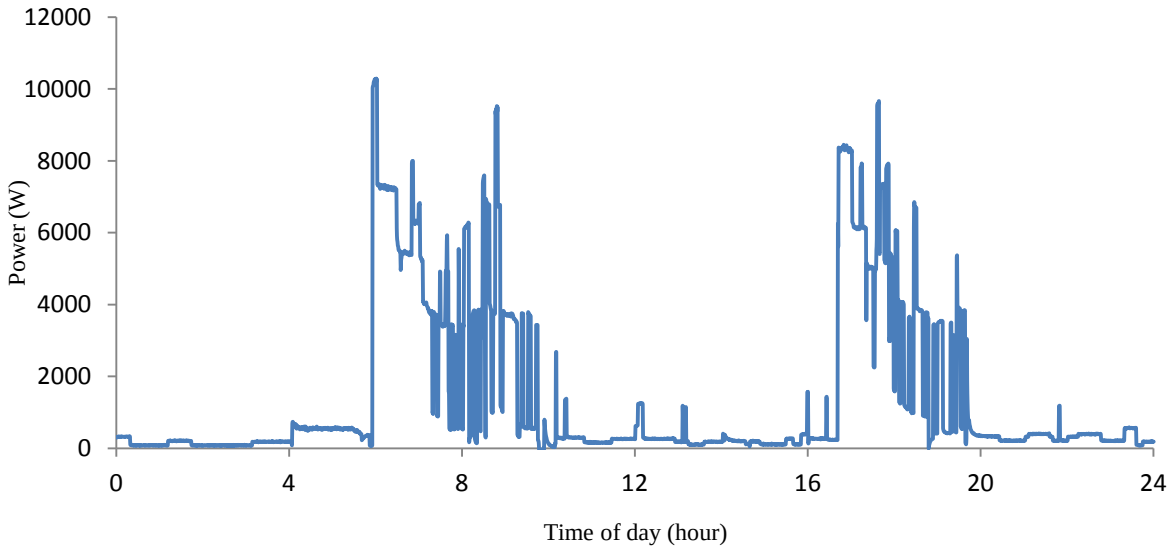

(a) Household electricity consumption

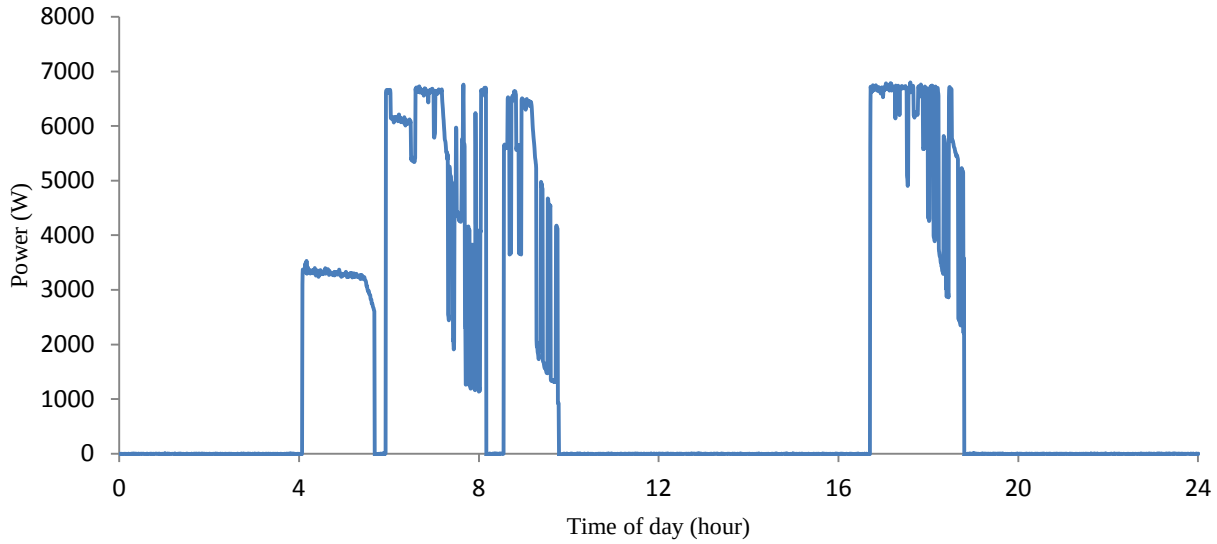

(b) Generator set power

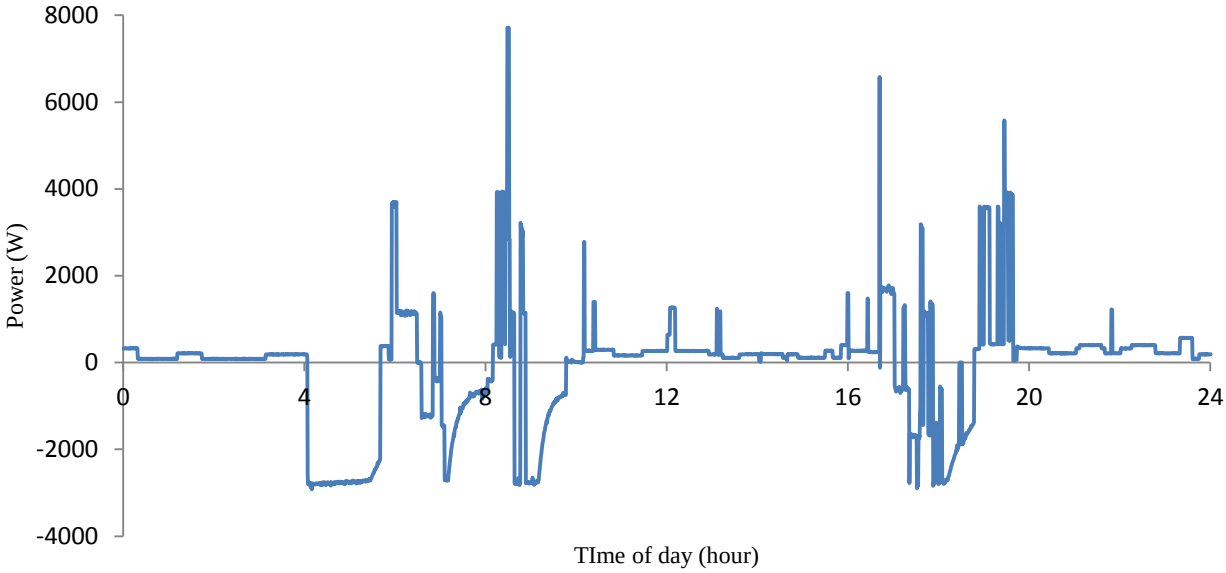

(c) Battery power

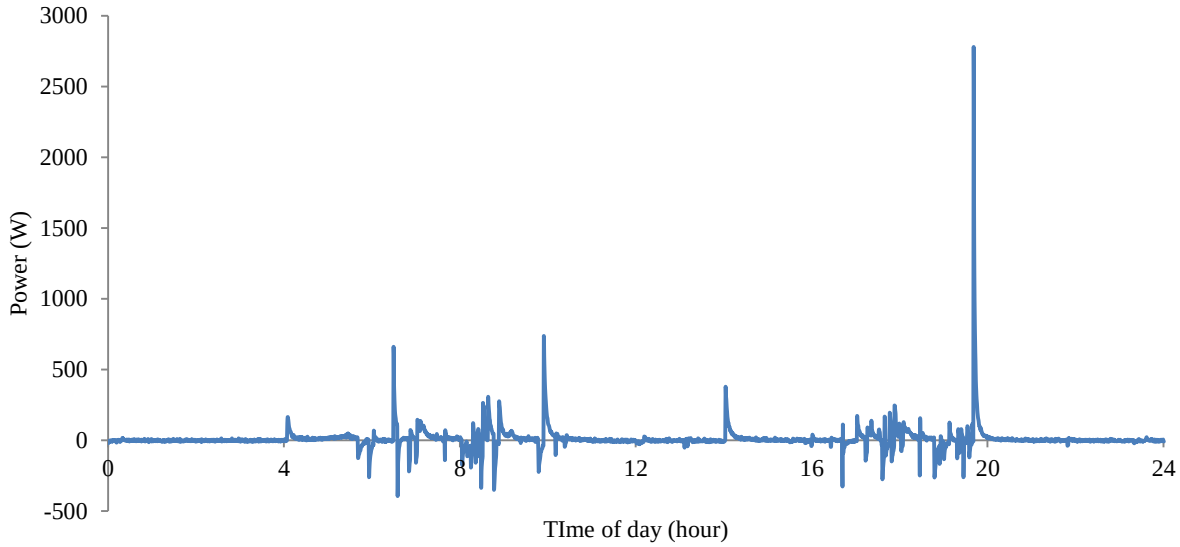

(d) Super capacitor power

Fig.6.7 Demands and supplying in the case 1

After presenting demonstration results from the trial test, a comparison was then carried out where one system was supplied by an engine only, and the other by a hybrid power source including generator set, batteries and supercapacitor module.

- Energy management strategy

Batteries and supercapacitor, as the main electrical storage and power sources, were operated over peak time and off-peak time. In order to make sure the engine worked with relativly high efficiency, the engine started at these two operational criteria,

① Peak hour, when the batteries and super capacitors cannot provide enough electricity to the load.
② For charging the batteries when the SOC of the batteries decreased to some low threshold level.

Additionally, there was once extra charging operation for the HEES before the first peak hour. Therefore, the HEES was ensured to have enough energy stored for the first peak hour after it discharged over the night time. The maximum charge power for the HEES was around 3000 W which is recommended by the manufacturer as the default value subject to the batteries' capacity.

The operational methods employed in the tests were the same as in the simulation. Section 5.4.1 provides the details.

- Criteria for efficiency calculation

Employing a hybrid power supply system, the test was executed over 24 hours. Batteries along with super capacitors, as electricity storage/supply sources, were operated in off-peak hours. On the other hand, the engine/generator worked with them when peak power demands were needed. When the SOC of the batteries decreased to a relatively low level, the engine switched on to charge batteries with a relatively high power output. Therefore, high efficiency operation of the engine was achieved.

According to the results from the test, several important efficiency indicators can be derived. The calculation is presented below and the definition of the parameters is provided in the list of *Symbols*,

(1) Waste heat recovery

Heat obtained was recovered from the cooling system and the exhaust gas of the engine/generator. Therefore, heat energy recovered was equal to the sum of them over the whole engine operation which was calculated by the series of equations below,

$$Q_{exh} = \frac{\sum_{i=1}^{K} \int_0^{T_i} p_{exh}(t, p_e) dt}{3600} \quad (6\text{-}1)$$

$$Q_{co} = \frac{\sum_{i=1}^{K} \int_0^{T_i} p_{co}(t, p_e) dt}{3600} \quad (6\text{-}2)$$

So,

$$Q = \frac{\sum_{i=1}^{K} \int_0^{T_i} p_{rec}(t, p_e) dt}{3600} \quad (6\text{-}3)$$

With

$$p_{rec}(t, p_e) = p_{exh}(t, p_e) + p_{co}(t, p_e) \quad (6\text{-}4)$$

(2) System efficiencies

Several important efficiency-related indicators can be produced. The calculation is described in the following sections.

Engine electric efficiency

The electric efficiency of the engine is the mean efficiency over the engine operation as follows:

$$\eta_{eng} = \frac{\sum_{i=0}^{K} \int_0^{T_i} f_{eng}(t, p_e) dt}{\sum_{i=0}^{K} T_i} \quad (6\text{-}5)$$

The electric efficiency of the storage system,

The electric efficiency of the storage system is equal to its charge efficiency multiplied by its charge/discharge transferring efficiency. Therefore, electric efficiency can be expressed as equation (6-6) below:

(6-6)

$$\eta_{storage} = \frac{\sum_{j=1}^{J}\left(\frac{\int_0^{T_j}\eta_{ch}(i) * f_{ch_{disc}}(t,p_e)dt}{\int_0^{T_j}dt}\right)}{\sum_{j=1}^{J} j}$$

(6-7)

$$\eta_{ch}(i) = \frac{\int_0^{T_i} f_{ch}(t,p_e)dt}{\int_0^{T_i} dt}$$

The overall electric efficiency of the system

System overall electric efficiency η_{sys} can be calculated by equation (6-8),

$$\eta_{sys} = (\eta_{eng} * T_{eng} + \eta_{storage} * T_{ees} + (\eta_{eng} + \eta_{storage}) * 0.5 * \mathrm{T}_{together})/(T_{eng} + T_{ees} + T_{together}) \quad (6\text{-}8)$$

- Test results

In case 1, the BMT-HEES was applied to a domestic dwelling requiring much more electrical power than a 6.5kW Yanmar engine/generator can provide. The test was based on 24-hour electricity demand to assess the feasibility and evaluate the performance of BMT-HEES.

The peak hour (electricity demands over 6.5 kW) lasted for 1.48 hours while the engine operated for 7.16 hours in total. The electricity demand profile in case 1 is illustrated in Fig.6.7 (a) while Fig.6.7 (b) to (d) demonstrate the details of the system dynamic response.

Basically, there were two high power periods. The first one started at 5 am 34 minutes with a 10.02 kW power demand while the second one was at 4 pm 25 minutes with a 6.25 kW power demand. The peak hour in this case was 1.48 hours and was when the generator set cooperated with the HEES discharging to supply high power demands (over 6.5 kW electrically). The rest of the time saw lower demands in the profile for 22.52 hours in total.

Fig. 6.7 (b) to (d) demonstrated the response curves of the engine, batteries and super capacitors respectively. The generator set output is illustrated in Fig. 6.7(b) where it started 3 times at the times of 5 am 34 minutes, 8 am 34 mintes and 4 pm 25 minutes where

corresponding power outputs were 6.61 kW, 5.63 kW and 5.62 kW respectively. There was an exceptional engine starting at the time 4 am 2 minutes for charging the HEES as mentioned before rather than being triggered by the high power demands.

Fig. 6.7 (c) shows the batteries where they experienced fluctuation over the operation. The positive values in the graph represent discharge power while negative ones are the charge power. Principally, the batteries had two different states –that is, charging or discharging. The batteries would be charged either after supplying electricity to the load along with the engine (at 8 am 23 minutes) or before peak demand (at 4 am 2 minutes). The batteries provided electricity to the load over most of the time within the 24 hour case study. Specifically, battery discharge can be divided into two different scenarios. Sometimes, the battery discharged to assist the engine for satisfying high demands (at 5 am 34 minutes), otherwise the batteries worked alone to deliver small amounts of power to the load (from 0am to 4 am 2

Table 6.3 Performance summaries and comparison for the case 1 study

Performance indicators		Tri-generation (with HEES)	Tri-generation (without HEES)
Energy(kWh)	Discharge energy from HEES	8.85	/
	Electric energy from engine	35.16	33.63
	Energy supplying to load directly from engine	25.03	33.63
	Energy for charging energy storage system	16.34	/
	Electricity consumed by load	33.63	33.63
	Thermal energy recovered	51.71	130.26
	Total energy over peak hours	11.78	11.78
Duration (hrs)	HEES discharge time	18.32	/
	Engine running	7.16	24
	Charge period for HEES	5.70	/
	Peak hour (energy demands above 6.5kW)	1.48	1.48
Efficiency (%)	HEES electric efficiency	24.38	/
	Engine electric efficiency	25.75	11.26
	Thermal efficiency	39.22	39.64
	System electric efficiency	25.07	11.26
	System overall efficiency	64.29	50.90
Power (W)	power from HEES	-2,920/7,715	/
	power from engine	0-6,800	0-10,290
	Load power	0-10,290	0-10,290

minutes). Battery power ranged from -2.92 kW to 7.72 kW over the 24 hours of operation.

Similarly, the 24-hour operation saw fluctuations of the super capacitors as depicted in Fig. 6.7 (d). The positive and negative values in the diagram represent the charge and discharge power respectively. The power provided or absorbed by the super capacitors was much less than that of the batteries. The power range of the super capacitors was between -395 W to 693 W most of the time. There was an exceptional point at 7 pm 25 minutes where the super capacitors discharged power of 2.78 kW. It is noticed that the batteries discharged 270 W at the same time point while the engine was switched off. Overall, the scale of the super capacitor module utilised in this system was small. Therefore, the electric power delivered from it was relatively limited. The contribution to high power demands from the super capacitors was minimal.

All of the relevant indicators for evaluating the performance of the system have been summaried in Table 6.3. The criteria for their calculation are provided in equations (6-1) to (6-8). The table also lists the corresponding indicators for the alternative CHP system with an engine only as comparison. According to Table 6.3, it can be easily seen that overall efficiency of the BMT-HEES (6.5 kW engine-based) was 64.29% while the tri-generation (10 kW engine-based) without HEES was 50.9%. This was mainly due to the fact that engine had to run continuously over the 24 hours to satisfy both low and high electrical demands without the assistance of the HEES. Therefore, the engine worked with lower electrical efficiency for most of the time. In contrast, the BMT-HEES system had better efficiency electrically and thermally, with 25.1% and 39.2% respectively. Furthermore, there was a dramatic decrease in the duty time of the engine, from 24 hours to 7.16 hours. During the rest of the time over 24 hours, the HEES delivered electricity previously provided by the engine to the load. Meanwhile, without integration of the HEES, excessive heat energy was generated by the engine due to its long-term operation, which was 2.5 times more than the BMT-HEES provided.

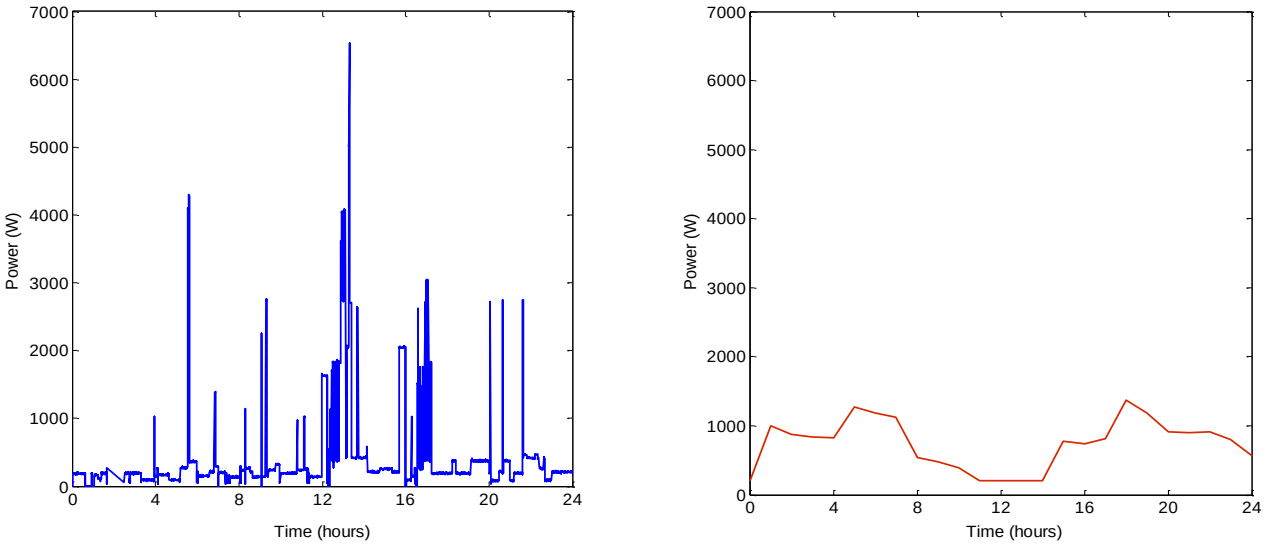

Fig.6.8 Household energy demands profile

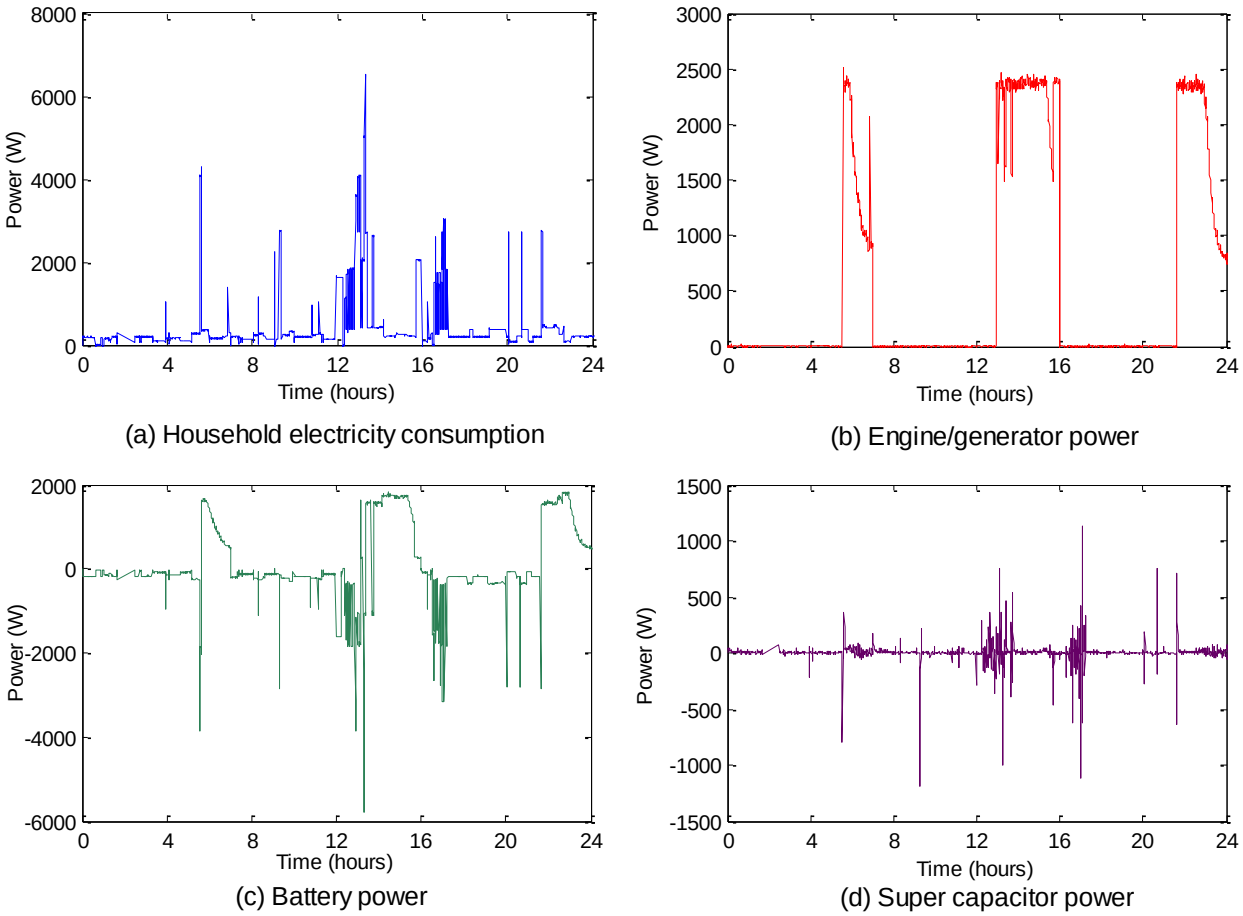

Fig. 6.9 Household electricity consumption and supplying profiles of power sources

A Case 2

- Energy consumption profiles in a household

Case study 2 selected another typical household in the UK. Fig. 6.8 (a) [14] shows the electricity and heat consumption/demand profile over 24 hours for the selected house. From the figure, it can be seen that the minimum demand of electrical power was around 100W and the maximum demand reached 6.544 kW. From Fig. 6.8 (a), it can also be seen that the electricity consumption was lower than 1 kW during the majority of the 24 hours while the peak demands happened over relatively short periods. For instance, at 1.18pm, the demand was as high as 6.544 kW before it plunged to 400 W 5 minutes later. The peak demands over 2.500 kW appeared 3 times, starting from 5.36am, 1.18pm, and 9.37pm. Electricity consumption for this household over 24 hours was 9.85 kWh in total.

Fig.6.8 (b) demonstrates the heat demand profile for the same house in the same day. Heat energy was used for space heating and hot water. According to the profile in Fig. 6.8 (b), the maximum heat demand was 1.375 kW while the minimum was 205W. The overall amount of heat required was 18.5 kWh for the day. Compared to the electricity profile, the heat profile had a slow and moderate variation during the 24 hours where there was no sudden change from time to time.

- Methodology

The energy management strategy in case 2 was the same as the one adopted in case 1 except that a 2.5 kW engine/generator was chosen to replace the previous one.

- Operational plan of the system

The HEES system supplied the electric power to meet the demand when the load was lower than 4000 W. The engine/generator ran along with the HEES to satisfy peak demands. In order to obtain higher overall efficiency for the BMT-HEES system, the engine/ generator was started and operated 3 times, namely, 6 – 7 am, 13 – 16 pm and 22 – 24 pm. During the running periods, the HEES was charged with the extra electricity from the engine/generator, making sure it had enough energy stored to supply electric power as required. Over most of

the rest of the time, electricity supplied to the electrical load came from the batteries and super capacitors.

- Dynamic performance of the energy storage system

In the test, the engine started and ran three times when the electric load demands were over 4.000 kW or the remaining energy stored in the HEES system was inadequate. Fig. 6.9 (a) shows the electricity consumption profile. The performance of the engine/generator is shown in Fig. 6.9 (b). When the engine/generator was running, it supplied electric power with assistance from the HEES system during peak times; otherwise, the engine/generator charged the HEES system at off-peak times until the HEES was fully charged. From Fig. 6.9 (b), it can be seen that the engine/generator was always running above half load. Therefore, high efficient operation of the BMT-HEES was achieved.

The test results of the HEES system are shown in Fig. 6.9 (c) and (d). The negative powers of the batteries in Fig. 6.9 (c) and the super-capacitor profile in Fig. 6.9 (d) represented the amount of electric power for charging, while the positive ones are the amount of electric power during discharge. The batteries were charged when the engine/generator started during off-peak hours to make sure there was enough energy stored in the HEES system. From Fig. 6.9 (d), it can be seen that the super-capacitor responded to the load fluctuation speedily. When electric demands varied, it released electricity with maximum capability promptly.

For the engine/generator, the transition time during operation represents how quickly the engine responds to load variation, which is normally around 3 to 10 seconds depending on engine types. From the test results, it can be seen that the HEES responded swiftly to the sudden change of load, which has a positive effect on engine operation. Consequently, engine had enough time to alter its output properly.

- Heat recovered

The total heat energy recovered from the engine during the 24 hour test was 21.07 kWh, while the heat consumption for the day was 18.5 kWh. The heat recovered was 14% more than the demand. Furthermore, due to the engine being operated at high loads, heat at higher temperature could be obtained. Therefore, the heat recovered during the test could fully

satisfy the requirement for the house over the 24 hours. The heat recovered was 40.1% of the fuel input.

- Electric efficiency and overall efficiency of the system

In the BMT-HEES system, an engine/generator rated 2.5 kW was used and coupled with the HEES system. The test results are listed in Table 6.4. Discharge efficiency of the storage system, engine efficiency and overall electric efficiency were 24.01%, 26.45% and 23.59% respectively.

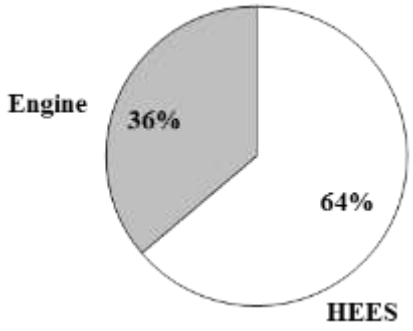

Fig .6.10 (a) Energy contribution

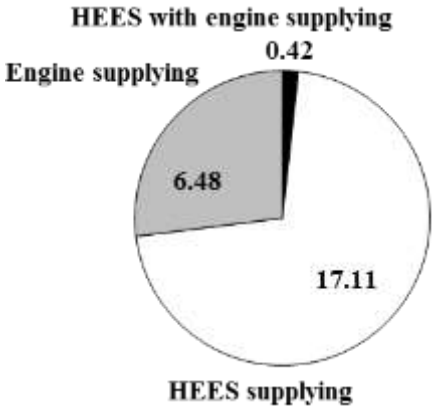

Fig. 6.10 (b) Operation duration (Hours)

Table 6.4 Performance comparison between the two electric systems

Performance indicators	Tri-generation without HEES	BMT-HEES	Improvement (%)
Engine nominal Power (kW)	6.500	2.500	--
Operational range (kW)	0 – 6.500	0 – 2.507	--
Engine operation duration (hours)	24.00	6.89	--
Storage system charge duration (hours)	--	6.48	--
Storage system discharge duration	--	17.52	--
Storage system charge efficiency (%)	--	26.10	--
Storage system discharge efficiency (%)	--	24.01	--
Average engine generator efficiency (%)	4.95	26.45	21.5
Overall electric efficiency (%)	4.95	23.59	18.6
Heat recovered (kWh)	75.01	20.07	--
Average heat recovery (%)	38.11	40.08	2.0
Overall CHP system efficiency (%)	43.06	63.67	20.6

For comparison, a tri-generation system without HEES was also assessed. The tri-generation was assumed to have a maximum power output 6.5 kW, to meet the maximum electricity demand; and it had similar electric efficiencies at different loads as the engine/generator in the BMT-HEES system. From Table 6.4, it can be seen that the average efficiency of the tri-generation system without HEES was only 4.95%. This was due to the fact that the engine frequently ran at very low loads (< 1.000 kW). The heat recovered from the tri-generation was 75.01 kW. It was 4 times that of the overall amount of heat required (18.5 kWh) for the day in the case 2 study. In other words, there was 56.51 kW of heat wasted.

Compared to the tri-generation without the HEES system with 4.95% electric efficiency, the BMT-HEES system had a much higher electric efficiency (23.59%). Furthermore, the overall BMT-HEES system efficiency increased from 43.06% to 63.67% where the improvement of the overall system efficiency was 47.86%, as shown in Table 6.4.

From the results, it was found that the engine/generator supplied 36% of the electric energy in 24 hours; the HEES system contributed 64% of the electricity needed. Fig. 6.10 (a) shows the percentage of electricity supplied from the engine/generator and the HEES system. Fig. 6.10 (b) illustrates the distribution of the operational durations of the engine/generator, the HEES and both of them. The HEES system supplied power for 17 hours 06 minutes at low load demand; while the engine/generator worked for 6.48 hours and supplied power and recharged the HEES system; only over the 0.41 peak hour, was the engine running together with the HEES system to supply the peak demand.

From the previous analyses, the BMT-HEES system performed much better than the conventional tri-generation system (engine only). For a BMT system integrated with a hybrid electric energy storage (HEES) system, a smaller engine/generator can be used to satisfy the same energy demands as the conventional off-grid/distributed tri-genration system. The smaller engine/generator was able to work at much higher electric efficiency due to the effect of peak shaving and valley filling from the HEES unit. The integrated BMT-HEES system can satisfy both electric and heat demands required by the house at high efficiency. Overall energy efficiency had dramatic increases and the duty time of the engine declined a lot in both case studies provided the HEES was integrated. However, the scale of the super capacitor module utilised in this system was relatively small. Therefore, the electricity delivered from it was relatively limited.

6.5 **Summary**

Chapter 6 has presented a series of trial tests for the BMT-HEES system from HEES system experiments to complete BMT-HEES case studies step by step.

The BMT-HEES consists of an engine-based conventional tri-genration system and the HEES system. After theoretical and trial tests, it can be concluded that the engine can work with relatively high power output to achieve high efficiency both electrically and thermally in the BMT-HEES.

Before investigating the complete BMT-HEES, a series of tests with regard to battery performance were carried out. Obviously, it was the optimal for the batteries to discharge with relatively small and slow current or power. Therefore, more electricity could be derived from the batteries for longer discharge duration, benefitting their life span as well.

After fundamental tests concerning key components of the BMT-HEES system, a performance test was carried out followed by the complete system investigation based on two case studies. Both the performance test and case studies validated that the complete BMT-HEES was a preferable energy system with relatively high energy efficiency, where the FEL energy management strategy was adopted for satisfying electrical load as a priority. Benefitting from the integration of the HEES, the whole system supplied energy to the demand in an effective and efficient way, which allowed the engine to work over limited duty time but with high efficiency. The HEES, supplied to the load over most of the 24 hours of operation except for the peak hours. Furthermore, a smaller engine/generator can be employed to work at much higher electric efficiency due to the peak shaving and valley filling from the HEES unit.

In summary, the BMT-HEES was an ideal option for stand-alone energy supply systems, especially in rural areas. The benefits of BMT-HEES include high energy efficiency, free of seasonal-dependence and environmental friendliness.

Chapter 7 Comparison of simulation and experimental performances

7.1 Introduction

In the previous chapters, the main purpose of the simulation work was to achieve reasonable prediction and assessment of the system performance prior to building a physical system. Furthermore, the models and system simulations could be improved and then provide beneficial suggestions for future investigations by comparing simulation and physical outcomes. In this chapter, a series of comparisons between simulation and experimental test results on the BMT-HEES system have been carried out. From the subsystem to complete system comparison, the system was improved along with individual components, such as cooling components, the engine with thermal and cooling properties, control strategies and batteries with charge features.

7.2 Engine system

In the physical system, a Yanmar diesel engine as the prime mover was fed with different bio-fuels, such as sun flower oil, rapeseed oil, croton oil etc. It could provide a maximum electrical power output of 6.5 kW and was coupled with the HEES to supply the electricity demand. Waste heat from both engine cooling system as well as exhaust gas recovery was stored in a hot water tank to supply heating and hot water.

In the simulation, the main task was to set up a model of the engine with mechanical and electrical properties. Additionally, both electrical and heat efficiencies of the specific engine were essential factors for the purpose of identifying the whole system. Fig. 7.1 (a) and (b) provide the illustration of the experimental test results of efficiency of the engine generator and fitting curves used in the modelling.

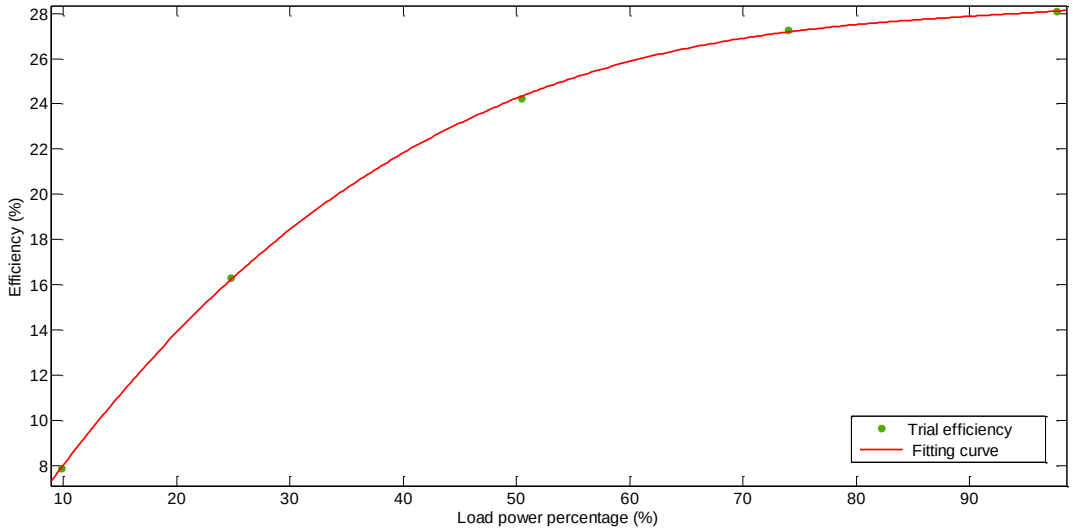

(a) Electrical efficiency

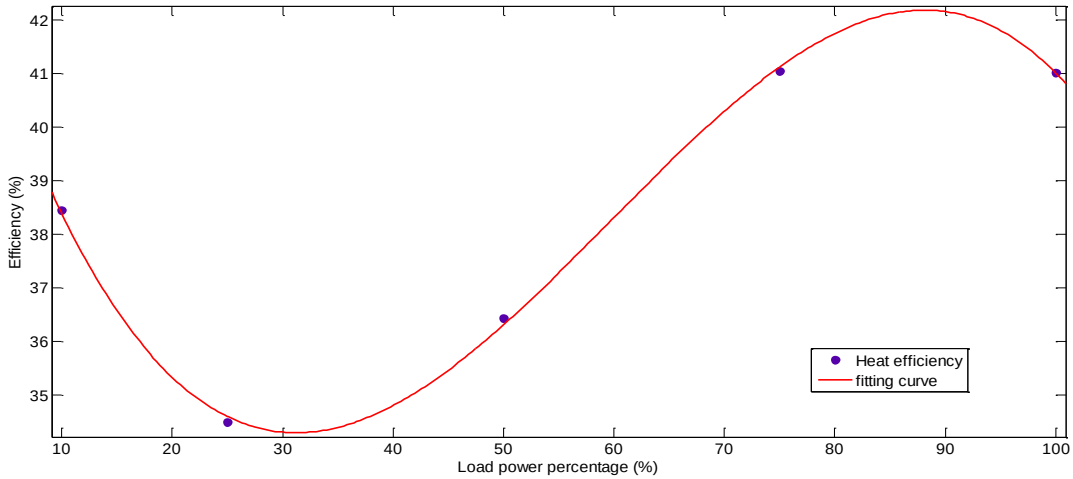

(b) Heat efficiency

Fig. 7.1 Engine efficiency and fitting curves

Fig. 7.1 (a) demonstrates the electrical efficiency of the engine and the curve fitted to the data. Curve fitting was achieved by a cubic polynomial equation as in equation (7-1).

$$F_e(x) = p1*x^3 + p2*x^2 + p3*x + p4 \quad (7\text{-}1)$$

Where,

p1 = 3.065e-005, p2 = -0.008542, p3 = 0.8236, p4 = 0.585

The coefficients have 96% confidence bounds.

Similarly, Fig. 7.1 (b) illustrates the heat efficiency in the trial test and its fitted curve. Curve fitting used equation (7-2),

$$f_h(x) = q1*x\hat{}3 + q2*x\hat{}2 + q3*x + q4 \quad (7\text{-}2)$$

$q1 = -8.567\ e^{-005}$, $q2 = 0.01533$, $q3 = -0.7064$, $q4 = 44.02$

The coefficients in this equation have 95% confidence bounds. The differences between trial test outcomes and the fitted curves are imperceptible. Therefore it is beneficial to use a model with the fitted curves to predict the electrical and thermal performance of the engine system.

7.3 **HEES system**

In this section, simulation results of the small HEES system are compared with the trial tests. The system employed both in simulation and trial test included 3 units of batteries (12 V/12 Ah each), a super capacitor (HCC 60 V/40 F module) and a charger/inverter. The essential criteria for comparison are charge /discharge process variables, such as current, voltage, power and conversion efficiency.

7.3.1 **System construction**

Fig. 5.16 and Fig. 3.7 illustrate the simulation models and trial test bench, respectively. In Fig. 5.16, batteries and super capacitors are linked in parallel and are charged or discharged by the charger/inverter with specific conversion efficiencies at different power levels. The generation of the control signals used to switch between charge and discharge processes were integrated into the programme without employment of a specific component in the simulation. This situation is different to the implementation in the trial bench shown in Fig. 3.7. Specifically, in the physical system, Siemens S7-200 PLC acted as the control device to produce the signal to trigger alternation of charge/discharge. Despite that, the rest of the components employed in both cases were similar.

7.3.2 **Single duration comparison**

A Discharge current

There are three lines with different colour in Fig. 7.2, which represent discharge current from the diverse components. Specifically, super capacitor and battery current are in red and blue, respectively. The total current from both batteries and super capacitors is in green. Fig. 7.2

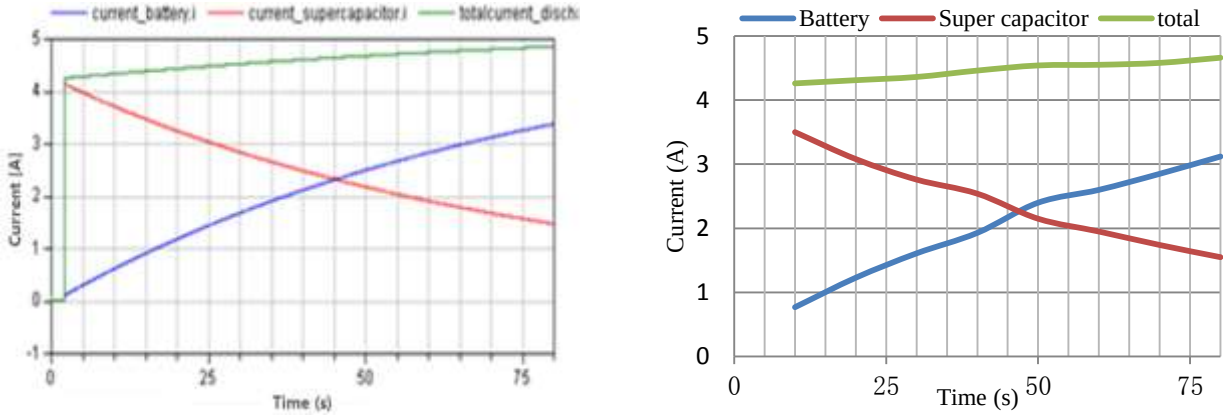

(a) Simulation *(b) Trial test*

Fig. 7.2 Discharge current comparison

(a) and (b) demonstrate similar outcomes from both simulation and physical tests. Super capacitor current decreased gradually as that of the battery rose. The overall current from both devices had a slight increase over this period.

- Super capacitor current

  In the simulation, the range of the super capacitor current iwas from 4.15 A (at the start of discharge) to 1.50 A (at the end of discharge). On the other hand, there was a narrower range in the trial tests for the super capacitors, between 3.51 A and 1.55 A.

- Battery current

  The battery current increased from 0.1 A (at the beginning) to 3.35 A (at the end) in the simulation. The measurements in trial test were from 0.75 A to 3.2 A.

- Current in total

The total current in the simulation slightly altered between 4.25 A and 4.85 A while the experimental results changed between 4.26 A to 4.75 A.

B Discharge voltage

Fig. 7.3 presents the results of the discharge voltage. Fig. 7.3 (a) illustrates that the DC voltage fell gradually from 39 V to 34 V in the simulation. In the practical experiments, it declined from 39 V to 36 V since the DC operational voltage of inverter ranged from 36 V to 39 V (shown in Fig. 7.3 (b)). However, both the simulation and experimental curves show a similar decay trend over the discharge period.

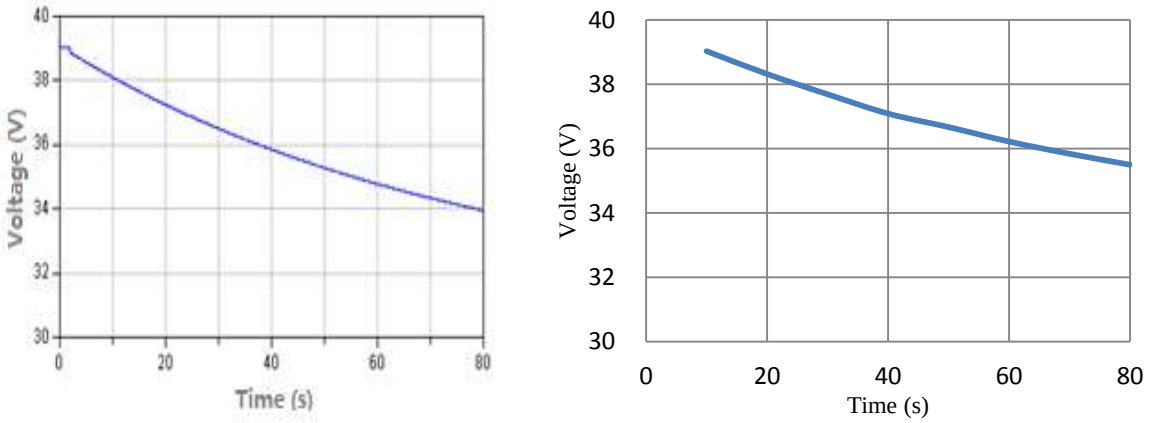

(a) Simulation outcomes *(b) Trial test outcomes*

Fig. 7.3 Discharge voltage comparison

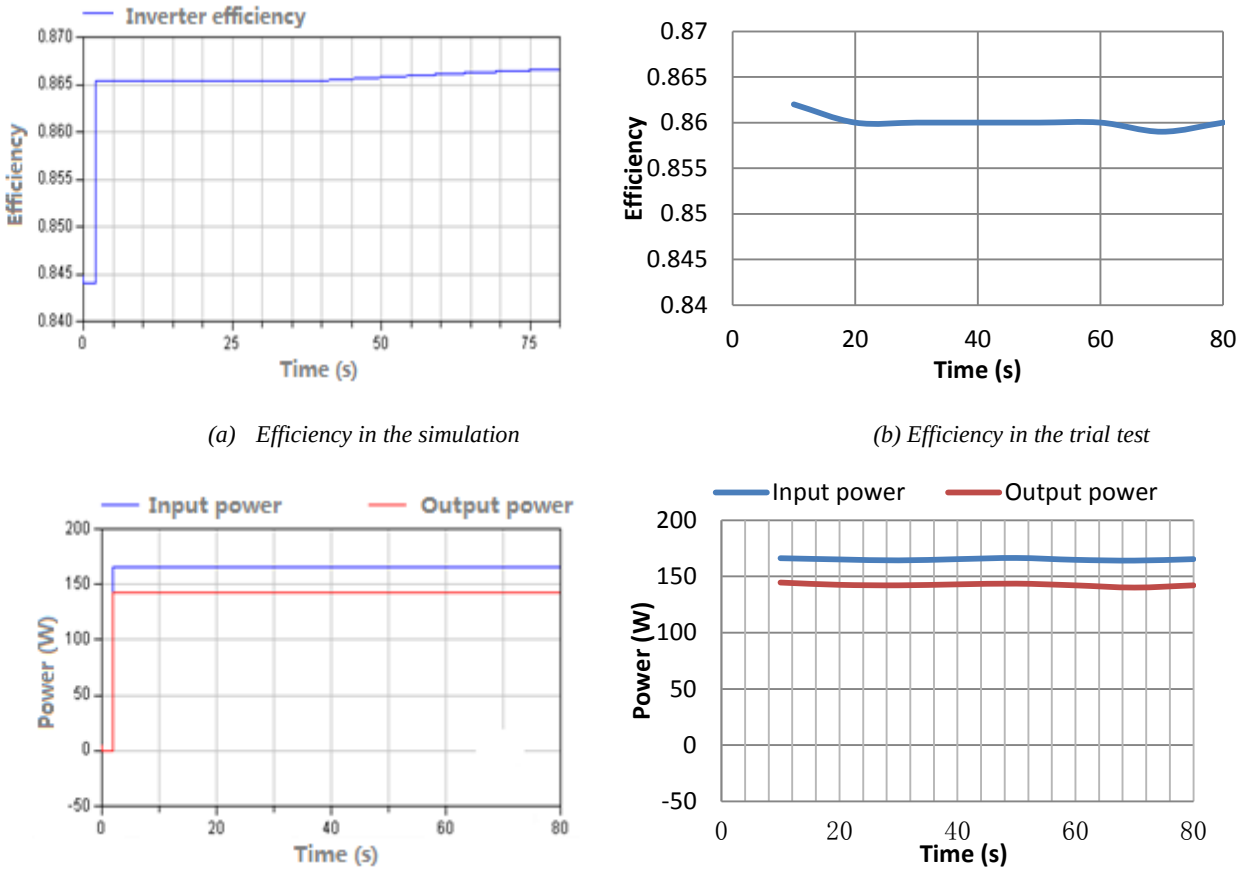

(a) Efficiency in the simulation

(b) Efficiency in the trial test

(c) Power in the simulation

(d) Power in the trial test

Fig.7.4 Efficiency and power of the inverter

C Power and efficiency

Fig. 7.4 shows the curves of inverter efficiency and input-output power. From the figure, it can be seen that the inverter efficiency was initially steady at 86.6% in the simulation curves but they increased gradually due to the current boost (as shown in Fig. 7.4 (a)). In the simulation, the inverter efficiency changed along with the circuit current. This fits with the general features of practical power devices higher efficiency for high power operation than in low power. Therefore, it is easy to undertand that the experimental results had almost constant efficiency since there was stable power required in the practical experiments (see as Fig. 7.4 (b)).

In Fig. 7.4 (c) and (d) the avarage input power is 165W while the average output power of the inverter is 143W in the physical tests. From these two diagrams, it can be observed that the output differences between them are within 2%, which is acceptable.

7.3.3 **HEES performance comparison over discharge/discharge operation**

Fig. 7.5 compares both trial test and simulation results regarding the current over the charge/discharge operation of the HEES. Blue, red and green lines are used to present super

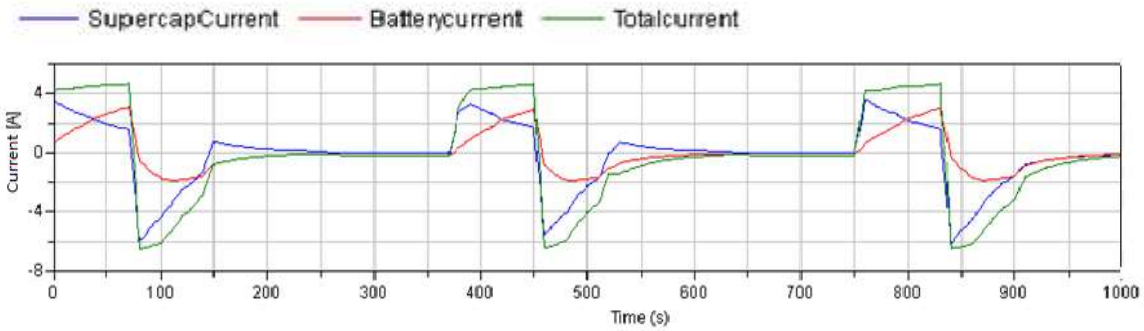

(a) Experimental outcomes

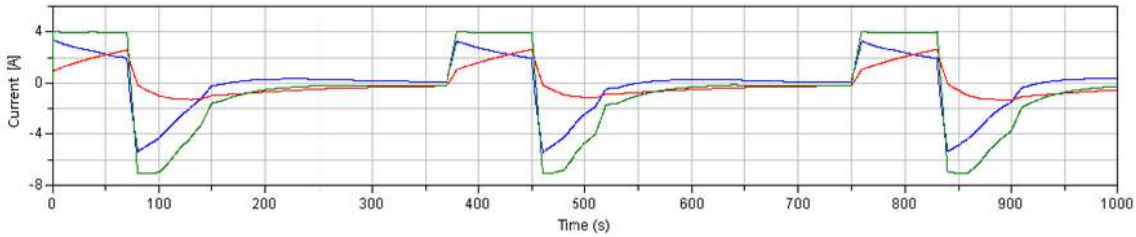

(b) Simulation outcomes

Fig. 7.5 Current comparison over the whole operation

capacitor, battery and total currents in both diagrams. Each current trace illustrates similar variation in both diagrams. There are slight differences between the simulation and physical outcomes as follows,

- The battery had an apparent difference at both the beginning and the end of the operation. The current decreased or increased promptly at both time points in the simulation but was relatively smooth over the physical operation in practice. The reason for that is due to the fact that the battery model has a voltage source and resistance. However, it was actually a chemical process during the physical operation. Meanwhile, the battery had less charge current than its physical counterpart due to different equivalent resistances between them.

- The simulation results of the super capacitor indicate that the model representation of the

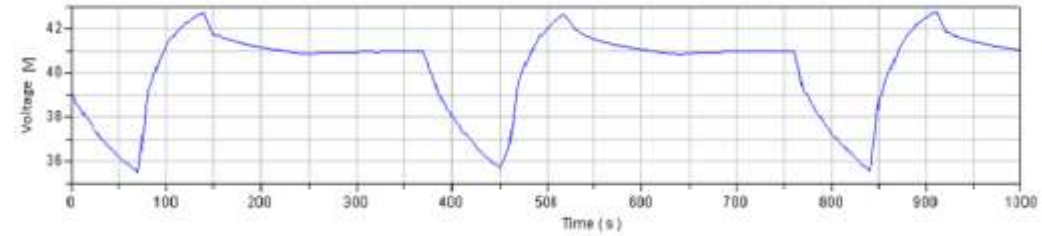

(a) Experimental outcomes

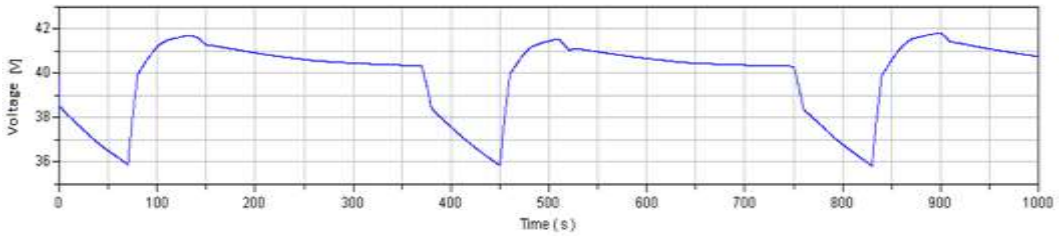

(b) Simulation outcomes

Fig. 7.6 Voltage comparison over the whole operation

physical component is more accurate than the battery. The difference between simulation and physical test was insignificant thanks to the simple electrical circuit of the super capacitor physically. Therefore, a simple model of the super capacitor can be used for practical operation with reasonable accuracy.

- The total current in both simulation and physical tests were in good agreement.

Fig. 7.6 demonstrates the voltage comparison over discharge/charge operation. Fig. 7.6 represents experimental and simulation test results. Decline and rise trends reflect discharge and charge, respectively. There were noticeable peaks over the charging duration in the physical test as in Fig. 7.6 (a) while the line in Fig. 7.6 (b) showed a slight reduction. Taking the time 145 s for example, the voltage increased rapidly to 42.8 V in Fig. 7.6 (a) while it went up gradually to 41.8 V in Fig. 7.6 (b). The error was 1 V, which is 2.3%. By contrast, the voltage had a faster decrease over the discharge operation in the simulation while the physical counterpart altered more smoothly, which can be seen from the duration between 380 s and 450 s by comparing the two graphs.

Overall, the simulation results modelled their practical counterparts over charge/discharge operation with good accuracy. Therefore, the HEES system models could be realistically integrated into the whole BMT-HEES for further investigation.

7.4 **BMT-HEES system simulation and trial test**

The aim of the whole project was to build up a tri-generation system fed by bio-fuel to satisfy domestic energy demands both electrically and thermally. Therefore, a domestic size tri-generation system was built up. A selected energy profile investigated by Lawson [14] was used as a typical case applied to the BMT-HEES which was validated by the simulation investigation and trial tests.

7.4.1 **Case 1 comparison of simulation and experimental results**

The main task of this research was to investigate a 6.5kW Yanmar engine-based BMT-HEES system. The load profiles in case 1 are shown in Fig. 7.7. There were two peak durations which happened from around 6am and 5pm. The maximum power reached 10,290 W while the minimum power demand was only 250W on this day. Basically, there were regular fluctuations between the times 0 and 6am, 12 and 16:30 where load power ranged from 290 W to 540 W, 250 W to 1390 W respectively. A series of diagrams from Fig. 7.7 to Fig. 7.10 illustrate the dynamic curves for case 1 both in experimental and simulation investigations. The uncertainties between experimental results and their simulation counterparts for case 1 are summarised in Table 7.1.

A Load profiles

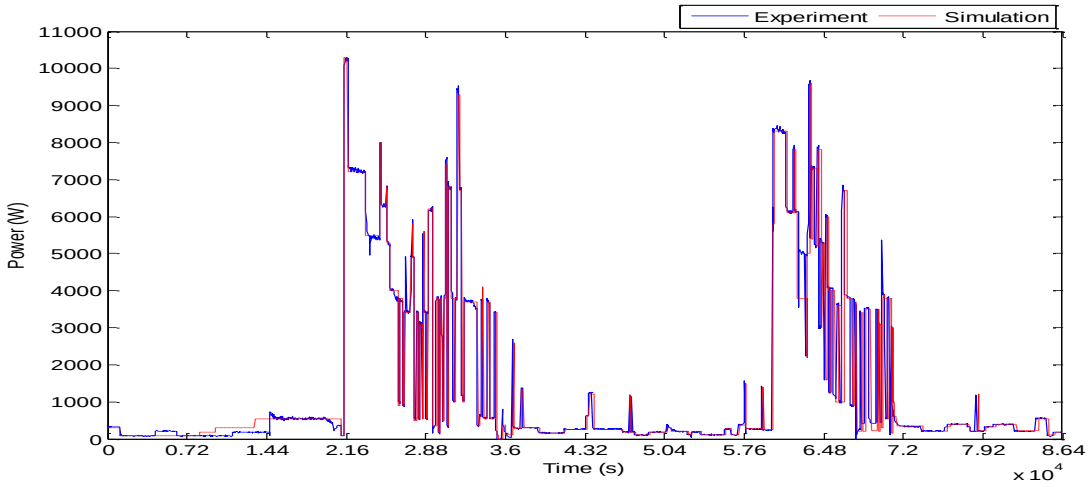

(a) Load profile comparison

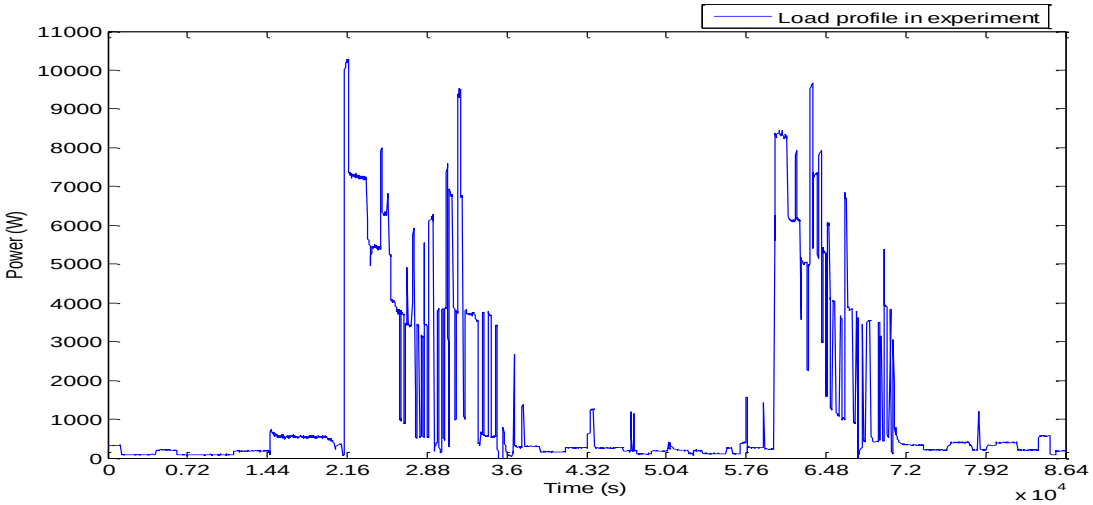

(b) In experiment

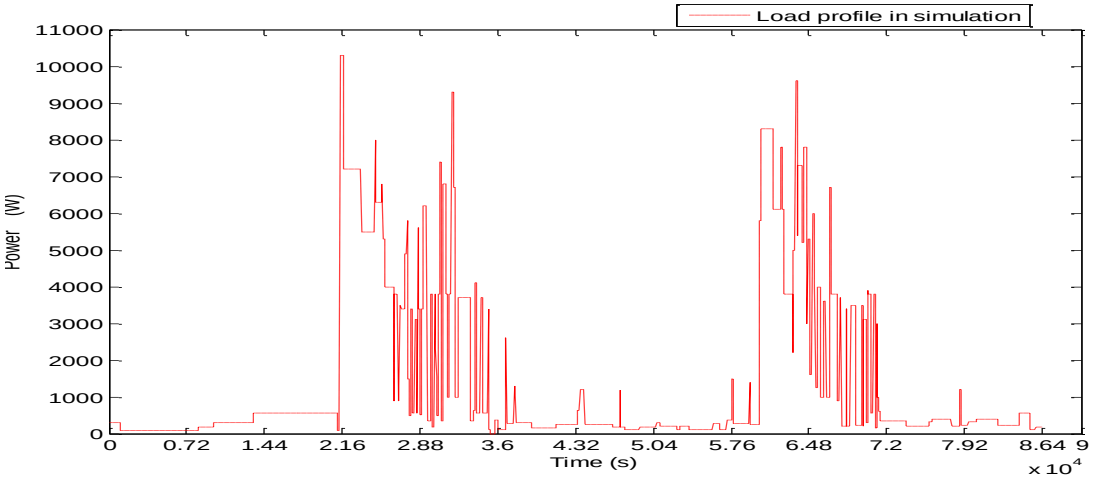

(c) In simulation

Fig. 7.7 Household electricity consumption over 24 hours

The load power data was detected by the power transmitters and transformed by the NI dock card. Fig. 7.7 (b) shows its profile per 30 seconds. The total number of data points was 2880 over 24 hours. In the simulation, the load profile was loaded by data table with 147 feature points which represented the fluctuation of the load power over 24 hours, the profile is shown in Fig. 7.7 (c).

B Engine performance

Engine power profiles in Fig. 7.8 for the experiments and simulation results show a similarity over 24 hours. Fig. 7.8 (a) shows the comparison for the outcomes in the practical experiment and the simulation. Fig. 7.8 (b) and (c) illustrate the details of both results. There were 3 times of engine duty period over 24 hours, from 14670 to 20430 seconds, from 21360 to 35190 seconds, and from 60150 to 67650 seconds. The engine switched on to charge the storage system over the first duty duration to ensure enough energy was can be stored in the energy storage system before the first peak hour of the electrical demand. The remaining two durations appeared in the peak hours from 6 am to 9 am and from 4 pm to 7 pm on this day. However, the most noticeable dissimilarity between these two profiles was the power range of the engine. Specifically, its maximum power was 6800 W in the practical tests while the counterpart in the simulation it was restricted to 6500 W.

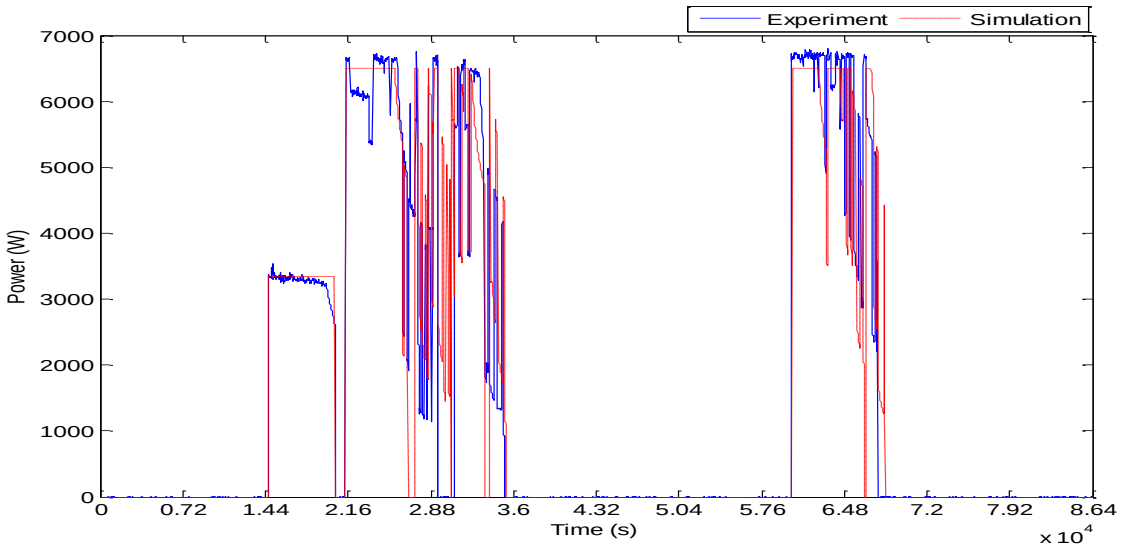

(a) Engine performance comparison

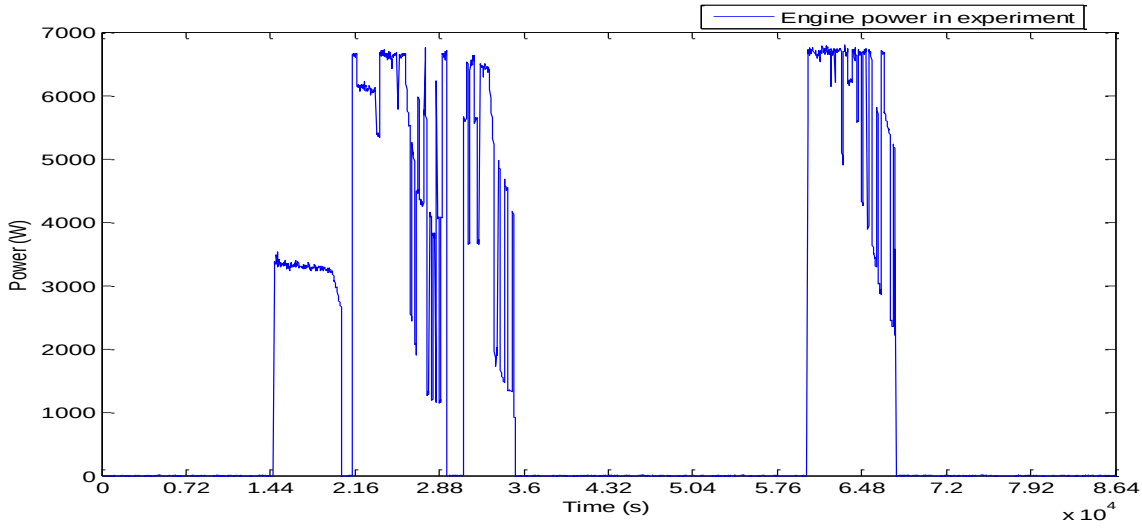

(b) In experiment

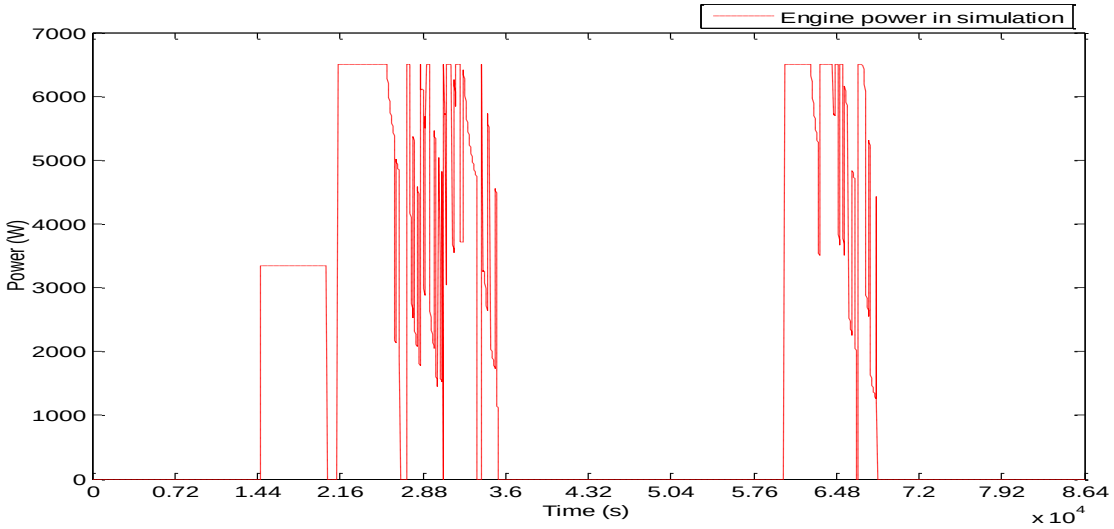

(c) In simulation

Fig.7.8 Engine power profiles over 24 hours

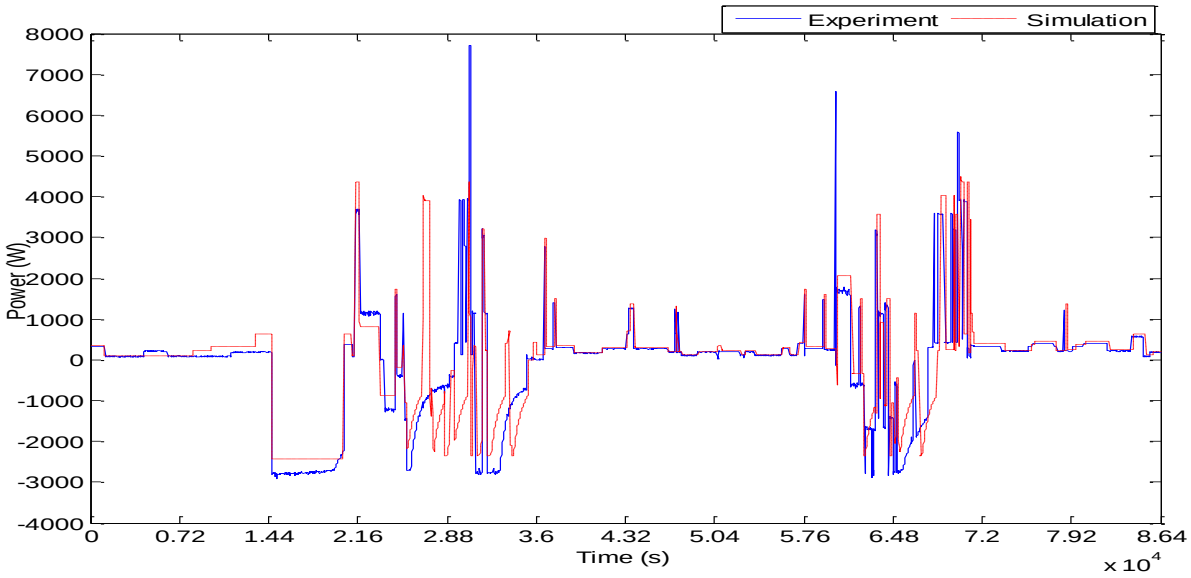

(a) Battery performance comparison

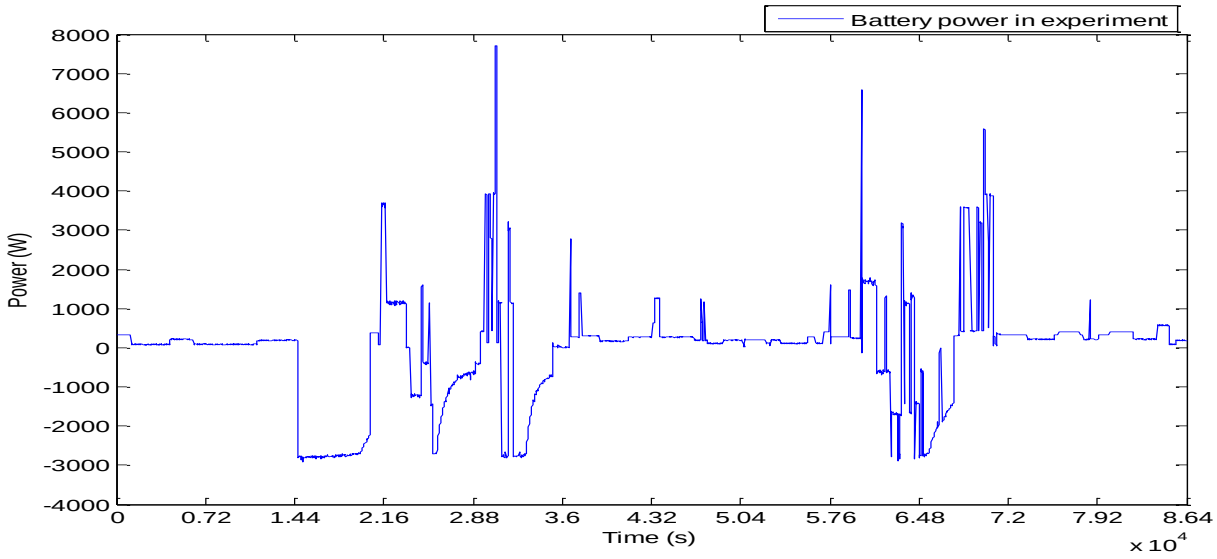

(b) In experiment

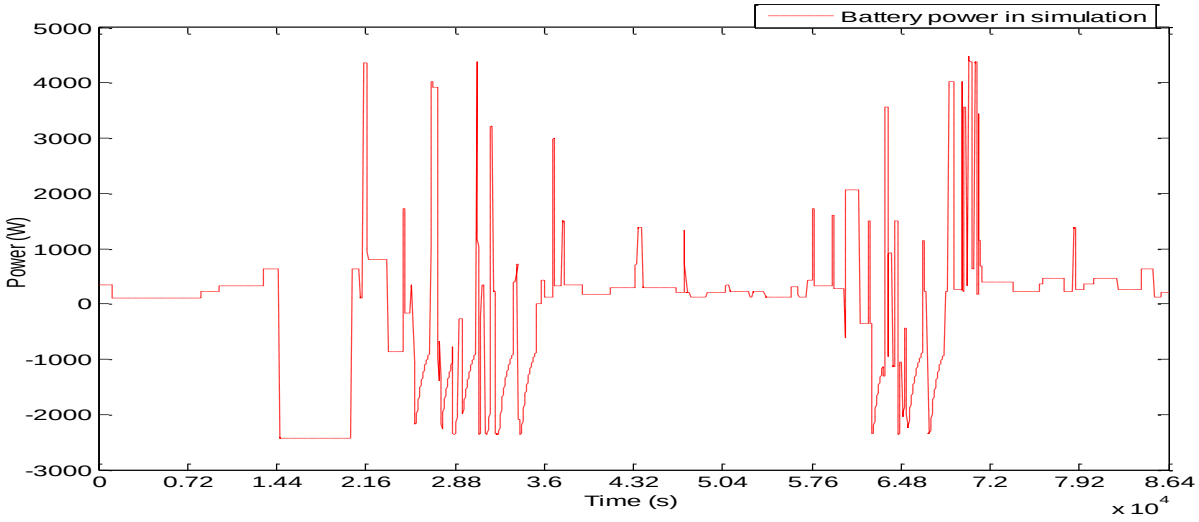

(c) In simulation

Fig.7.9 Battery power profiles over 24 hours

C Battery performance

The series of diagram in Fig. 7.9 illustrate the battery performance both in experiment and simulation. The batteries were operated most of the time (over 18 hours) within the 24-hour test. They were able to cover the fluctuation of the load power profile with a range between -2,920 W and 7,715 W in the practical system (shown as Fig. 7.9 (b)) and from -2364 W to 4373 W in simulation (shown as Fig. 7.9 (c)). The negative values in Fig. 7.9 represent the power for charging while positive one stands for power discharged from batteries.

D Super capacitor performance

The super capacitors provided limited energy and power to the system compared to the batteries. However, they responded to the sudden change of the load demands promptly. Practically, when the load increased unexpectedly by a large amount, in which case they provided the power needed to compensate the power of the battery in the practical test. However, in the simulation this job was taken by the engine. This case could be found at the time 7 pm 25 minutes (70860 s). Fig. 7.10 illustrates the details. The power of the super capacitors in the practical test ranged from -395 W to 2,781 W (shown as Fig. 7.10 (b)) while in simulation it was from -1532.7 W to 1520.0 W (shown as Fig. 7.10 (c)). Again, the negative value represents power for charging while the positive stands for power discharged.

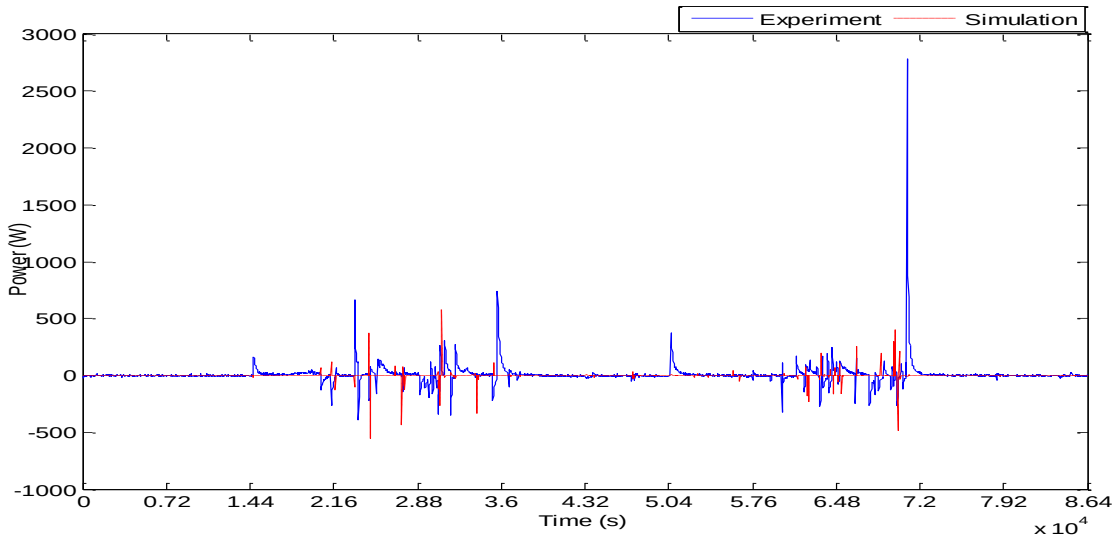

(a) Super capacitor performance comparison

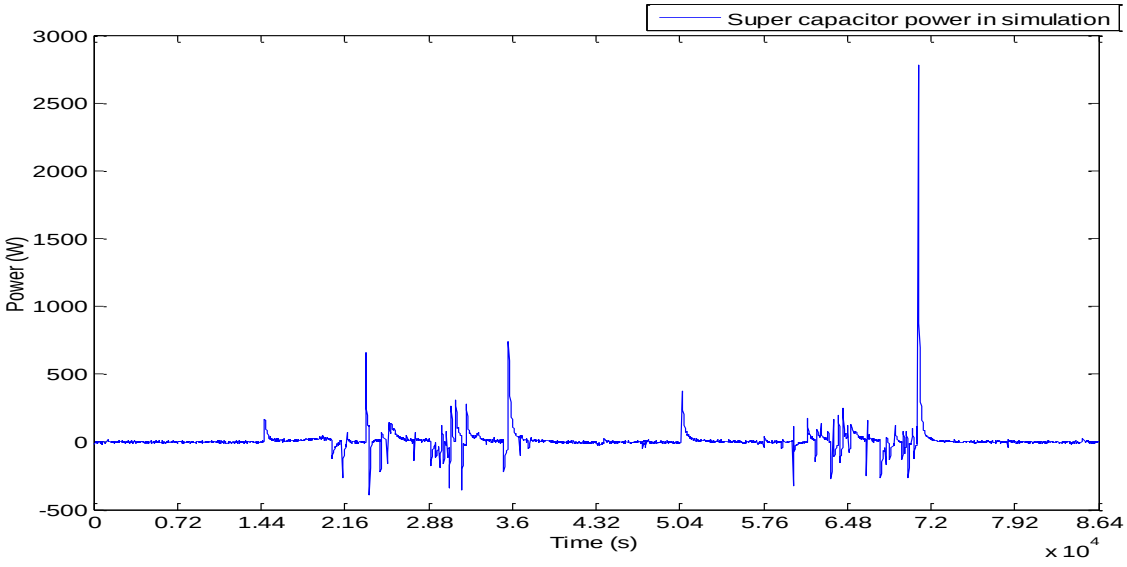

(b) In experiment

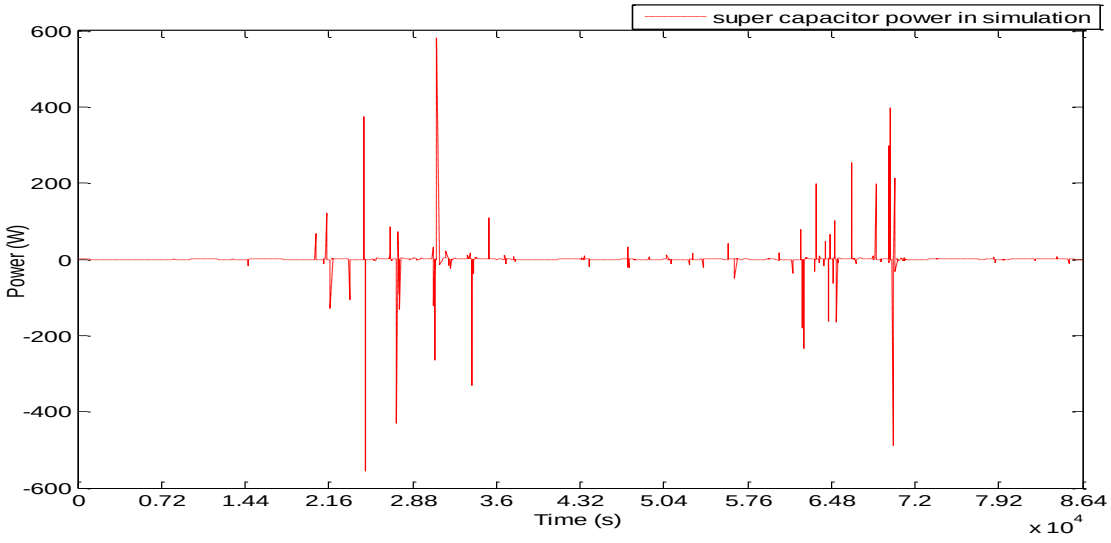

(c) In simulation

Fig. 7.10 Super capacitor power profile over 24 hours

E Indicator summary

Table 7.1 summarises the performance indicators and their comparisons over the investigations. Four aspects have been compared, including energies, duration, efficiencies and power range. For instance, the electricity consumed over 24 hours was 33.63 kWh in the experiment and 33.13 kWh in the simulation with an uncertainty of 1.49%. The engine was operated for 7.16 hours and 7.22 hours in the experiment and simulation, respectively. Meanwhile, the uncertainty between them was 0.84%. In terms of overall system efficiency, it was 63.70% and 63.27% in experiment and simulation, respectively.

Table 7.1 Outcomes comparison between experiment and simulation in case 1 study

		Trail test	Simulation	Uncertainties (%)
Energy (kWh)	Electric energy from engine	35.16	35.49	0.94
	Energy supplying to load directly from engine	25.03	25.16	0.51
	Electricity consumed by load	33.63	33.13	1.49
	Thermal energy recovered	51.71	52.65	1.82
	Peak energy	11.78	11.66	1.02
Duration (hours)	Battery discharge time	18.32	18.13	1.04
	Engine running	7.16	7.22	0.84
	Charge period for batteries	5.7	5.8	1.75
	Peak hour (energy demands above 6.5kW)	1.48	1.50	1.35
Efficiencies (%)	Batteries electric efficiency	23.23	22.83	1.72
	Super capacitors electric efficiency	25.53	24.94	2.31
	Engine electric efficiency	25.75	25.46	1.13
	Thermal efficiency	39.22	38.86	0.92
	System electric efficiency	24.78	24.41	1.5
	System overall efficiency	63.70	63.27	0.68
Power range (W)	power from super capacitors	-395/2,781	-532.7/1520.0	-
	power from battery	-2,920/7,715	-2364/4373	-
	power from engine	0/6,800	0/6500	-
	Load power	0/10,290	0/10,290	-

All of the indicators for the experiment and the simulation were quite close as shown in Table 7.1 where all uncertainties in the tables were within 2.3%. This confirmed that the models of the system matched the physical system well.

First of all, the load profile fed into the system model did not have the same accuracy as the one adopted in the experiment.

Secondly, the charge method for the energy storage system in the simulation was an approximate curve from the battery performance test. Therefore, the batteries charged with the same curve when they were in different situations. The charge curve in the simulation was adjusted according to the capacities of the batteries. For example, the bulk charge would take longer after batteries experienced large discharge.

Thirdly, uncertainty factors in the experiment, such as measuring error of the detecting devices, temperature influences, power and load fluctuations etc. would give rise to the difference between experiment and simulation.

For the statistical calculation, the system performance in the experiment and simulation matched well. However, there is potential for improving the dynamic response of the system with a higher accuracy.

7.4.2 **Case 2 comparison of simulation and experimental results**

In case 2, the domestic electricity consumption over 24 hours in another dwelling was employed. From Fig. 7.11, it can be seen that the minimum demand of electrical power was around 100 W and the peak demand reached 6544 W. Meanwhile, the electricity consumption was lower than 1 kW during the majority of the 24 hours while the peak demands lasted for relatively short periods. For instance, at 1 pm 11 minutes (47448 s), the demand was as high as 6.544 kW before it dropped to 400 W 5 minutes later. The peak demands over 2.500 kW appeared 3 times, starting from 5 am 22 minutes (19296 s), 1 pm 11 minutes (47448 s), and 9 pm 22 minutes (76932 s). Electricity consumption for this household over 24 hours was 9.85 kWh in total.

The key performance indicators are summarised in Table. 6.2. The series of diagrams form in Fig. 7.11 to Fig. 7.14 provide the load power scenario, batteries power scenario, super-capacitor power scenario and engine/generator power supply both in test and simulation.

A Load power profiles

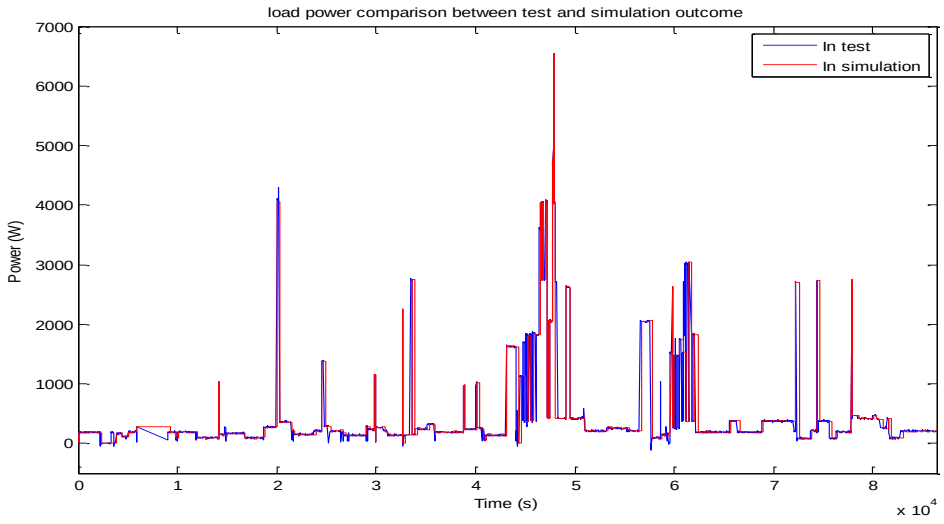

(a) Load profiles comparison

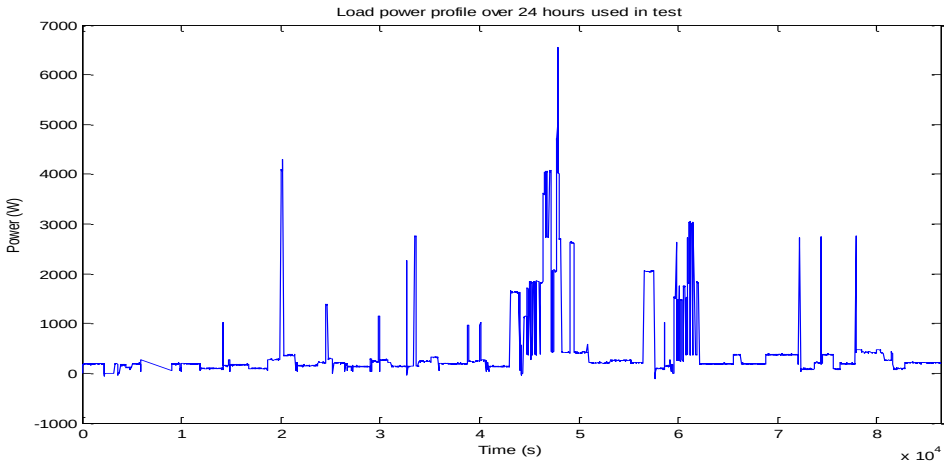

(b) In test

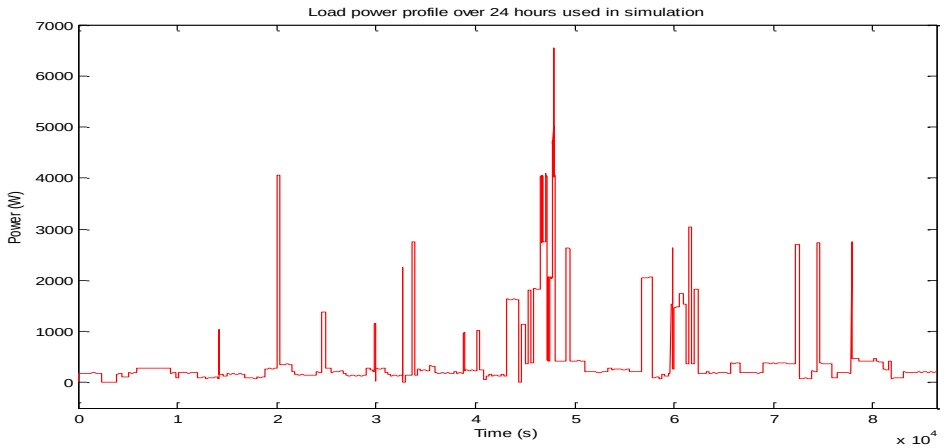

(c) In simulation

Fig.7.11 Load power profile over 24 hours

Fig. 7.11 compares the load power scenario in case 2 over 24 hours in the test and simulation respectively. There is a slight difference between them due to the dissimilar data format required by Dymola modelling. Load power data was fed into the simulation via the model *time table* in which variation between different time points is not permitted. That meant the trip points were only allowed to be set at same time point. Therefore, the original power data file needed to be revised in *Dymola* data format. Furthermore, the data points in *time table* are limited and some less-significant data was ignored to satisfy this requirement.

B Battery profiles

According to Fig. 7.12, the battery power profiles had quite similar features both in test and simulation. Apparently, there were three durations for battery charge in both investigations while the battery performance was satisfactory in meeting the electrical demand. However, the power range was different between simulation and trial tests. The batteries were operated within the range from -5800.38 to 1841.798 W in the physical system (shown as Fig. 7.12 (b)) while the power varied between -4043.5 and 2421.6 W in the simulation (shown as Fig. 7.12 (c)).

C Super-capacitor profile

The super-capacitor performance shown in Fig. 7.13 revealed their prompt response capability both in the tests and simulation. However, they contributed limited energy to the system over any longer duration. The power of the super-capacitors ranged from 563 to -595 W in the trial tests (shown as Fig. 7.13 (b)) while they were within the power spectrum from -728 W to 856 W in simulation (shown as Fig. 7.13(c)). Apparently, less energy was provided by the super capacitors in the trial test than in simulation. Here, the positive and negative values represent charge and discharge power respectively.

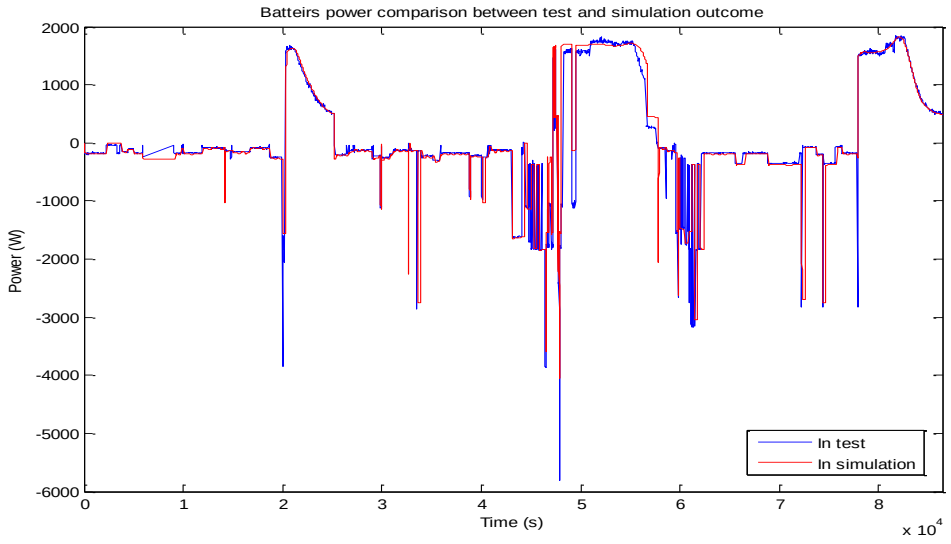

(a) Battery performance conparison

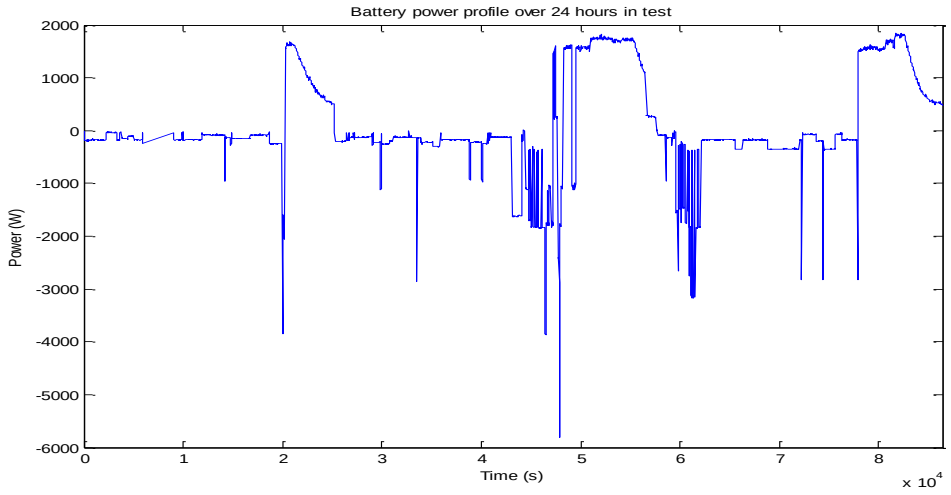

(b) In test

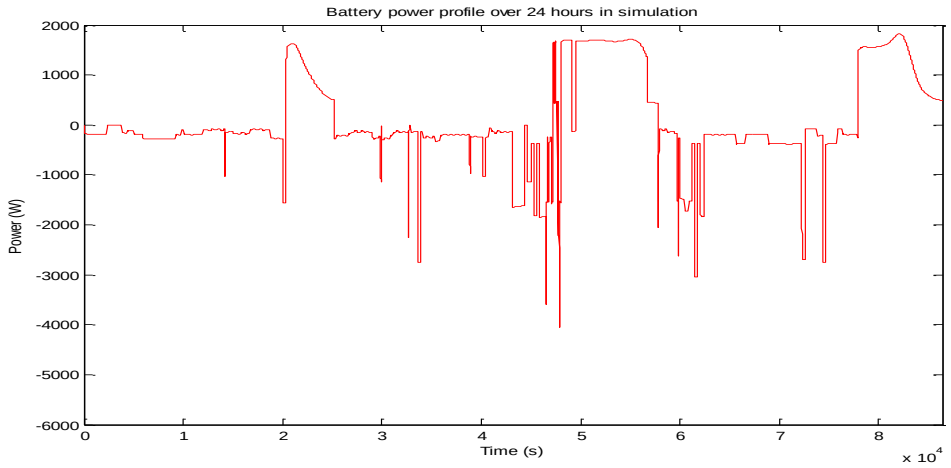

(c) In simulation

Fig. 7.12 Battery power profile over 24 hours

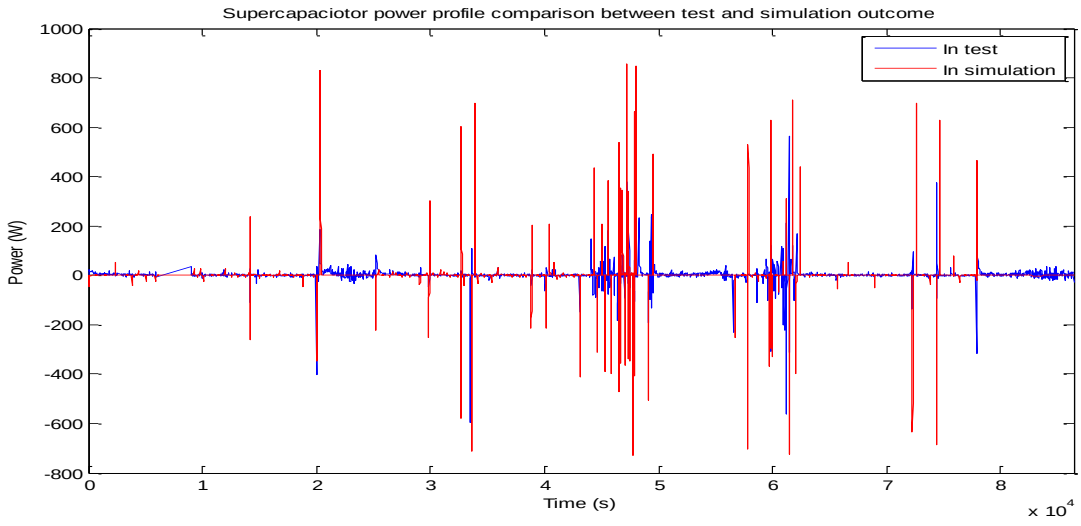

(a) Super capacitor performance comparison

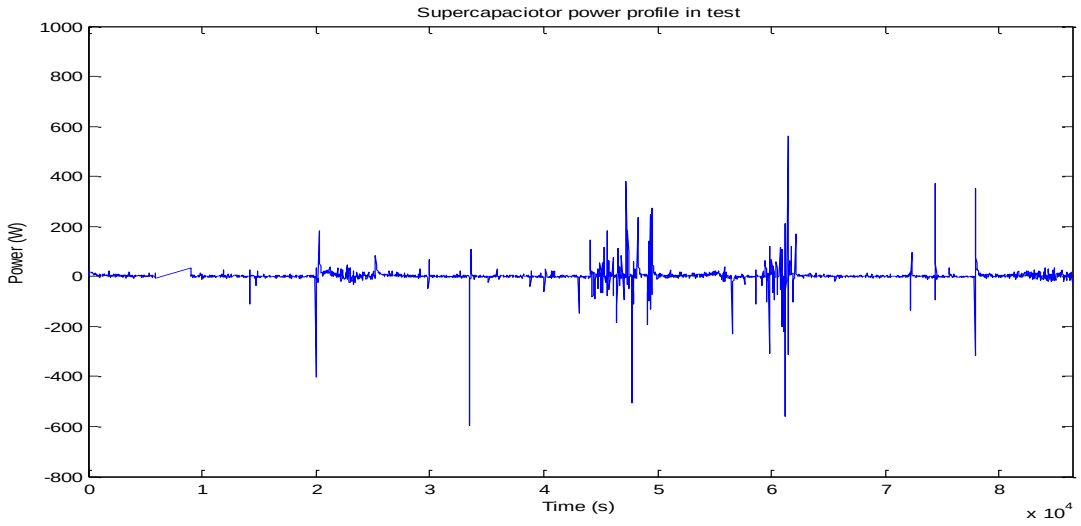

(b) In test

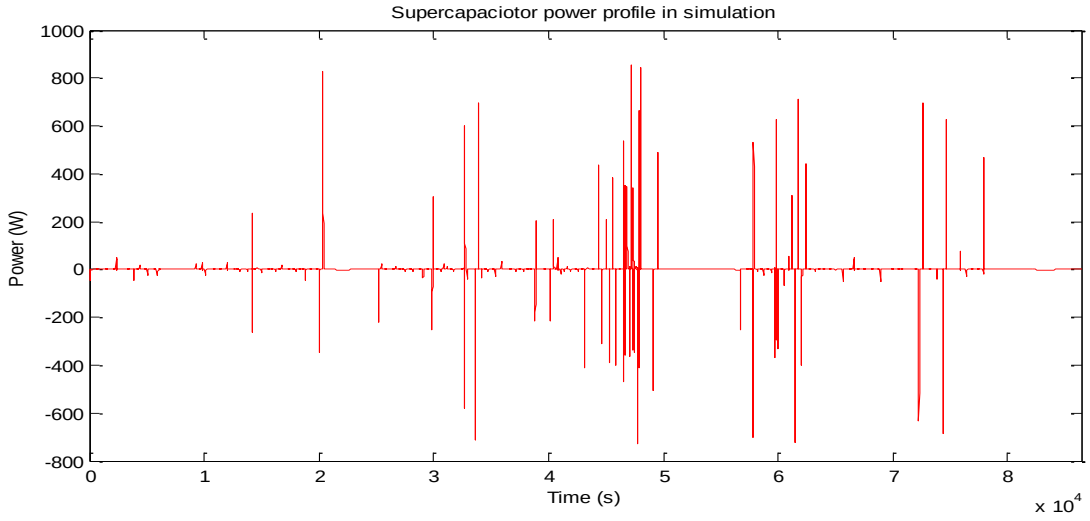

(c) In simulation

Fig. 7.13 Super-capacitor power profile over 24 hours

D Engine/generator power profile

Fig. 7.14 compares simulation and trial tests outcomes regarding engine performance over the

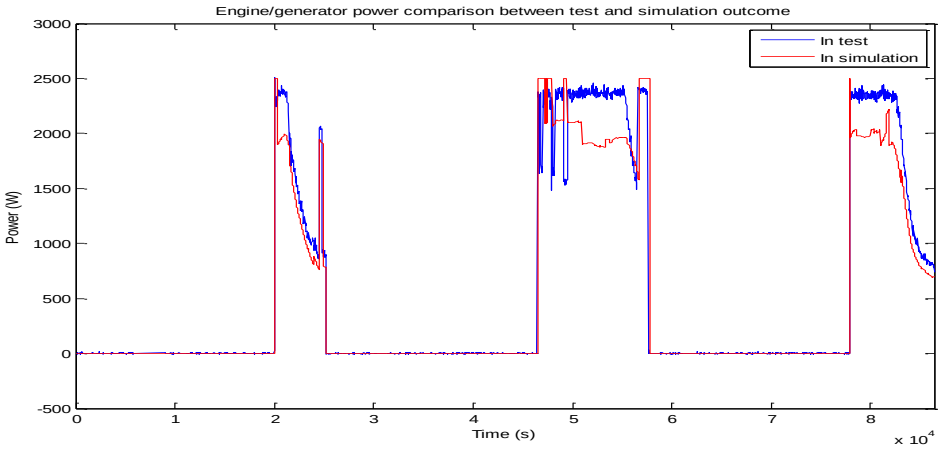

(a) Engine performance comparison

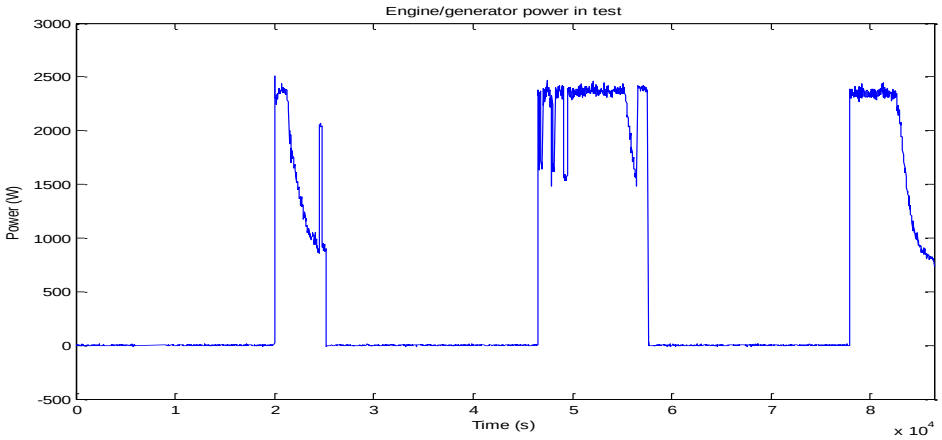

(b) In test

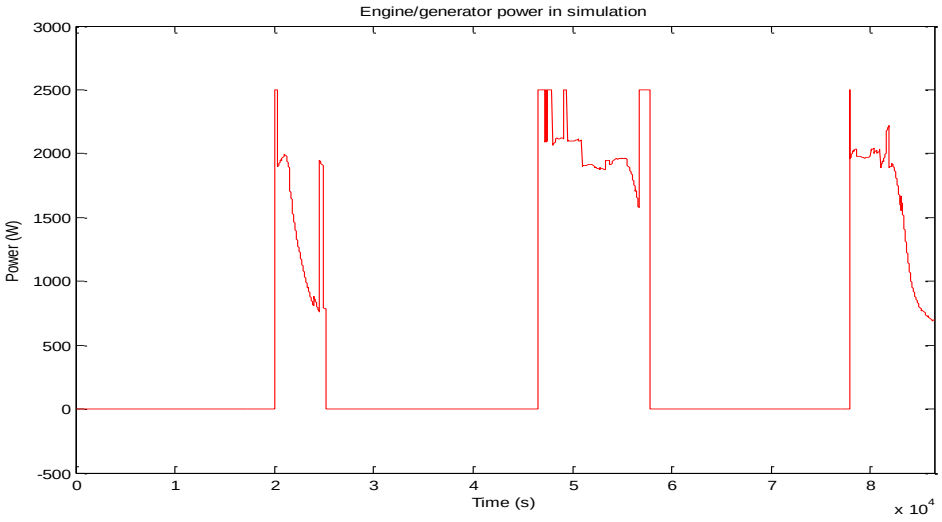

(c) In simulation

Fig. 7.14 Engine/generator power profile over 24 hours

24 hours studied. The engine operated three times over the 24 hour investigation. The signal for triggering the engine launch depended on the load power level as explained previously. The overall operation duration was 6.89 hours in the experimental tests while 6.87 hours was used in simulation provided that the same strategy was employed for both investigations.

E Comparisons for the key performance indicators

Table 7.2 lists some key performance indicators for comparing between test and simulation outcomes. A series of efficiency comparisons confirm that the differences between test and simulation results were insignificant and all of the deviations were within 2.6%. Engine start time points revealed that the engine launched three times and the total running duration was 6.89 hours in test and 6.87 hours in simulation. During the rest of the time over 24 hours, the HEES system provided electricity to satisfy the load demand. Obviously, the overall system efficiency is higher than when a single engine without energy storage is used to provide a 24-hour supply. The energy storage system supplied less energy in simulation than that in the tests. They provided a maximum power of 5800 W to the load in the practical tests while it was 4044 W in the simulation. On the other hand, the simulation results regarding the super-capacitor power was higher than in the test.

Table 7.2 Outcomes comparison between physical test and simulation

	Outcomes from trial test	Outcomes from simulation	Uncertainty (%)
Charge efficiency of HEES	22.56	23.14	2.57
Discharge efficiency of HEES	20.69	21.21	2.51
Engine efficiency(with HEES)	26.49	25.93	2.11
Engine efficiency (without HEES)	4.95	5.003	1.07
Overall electrical efficiency	23.59	23.57	0.085
Average heat recovery efficiency (BMT-HEES) (%)	40.08	40.05	0.74
Overall system efficiency (BMT-HEES) (%)	63.67	63.62	0.78
Batteries power range (W)	-5800.38 to 1841.798	-4043.5 to 2421.6	-
Super-capacitor power range (W)	562.7445 to -594.687	-728.3670 to 856.378	-
Engine/generator power range (W)	0-2507.5	0-2500	-
Engine operation duration (Hours)	6.89	6.87	0.3
Storage system charge duration (Hours)	6.48	6.46	0.31
Storage system discharge duration (Hours)	16.62	17.05	2.59

7.5 **Conclusions**

A series of comparisons between physical and simulation tests have been carried out in this chapter, ranging from the individual unit to the whole system investigation over 24 hours for two case studies. The simulation and test results validate the effectiveness of the developed technologies. All uncertainties between test results and their simulation counterparts were within 2.6% in terms of the whole system investigation.

The engine model was set up on the basis of mechanical and electrical principles and meanwhile, electrical and heat efficiency acquired from the physical test was taken into account in terms of calculation both for trial test and simulation. The HEES performance comparison between trial test and simulation confirmed that the uncertainties were limited to a reasonable range which will support further prototype development. All of the the experimental results agreed well with the simulation with a difference of less than 2.6% in both between the cases. Therefore, the system models could be used to forecast or predict system performance with reasonable accuracy when different energy scenarios are considered before a trial test is carried out.

Chapter 8 Conclusion and future work

8.1 Introduction

In this chapter, the main issues regarding the development of a bio-fuel micro-tri-generation system (BMT) with hybrid electrical energy storage (HEES) are concluded based on the in-depth analysis and discussion given in previous chapters. The key innovations and findings from this research work are summarised. Afterwards, further work for improvements and future development in this research field are provided with a focus on the integration of BMT and HEES.

8.2 Key issues in this investigation

The utilisation of new and renewable energy is high on international and national agendas. Historically, bio-fuels and tri-generation have been extensively explored in the literature and commonly regarded as two promising technologies to combat climate change and the global energy crisis.

Bio-fuels (especially bio-diesels for engines) are a cost-effective substitute for conventional fossil fuels to reduce CO_2 emissions and, counter general concerns for fuel security. Conventional tri-generation systems (e.g. CCHP) can be found in use in medium- and large-scale applications and micro-tri-generation systems are utilised in household or other domestic applications. These systems are generally effective but suffer from relatively poor dynamic response, low energy efficiency, and high initial and operational costs. The related technologies are still evolving with regard to component-level and system-level optimisation, interconnection and grid connection.

This work was concerned with the development of innovative technologies to integrate bio-fuels and energy storage system (including super-capacitors and batteries) into the tri-generation system whilst still improving the system performance, energy efficiency and cost-effectiveness. The primary goal of this PhD research was to simulate and build up a bio-fuel-based micro-tri-generation system with hybrid electrical energy storage which could meet the domestic energy demands for electricity, heating and cooling with low fuel consumption, low emissions and high electrical, thermal and cost efficiency.

There were five crucial technical issues this work has addressed:

1) Study of domestic energy consumption. This system is primarily applied to the domestic environment and it was necessary to survey domestic energy consumptions and find out the potential demand characteristics in order to select the size and the capacity of the BMT system.

2) Investigation into energy storage systems and related technologies. This was a key technical task central to this research. The compatibility of energy storage systems with the operation of a diesel engine was taken into account along with consideration of the application characteristics.

3) Survey of energy management strategies, mathematical algorithms and control systems. The energy management strategy is key to the efficient operation of a tri-generation system but strongly depends on the specific goals the users want to achieve from the system. Therefore, detailed comparison and analysis of various potential strategies for the domestic tri-generation applications have been conducted in order to ensure effective energy utilisation.

4) Computational models and simulation of the system. Simulation is a useful approach to relieve burdensome experiments and to provide guidelines on constructing a physical BMT-HEES. This was done in the "Dymola" environment with the help of advanced energy management strategies. The models in turn were validated by the experimental results. The system parameters could be modified and evaluated to improve the system design.

5) The design, implementation and testing of the BMT-HEES system. This was the final realisation stage to follow the optimised system design and to build the physical system unit by unit, and experimentally validate the proposed system.

8.3 **Conclusion from this study**

Research findings are summarised in the areas of completed work.

8.3.1 **Energy demand survey in the UK households**

Undoubtedly, a domestic tri-generation system should satisfy both electricity consumption and heat (or/ and cooling) demands. However, heat and power consumptions are very dissimilar from each other in practice. Heat demand changes very slowly while electricity may vary rapidly within millisecond if demanded. Moreover, domestic heat demands have apparently seasonal differences but the variation over one single day is relatively slow while the electricity demands fluctuate dramatically within each day but have a good repeatability over the year. The daily electricity demands fluctuated over a wide range from several-hundred watts for the majority of the time to several kilo watts for a very short period.

In this investigation, relevant technologies and experiences relating to tri-generation have been surveyed. The investigations were concentrated with tri-generation systems and dynamic energy consumption in UK households using various available statistical data. From extensive studies on existing engine-based tri-generation systems, it was necessary to include an electrical energy storage system to ensure fuel savings and energy efficiency enhancement. As a result, electrical energy storage technologies were examined in the literature review and a hybrid electrical energy storage was considered to achieve both power and energy benefits in the integrated system. A Yanmar engine with output power of 6.5 kW was selected as the prime mover in the investigation.

8.3.2 **Energy storage system**

Electrical storage devices can be generally divided into two groups according to their application, namely an energy device group and a power device group. After considering comprehensive factors, including cost, applications and physical size, batteries and super-capacitors were selected as key components in the storage system. From the tests, it was found that super-capacitors exhibited superior dynamic properties in response to electrical demand changes. However, they have a low energy density and could only provide electricity over a short period of time (in seconds). This drawback could be compensated by the use of batteries in hybrid systems. In contrast, batteries have a higher energy density which can sustain a relatively long period of supply. During the operation, the super-capacitor would first provide a large current to meet the transient demand from the load but this would soon reduce and the load would then be supported by the batteries.

Despite the merits of the HEES, specific performance indicators should be evaluated by performing physical tests on a prototype system. This was achieved by conducting a series of preliminary tests. In the tests, the super capacitors were activated promptly both in charging and discharging cycles and thus considered to be appropriate to satisfy household electrical loads with sound dynamic response. However, due to the parallel connection between the batteries and the super capacitors, there was a voltage difference between them at the float-charging stage causing electrical current to rush from the super-capacitors into the batteries even though both were in charging mode. Therefore, diodes were added to stop this from happening when developing the complete BMT-HEES.

8.3.3 **Modelling and simulation**

Through the preliminary tests on the HEES, the properties and characteristics of the components were understood, which served as the basis of the system models. System models were constructed and system performance assessed by case studies which were of typical domestic electrical consumption profiles over a single day as reported in the literature.

Modelling and simulation provided guide information prior to the physical development of the system. Following extensive theoretical analysis, core component models were built up in the "Dymola" environment, including batteries, super capacitor, engine, power conversion devices (inverter/charger), and controller.

In the simulation, optimal energy management strategies were examined and compared in order to manage the energy distribution at high operational efficiency. From simulation tests, the targets of fuel savings and high energy efficiency were achieved. When employing a 6.5 kW Yanmar engine in the BMT-HEES, the overall energy efficiency increased from 47.6% to 63.9% and especially, the electrical efficiency has improved dramatically from 7.2% to 25.2%.

8.3.4 **Energy management strategy**

After the physical structure of the energy system was designed, the energy management strategy was the next critical issue for optimising performance of the system.

For this research electrical consumption was identified as a key factor for system operation due to the rapid transient fluctuations for the household demands. The operational approach

in the BMT-HEES could be described with three different states according to the interaction between the engine/generation system and HEES. In State 1, electrical power was supplied from both the engine/generator and the HEES system (for peak hours). In State 2, the engine was still running to supply power to the load and in the meantime to charge the HEES (for off-peak hours). State 3 described the situation when the electrical load was low and the HEES system operates alone to meet household demands and the engine was shut down (for night hours). The economic benefits were obvious here. On the basis of this optimisation of the algorithm was considered for best coordinating the operation of the engine/generator and the HEES at high efficiency.

8.3.5 **Integrated physical system tests**

The BMT-HEES system was developed after gaining an in-depth understanding of the component and system performance as well as a carrying out a system design and performance prediction in computational simulation. Case studies were used to compare the BMT-HEES with engine-based tri-generation without electrical energy storage.

It was found: the use of a BMT-HEES allowed a smaller engine to satisfy the same energy demands. Dynamic performance was improved owing to the integration of the HEES. With optimal energy management strategies, the engine was allowed to operate over shorter durations and at higher energy efficiency compared to the engine-based tri-generation (without HEES). The BMT-HEES satisfied electrical and thermal demands with just the required amount of energ generated. As a result, the system performance and energy efficiency were greatly improved.

8.3.6 **Comparison between simulation and experimental results**

The BMT-HEES system was improved based on the investigation both from simulation and preliminary experiments. Experimental results were in good agreement with the simulation results in all aspects examined. The differences between them were within 2.6%, which ensured that the system models had reliable accuracy for performance assessment and prediction.

8.4 **Recommendation for future work**

The aim of developing a BMT-HEES system to satisfy expected domestic energy demands has been achieved. In future work, there are some potential areas for the developed technologies to be expanded. Fig. 8.1 illustrates some potential applications involving the BMT-HEES, including hybrid energy systems, power-grid based systems, shore power and solar energy systems. The system can be incorporated with other types of bio-fuel or other

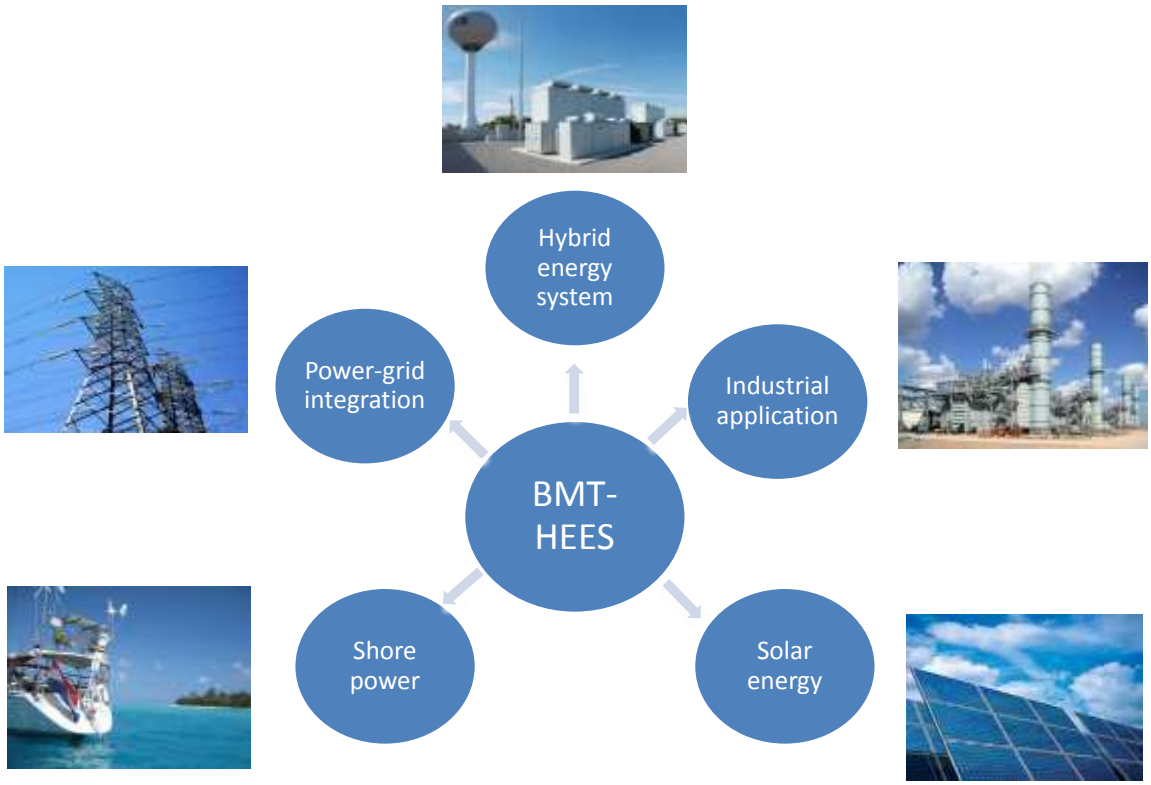

Fig. 8.1 Expandability of the BMT-HEES

sources of new and renewable energy (wind, solar, geothermal, biomass etc.), depending on the availability of the energy and location of the system. Furthermore, this system can be scaled up for larger commercial and industrial environments. Also, it can be incorporated with energy networks and smart grids. As illustrated in Fig. 8.2, there is potential for applications of the BMT-HEES which include some renewable energy. In this case, solar energy collected by the solar panel could be used to charge both batteries and super-capacitors with little conversion loss. DC power sources could act as extra energy sources to supply peak demands along with AC power from the generator. Furthermore, solar power could be linked with a generator via an inverter to supply AC power demands to increase AC power capacity.

In addition, the BMT-HEES could be expanded into a shore power system by updating the system construction. Fig. 8.3 shows one possible shore power system that could integrate with the BMT-HEES. The majority of components in this system are similar to the system described in this study with some additions (transformers, relays and circuit breakers) to upgrade the capacity of the energy supply.

Finally, in addition to the small-scale domestic environment, the physical system could be scaled up to be used in larger commercial and industrial environments. The developed system could not only be used as a stand-alone energy system, but also be inter-connected with neighbouring energy systems or connected with the power grid as a distributed generation set if there was a need for (or a surplus of) the generated electricity. Without doubt, this would require further work on this inter-disciplinary topic as well as new innovations in the fields of energy networks and smart grids.

8.5 Summary

This chapter provided the key challenges, solutions and findings related to the development of the BMT-HEES from this EPSRC-sponsored PhD work. Moreover, some potential applications and areas for improvements have been provided for consideration for further work.

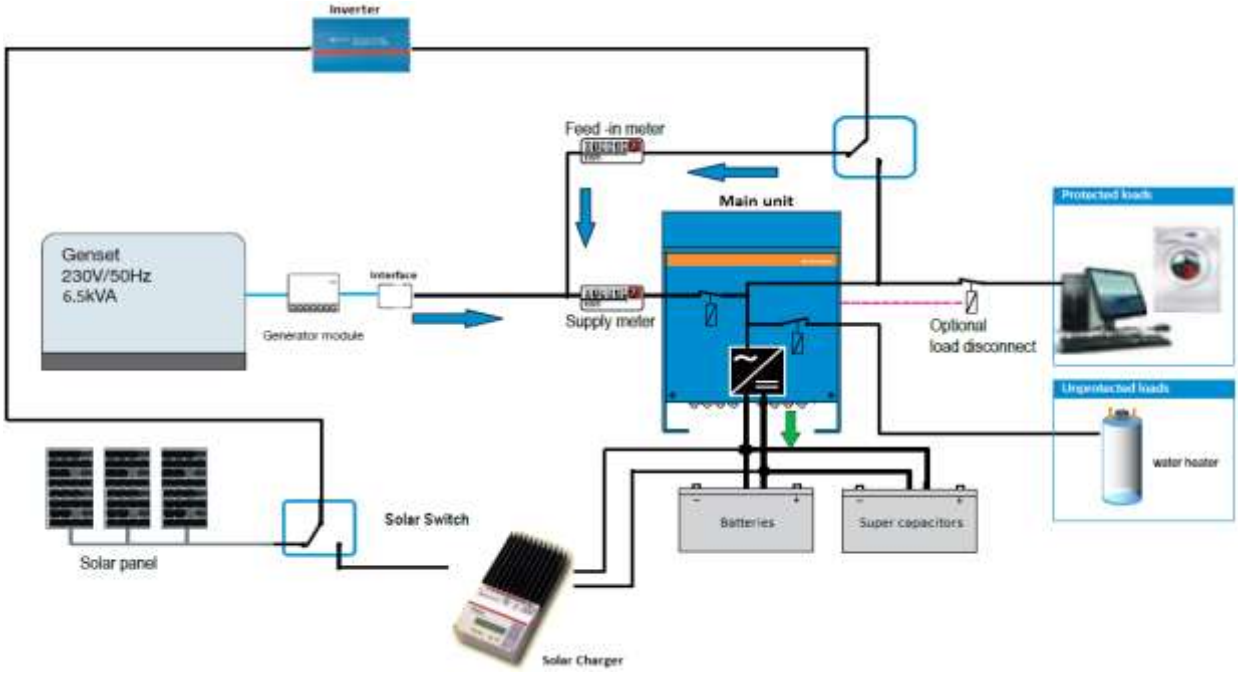

Fig. 8.2 BMT-HEES combining with other power sources

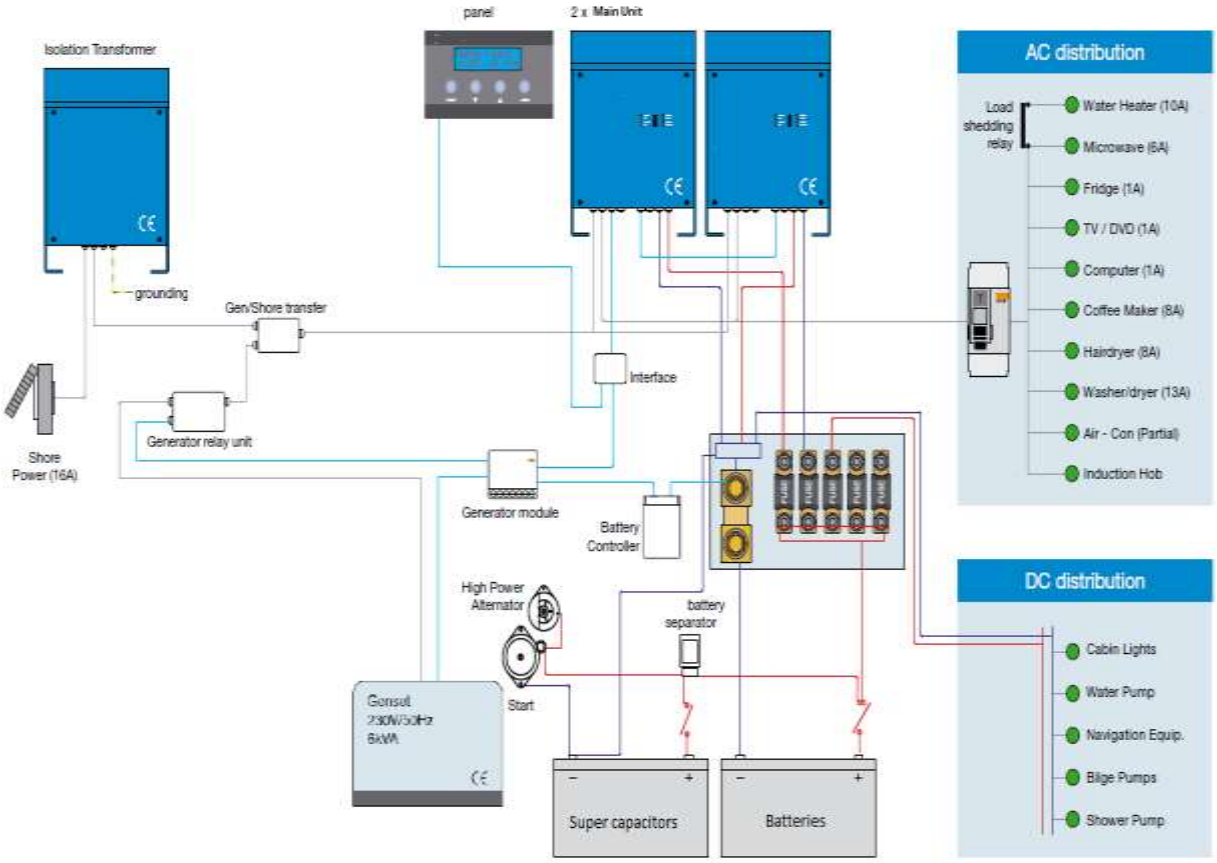

Fig. 8.3 BMT-HEES integrating with other power sources

References

1. (OPSI), O.o.P.S.I., *Climate Change Act 2008*, O.o.P.S.I. (OPSI), Editor 2008.
2. plc, A.T., *Analysis of Renewables Growth to 2020*, 2010.
3. DECC, *UK Renewable Energy Roadmap Update 2012*, DECC, Editor 2012: UK.
4. Fisher, J., *Reducing Household Energy Use and Carbon Emissions: the potential for promoting significant and durable changes through group participation*, in *Proceedings of Conference: IESD PhD Conference: Energy and Sustainable Development*2010: Leicester, UK.
5. DECC, *Electricity statistics*, d.o.e.a.c. change, Editor 2011. p. 120.
6. DECC, *Feed in Tariff generation*, 2012.
7. DECC, *Feed in Tariff capacity*, 2012.
8. D.H. Qi, H. Chen, L.M. Geng, Y. ZH. Bian, *Experimental studies on the combustion characteristics and performance of a direct injection engine fueled with biodiesel/diesel blends.* Energy Conversion and Management, 2010. **51**(12): p. 2985-2992.
9. DECC, *Domestic energy consumption*, DECC, Editor 2011, Department for Energy and Climate Change Publisher: data.gov.uk.
10. Ofgem, *Typical domestic energy consumption figures - factsheet*. 18/01/2011; Available from: http://www.ofgem.gov.uk/Pages/MoreInformation.aspx?file=domestic%20energy%20consump%20fig%20FS.pdf&refer=Media/FactSheets.
11. S. Firth, K. Lomas, A. Wright, R. Wall, *Identifying trends in the use of domestic appliances from household electricity consumption measurements.* Energy and Buildings, 2008. 40(5): p. 926-936.
12. G. Wood, M. Newborough, *Dynamic energy-consumption indicators for domestic appliances: environment, behaviour and design.* Energy and Buildings, 2003. **35**(8): p. 821-841.
13. DECC, *The impact of changing energy use patterns in buildings on peak electricity demand in the UK*, DECC, Editor 2008.
14. R. Lawson, *A study of the energy usage in domestic UK dwellings to aid the development of domestic combined heat and power(CHP) and micro renewable technologies*, in *Renewable Energy* 2010, Newcastle university. p. 121-127.
15. *K.K. Gupta, A. Rehman, R.M. Sarviya, Bio-fuels for the gas turbine: A review.* Renewable and Sustainable Energy Reviews, 2010. **14**(9): p. 2946-2955.
16. S. A. Basha, K. R. Gopal, S. Jebaraj, *A review on biodiesel production, combustion, emissions and performance.* Renewable and Sustainable Energy Reviews, 2009. **13**(6–7): p. 1628-1634.
17. L.G. Schumacher, S.C. Borgelt, D. Fosseen, W. Goetz, W.G. Hires., *Heavy-duty engine*

exhaust emission tests using methyl ester soybean oil/diesel fuel blends. Bioresource Technology, 1996. **57**(1): p. 31-36.

18. A. Murugesan, C. Umarani, R. Subramanian, N. Nedunchezhian, *Bio-diesel as an alternative fuel for diesel engines—A review.* Renewable and Sustainable Energy Reviews, 2009. **13**(3): p. 653-662.
19. C.D. Rakopoulos, K.A. Antonopoulos, D.C. Rakopoulos, D.T. Hountalas, E.G. Giakoumis, *Comparative performance and emissions study of a direct injection Diesel engine using blends of Diesel fuel with vegetable oils or bio-diesels of various origins.* Energy Conversion and Management, 2006. **47**(18–19): p. 3272-3287.
20. Wang, Y.D., et al., *An experimental investigation of the performance and gaseous exhaust emissions of a diesel engine using blends of a vegetable oil.* Applied Thermal Engineering, 2006. **26**(14–15): p. 1684-1691.
21. P. McCarthy, M.G. Rasul, S. Moazzem, *Analysis and comparison of performance and emissions of an internal* combustion *engine fuelled with petroleum diesel and different bio-diesels.* Fuel, 2011. **90**(6): p. 2147-2157.
22. Y. Huangfu, J.Y. Wu, R.Z. Wang, X.Q. Kong, B.H. Wei, *Evaluation and analysis of novel micro-scale combined cooling, heating and power (MCCHP) system.* Energy Conversion and Management, 2007. **48**(5): p. 1703-1709.
23. J.L. Míguez, S. Murillo, J. Porteiro, L.M. López, *Feasibility of a new domestic CHP trigeneration with heat pump: I. Design and development.* Applied Thermal Engineering, 2004. **24**(10): p. 1409-1419.
24. J. Porteiro, J.L. Míguez, S. Murillo, L.M. López, *Feasibility of a new domestic CHP trigeneration with heat pump: II. Availability analysis.* Applied Thermal Engineering, 2004. **24**(10): p. 1421-1429.
25. G. Gigliucci, L. Petruzzi, E. Cerelli, A. Garzisi, A. La Mendola, *Demonstration of a residential CHP system based on PEM fuel cells.* Journal of Power Sources, 2004. **131**(1–2): p. 62-68.
26. D.W. Wu, R.Z. Wang, *Combined cooling, heating and power: A review.* Progress in Energy and Combustion Science. **32**(5-6): p. 459-495.
27. X.Q. Kong, *Experimental study on a continuous adsorption water chiller with novel design,.* Journal of Engineering Thermophysics, 2005. **28**: p. 218-230.
28. Y.Cai, J. Ren, X. Wang. *The Application and Economic Evaluation of DES: Discussion on DES Based CCHP*. in *Power and Energy Engineering Conference (APPEEC), 2010 Asia-Pacific*. 2010.
29. P.Amid, , F. Saffaraval, M. Saffar-avval. *Feasibility study of different scenarios of CCHP for a residential complex*. in *Innovative Technologies for an Efficient and Reliable Electricity Supply (CITRES), 2010 IEEE Conference on*. 2010.

30. N.Badea, , C. Vlad, A. Stolan. *Comparative study of energy performance for two mCCHP systems used in domestic residence*. in *Electrical and Electronics Engineering (ISEEE), 2010 3rd International Symposium on*. 2010.
31. W. Yang, K. Guo, *Analysis on Energy Saving for a Cool, Heat and Power Cogeneration System with a Micro Gas Turbine*. in *Power and Energy Engineering Conference (APPEEC), 2010 Asia-Pacific*. 2010.
32. N. Anglani, G. Petrecca, *Fossil fuel and biomass fed distributed generation and utility plants: Analysis of energy and environmental performance indicators*. in *Power Electronics for Distributed Generation Systems (PEDG), 2010 2nd IEEE International Symposium on*. 2010.
33. J. Galvão, S.Leitão, S.Malheiro, T. Gaio, *Biofuel for the energy efficiency on a building with small CCHP*. in *Clean Electrical Power, 2009 International Conference on*. 2009.
34. J. F. Wang, Y. P Dai, Z. X. Sun, *A new combined cooling, heating and power system driven by solar energy.* Renewable Energy, 2009. **34**(12): p. 2780-2788.
35. F. Immovilli, A. Bellini, C. Bianchini, G. Franceschini, *Solar Trigeneration for Residential Applications, a Feasible Alternative to Traditional Micro-Cogeneration and Trigeneration Plants*. in *Industry Applications Society Annual Meeting, 2008. IAS '08. IEEE*. 2008.
36. M. S. Carmeli, F. Castelli-Dezza, G. Marchegiani, M. Mauri, L. Piegari, D. Rosati, *Hybrid PV-CHP distributed system: Design aspects and realization*. in *Clean Electrical Power, 2009 International Conference on*. 2009.
37. P. Gang, , L. Jing, J. Jie, *Design and analysis of a novel low-temperature solar thermal electric system with two-stage collectors and heat storage units.* Renewable Energy, 2011. **36**(9): p. 2324-2333.
38. L. Petrucci, C. Boccaletti, B. Francois, P. Di Felice, *Hybrid trigeneration system management with a double DC-bus configuration on the electrical side*. in *Advanced Electromechanical Motion Systems & Electric Drives Joint Symposium, 2009. ELECTROMOTION 2009. 8th International Symposium on*. 2009.
39. N. Badea, I. Voncila, M. Oanca, I. Paraschiv, *Analysis by indicators performance of the conceptual structures mCCHP-SE using renewable energy sources*. in *Electrical and Electronics Engineering (ISEEE), 2010 3rd International Symposium on*. 2010.
40. X.Y. Meng, F.H. Yang, Z.W. Bao, J.Q. Deng, N.N. Serge, Z.X. Zhang ,*Theoretical study of a novel solar trigeneration system based on metal hydrides.* Applied Energy, 2010. **87**(6): p. 2050-2061.
41. Y.D. Wang, Y. Huang, E. Chiremba, A.P. Roskilly, N. Hewitt, Y.L. Ding, D.W. Wu, H.D. Yu, X.P. Chen, Y.P. Li, J.C. Huang, R.Z. Wang, J.Y. Wu, Z.Z. Xia, C.Q. Tan, *An investigation of a household size trigeneration running with hydrogen.* Applied Energy, 2011. **88**(6): p. 2176-2182.
42. M. Goodell, *City of Austin Dedicates New "Super-Efficient" 4.5 Megawatt Trigeneration*

Plant 2004, Available from: http://cogeneration.net/Trigeneration%20Advantages.htm.

43. I. Stambler, , *4.6MW plant with an indirect fired 2600 ton chiller at 76.8% efficiency.* Gas Turbine World, 2004.
44. M.J. Mercer, *CHP Gets New Spin*, in *Diesel and Gas Turbine Worldwide* 2004.
45. C.f.B.I.T Center, *CHP for Buildings Integration Test Center at University of Maryland*. Guide book, 2001.
46. R.Z. Wang, R.G. Oliveira, *Adsorption refrigeration—An efficient way to make good use of waste heat and solar energy.* Progress in Energy and Combustion Science, 2006. **32**(4): p. 424-458.
47. A.R. JoséParise, C. Luis, M. Castillo, P.M. Rui, B.M. Jesús, V.C. José, *A study of the thermodynamic performance and CO2 emissions of a vapour compression bio-trigeneration system.* Applied Thermal Engineering, 2011. **31**(8-9): p. 1411-1420.
48. P.J. Mago, L.M. Chamra, *Analysis and optimization of CCHP systems based on energy, economical, and environmental considerations.* Energy and Buildings, 2009. **41**(10): p. 1099-1106.
49. E. Cardona, A. Piacentino, F. Cardona, *Matching economical, energetic and environmental benefits: An analysis for hybrid CHCP-heat pump systems.* Energy Conversion and Management, 2006. **47**(20): p. 3530-3542.
50. A. Piacentino, F. Cardona, *An original multi-objective criterion for the design of small-scale polygeneration systems based on realistic operating conditions.* Applied Thermal Engineering, 2008. **28**(17-18): p. 2391-2404.
51. E. Cardona, A. Piacentino, *A Validation Methodology for a Combined Heating Cooling and Power (CHCP) Pilot Plant.* Journal of Energy Resources Technology, 2004. **126**(4): p. 285-292.
52. A.A. Jalalzadeh-Azar, *A Comparison of Electrical- and Thermal-Load-Following CHP Systems.* ASHRAE Transactions, 2004. **110**: p. 85-94.
53. P.J. Mago, N. Fumo, L.M. Chamra, *Performance analysis of CCHP and CHP systems operating following the thermal and electric load.* International Journal of Energy Research, 2009. **33**(9): p. 852-864.
54. E. Cardona, A. Piacentino, *A methodology for sizing a trigeneration plant in mediterranean areas.* Applied Thermal Engineering, 2003. **23**(13): p. 1665-1680.
55. H. Li, L. Fu, K.C Geng, Y. Jiang, *Energy utilization evaluation of CCHP systems.* Energy and Buildings, 2006. **38**(3): p. 253-257.
56. G. Chicco, P. Mancarella, *From cogeneration to trigeneration: Profitable alternatives in a competitive market.* IEEE Transactions on Energy Conversion, 2006. **21**(1): p. 265-272.
57. Z.G. Sun, R.Z. Wang, W.Z. Sun, *Energetic efficiency of a gas-engine-driven cooling and heating system.* Applied Thermal Engineering, 2004. **24**(5–6): p. 941-947.

58. R. Zogg, K. Roth, J. Brodrick, *Using CHP systems in commercial buildings.* Ashrae Journal, 2005. **47**(9): p. 33-35.

59. N. Fumo, P.J. Mago, L.M. Chamra, *Cooling, heating, and power energy performance for system feasibility.* Proceedings of the Institution of Mechanical Engineers Part a-Journal of Power and Energy, 2008. **222**(A4): p. 347-354.

60. M. Liu, Y. Shi, F. Fang, *A new operation strategy for CCHP systems with hybrid chillers.* Applied Energy, 2012. **95**(0): p. 164-173.

61. M. Liu, Y. Shi, F. Fang, *Optimal power flow and PGU capacity of CCHP systems using a matrix modeling approach.* Applied Energy, 2013. **102**(0): p. 794-802.

62. M. Sakawa, K. Kato, S. Ushiro, *Operational planning of district heating and cooling plants through genetic algorithms for mixed 0-1 linear programming.* European Journal of Operational Research, 2002. **137**(3): p. 677-687.

63. P. Ahmadi, I. Dincer, *Exergoenvironmental analysis and optimization of a cogeneration plant system using Multimodal Genetic Algorithm (MGA).* Energy, 2010. **35**(12): p. 5161-5172.

64. M. Burer, K. Tanaka, D. Favrat, K. Yamada, *Multi-criteria optimization of a district cogeneration plant integrating a solid oxide fuel cell–gas turbine combined cycle, heat pumps and chillers.* Energy, 2003. **28**(6): p. 497-518.

65. G. Abdollahi, M. Meratizaman, *Multi-objective approach in thermoenvironomic optimization of a small-scale distributed CCHP system with risk analysis.* Energy and Buildings, 2011. **43**(11): p. 3144-3153.

66. H. Ghaebi, M.H. Saidi, P. Ahmadi, *Exergoeconomic optimization of a trigeneration system for heating, cooling and power production purpose based on TRR method and using evolutionary algorithm.* Applied Thermal Engineering, 2012. **36**(0): p. 113-125.

67. R. Lahdelma, H. Hakonen, *An efficient linear programming algorithm for combined heat and power production.* European Journal of Operational Research, 2003. **148**(1): p. 141-151.

68. A. Rong, R. Lahdelma, *An efficient linear programming model and optimization algorithm for trigeneration.* Applied Energy, 2005. **82**(1): p. 40-63.

69. S. Makkonen, R. Lahdelma, *Non-convex power plant modelling in energy optimisation.* European Journal of Operational Research, 2006. **171**(3): p. 1113-1126.

70. A. Rong, R. Lahdelma, P.B. Luh, *Lagrangian relaxation based algorithm for trigeneration planning with storages.* European Journal of Operational Research, 2008. **188**(1): p. 240-257.

71. H.J. Cho, P.J. Mago, R. Luck, L.M. Chamra, *Evaluation of CCHP systems performance based on operational cost, primary energy consumption, and carbon dioxide emission by utilizing an optimal operation scheme.* Applied Energy, 2009. **86**(12): p. 2540-2549.

72. S.G. Tichi, M.M. Ardehali, M.E. Nazari, *Examination of energy price policies in Iran for optimal configuration of CHP and CCHP systems based on particle swarm optimization algorithm.* Energy Policy, 2010. **38**(10): p. 6240-6250.

73. O.M. Toledo, D.O. Filho, A.S. Diniz, *Distributed photovoltaic generation and energy storage systems: A review.* Renewable and Sustainable Energy Reviews, 2010. **14**(1): p. 506-511.
74. H.S. Chen, T.N. Cong, W. Yang, C.Q Tan, Y.L. Li, Y.L. Ding, *Progress in electrical energy storage system: A critical review.* Progress in Natural Science, 2009. **19**(3): p. 291-312.
75. I. Hadjipaschalis, A. Poullikkas, V. Efthimiou, *Overview of current and future energy storage technologies for electric power applications.* Renewable and Sustainable Energy Reviews, 2009. **13**(6–7): p. 1513-1522.
76. P.J. Hall, E.J. Bain, *Energy-storage technologies and electricity generation.* Energy Policy, 2008. **36**(12): p. 4352-4355.
77. A. Nourai, *Large-scale electricity storage technologies for energy management*. 2002 IEEE Power Engineering Society Summer Meeting, Vols 1-3, Conference Proceedings2002. 310-315.
78. A. Oudalov, D. Chartouni, C. Ohler, G. Linhofer, *Value analysis of battery energy storage applications in power systems*. 2006 IEEE/PES Power Systems Conference and Exposition. Vols 1-52006. 2206-2211.
79. M. Conte, P.P. Prosini, S. Passerini, *Overview of energy/hydrogen storage: state-of-the-art of the technologies and prospects for nanomaterials.* Materials Science and Engineering: B, 2004. **108**(1–2): p. 2-8.
80. J.P. Deane, B.P. Ó Gallachóir, E.J. McKeogh, *Techno-economic review of existing and new pumped hydro energy storage plant.* Renewable and Sustainable Energy Reviews, 2010. **14**(4): p. 1293-1302.
81. M. Conte, A. Iacobazzi, M. Ronchetti, R. Vellone, *Hydrogen economy for a sustainable development: state-of-the-art and technological perspectives.* Journal of Power Sources, 2001. **100**(1–2): p. 171-187.
82. G. Smith, *Storage batteries, including operation, charging, maintenance and repair* 1968, London: Pitman.
83. F.D. González, A. Sumper, O.G. Bellmunt, R.V. Robles, *A review of energy storage technologies for wind power applications.* Renewable and Sustainable Energy Reviews, 2012. **16**(4): p. 2154-2171.
84. A. Kirubakaran, S. Jain, R.K. Nema, *A review on fuel cell technologies and power electronic interface.* Renewable and Sustainable Energy Reviews, 2009. **13**(9): p. 2430-2440.
85. P. Thounthong, S. Raël, B. Davat, *Energy management of fuel cell/battery/supercapacitor hybrid power source for vehicle applications.* Journal of Power Sources, 2009. **193**(1): p. 376-385.
86. P. Thounthong, S. Raël, B. Davat, *Control strategy of fuel cell/supercapacitors hybrid power sources for electric vehicle.* Journal of Power Sources, 2006. **158**(1): p. 806-814.
87. K.E. Nielsen, M. Molinas, *Superconducting Magnetic Energy Storage (SMES) in power*

systems with renewable energy sources. in *Industrial Electronics (ISIE), 2010 IEEE International Symposium on*. 2010.

88. W.F. Pickard, A.Q. Shen, N.J. Hansing, *Parking the power: Strategies and physical limitations for bulk energy storage in supply–demand matching on a grid whose input power is provided by intermittent sources.* Renewable and Sustainable Energy Reviews, 2009. **13**(8): p. 1934-1945.
89. M. Sander, R. Gehring, H. Neumann, T. Jordan, *LIQHYSMES storage unit – Hybrid energy storage concept combining liquefied hydrogen with Superconducting Magnetic Energy Storage.* International Journal of Hydrogen Energy, 2012. **37**(19): p. 14300-14306.
90. L. Xu, *On the Key Techniques of Supercapacitors' Application in the Hybrid Power System of Crane*. SHIP &OCEAN ENGINEERING(CHINA), 2008.
91. J.N. Marie-Francoise, H. Gualous, R. Outbib, A. Berthon, *A 42V Power Net with supercapacitor and battery for automotive applications.* Journal of Power Sources, 2005. **143**(1–2): p. 275-283.
92. K.T. Chau, Y.S. Wong, *Hybridization of energy sources in electric vehicles.* Energy Conversion and Management, 2001. **42**(9): p. 1059-1069.
93. B. Zupančič, A. Sodja, *Advanced Multi-Domain Modelling: Advantages and Dangers*. in *Computer Modelling and Simulation (UKSim), 2011 UkSim 13th International Conference on*. 2011.
94. M. Dempsey, *Dymola for Multi-Engineering Modelling and Simulation*. in *Vehicle Power and Propulsion Conference, 2006. VPPC '06. IEEE*. 2006.
95. R.J. Smith, *Circuits, devices, and systems : a first course in electrical engineering* ed. S. Elliot1992, New York :Wiley. 868.
96. Y.S Kung, N.V. Quynh, N.T. Hieu, C.C. Huang, L.C Huang, *Simulink/Modelsim Co-Simulation and FPGA Realization of Speed Control IC for PMSM Drive.* Procedia Engineering, 2011. **23**(0): p. 718-727.
97. D. Grenier, L.A. Dessaint, O. Akhrif, Y. Bonnassieux, B.L. Pioufle, *Experimental nonlinear torque control of a permanent-magnet synchronous motor using saliency.* Industrial Electronics, IEEE Transactions on, 1997. **44**(5): p. 680-687.
98. M. Ceraolo, *New dynamical models of lead-acid batteries.* Power Systems, IEEE Transactions on, 2000. **15**(4): p. 1184-1190.
99. S. Barsali, M. Ceraolo, *Dynamical Models of Lead-Acid Batteries: Implementation Issues.* Power Engineering Review, IEEE, 2002. **22**(2): p. 63-63.
100. R.A. Jackey, *A Simple, Effective Lead-Acid Battery Modeling Process for Electrical System Component Selection*. 2007.
101. M.E. Glavin, P.K. Chan, S. Armstrong, W.G. Hurley, *A stand-alone photovoltaic supercapacitor battery hybrid energy storage system*. in *Power Electronics and Motion*

Control Conference, 2008. EPE-PEMC 2008. 13th. 2008.

102. M. Uzunoglu, M.S. Alam, *Modeling and Analysis of an FC/UC Hybrid Vehicular Power System Using a Novel-Wavelet-Based Load Sharing Algorithm.* Energy Conversion, IEEE Transactions on, 2008. **23**(1): p. 263-272.
103. M. Uzunoglu, O.C. Onar, M.S. Alam, *Modeling, control and simulation of a PV/FC/UC based hybrid power generation system for stand-alone applications.* Renewable Energy, 2009. **34**(3): p. 509-520.
104. S.M. Halpin, R.L. Spyker, R.M. Nelms, R.F. Burch, *Application of double-layer capacitor technology to static condensers for distribution system voltage control.* Power Systems, IEEE Transactions on, 1996. **11**(4): p. 1899-1904.
105. R.L. Spyker, R.M. Nelms, *Classical equivalent circuit parameters for a double-layer capacitor*. Aerospace and Electronic Systems, IEEE Transactions on, 2000. **36**(3): p. 829-836.
106. S.M. Naylor, V. Pickert, D.J. Atkinson, *Fuel Cell Drive Train Systems -- Driving Cycle Evaluation of Potential Topologies*. in *Vehicle Power and Propulsion Conference, 2006. VPPC '06. IEEE*. 2006.
107. A.K. Shukla, A. Banerjee, M.K. Ravikumar, A. Jalajakshi, *Electrochemical capacitors: Technical challenges and prognosis for future markets.* Electrochimica Acta, (0).
108. B. Andrew, *Ultracapacitors: why, how, and where is the technology*. Journal of Power Sources, 2000. **91**(1): p. 37-50.

Appendices

Appendix-1 PLC programme in primary test

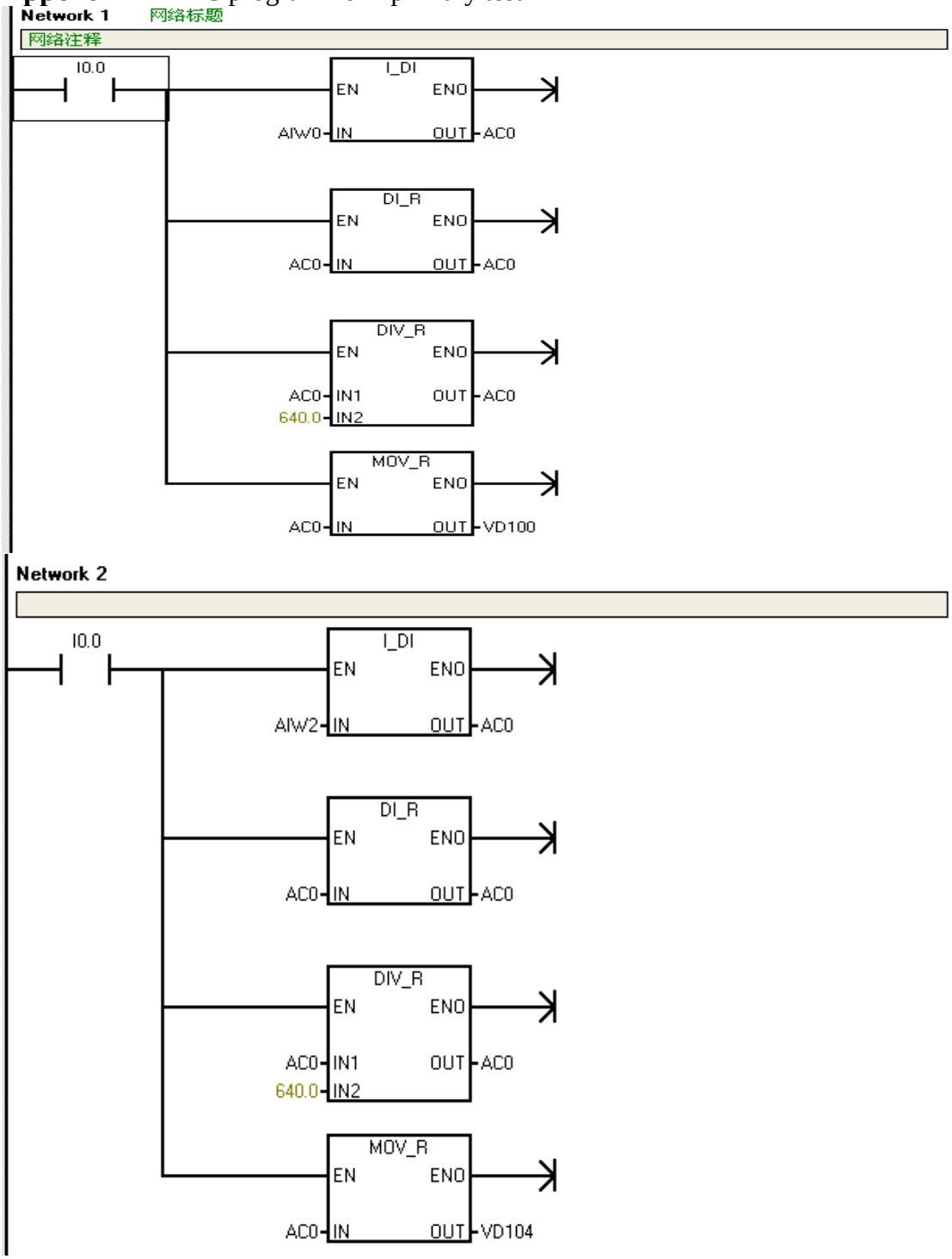

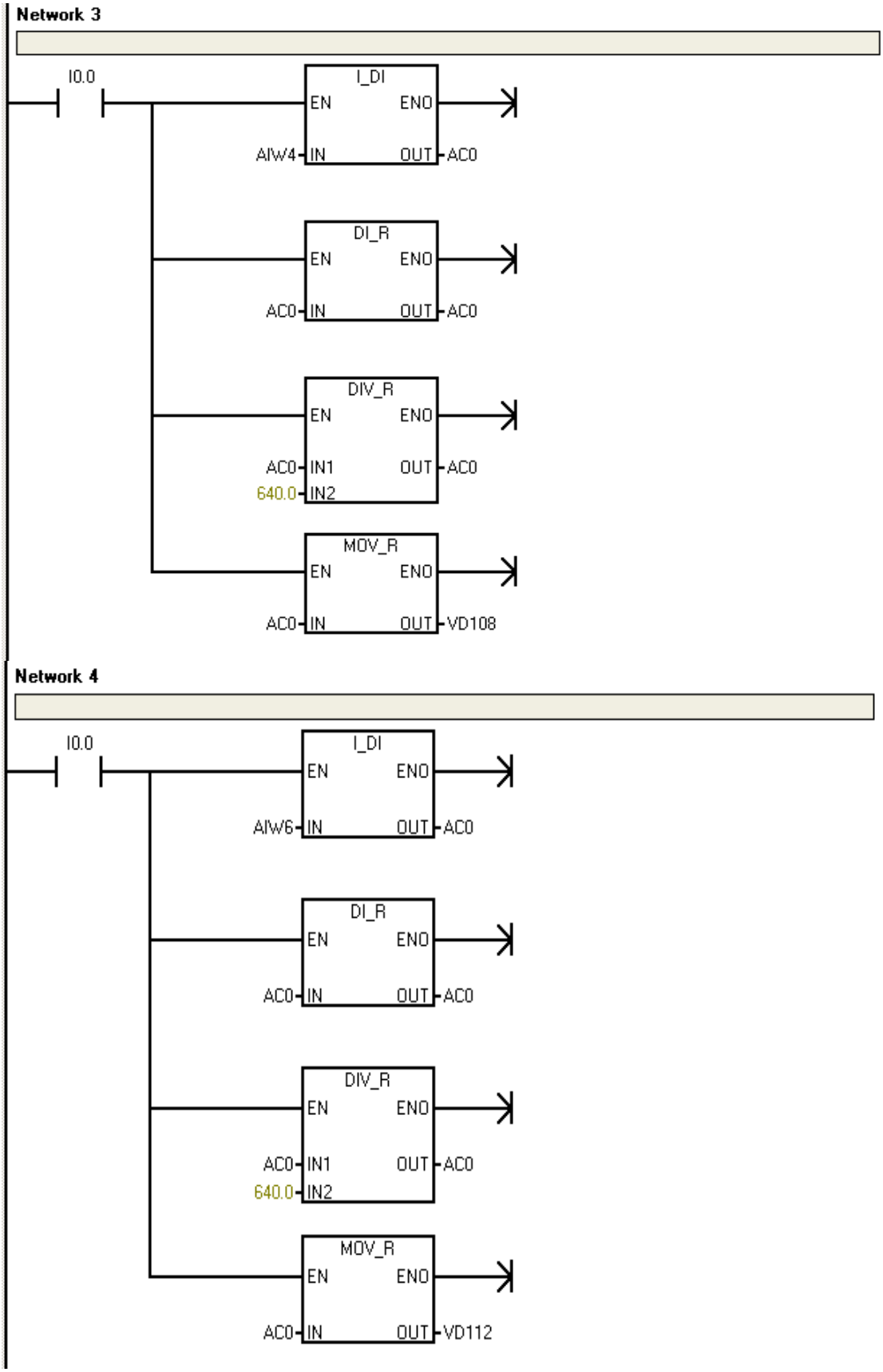
Network 3
I0.0
I_DI
EN
ENO
AIW4
IN
OUT
AC0
DI_R
EN
ENO
AC0
IN
OUT
AC0
DIV_R
EN
ENO
AC0
IN1
OUT
AC0
640.0
IN2
MOV_R
EN
ENO
AC0
IN
OUT
VD108
Network 4
I0.0
I_DI
EN
ENO
AIW6
IN
OUT
AC0
DI_R
EN
ENO
AC0
IN
OUT
AC0
DIV_R
EN
ENO
AC0
IN1
OUT
AC0
640.0
IN2
MOV_R
EN
ENO
AC0
IN
OUT
VD112

Network 5

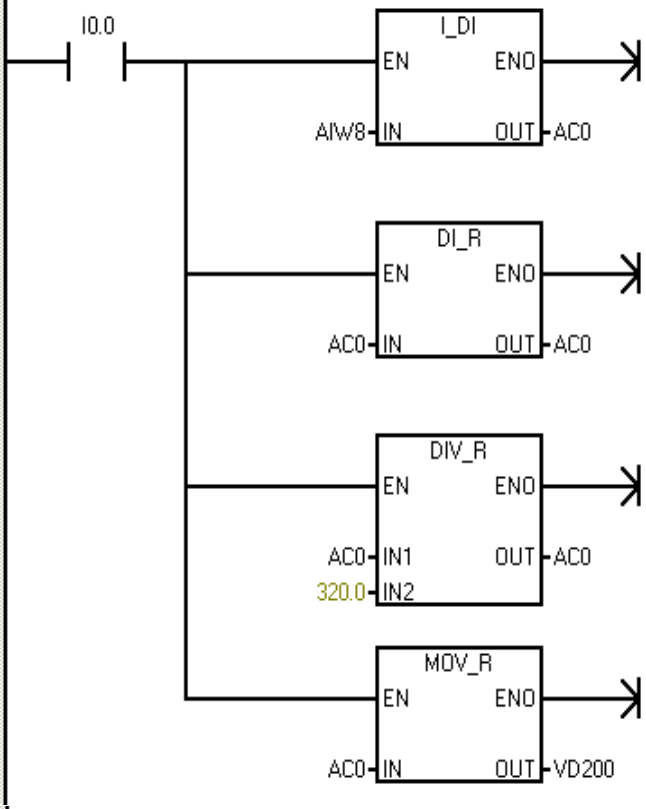

Network 6

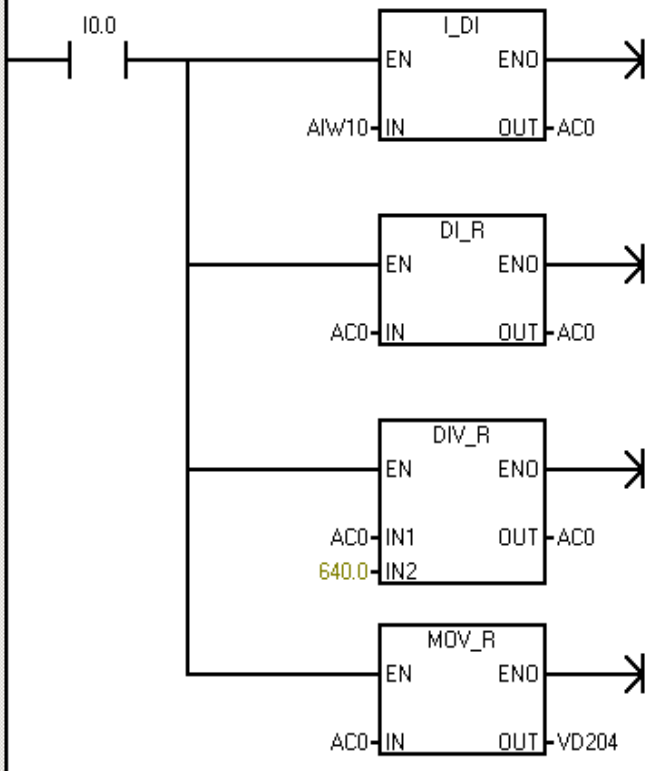

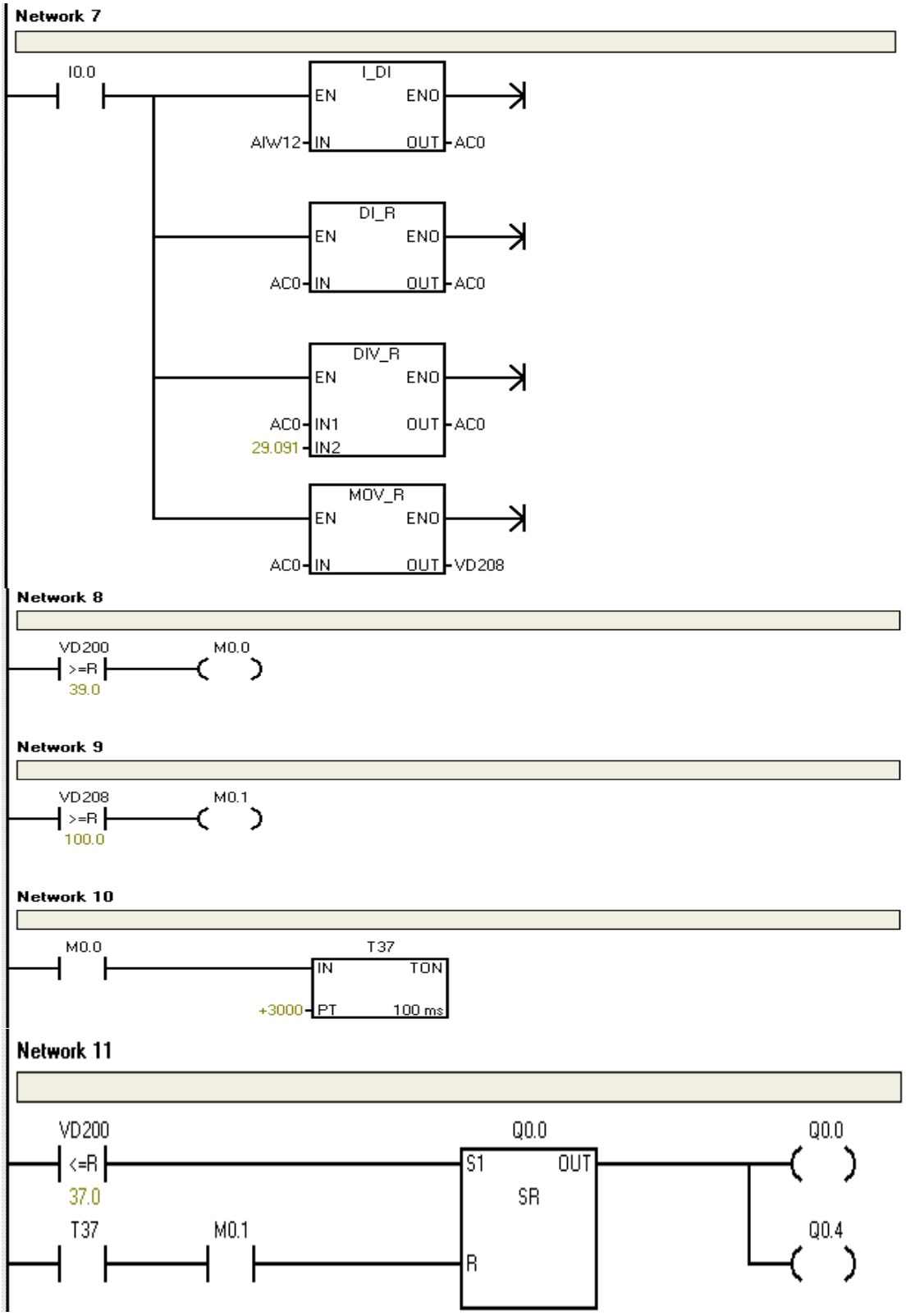
Network 7
I0.0
I_DI
EN
ENO
AIW12
IN
OUT
AC0
DI_R
EN
ENO
AC0
IN
OUT
AC0
DIV_R
EN
ENO
AC0
IN1
OUT
AC0
29.091
IN2
MOV_R
EN
ENO
AC0
IN
OUT
VD208
Network 8
VD200
>=R
39.0
M0.0
Network 9
VD208
>=R
100.0
M0.1
Network 10
M0.0
T37
IN
TON
+3000
PT
100 ms
Network 11
VD200
<=R
37.0
Q0.0
S1
OUT
SR
R
Q0.0
T37
M0.1
Q0.4

Appendix-2

Spring case

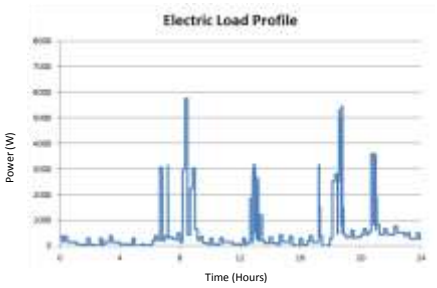

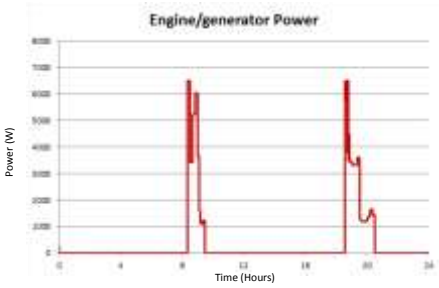

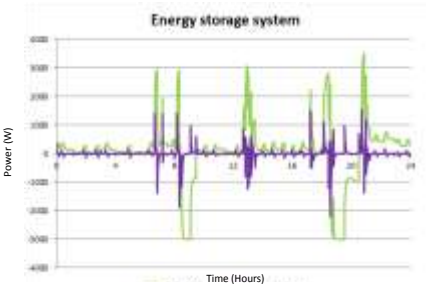

Spring	6.5kWengine and 600AH/24V batteries and 30V/4573F Supercapacitor	10kW Engine
Engine electric efficiency	20.79	3.84
Engine thermal efficiency	37.29	41.93
Battery efficiency	18.49	--
Super capacitor efficiency	20.56	--
electricity consumption	11.96	11.96
Engine electricity supplying	9.59	11.96
Battery discharge	8.22	--
Super capacitor discharge	0.68	--
energy charged	6.05	--
Engine running time(hours)	3.12	24
Charge duration	3.03	--
Heat recovered (kWh)	15.98	118.87

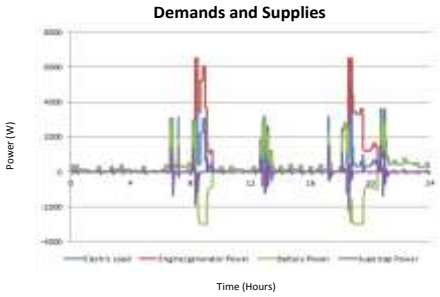

Summer case

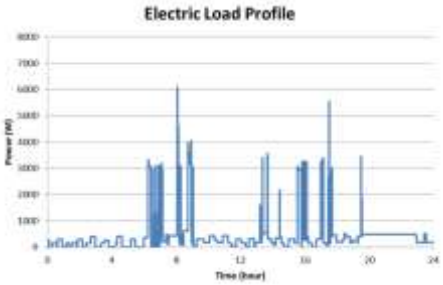

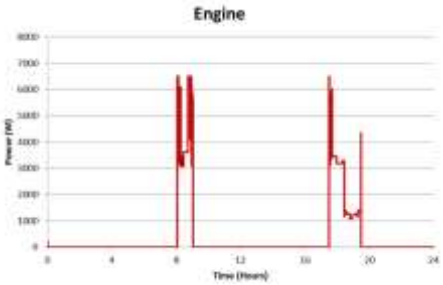

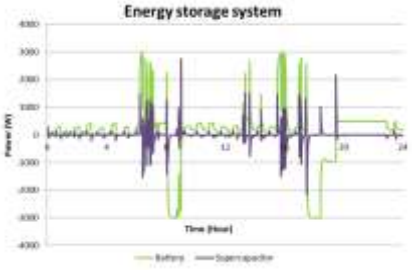

Summer	6.5kWengine and 600AH/24V batteries and 30V/4573F Supercapacitor	10kW Engine
Engine electric efficiency	21.21	3.67
Engine thermal efficiency	36.96	41.95
Battery efficiency	15.94	--
Super capacitor efficiency	17.94	--
electricity consumption	11.01	11.01
Engine electricity supplying	9.04	11.01
Battery discharge	8.35	--
Super capacitor discharge	0.85	--
energy charged	6.57	--
Engine running time(hours)	2.97	24
Charge duration	2.94	--
Heat recovered (kWh)	14.91	105.01

Autumn case

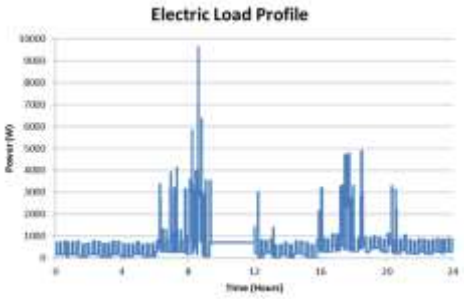

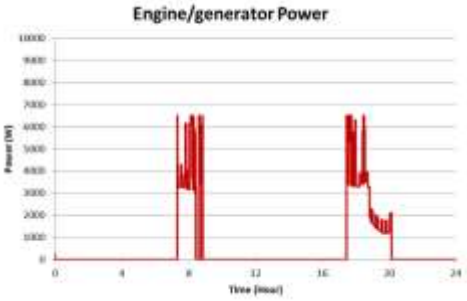

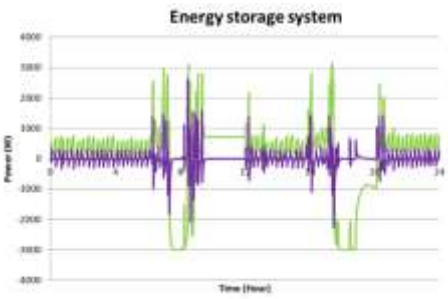

Autumn	6.5kWengine and 600AH/24V batteries and 30V/4573FSupercapacitor	10kW Engine
Engine electric efficiency	22.70	5.15
Engine thermal efficiency	37.45	40.86
Battery efficiency	20.15	--
Super capacitor efficiency	22.26	--
electricity consumption	16.06	16.06
Engine electricity supplying	14.02	16.06
Battery discharge	10.77	--
Super capacitor discharge	1.38	--
energy charged	9.17	--
Engine running time(hours)	4.04	24
Charge duration	3.99	--
Heat recovered (kWh)	22.20	118.17

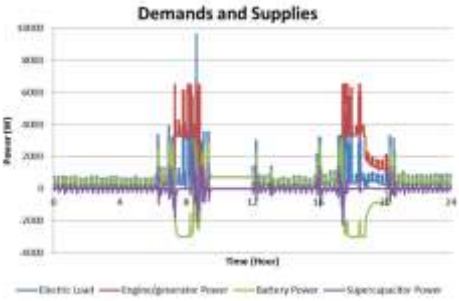

Winter case

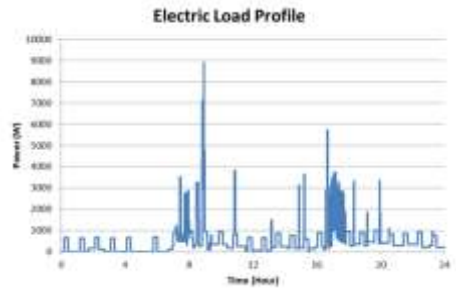

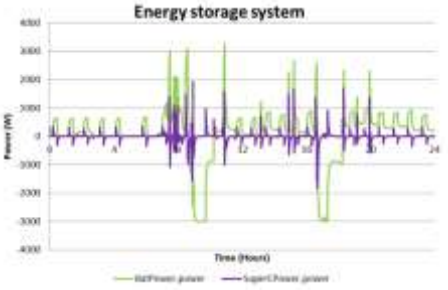

winter	6.5kWengine and 600AH/24V batteries and 30V/4573FSupercapacitor	10kW Engine
Engine electric efficiency	21.72	4.14
Engine thermal efficiency	36.95	41.57
Battery efficiency	17.16	--
Super capacitor efficiency	17.16	--
electricity consumption	12.49	12.49
Engine electricity supplying	9.57	12.49
Battery discharge	8.60	--
Super capacitor discharge	0.83	--
energy charged	5.86	--
Engine running time(hours)	3.22	24
Charge duration	2.97	--
Heat recovered (kWh)	15.53	99.90